

THE UNIVERSITY OF MANITOBA

THREE DIMENSIONAL ANALYSIS OF
HARMONIC WAVES IN A PERIODICALLY
LAMINATED MEDIUM

BY

JOHNNY KHEE-THAI YEO

A THESIS

SUBMITTED TO THE FACULTY OF GRADUATE STUDIES
IN PARTIAL FULFILLMENT OF THE REQUIREMENT FOR THE DEGREE
MASTER OF SCIENCE

DEPARTMENT OF CIVIL ENGINEERING

WINNIPEG, MANITOBA

MAY 1983

THREE DIMENSIONAL ANALYSIS OF
HARMONIC WAVES IN A PERIODICALLY
LAMINATED MEDIUM

BY

JOHNNY KHEE-THAI YEO

A thesis submitted to the Faculty of Graduate Studies of
the University of Manitoba in partial fulfillment of the requirements
of the degree of

MASTER OF SCIENCE

©[✓] 1983

Permission has been granted to the LIBRARY OF THE UNIVER-
SITY OF MANITOBA to lend or sell copies of this thesis, to
the NATIONAL LIBRARY OF CANADA to microfilm this
thesis and to lend or sell copies of the film, and UNIVERSITY
MICROFILMS to publish an abstract of this thesis.

The author reserves other publication rights, and neither the
thesis nor extensive extracts from it may be printed or other-
wise reproduced without the author's written permission.

ACKNOWLEDGEMENT

The author would like to express his sincere gratitude to his advisor, Professor A.H. Shah of the Department of Civil Engineering for supervising this thesis. His guidance, encouragement and friendship are gratefully acknowledged.

Special appreciation goes to Prof. S.K. Datta of Colorado University for his careful reading of the thesis. His guidance and comment on this work proved to be invaluable.

The author would like to thank his friends, especially Julia Shim and Siok-Li Lee who one way or another contributed to the final copy of this thesis.

Finally, the author is deeply indebted to his parents and family for their emotional support and encouragement.

TABLE OF CONTENTS

	PAGE
LIST OF TABLES	vi
LIST OF FIGURES	vii
NOMENCLATURE	xi

CHAPTER

1	INTRODUCTION	1
	1.1 LITERATURE REVIEW	1
	1.2 PRESENT SCOPE	3
2.	HARMONIC WAVES IN A PERIODICALLY LAMINATED MEDIUM: FINITE ELEMENT METHOD (F.E.M.)	4
	2.1 INTRODUCTION	4
	2.2 EQUATION OF LINEAR ELASTICITY	4
	2.3 TRACTION AND DISPLACEMENT CONTINUITY	6
	2.4 DISPLACEMENT EQUATIONS	8
	2.5 FORMULATION OF ELEMENTAL STIFFNESS AND MASS MATRICES	9
	2.6 GENERATION OF EIGENVALUE AND EIGENVECTOR PROBLEMS	11
	2.7 ANTIPLANE AND PLANE STRAIN MOTIONS	12
	2.7.1 Antiplane Strain	13
	2.7.2 Plane Strain	14
3.	OTHER THEORIES ON WAVE PROPAGATION IN A STRATIFIED MEDIUM	16
	3.1 INTRODUCTION	16
	3.2 EFFECTIVE MODULUS METHOD	16
	3.2.1 Stress-Strain Relationship	17
	3.2.2 Effective Elastic Constants	21
	3.2.3 Displacement Equations of Motion	23
	3.2.4 Antiplane and Plane Strain Motion	24

	PAGE
3.3 EFFECTIVE STIFFNESS METHOD	25
3.3.1 Kinematic and Smoothing Operation	26
3.3.2 Displacement Equations of Motion	34
3.3.3 Propagation of Plane Harmonic Waves	37
3.3.4 Antiplane and Plane Strain Motion	38
4. NUMERICAL RESULTS AND DISCUSSION	42
4.1 INTRODUCTION	42
4.2 ISOTROPIC LAMINATED MEDIUM	43
4.3 FIBER-REINFORCED BORON-ALUMINIUM COMPOSITE	45
4.4 GRAPHITE-EPOXY FIBER REINFORCED COMPOSITE	49
4.4.1 Graphite-Epoxy Composite (i)	50
4.4.2 Graphite-Epoxy Composite (ii)	51
4.5 COMPARISON OF THREE METHODS: Effective Modulus, Effective Stiffness and Finite Element Method	52
4.6 CONCLUSION	53
REFERENCES	55
APPENDICES	58
APPENDIX A DERIVATION OF THE INTERPOLATION FUNCTION	58
APPENDIX B INTEGRATION OF INTERPOLATION FUNCTION	62
APPENDIX C EVALUATION OF THE INTEGRAL IN ENERGY EQUATION (EQ. 2.10 OF CHAPTER 2)	64
APPENDIX D ASSEMBLY PROCESS OF STIFFNESS MATRIX	74
APPENDIX E EVALUATION OF EULER EQUATION (EQ. 3.43 OF CHAPTER 3)	77
APPENDIX F ELEMENTS OF THE IMPEDANCE MATRIX	80
APPENDIX G FORMULA TO CALCULATE THE MATERIAL CONSTANTS OF GRAPHITE-EPOXY FIBER-REINFORCED COMPOSITE	83

	PAGE
APPENDIX H FORTRAN PROGRAM FOR THE EFFECTIVE MODULUS METHOD . .	86
APPENDIX I FORTRAN PROGRAM FOR THE EFFECTIVE STIFFNESS METHOD	91
APPENDIX J FORTRAN PROGRAM FOR THE FINITE ELEMENT METHOD . . .	97
TABLES	120
FIGURES	126

LIST OF TABLES

<u>NUMBER</u>		<u>PAGE</u>
4.1	Material Constants of Isotropic Laminae	121
4.2	Material Constants for Fiber-reinforced Boron Aluminium Composite	122
4.3	Material Constants for Graphite-epoxy Composite (i) . .	123
4.4	Material Constants for Graphite-epoxy Composite (ii) . .	124
4.5	Material Constants of Transversely Isotropic Laminae . .	125

LIST OF FIGURES

<u>NUMBER</u>		<u>PAGE</u>
2.1	Geometry of periodically laminated infinite medium. . .	127
3.1	Typical finite laminated medium showing shear stresses acting on the surface of the medium.	128
3.2	Laminated layers subjected to tangential traction. . .	129
3.3	Laminated medium used for the Effective Stiffness Method showing the layer properties and local coordinates. . .	130
3.4	Pair of reinforcing and matrix layers.	131
4.1	Lowest symmetric SH mode propagating in the direction of the layering for isotropic material.	132
4.2	Phase velocity vs. wave number plot for the lowest antisymmetric mode (SV) propagating in the direction of the layering.	133
4.3	Lowest symmetric P mode propagating in the direction of the layering.	134
4.4	Lowest transverse (SV) and longitudinal (P) mode propagating normal to the layering.	135
4.5	Lowest transverse (SV) and longitudinal (P) mode propagating in the direction of the layering for anisotropic material.	136
4.6	Lowest SH, SV and P mode propagating normal to the layering for anisotropic material, $\alpha = 0^\circ$, $\phi = 90^\circ$	137
4.7	Lowest SH, SV and P mode propagating along x-y plane, $\phi = 0^\circ$	138
4.8	Lowest SH, SV and P mode propagating along x-y plane, $\phi = 30^\circ$	139
4.9	Lowest SH, SV and P mode propagating along x-y plane, $\phi = 60^\circ$	140
4.10	Lowest SH, SV and P mode propagating along x-y plane, $\phi = 90^\circ$	141
4.11	Lowest SH, SV and P mode propagating along y-z plane, $\phi = 0^\circ$	142
4.12	Lowest SH, SV and P mode propagating along y-z plane, $\phi = 30^\circ$	143
4.13	Lowest SH, SV and P mode propagating along y-z plane, $\phi = 60^\circ$	144
4.14	Lowest SH, SV and P mode propagating along y-z plane, $\phi = 90^\circ$	145

	PAGE
4.15 Lowest SH, SV and P mode propagating along x-z plane, $\alpha=0^\circ$	146
4.16 Lowest SH, SV and P mode propagating along x-z plane, $\alpha=30^\circ$	147
4.17 Lowest SH, SV and P mode propagating along x-z plane, $\alpha=60^\circ$	148
4.18 Lowest SH, SV and P mode propagating along x-z plane, $\alpha=90^\circ$	149
4.19 Frequency vs. vertical angle plot for SH mode propagating on x-y plane.	150
4.20 Frequency vs. vertical angle plot for SV mode propagating on x-y plane.	151
4.21 Frequency vs. vertical angle plot for P mode propagating on x-y plane.	152
4.22 Frequency vs. vertical angle plot for lowest SH mode propagating on y-z plane.	153
4.23 Frequency vs. vertical angle plot for lowest SV mode propagating on y-z plane.	154
4.24 Frequency vs. vertical angle plot for lowest P mode propagating on y-z plane.	155
4.25 Frequency vs. horizontal angle plot for lowest SH mode propagating on x-z plane.	156
4.26 Frequency vs. horizontal angle plot for lowest SV mode propagating on x-z plane.	157
4.27 Frequency vs. horizontal angle plot for lowest P mode propagating on x-z plane.	158
4.28 Curves of constant \bar{k} for lowest SH mode, $\alpha=0^\circ$	159
4.29 Curves of constant \bar{k} for lowest SH mode, $\alpha=90^\circ$	160
4.30 Curves of constant \bar{k} on x-y plane, $\alpha=0^\circ$	161
4.31 Lowest 5 branches for curves of constant \bar{k} on x-y plane, $\alpha=45^\circ$	162
4.32 Lowest 5 branches for curves of constant \bar{k} on y-z plane, $\alpha=90^\circ$	163
4.33 Lowest 5 branches for $\alpha=0^\circ$, $\bar{\eta} = 0.0$	164
4.34 Lowest 5 branches for $\alpha=45^\circ$, $\bar{\eta} = 0.0$	165
4.35 Lowest 5 branches for $\alpha=90^\circ$, $\bar{\eta} = 0.0$	166

	PAGE
4.36 Frequency vs. wave number plot for lowest SH mode, $\bar{\eta} = 0.0$ and $\bar{\eta} = 1/13$	167
4.37 Lowest 5 branches for $\alpha = 45^\circ$, $\bar{\eta} = 1/26$	168
4.38 Lowest 5 branches for $\alpha = 45^\circ$, $\bar{\eta} = 1/13$	169
4.39 Lowest 3 branches for wave propagating on x-y plane, $\alpha=0^\circ$, $\phi = 45^\circ$	170
4.40 Lowest 3 branches for wave propagating on y-z plane, $\alpha=90^\circ$, $\phi = 45^\circ$	171
4.41 Lowest 3 branches for wave propagating on x-z plane, $\alpha=45^\circ$, $\phi = 0^\circ$	172
4.42 Lowest 3 branches for wave propagating at $\alpha = 45^\circ$, $\phi = 45^\circ$	173
4.43 Lowest 3 branches for curves of constant \bar{k} , $\alpha = 0^\circ$	174
4.44 Lowest 3 branches for curves of constant \bar{k} , $\alpha = 45^\circ$	175
4.45 Lowest 3 branches for curves of constant \bar{k} , $\alpha = 90^\circ$	176
4.46 Lowest branch for constant $\bar{\eta}$, $\alpha = 45^\circ$	177
4.47 Lowest 3 branches for wave propagating on x-y plane, $\alpha=0^\circ$, $\phi = 45^\circ$; $\bar{d} = 9$	178
4.48 Lowest 3 branches for wave propagating on y-z plane, $\alpha=90^\circ$, $\phi = 45^\circ$; $\bar{d} = 9$	179
4.49 Lowest 3 branches for wave propagating on x-z plane, $\alpha=45^\circ$, $\phi = 0^\circ$; $\bar{d} = 9$	180
4.50 Lowest 3 branches for wave propagating at $\alpha = 45^\circ$, $\phi = 45^\circ$, $\bar{d} = 9$.	181
4.51 Lowest 3 branches for curves of constant \bar{k} , $\alpha = 0^\circ$; $\bar{d} = 9$	182
4.52 Lowest 3 branches for curves of constant \bar{k} , $\alpha = 45^\circ$; $\bar{d} = 9$	183
4.53 Lowest 3 branches for curves of constant \bar{k} , $\alpha = 90^\circ$; $\bar{d} = 9$	184
4.54 Lowest branch for constant $\bar{\eta}$, $\alpha = 45^\circ$; $\bar{d} = 9$	185
4.55 Lowest 3 branches for wave propagating on x-y plane, $\alpha = 0^\circ$ $\phi = 45^\circ$	186
4.56 Lowest 3 branches for wave propagating on y-z plane, $\alpha=90^\circ$ $\phi = 0^\circ$	187

	PAGE
4.57 Lowest 3 branches for wave propagating on x-z plane, $\alpha=45^\circ$ $\phi = 0^\circ$	188
4.58 Lowest 3 branches for wave propagating at $\alpha = 45^\circ$, $\phi = 45^\circ$	189
4.59 Lowest 3 branches for curves of constant \bar{k} , $\alpha = 0^\circ$. . .	190
4.60 Lowest 3 branches for curves of constant \bar{k} , $\alpha = 45^\circ$. . .	191
4.61 Lowest 3 branches for curves of constant \bar{k} , $\alpha = 90^\circ$. . .	192
4.62 Lowest branch for constant $\bar{\eta}$, $\alpha = 45^\circ$	193
4.63 Lowest 3 branches for wave propagating on x-y plane, $\alpha = 0^\circ$ $\phi = 45^\circ$; $\bar{d} = 9$	194
4.64 Lowest 3 branches for wave propagating at y-z plane, $\alpha=90^\circ$ $\phi = 45^\circ$; $\bar{d} = 9$	195
4.65 Lowest 3 branches for wave propagating at x-z plane, $\alpha=45^\circ$ $\phi = 0^\circ$; $\bar{d} = 9$	196
4.66 Lowest 3 branches for wave propagating at $\alpha = 45^\circ$, $\phi = 45^\circ$; $\bar{d} = 9$	197
4.67 Lowest 3 branches for curves of constant \bar{k} , $\alpha = 0^\circ$; $\bar{d} = 9$	198
4.68 Lowest 3 branches for curves of constant \bar{k} , $\alpha = 45^\circ$; $\bar{d} = 9$	199
4.69 Lowest 3 branches for curves of constant \bar{k} , $\alpha = 90^\circ$; $\bar{d} = 9$	200
4.70 Lowest branch for constant $\bar{\eta}$, $\alpha = 45^\circ$; $\bar{d} = 9$	201
4.71 Lowest SV mode for wave propagating through 3 isotropic media with different thicknesses	202
4.72 Lowest SH mode for wave propagating through 3 isotropic media with different thicknesses	203

NOMENCLATURE

\bar{A}, \bar{B} $\bar{U}, \bar{V}, \bar{W}$	Amplitude of propagating wave
$[A_1], [B_1]$	Stiffness and Mass matrix of the laminated media
$C_{\ell,n}^{(i)}$	Material constants of the (i) th lamina (i) = f : reinforcing layer (i) = m : matrix layer $\ell = 1, 2, 3 \dots 6$ $n = 1, 2, 3 \dots 6$
c	Phase Velocity
d	Thickness of a unit cell
$d_1, d_f, 2h^{(1)}$	Thickness of reinforced layer
$d_2, d_m, 2h^{(2)}$	Thickness of matrix layer
\bar{d}	Ratio of thicknesses of reinforced layer and the matrix layer
$f_m (\eta_i)$	Interpolation function, $m = 1, 2, 3, 4$
I, (i)	Superscript (i) and I represent the same quantity, i.e., the (i) th or I th lamina
$[k_i], [m_i]$	Stiffness and mass matrix of the (i) th lamina
\bar{k}, ξ	Dimensionless wave number
k, k_x, k_y, k_z	Wave number and the x-, y- and z-component of the wave number
$\{r_i\}$	Matrix of nodal quantities for the (i) th lamina
$\{R\}$	Matrix of nodal quantities for the entire media
$[S^a], [S^p]$	Impedance matrix
t, T	Time, superscript denotes transpose
$T_{kin}^{(i)}, V_{Pot}^{(i)}$	Kinetic energy and potential energy of the (i) th lamina (i) = f : reinforced layer (i) = m : matrix layer

U_I, V_I, W_I	x-, y- and z-component of the global displacement of the (i) th lamina
$\bar{U}_I, \bar{V}_I, \bar{W}_I$	Complex conjugate of U_I, V_I, W_I
$U_o^{ft,mk}, V_o^{ft,mk}$	Local displacement of mid plane of the k th pair of reinforcing and matrix layer.
$W_o^{fk,mk}$	
u_i, v_i, w_i	nodal x-, y- and z-displacement of the i th node
α, ϕ	Horizontal and vertical angle
β	Nondimensional phase velocity
$\gamma^{(i)}, \epsilon^{(i)}$	Shear strain and axial strain of the (i) th lamina (i) = f reinforced layer (i) = m matrix layer
γ	Ratio of shear modulus
η	Nondimensional ratio of thicknesses of reinforced layer and the total thickness of the unit cell
η_i	Generalized coordinate of the (i) th lamina
$\bar{\eta}$	Nondimensional y-component of wave number
θ	Ratio of mass densities
$\lambda_1, \lambda_2, \lambda_3$	Lagrangian multiplier
Λ	Wavelength
μ	Shear Modulus, Lamé's constant
ν	Poisson's ratio
$\rho^{(i)}$	Density of (i) th lamina (i) = f : reinforcing layer (i) = m ; matrix layer
$\sigma^{(i)}$	Stresses of the (i) th lamina
τ_i	Nodal shear stress parallel to x-y plane at i th node

σ_i	Nodal normal stress parallel to y-axis at i^{th} node
τ_i	Nodal shear stress parallel to y-z plane at i^{th} node
ω	Frequency
Ω	Normalized nondimensional frequency

CHAPTER 1

INTRODUCTION

1.1 LITERATURE REVIEW

The increasing use of composite materials like fibre-reinforced composite and graphite-epoxy composite in a variety of structural applications has generated extensive research efforts in the area of dynamic behaviour of periodically laminated media. In the past two decades, various approximate theories and exact solutions for wave propagation in the laminated media have been proposed.

The early approximate theory was made by specifying the behaviour of the plate through its thickness. The most common of which is the Love-Kirchhoff hypothesis [1, 2, 3]. But, when the material properties differ appreciably from layer to layer and/or when a high degree of orthotropy exists in one or more layers, the validity of these theories was found to be questionable [4]. To improve these approximate theories, the effect of transverse shear deformation has been included. This approach produced satisfactory results for the static analysis of thick laminates [5]. Later, Nelson and Lorch [6] introduced a refined theory that includes transverse shear, transverse normal and quadratic terms in the kinematic assumption.

Postma [7], Rytov [8], and White and Angona [9] then developed the effective modulus theory on the basis of both static and dynamic consideration. This is the approximate elasticity solutions in which attempts were made to bridge the gap between the approximate plate theories and the general theory of elasticity formulations, by smoothing and averaging procedures on special laminates with periodic structure

through thickness. However, this method does not account for the effects of the geometric dispersion. Therefore, an effective stiffness method was proposed by Sun, Achenbach and Herrmann [10, 11, 12]. This method was then developed in more detail by other investigators [13, 14, 15].

Other approximate approaches that have been used extensively are the mixture theory [16, 17, 18], the theory of interacting continuum [19, 20], and the new quotient method [21, 22]. Recently, Mengi et al [23] used higher order plate theory together with a smoothing operation to study the dispersion characteristic of two-layer periodic laminated media.

In addition to the approximate analysis mentioned above, exact solutions for wave propagating in laminated media have also been presented in the literature. Most actual analyses are based on two-dimensional equations where each laminate is isotropic. The antiplane [24-26] and plane strain [27] problems have been dealt with by imposing the displacement and stress continuity conditions at the interfaces. Recently, Delph et al. [28-30] have done extensive work in using Floquet's theory in conjunction with the elasticity solution to analyse the dispersion characteristic for harmonic wave propagation through laminated media. Dispersion relations for laminated composites in a three-dimensional setting have been obtained by Kulkarni and Pagano [31], where the solution for vibration frequencies for cylindrical bending has been presented. Yamada and Nemat-Nasser [32] have also examined the dispersive effects in layered orthotropic elastic composites, where the direction of the corresponding harmonic waves makes an arbitrary angle with respect to the layers.

In most of the analysis mentioned above, the laminae were assumed to be isotropic. The most recent work was done by Shah and Datta [33] in which the finite element method is presented for studying harmonic wave propagation in a periodically laminated medium, where each lamina may have anisotropic properties. However, in their work, antiplane and plane strain motions are dealt with separately. The method used is discussed in detail in Ref. [33].

1.2 PRESENT SCOPE

In this thesis, the finite element method or stiffness method proposed by Shah and Datta [33], for the antiplane and plane strain motions, is extended to three-dimensional problems. The method and formulation technique used is discussed in Chapter 2. In order to assess the accuracy of this method, numerical results are first compared with the results obtained by the effective modulus [7] and effective stiffness methods [11]. But first of all, the effective modulus and effective stiffness method have to be extended to handle a three dimensional analysis for anisotropic materials. These will be discussed and formulated in Chapter 3. Numerical results are then presented for fiber-reinforced composite and graphite-epoxy composite with different layer thicknesses. The computer programs used to assist the numerical computation are listed in Appendix H, I and J. The first computer program is written for the three dimensional analysis of wave propagation through laminated layers using the effective modulus method. The second is for an effective stiffness analysis while Appendix J is the computer program written to solve the same problem using the finite element method.

CHAPTER 2

HARMONIC WAVES IN A PERIODICALLY LAMINATED MEDIUM:

FINITE ELEMENT METHODS (F.E.M.)

2.1 INTRODUCTION

In this chapter, the behaviour of harmonic waves propagating in a periodically layered, infinite, elastic body is examined. In most previous studies on the similar subject mentioned in Chapter 1, each lamina was assumed to be isotropic. However, in order to be more general, the present analysis will deal with three dimensional, anisotropic lamina. In this method, an interpolation function is assumed for each lamina which is characterized by a discrete number of generalized coordinates at the interfaces. These generalized coordinates are the interface displacements and stresses, thus ensuring the continuity of these quantities across the boundary planes. By applying Hamilton's principle [34] and using Floquet's theory [35], the dispersion equation is obtained. The solutions of this equation yield the frequency-wave-number relationships. In the following, the method will be discussed in detail.

2.2. EQUATION OF LINEAR ELASTICITY

In the following, harmonic waves propagating through a periodically layered, elastic body of unbounded extent is considered. For the purpose of this discussion, a two-layered periodically laminated elastic body, as shown in Fig.2.1, is considered though the method presented can be applied to any number of periodicity. Any two adjacent laminae in the body then compose a unit cell. Both laminae in the unit cell are assumed to be homogeneous, orthorhombic and perfectly bonded to contiguous

layers. The two laminae of a typical unit cell, C_n , as shown in Fig. 2.1, have elastic constants $(C_{11}^{(i)}, C_{12}^{(i)}, C_{13}^{(i)}, C_{22}^{(i)}, C_{23}^{(i)}, C_{33}^{(i)}, C_{44}^{(i)}, C_{55}^{(i)}, C_{66}^{(i)})$; $(C_{11}^{(i+1)}, C_{12}^{(i+1)}, C_{13}^{(i+1)}, C_{22}^{(i+1)}, C_{23}^{(i+1)}, C_{33}^{(i+1)}, C_{44}^{(i+1)}, C_{55}^{(i+1)}, C_{66}^{(i+1)})$, thickness $(2 h^{(i)}, 2 h^{(i+1)})$ and densities $(\rho^{(i)}, \rho^{(i+1)})$, respectively. For a particular lamina, the relevant stress-strain relations are

$$\begin{Bmatrix} \sigma_{xx}^{(i)} \\ \sigma_{yy}^{(i)} \\ \sigma_{zz}^{(i)} \\ \sigma_{yz}^{(i)} \\ \sigma_{xz}^{(i)} \\ \sigma_{xy}^{(i)} \end{Bmatrix} = \begin{bmatrix} C_{11}^{(i)} & C_{12}^{(i)} & C_{13}^{(i)} & 0 & 0 & 0 \\ C_{12}^{(i)} & C_{22}^{(i)} & C_{23}^{(i)} & 0 & 0 & 0 \\ C_{13}^{(i)} & C_{23}^{(i)} & C_{33}^{(i)} & 0 & 0 & 0 \\ 0 & 0 & 0 & C_{44}^{(i)} & 0 & 0 \\ 0 & 0 & 0 & 0 & C_{55}^{(i)} & 0 \\ 0 & 0 & 0 & 0 & 0 & C_{66}^{(i)} \end{bmatrix} \begin{Bmatrix} \epsilon_{xx}^{(i)} \\ \epsilon_{yy}^{(i)} \\ \epsilon_{zz}^{(i)} \\ \gamma_{yz}^{(i)} \\ \gamma_{xz}^{(i)} \\ \gamma_{xy}^{(i)} \end{Bmatrix} \quad (2.1)$$

where $\sigma_{mn}^{(i)}$ represent the stress and $\epsilon_{mn}^{(i)}, \gamma_{mn}^{(i)}$ represent the strain of the I^{th} (superscript (i)) lamina.

Let $U_I(x_i, y_i, z_i, t)$, $V_I(x_i, y_i, z_i, t)$ and $W_I(x_i, y_i, z_i, t)$ be the Cartesian components of the displacement in the x, y and z directions respectively, for the I^{th} lamina. The strain components in the $(i)^{\text{th}}$ lamina can then be expressed as

$$\begin{aligned} \epsilon_{xx}^{(i)} &= \frac{\partial U_I}{\partial x_i} & \epsilon_{yy}^{(i)} &= \frac{\partial V_I}{\partial y_i} & \epsilon_{zz}^{(i)} &= \frac{\partial W_I}{\partial z_i} \\ \gamma_{yz}^{(i)} &= \left(\frac{\partial W_I}{\partial y_i} + \frac{\partial V_I}{\partial z_i} \right) & \gamma_{xz}^{(i)} &= \left(\frac{\partial W_I}{\partial x_i} + \frac{\partial U_I}{\partial z_i} \right) & \gamma_{xy}^{(i)} &= \left(\frac{\partial V_I}{\partial x_i} + \frac{\partial U_I}{\partial y_i} \right) \end{aligned} \quad (2.2)$$

Substituting Eqs. 2.2 into Eqs. 2.1, the stress-displacement relationships may be obtained. Substitution of these stress-displacement relationships into the stress equations of motion leads to Navier's equation of motion [36]. The solution to these Navier equations give the displacement and stresses in each lamina. At present, no analytical solutions to these Navier's equations are available. Thus, in this thesis, a finite element method is proposed to solve the problem.

2.3 TRACTION AND DISPLACEMENT CONTINUITY

For a two-layered periodically laminated elastic body, the continuities of traction and displacement at the interface between two consecutive lamina (1) and (2), and (2) and (3) are:

$$\begin{aligned}
 U_2(x_2, -h^{(2)}, z_2, t) &= U_1(x_1, h^{(1)}, z_1, t) \\
 V_2(x_2, -h^{(2)}, z_2, t) &= V_1(x_1, h^{(1)}, z_1, t) \\
 W_2(x_2, -h^{(2)}, z_2, t) &= W_1(x_1, h^{(1)}, z_1, t) \\
 \sigma_{yx}^{(2)}(x_2, -h^{(2)}, z_2, t) &= \sigma_{yx}^{(1)}(x_1, h^{(1)}, z_1, t) \\
 \sigma_{yy}^{(2)}(x_2, -h^{(2)}, z_2, t) &= \sigma_{yy}^{(1)}(x_1, h^{(1)}, z_1, t) \\
 \sigma_{yz}^{(2)}(x_2, -h^{(2)}, z_2, t) &= \sigma_{yz}^{(1)}(x_1, h^{(1)}, z_1, t)
 \end{aligned} \tag{2.3}$$

and

$$\begin{aligned}
 U_2(x_2, h^{(2)}, z_2, t) &= U_3(x_3, -h^{(1)}, z_3, t) \\
 V_2(x_2, h^{(2)}, z_2, t) &= V_3(x_3, -h^{(1)}, z_3, t) \\
 W_2(x_2, h^{(2)}, z_2, t) &= W_3(x_3, -h^{(1)}, z_3, t) \\
 \sigma_{yx}^{(2)}(x_2, h^{(2)}, z_2, t) &= \sigma_{yx}^{(3)}(x_3, -h^{(1)}, z_3, t)
 \end{aligned}$$

$$\begin{aligned}\sigma_{yy}^{(2)}(x_2, h^{(2)}, z_2, t) &= \sigma_{yy}^{(3)}(x_3, -h^{(1)}, z_3, t) \\ \sigma_{yz}^{(2)}(x_2, h^{(2)}, z_2, t) &= \sigma_{yz}^{(3)}(x_3, -h^{(1)}, z_3, t)\end{aligned}\quad (2.4)$$

Using Floquet's theory [35], Eqs. 2.4 can be rewritten as

$$\begin{aligned}U_2(x_2, h^{(2)}, z_2, t) &= U_1(x_1, -h^{(1)}, z_1, t) e^{ik_y d} \\ V_2(x_2, h^{(2)}, z_2, t) &= V_1(x_1, -h^{(1)}, z_1, t) e^{ik_y d} \\ W_2(x_2, h^{(2)}, z_2, t) &= W_1(x_1, -h^{(1)}, z_1, t) e^{ik_y d} \\ \sigma_{yx}^{(2)}(x_2, h^{(2)}, z_2, t) &= \sigma_{yx}^{(1)}(x_1, -h^{(1)}, z_1, t) e^{ik_y d} \\ \sigma_{yy}^{(2)}(x_2, h^{(2)}, z_2, t) &= \sigma_{yy}^{(1)}(x_1, -h^{(1)}, z_1, t) e^{ik_y d} \\ \sigma_{yz}^{(2)}(x_2, h^{(2)}, z_2, t) &= \sigma_{yz}^{(1)}(x_1, -h^{(1)}, z_1, t) e^{ik_y d}\end{aligned}\quad (2.5)$$

where k_y is the Floquet wave number in the y-direction and

$$d = 2(h^{(1)} + h^{(2)})$$

By writing the equations in this form, the stresses and displacements at the interface of two consecutive laminae are automatically satisfied.

The dispersion equation for harmonic-wave propagation is obtained by using Eqs. 2.3 and 2.5. For two dimensional isotropic laminates, Delph, Herrmann, and Kaul [29, 30] used exact solutions to Navier's equations of motion together with continuity conditions and Floquet's theory equation (2.3) and (2.5) to obtain the exact dispersion relationship. For two dimensional anisotropic laminates, Shah and Datta [33] proposed an approximate method by expressing the displacement components in each lamina in terms of interpolation functions and then employed Eqs. 2.3 and 2.5 to obtain the approximate dispersion relationship. For three dimensional analysis, Yamada and Nemat-Nasser [32] proposed an

approximate analysis and an approximate method called the new quotient method for waves propagating through a layered orthotropic elastic composite. In this thesis, the approach by Shah and Datta [33] has been adopted and extended to three dimensional analysis. This method is chosen because of its simplicity and accuracy in the two-dimensional analysis.

2.4 DISPLACEMENT EQUATIONS

In this three dimensional analysis to obtain the approximate dispersion equations, the displacements have to be defined first. The displacement components in each lamina are expressed in terms of interpolation functions as

$$\begin{Bmatrix} U_I \\ V_I \\ W_I \end{Bmatrix} = \bar{E} \begin{bmatrix} u_i & u_j & \frac{\chi_i}{c_{66}^{(i)}} - \frac{\partial v_i}{\partial x} & \frac{\chi_j}{c_{66}^{(i)}} - \frac{\partial v_j}{\partial x} \\ v_i & v_j & \frac{1}{c_{22}^{(i)}} \left\{ \sigma_i - c_{12}^{(i)} \frac{\partial u_i}{\partial x} - c_{23}^{(i)} \frac{\partial w_i}{\partial z} \right\} & \frac{1}{c_{22}^{(i)}} \left\{ \sigma_j - c_{12}^{(i)} \frac{\partial u_j}{\partial x} - c_{23}^{(i)} \frac{\partial w_j}{\partial z} \right\} \\ w_i & w_j & \frac{\tau_i}{c_{44}^{(i)}} - \frac{\partial v_i}{\partial z} & \frac{\tau_j}{c_{44}^{(i)}} - \frac{\partial v_j}{\partial z} \end{bmatrix} \begin{Bmatrix} f_1(\eta_i) \\ f_2(\eta_i) \\ f_3(\eta_i) \\ f_4(\eta_i) \end{Bmatrix} \quad (2.6)$$

where $j = i + 1$, $\bar{E} = e^{i(k_x x + k_z z - \omega t)}$

$$f_1(\eta_i) = \frac{1}{4} (2 - 3 \eta_i + \eta_i^3)$$

$$f_2(\eta_i) = \frac{1}{4} (2 + 3 \eta_i - \eta_i^3)$$

$$f_3(\eta_i) = \frac{h^{(i)}}{4} (1 - \eta_i - \eta_i^2 + \eta_i^3)$$

$$f_4(\eta_i) = \frac{h^{(i)}}{4} (-1 - \eta_i + \eta_i^2 + \eta_i^3) \text{ in which } \eta_i = y_i / h^{(i)} \text{ is the natural coordinate}$$

$u_i, v_i, w_i, \chi_i, \sigma_i$ and τ_i are the i^{th} nodal value given

$$\text{by } \{u_i, \chi_i, v_i, \sigma_i, w_i, \tau_i\}^T = \{U_I, \sigma_{yx}^{(i)}, V_I, \sigma_{yy}^{(i)}, W_I, \sigma_{yz}^{(i)}\}^T_{y_i = -h_i^{(i)}}$$

Similarly, $\{u_j, \chi_j, v_j, \sigma_j, w_j, \tau_j\}^T = \{U_I, \sigma_{yx}^{(i)}, V_I, \sigma_{yy}^{(i)}, W_I, \sigma_{yz}^{(i)}\}_{y_i=h}^{(i)}$

k_x, k_z are the wave numbers in the x and z directions respectively where

$k_x = \frac{2\pi}{\Lambda_x}, k_z = \frac{2\pi}{\Lambda_z}$. Λ_x, Λ_z , are the wavelengths in the x and z directions,

respectively, and ω is the circular frequency. Superscript T denotes a transpose.

The interpolation function $f_m(\eta_i)$ is chosen in order to satisfy the stress and displacement continuity at the interface.

The complete derivation of Eqs. 2.6 is given in Appendix A. In Eqs. 2.6, if the z-component of the displacement is suppressed, the problem is reduced to a two dimensional plane-strain problem similar to that outlined in [33].

2.5 FORMULATION OF ELEMENTAL STIFFNESS AND MASS MATRICES

The potential energy and kinetic energy [34] for the (i)th lamina are

$$V_{\text{pot}}^{(i)} = \frac{1}{2} \int_0^{\Lambda_z} \int_0^{\Lambda_x} \int_{-h}^{h(i)} \{ \sigma_{xx} \bar{\epsilon}_{xx} + \sigma_{yy} \bar{\epsilon}_{yy} + \sigma_{zz} \bar{\epsilon}_{zz} + \sigma_{yz} \bar{\gamma}_{yz} + \sigma_{xz} \bar{\gamma}_{xz} + \sigma_{xy} \bar{\gamma}_{xy} \} dy dx dz$$

$$T_{\text{kin}}^{(i)} = \frac{\omega^2}{2} \int_0^{\Lambda_z} \int_0^{\Lambda_x} \int_{-h}^{h(i)} \rho^{(i)} \{ U_I \bar{U}_I + V_I \bar{V}_I + W_I \bar{W}_I \} dy dx dz \quad (2.7)$$

where a bar over a quantity designates the complex conjugate.

Using the assumed displacement (2.6) and substituting it into the potential and kinetic energy expression, equations (2.7), lead to the forms given in matrix notation as

$$V_{\text{pot}}^{(i)} = \frac{1}{2} \{\bar{r}_i\}^T [k_i] \{r_i\}$$

$$T_{\text{kin}}^{(i)} = \frac{\omega^2}{2} \{\bar{r}_i\}^T [m_i] \{r_i\} \quad (2.8)$$

where $\{r_i\}^T = \{u_i, \chi_i, v_i, \sigma_i, w_i, \tau_i, u_j, \chi_j, v_j, \sigma_j, w_j, \tau_j\}^T$
 and $[k_i]$ and $[m_i]$ are the stiffness and mass matrices of the (i)th
 lamina.

The long hand expression for $(V_{\text{pot}}^{(i)} - T_{\text{kin}}^{(i)})$ can be obtained by substituting the stress-strain relationship, which are functions of the nodal values, into Eqs. 2.7. This expression is shown as:

$$\begin{aligned}
 V_{\text{pot}}^{(i)} - T_{\text{kin}}^{(i)} = & \frac{\Lambda_x \Lambda_z}{2} \{C_{11}^{(i)} k_x^2 h^{(i)} \int_{-1}^1 U_I \bar{U}_I d\eta_i + C_{12}^{(i)} ik_x \int_{-1}^1 (U_I \bar{V}'_I - V_I \bar{U}'_I) d\eta_i \\
 & + C_{13}^{(i)} h^{(i)} k_x k_z \int_{-1}^1 (W_I \bar{U}_I + U_I \bar{W}_I) d\eta_i + \frac{C_{22}^{(i)}}{h^{(i)}} \int_{-1}^1 V_I \bar{V}'_I d\eta_i \\
 & + C_{23}^{(i)} ik_z \int_{-1}^1 (W_I \bar{V}'_I - V_I \bar{W}_I) d\eta_i + C_{33}^{(i)} k_z^2 h^{(i)} \int_{-1}^1 W_I \bar{W}_I d\eta_i \\
 & + \frac{C_{44}^{(i)}}{h^{(i)}} \int_{-1}^1 W_I \bar{W}'_I d\eta_i + C_{44}^{(i)} ik_z \int_{-1}^1 (V_I \bar{W}'_I - W_I \bar{V}'_I) d\eta_i \\
 & + C_{44}^{(i)} k_z^2 h^{(i)} \int_{-1}^1 V_I \bar{V}_I d\eta_i + C_{55}^{(i)} h^{(i)} k_x^2 \int_{-1}^1 W_I \bar{W}_I d\eta_i \\
 & + C_{55}^{(i)} h^{(i)} k_x k_z \int_{-1}^1 (W_I \bar{U}_I + U_I \bar{W}_I) d\eta_i + C_{55}^{(i)} k_z^2 h^{(i)} \int_{-1}^1 U_I \bar{U}_I d\eta_i \\
 & + C_{66}^{(i)} h^{(i)} k_x^2 \int_{-1}^1 V_I \bar{V}_I d\eta_i + C_{66}^{(i)} ik_x \int_{-1}^1 (V_I \bar{U}'_I - U_I \bar{V}'_I) d\eta_i \\
 & + \frac{C_{66}^{(i)}}{h^{(i)}} \int_{-1}^1 U_I \bar{U}'_I d\eta_i - \rho_i h^{(i)} \omega^2 \int_{-1}^1 U_I \bar{U}_I d\eta_i \\
 & - \rho_i h^{(i)} \omega^2 \int_{-1}^1 V_I \bar{V}_I d\eta_i - \rho_i h^{(i)} \omega^2 \int_{-1}^1 W_I \bar{W}_I d\eta_i
 \end{aligned}$$

in which η_i is the natural coordinate.

$$i = \sqrt{-1}$$

and the prime denotes the differentiation with respect to η_i .

The evaluations of the integrals of Eq. 2.10 are shown in Appendix B and Appendix C.

Making use of Eqs. 2.8, the expression (2.10) can be rewritten as

$$\begin{aligned} (V_{\text{pot}}^{(i)} - T_{\text{kin}}^{(i)}) &= \frac{1}{2} \{\bar{r}_i\}^T \{[k_i] - \omega^2 [m_i]\} \{r_i\} \\ &= \frac{1}{2} \{\bar{r}_i\}^T [S^a] \{r_i\} \end{aligned} \quad (2.11)$$

where the impedance matrix $[S^a]$ is Hermitian.

2.6 GENERATION OF EIGENVALUE AND EIGENVECTOR PROBLEMS

Consider an m-layer periodicity. Floquet's relationship (2.5) can be written as

$$\begin{aligned} &\{u_{m+1}, \chi_{m+1}, v_{m+1}, \sigma_{m+1}, w_{m+1}, \tau_{m+1}, u_{m+2}, \chi_{m+2}, v_{m+2}, \tau_{m+2}, w_{m+2}, \tau_{m+2}\}^T \\ &= \{u_1, \chi_1, v_1, \sigma_1, w_1, \tau_1, u_2, \chi_2, v_2, \sigma_2, w_2, \tau_2\}^T e^{ik_y d} \\ &\text{where } d = \sum_{i=1}^m 2 h^{(i)} \end{aligned} \quad (2.12)$$

By applying Hamilton's Principle to (2.11) and then utilizing Floquet's relation (2.12), the equilibrium equations for nodes 1 to m can be written. After rearranging terms, these equations yield the dispersion relation as an algebraic eigenvector problem,

$$[A_3] \{R_3\} = \omega^2 [B_3] \{R_3\} \quad (2.13)$$

where $\{R_3\}^T = \{u_1, \chi_1, v_1, \sigma_1, w_1, \tau_1, u_2, \chi_2, \dots, w_m, \tau_m\}^T$

and $[A_3]$ and $[B_3]$ are $6m \times 6m$ matrices with complex-valued polynomial elements which are functions of material and geometric properties, wave number k_x , k_y and k_z and frequency ω .

The roots of the dispersion relation

$$\det \left| [A_3] - \omega^2 [B_3] \right| \quad (2.14)$$

define a surface in frequency-wave-number space which is generally discontinuous at $k_y = \frac{n\pi}{d}$, $n = 1, 2, \dots$. The assembly process of Eq. 2.14 is outlined in Appendix D using the form of an impedance matrix. A detailed discussion of the dispersion surface has been reported by Delph, Harrmann, and Kaul [28, 30]. It has also been shown by Shah and Datta [33] that, for a two dimensional analysis, the numerical results obtained by this finite element method are in close agreement with the exact solution for isotropic laminates. In this study numerical results are presented for three dimensional analysis on boron-aluminium composites and graphite-epoxy composites. Attention is focused on the lowest three branches (SH, SV, and P) of the dispersion curve for real wave number k ($k = \frac{2\pi}{\lambda}$). The reason for concentrating on the lowest 3 branches is that for a structural dynamic problem, it is the lower frequencies that cause the most severe problems. SH is the lowest out of plane mode, SV is the lowest transverse mode and P is the lowest longitudinal mode propagating in any arbitrary direction through the lamina. SH, SV and P modes of the dispersion curve are defined in the following section.

2.7 ANTIPLANE AND PLANE STRAIN MOTIONS

The derivation of the dispersion relation in this Chapter is for the general three-dimensional case. However, with a simple modification, the dispersion relations for antiplane and plane strain motions can be obtained. The method of obtaining these dispersion relations will be discussed in the following.

2.7.1 ANTIPLANE STRAIN

For the antiplane motion, the equation of displacement is given as

$$W_I(x_i, y_i, 0, t) = \{f_1(\eta_i) w_i + f_2(\eta_i) w_j + f_3(\eta_i) \frac{\tau_i}{C_{44}^{(i)}} + f_4(\eta_i) \frac{\tau_j}{C_{44}^{(i)}}\} e^{i(k_x x - \omega t)} \quad (2.15a)$$

where $f_m(\eta_i)$, k_x, ω are defined in Eq. 2.6

$$w_i = W_I(x_i, -h^{(i)}, 0); \quad w_j = W_I(x_i, h^{(i)}, 0) \quad (2.15b)$$

$$\tau_i = \sigma_{yz}^{(i)}(x_i, -h^{(i)}, 0); \quad \tau_j = \sigma_{yz}^{(i)}(x_i, h^{(i)}, 0) \text{ at a particular time } t.$$

Eq. 2.15b is obtained by substituting the conditions

$U_I = V_I = \sigma_{yx}^{(i)} = \sigma_{yy}^{(i)} = 0.0$ into Eq. 2.6. Then, the potential energy and kinetic energy for the (i)th lamina are obtained by integrating over both the lamina thickness and the wavelength Λ .

$$V_{\text{pot}}^{(i)} = \frac{1}{2} \int_0^\Lambda \int_{-h^{(i)}}^{h^{(i)}} [C_{44}^{(i)} \gamma_{yz}^{(i)} \bar{\gamma}_{yz}^{(i)} + C_{55}^{(i)} \gamma_{xz}^{(i)} \bar{\gamma}_{xz}^{(i)}] dx_i dy_i$$

$$T_{\text{kin}}^{(i)} = \frac{\omega^2}{2} \int_0^\Lambda \int_{-h^{(i)}}^{h^{(i)}} \rho^{(i)} W_I \bar{W}_I dx_i dy_i \quad (2.16)$$

After differentiating the assumed displacement field, its substitution into the potential and kinetic energy expression leads to forms given in matrix notation by

$$V_{\text{pot}}^{(i)} = \frac{1}{2} \{\bar{r}_1\}^T [k_1] \{r_1\}$$

$$T_{\text{kin}}^{(i)} = \frac{1}{2} \{\bar{r}_1\}^T [m_1] \{r_1\} \quad (2.17)$$

where $\{r_1\}^T = \{w_i, \tau_i, w_j, \tau_j\}^T$

$[k_1]$ and $[m_1]$ are the stiffness and mass matrices of the lamina.

If m-layer periodicity is considered, Floquet's relation Eq. 2.5 can be written as,

$$\{w_{m+1} \tau_{m+1} w_{m+2} \tau_{m+2}\}^T = \{w_1 \tau_1 w_2 \tau_2\}^T e^{ik_y d} \quad (2.18)$$

where $d = \sum_{i=1}^m 2 h^{(i)}$

By applying Hamilton's Principle and using Floquet's relation, the equilibrium equations for the nodes can be written. These equations yield the dispersion relation as an algebraic eigenvalue problem as in Eq. 2.13. However, for this case,

$$\{R_1\} = \{w_1, \tau_1, \dots, w_m, \tau_m\}^T$$

and [A], and [B] are $2m \times 2m$ matrices.

The lowest frequency obtained by solving the dispersion relation $\det [A_1] - \omega^2 [B_1] = 0$

is the frequency of the lowest SH mode of the propagating waves.

2.7.2 Plane Strain

Similarly, the dispersion relations for plane strain motion can be obtained by substituting the conditions

$$W_I = \sigma_{yz}^{(i)} = 0 \text{ into Eq. 2.6}$$

It is given in the form

$$\begin{Bmatrix} U_I \\ V_I \end{Bmatrix} = e^{i(k \cdot x - \omega t)} \begin{bmatrix} u_i & u_j & \frac{\chi_i}{C_{66}^{(i)}} - \frac{\partial v_i}{\partial x_i} & \frac{\chi_j}{C_{66}^{(i)}} - \frac{\partial v_j}{\partial x_i} \\ v_i & v_j & -\frac{C_{12}^{(i)}}{C_{22}^{(i)}} \frac{\partial u_i}{\partial x_i} + \frac{\sigma_i}{C_{22}^{(i)}} & -\frac{C_{12}^{(i)}}{C_{22}^{(i)}} \frac{\partial u_j}{\partial x_i} + \frac{\sigma_j}{C_{22}^{(i)}} \end{bmatrix} \begin{Bmatrix} f_1(\eta_i) \\ f_2(\eta_i) \\ f_3(\eta_i) \\ f_4(\eta_i) \end{Bmatrix}$$

where $u_i, v_i, \chi_i, \sigma_i$ are defined in Eq. 2.6

The potential energy and kinetic energy for (i)th lamina become

$$V_{\text{pot}}^{(i)} = \frac{1}{2} \int_0^{\Lambda} \int_{-h^{(i)}}^{h^{(i)}} [\sigma_{xx} \bar{\epsilon}_{xx}^{(i)} + \sigma_{yy} \bar{\epsilon}_{yy}^{(i)} + \sigma_{xy} \bar{\gamma}_{xy}^{(i)}] dx_i dy_i$$

$$T_{\text{kin}}^{(i)} = \frac{\omega^2}{2} \int_0^{\Lambda} \int_{-h^{(i)}}^{h^{(i)}} \rho^{(i)} [U_I \bar{U}_I + V_I \bar{V}_I] dx_i dy_i \quad (2.20)$$

Following the same step as in 2.7.1, after differentiating the assumed displacement field and substituting it into the potential and kinematic energy expression, the form obtained is

$$V_{\text{pot}}^{(i)} = \frac{1}{2} \{\bar{r}_2\}^T [k_2] \{r_2\}$$

$$T_{\text{kin}}^{(i)} = \frac{1}{2} \{\bar{r}_2\}^T [m_2] \{r_2\} \quad (2.21)$$

where $\{r_2\}^T = \{u_1, \chi_1, v_1, \sigma_1, u_j, \chi_j, v_j, \sigma_j\}^T$

The $[k_2]$ and $[m_2]$ are the stiffness and mass matrices.

Similarly, by applying Hamilton's Principle and Floquet's relation to a m-layer periodicity lamina, the dispersion relation can be obtained as

$$[A_2] \{R_2\} = \omega^2 [B_2] \{R_2\} \quad (2.22)$$

where $\{R_2\}^T = \{u_1, \chi_1, \dots, v_m, \sigma_m\}^T$

and $[A_2]$ and $[B_2]$ are 4 m x 4 m matrices.

When $k_x = 0$, the dispersion equation (2.22) yields 2(2 m x 2 m) equations. One of these equations is the dispersion equation for longitudinal (P) waves propagating in the direction of propagating waves, while the other is for shear (SV) waves propagating normal to the direction of propagating waves.

The dispersion relation for plane strain and antiplane strain motion, derived above by inputting the proper conditions into Eq. 2.6, is the same as that derived by Shah and Datta [33].

CHAPTER 3

OTHER THEORIES ON WAVE PROPAGATION IN A STRATIFIED MEDIUM

3.1 INTRODUCTION

The practical importance of laminated and fiber reinforced composites has stimulated many analytical studies of these materials. For this kind of laminated medium, Postma [7], Rytov [8] and White and Angona [9] have computed the effective elastic constants on the basis of both static and dynamic consideration. However, it was shown in [11] that this effective modulus theory has limited applicability for wave propagation in practical laminates where ratio of layer stiffness is high. (Shear modulus of reinforced layer/shear modulus of matrix layer = 50) Sun, Achenbach and Herrmann [11, 12, 13] then proposed the effective stiffness theory. These two theories are based on a two-dimensional analysis performed on a stratified medium consisting of alternating plane, parallel layers of two homogeneous isotropic materials.

In this chapter, these two theories will be extended to accommodate a three dimensional analysis on the medium that consists of either isotropic or anisotropic materials. The governing dispersion equations for these two theories will be derived based on Postma's [7] presentation and Sun et al's [11] continuum theory. The results obtained by using these theories will be compared with those produced from the finite element method.

3.2 EFFECTIVE MODULUS METHOD

The customary approach in constructing a theory to describe the mechanical behaviour of a laminated composite consists of replacing the

composite by a homogeneous and isotropic medium whose material constants are determined in terms of the geometry and the material properties of the constituents of the composite. Theories of this type are termed "effective modulus theories". In the following discussion, Postma's [7] approach is followed closely but his approach is extended to a three dimensional case with either isotropic or anisotropic laminae.

3.2.1 Stress-Strain Relationship

Fig. 3.1 shows a typical laminated medium. For the purpose of this discussion, a layered structure consisting of alternating plane, parallel layers of materials which can be regarded as anisotropic, is considered. Supposing Hooke's law is valid, it can be expressed in matrix form as

$$\{\sigma\} = [C] \{\gamma\} \quad (3.1)$$

where

$$\{\sigma\}^T = \langle \sigma_{xx} \quad \sigma_{yy} \quad \sigma_{zz} \quad \sigma_{yz} \quad \sigma_{xz} \quad \sigma_{xy} \quad \rangle$$

$$\{\gamma\}^T = \langle \epsilon_{xx} \quad \epsilon_{yy} \quad \epsilon_{zz} \quad \gamma_{yz} \quad \gamma_{xz} \quad \gamma_{xy} \quad \rangle$$

σ_{xx} means the normal component of the traction across a surface element perpendicular to the x-axis etc.

σ_{yz} = the tangential component parallel to the y-axis of the traction across a surface element perpendicular to the z-axis, etc.

and ϵ_{xx} = linear dilatation of line elements in the direction of the x-axis in the unstrained state

γ_{yz} = decrease in angle between two line elements which are parallel to the y and z axes in the unstrained state

[C] is the coefficient matrix consisting of material constants.

It is clear that Eq. 3.1 is the same as Eq. 2.1. If U, V and W are the cartesian components of the displacement, the strain-displacement relationship shown in Eq. 2.2 also holds for this case.

Consider now a stratified medium consisting of a large number of alternating plane, parallel layers of two homogeneous anisotropic materials for which their elastic constants are $(C_{11}^{(1)}, C_{12}^{(1)}, C_{13}^{(1)}, C_{22}^{(1)}, C_{23}^{(1)}, C_{33}^{(1)}, C_{44}^{(1)}, C_{55}^{(1)}, C_{66}^{(1)})$; $(C_{11}^{(2)}, C_{12}^{(2)}, C_{13}^{(2)}, C_{22}^{(2)}, C_{23}^{(2)}, C_{33}^{(2)}, C_{44}^{(2)}, C_{55}^{(2)}, C_{66}^{(2)})$ respectively. The layer thickness and density for the first material is d_1 and $\rho^{(1)}$; for the second it is d_2 and $\rho^{(2)}$. Comparing d_1 and d_2 with that defined in Chapter 2, $d_1 = 2 h^{(1)}$; $d_2 = 2 h^{(2)}$. With the coordinate axes shown in Fig. 3.1 and consider an elementary rectangular parallelepiped with faces parallel to the coordinate planes, let the height of the parallelepiped be $n(d_1 + d_2)$ where n is an integer, and let the length and width be L and B respectively. To simplify the problem, the following calculations are based on a unit cell, that is $n = 1$.

On the face perpendicular to the y-axis, a traction σ_{yy} such that there are no tangential components σ_{xy} and σ_{zy} is applied. Similarly, on the face perpendicular to the x-axis, only the normal tractions $\sigma_{xx}^{(1)}$ on the layer d_1 and a normal traction $\sigma_{xx}^{(2)}$ on the layer d_2 are present. On the face perpendicular to the z-axis, there will be normal tractions $\sigma_{zz}^{(1)}$ and $\sigma_{zz}^{(2)}$. The normal tractions $\sigma_{xx}^{(1)}, \sigma_{xx}^{(2)}, \sigma_{zz}^{(1)}, \sigma_{zz}^{(2)}$ are such that $\epsilon_{xx}^{(1)} = \epsilon_{xx}^{(2)} = \epsilon_{xx}$ and $\epsilon_{zz}^{(1)} = \epsilon_{zz}^{(2)} = \epsilon_{zz}$ where $\epsilon_{xx}^{(1)}$ is the linear dilatation of a linear element in the direction of the x-axis in the layers d_1 , etc. This restriction holds in order to insure the continuity of the displacement as a function of the radius vector. The linear dilatation of a linear element parallel to the y-axis in the d_1 and d_2 layers are

$\epsilon_{yy}^{(1)}$ and $\epsilon_{yy}^{(2)}$ respectively. In general, $\epsilon_{yy}^{(1)}$ is not equal to $\epsilon_{yy}^{(2)}$.

For the first anisotropic medium, Hooke's law gives

$$\begin{aligned}\sigma_{xx}^{(1)} &= C_{11}^{(1)} \epsilon_{xx} + C_{12}^{(1)} \epsilon_{yy}^{(1)} + C_{13}^{(1)} \epsilon_{zz} \\ \sigma_{yy}^{(1)} &= C_{12}^{(1)} \epsilon_{xx} + C_{22}^{(1)} \epsilon_{yy}^{(1)} + C_{23}^{(1)} \epsilon_{zz} \\ \sigma_{zz}^{(1)} &= C_{13}^{(1)} \epsilon_{xx} + C_{23}^{(1)} \epsilon_{yy}^{(1)} + C_{33}^{(1)} \epsilon_{zz}\end{aligned}\quad (3.2a)$$

Hooke's law for the second anisotropic layer is obtained by replacing the superscript (1) of the above equation by a superscript (2) . This set of equations will be designated as (3.2b). If the weighed average tractions on the faces perpendicular to the x-axis and z-axis are considered, they become

$$\begin{aligned}\sigma_{xx} &= \frac{\sigma_{xx}^{(1)} d_1 + \sigma_{xx}^{(2)} d_2}{d_1 + d_2} \\ \sigma_{zz} &= \frac{\sigma_{zz}^{(1)} d_1 + \sigma_{zz}^{(2)} d_2}{d_1 + d_2}\end{aligned}\quad (3.3)$$

While the traction on the face perpendicular to the y-axis remains as

$$\sigma_{yy}.$$

By substituting Eqs. 3.2a and 3.2b into Eq. 3.3, the equation

become:

$$\begin{aligned}(d_1+d_2)\sigma_{xx} &= [d_1 C_{11}^{(1)} + d_2 C_{11}^{(2)}] \epsilon_{xx} + d_1 C_{12}^{(1)} \epsilon_{yy}^{(1)} + d_2 C_{12}^{(2)} \epsilon_{yy}^{(2)} + [d_1 C_{13}^{(1)} + d_2 C_{13}^{(2)}] \epsilon_{zz} \\ (d_1+d_2)\sigma_{yy} &= [d_1 C_{12}^{(1)} + d_2 C_{12}^{(2)}] \epsilon_{xx} + d_1 C_{22}^{(1)} \epsilon_{yy}^{(1)} + d_2 C_{22}^{(2)} \epsilon_{yy}^{(2)} + [d_1 C_{23}^{(1)} + d_2 C_{23}^{(2)}] \epsilon_{zz} \\ (d_1+d_2)\sigma_{zz} &= [d_1 C_{13}^{(1)} + d_2 C_{13}^{(2)}] \epsilon_{xx} + d_1 C_{23}^{(1)} \epsilon_{yy}^{(1)} + d_2 C_{23}^{(2)} \epsilon_{yy}^{(2)} + [d_1 C_{33}^{(1)} + d_2 C_{33}^{(2)}] \epsilon_{zz}\end{aligned}\quad (3.4)$$

If ϵ_{yy} is defined by

$$(d_1 + d_2) \epsilon_{yy} = d_1 \epsilon_{yy}^{(1)} + d_2 \epsilon_{yy}^{(2)} \quad (3.5)$$

then ϵ_{yy} is the overall dilatation of a linear element parallel to the

y-axis, which contains an equal number of sections through the layers d_1 and d_2 .

By substituting Eqs. 3.2a and 3.2b into Eq. 3.5, $\epsilon_{yy}^{(1)}$ and $\epsilon_{yy}^{(2)}$ can be expressed as:

$$\epsilon_{yy}^{(1)} = \frac{[c_{12}^{(2)} - c_{12}^{(1)}]\epsilon_{xx} + (\bar{d} + 1)c_{22}^{(2)}\epsilon_{yy} + [c_{23}^{(2)} - c_{23}^{(1)}]\epsilon_{zz}}{[c_{22}^{(1)} + c_{22}^{(2)}\bar{d}]}$$

$$\epsilon_{yy}^{(2)} = \frac{-\bar{d}[c_{12}^{(2)} - c_{12}^{(1)}]\epsilon_{xx} + (\bar{d} + 1)c_{22}^{(1)}\epsilon_{yy} - \bar{d}[c_{23}^{(2)} - c_{23}^{(1)}]\epsilon_{zz}}{[c_{22}^{(1)} + c_{22}^{(2)}\bar{d}]}$$

in which \bar{d} is defined as $\frac{d_1}{d_2}$ (3.6)

In order to get the relation between the normal stresses and the strains, Eq. 3.6 is substituted into Eq. 3.4 to obtain

$$D \sigma_{xx} = \{[\bar{d}c_{11}^{(1)} + c_{11}^{(2)}][c_{22}^{(1)} + \bar{d}c_{22}^{(2)}] - \bar{d}[c_{12}^{(1)} - c_{12}^{(2)}]^2\}\epsilon_{xx}$$

$$+ (\bar{d} + 1)[\bar{d}c_{12}^{(1)}c_{22}^{(2)} + c_{12}^{(2)}c_{22}^{(1)}]\epsilon_{yy}$$

$$+ \bar{d}[c_{12}^{(1)} - c_{12}^{(2)}][c_{23}^{(2)} - c_{23}^{(1)}] + [c_{22}^{(1)} + \bar{d}c_{22}^{(2)}][\bar{d}c_{13}^{(1)} + c_{13}^{(2)}]\epsilon_{zz}$$

(3.7a)

$$D \sigma_{yy} = \{[c_{22}^{(1)} + \bar{d}c_{22}^{(2)}][\bar{d}c_{12}^{(1)} + c_{12}^{(2)}] + \bar{d}[c_{12}^{(2)} - c_{12}^{(1)}][c_{22}^{(1)} - c_{22}^{(2)}]\}\epsilon_{xx}$$

$$+ (\bar{d} + 1)^2 c_{22}^{(1)} c_{22}^{(2)} \epsilon_{yy}$$

$$+ \{\bar{d}[c_{22}^{(1)} - c_{22}^{(2)}][c_{23}^{(2)} - c_{23}^{(1)}] + [\bar{d}c_{23}^{(1)} + c_{23}^{(2)}][c_{22}^{(1)} + \bar{d}c_{22}^{(2)}]\}\epsilon_{zz}$$

$$D \sigma_{zz} = \{[\bar{d}c_{13}^{(1)} + c_{13}^{(2)}][c_{22}^{(1)} + \bar{d}c_{22}^{(2)}] + \bar{d}[c_{12}^{(2)} - c_{12}^{(1)}][c_{23}^{(1)} - c_{23}^{(2)}]\}\epsilon_{xx}$$

$$+ \{(\bar{d} + 1)[\bar{d}c_{23}^{(1)}c_{22}^{(2)} + c_{23}^{(2)}c_{22}^{(1)}]\}\epsilon_{yy}$$

$$+ \{[\bar{d}c_{33}^{(1)} + c_{33}^{(2)}][c_{22}^{(1)} + \bar{d}c_{22}^{(2)}] - \bar{d}[c_{23}^{(2)} - c_{23}^{(1)}]^2\}\epsilon_{zz}$$

(3.7b)

$$\text{where } D = (\bar{d} + 1) [c_{22}^{(1)} + \bar{d} c_{22}^{(2)}] \quad (3.7c)$$

In the same way, if a tangential traction σ_{xy} is applied to the faces perpendicular to the y-axis as shown in Fig. 3.2, the following is obtained:

$$(d_1 + d_2) \gamma_{xy} = d_1 \gamma_{xy}^{(1)} + d_2 \gamma_{xy}^{(2)}$$

since $\sigma_{xy}^{(1)} = c_{66}^{(1)} \gamma_{xy}^{(1)} = c_{66}^{(2)} \gamma_{xy}^{(2)}$

Therefore, σ_{xy} can be expressed as

$$\sigma_{xy} = \frac{(\bar{d} + 1) c_{66}^{(1)} c_{66}^{(2)}}{\bar{d} c_{66}^{(2)} + c_{66}^{(1)}} \gamma_{xy} \quad (3.8a)$$

Similarly, for the traction σ_{zy} ,

$$\sigma_{zy} = \frac{(\bar{d} + 1) c_{44}^{(1)} c_{44}^{(2)}}{\bar{d} c_{44}^{(2)} + c_{44}^{(1)}} \gamma_{zy} \quad (3.8b)$$

Finally, by applying a tangential force $\sigma_{zx}^{(1)} Ld_1$ to the face perpendicular to the z-axis of the d_1 layer and a tangential force $\sigma_{zx}^{(2)} Ld_2$ to the corresponding face of the d_2 layers and based on the fact that $\gamma_{zx}^{(1)}$ must be equal to $\gamma_{zx}^{(2)}$ in order to insure the continuity of the displacement, it is found that $\sigma_{zx}^{(1)} = c_{55}^{(1)} \gamma_{zx}$; $\sigma_{zx}^{(2)} = c_{55}^{(2)} \gamma_{zx}$. By taking σ_{zx} as the average tangential traction on the parallelepiped, σ_{zx} can be expressed as

$$\sigma_{zx} = \frac{c_{55}^{(1)} \bar{d} + c_{55}^{(2)}}{(\bar{d} + 1)} \gamma_{zx} \quad (3.8c)$$

3.2.2 Effective Elastic Constants

By comparing these results with Eq. 3.1, the static effective elastic constants of the layered composite are found to be:

$$\begin{aligned}
 \bar{c}_{11} &= \frac{[\bar{d}c_{11}^{(1)} + c_{11}^{(2)}] [c_{22}^{(1)} + \bar{d}c_{22}^{(2)}] - \bar{d}[c_{12}^{(1)} - c_{12}^{(2)}]^2}{(1 + \bar{d}) [c_{22}^{(1)} + \bar{d} c_{22}^{(2)}]} \\
 \bar{c}_{12} &= \frac{[c_{22}^{(1)} c_{12}^{(2)} + \bar{d}c_{12}^{(1)} c_{22}^{(2)}]}{c_{22}^{(1)} + \bar{d} c_{22}^{(2)}} \\
 \bar{c}_{13} &= \frac{[\bar{d}c_{13}^{(1)} + c_{13}^{(2)}] [c_{22}^{(1)} + \bar{d}c_{22}^{(2)}] + \bar{d} [c_{12}^{(1)} - c_{12}^{(2)}] [c_{23}^{(2)} - c_{23}^{(1)}]}{(1 + \bar{d}) [c_{22}^{(1)} + \bar{d} c_{22}^{(2)}]} \\
 \bar{c}_{22} &= \frac{(1 + \bar{d}) c_{22}^{(1)} c_{22}^{(2)}}{[c_{22}^{(1)} + \bar{d} c_{22}^{(2)}]} \\
 \bar{c}_{23} &= \frac{\bar{d} c_{23}^{(1)} c_{22}^{(2)} + c_{23}^{(2)} c_{22}^{(1)}}{[c_{22}^{(1)} + \bar{d} c_{23}^{(2)}]} \\
 \bar{c}_{33} &= \frac{[\bar{d}c_{33}^{(1)} + c_{33}^{(2)}] [c_{22}^{(1)} + \bar{d}c_{22}^{(2)}] - \bar{d} [c_{23}^{(1)} - c_{23}^{(2)}]^2}{(1 + \bar{d}) [c_{22}^{(1)} + \bar{d} c_{22}^{(2)}]} \\
 \bar{c}_{44} &= \frac{(1 + \bar{d}) c_{44}^{(1)} c_{44}^{(2)}}{\bar{d} c_{44}^{(2)} + c_{44}^{(1)}} \\
 \bar{c}_{55} &= \frac{c_{55}^{(1)} \bar{d} + c_{55}^{(2)}}{(\bar{d} + 1)} \\
 \bar{c}_{66} &= \frac{(1 + \bar{d}) c_{66}^{(1)} c_{66}^{(2)}}{\bar{d} c_{66}^{(2)} + c_{66}^{(1)}}
 \end{aligned} \tag{3.9}$$

For plane strain problems, Eqs. 3.9 reduce to the form presented by Shah and Datta [37] which is similar to that listed in [7]. This supports the derivation of the effective constants for three dimensional analysis.

3.2.3. Displacement Equations of Motion

The equations of motion for the layered medium are defined as:

$$\begin{aligned} \frac{\partial \sigma_{xx}}{\partial x} + \frac{\partial \sigma_{xy}}{\partial y} + \frac{\partial \sigma_{xz}}{\partial z} &= \rho \frac{\partial^2 U}{\partial t^2} \\ \frac{\partial \sigma_{xy}}{\partial x} + \frac{\partial \sigma_{yy}}{\partial y} + \frac{\partial \sigma_{yz}}{\partial z} &= \rho \frac{\partial^2 V}{\partial t^2} \\ \frac{\partial \sigma_{xz}}{\partial x} + \frac{\partial \sigma_{yz}}{\partial y} + \frac{\partial \sigma_{zz}}{\partial z} &= \rho \frac{\partial^2 W}{\partial t^2} \end{aligned} \quad (3.10)$$

where U, V, and W are the displacement components in the x, y and z direction respectively.

$$\rho = \frac{\rho^{(1)} \bar{d} + \rho^{(2)}}{1 + \bar{d}} \quad \text{is the effective mass density}$$

t is the time

From Eqs. 3.1, 3.7, 3.8 and 3.10, the governing field equations of motions are:

$$(\bar{c}_{11} \frac{\partial^2}{\partial x^2} + \bar{c}_{66} \frac{\partial^2}{\partial y^2} + \bar{c}_{55} \frac{\partial^2}{\partial z^2}) U + (\bar{c}_{12} + \bar{c}_{66}) \frac{\partial^2 V}{\partial x \partial y} + (\bar{c}_{13} + \bar{c}_{55}) \frac{\partial^2 W}{\partial x \partial z} = \rho \ddot{U}$$

$$(\bar{c}_{66} + \bar{c}_{12}) \frac{\partial^2 U}{\partial x \partial y} + (\bar{c}_{66} \frac{\partial^2}{\partial x^2} + \bar{c}_{22} \frac{\partial^2}{\partial y^2} + \bar{c}_{44} \frac{\partial^2}{\partial z^2}) V + (\bar{c}_{23} + \bar{c}_{44}) \frac{\partial^2 W}{\partial y \partial z} = \rho \ddot{V}$$

$$(\bar{c}_{55} + \bar{c}_{13}) \frac{\partial^2 U}{\partial x \partial z} + (\bar{c}_{44} + \bar{c}_{23}) \frac{\partial^2 V}{\partial y \partial z} + (\bar{c}_{55} \frac{\partial^2}{\partial x^2} + \bar{c}_{44} \frac{\partial^2}{\partial y^2} + \bar{c}_{33} \frac{\partial^2}{\partial z^2}) W = \rho \ddot{W}$$

$$\text{where } \ddot{U} = \frac{\partial^2 U}{\partial t^2} \text{ etc}$$

(3.11)

If the displacement equations are defined as:

$$\begin{aligned}
 U &= \bar{U} e^{ik_x x + ik_y y + ik_z z - i\omega t} \\
 V &= \bar{V} e^{ik_x x + ik_y y + ik_z z - i\omega t} \\
 W &= \bar{W} e^{ik_x x + ik_y y + ik_z z - i\omega t}
 \end{aligned} \tag{3.12}$$

where k_x , k_y and k_z are the wave numbers

\bar{U} , \bar{V} and \bar{W} are amplitudes

ω is the circular frequency of the propagating wave,

and substituting these into Eq. 3.11, the governing field equations will result in a standard eigenvalue problem which can easily be solved. In matrix form, the equations are:

$$\begin{aligned}
 & \begin{bmatrix} \bar{C}_{11}k_x^2 + \bar{C}_{66}k_y^2 + \bar{C}_{55}k_z^2 & (\bar{C}_{12} + \bar{C}_{66})k_x k_y & (\bar{C}_{13} + \bar{C}_{55})k_x k_z \\ (\bar{C}_{66} + \bar{C}_{12})k_x k_y & \bar{C}_{66}k_x^2 + \bar{C}_{22}k_y^2 + \bar{C}_{44}k_z^2 & (\bar{C}_{23} + \bar{C}_{44})k_y k_z \\ (\bar{C}_{55} + \bar{C}_{13})k_x k_z & (\bar{C}_{23} + \bar{C}_{44})k_y k_z & \bar{C}_{55}k_x^2 + \bar{C}_{44}k_y^2 + \bar{C}_{33}k_z^2 \end{bmatrix} \begin{Bmatrix} \bar{U} \\ \bar{V} \\ \bar{W} \end{Bmatrix} = \\
 + \omega^2 & \begin{bmatrix} \rho & 0 & 0 \\ 0 & \rho & 0 \\ 0 & 0 & \rho \end{bmatrix} \begin{Bmatrix} \bar{U} \\ \bar{V} \\ \bar{W} \end{Bmatrix} \tag{3.13}
 \end{aligned}$$

In compact form, it is expressed as:

$$\begin{aligned}
 [A_1] \{x_i\} &= \omega^2 [B_1] \{x_i\} \\
 \text{where } \{x_i\}^T &= \{\bar{U} \bar{V} \bar{W}\}^T \tag{3.14a}
 \end{aligned}$$

The dispersion relationship similar to Eq. 2.14 is given by

$$\det [[A_1] - \omega^2 [B_1]] = 0 \tag{3.14b}$$

3.2.4 Antiplane and Plane Strain Motion

Similar to section 2.7, the equations for antiplane and plane strain motions can be obtained by substituting the governing conditions into Eq. 3.13.

For antipane strain motion,

$$\bar{U} = \bar{V} = 0$$

Then, the $[A_1]$ and $[B_1]$ matrices of Eq. 3.14 reduces to $m \times m$ matrix for a m -layer periodicity medium

For plane strain motion,

$$\bar{W} = 0$$

Then, the $[A_1]$ and $[B_1]$ matrices of Eq. 3.14 are $2m \times 2m$ matrices for an m -layer periodicity medium.

The definition of SH, SV and P mode of propagating wave is similar to section 2.7.

3.3. EFFECTIVE STIFFNESS METHOD

Herrmann and Achenbach [10] have proposed a conceptually different approach to constructing continuum models for the dynamic analysis of directionally reinforced composites. Instead of introducing a representative homogeneous medium by means of "effective moduli"; representative elastic moduli are used for the matrix, and the elastic and geometric properties of the reinforcing elements are combined into effective stiffnesses. Certain assumptions are made regarding the deformation of the reinforcing elements. With these assumptions and by applying a smoothing operation, approximate kinetic and strain energy densities for the composite material are obtained. Hamilton's principle is then applied to yield the displacement equations of motion. The displacements for both the reinforcing layers and the matrix layers are expressed as linear expansion about the mid-planes of the layers. In this manner, effective stiffnesses are introduced for both the matrix layers and the reinforcing layers. This theory is distinguished from the effective modulus theory

primarily because bending, shear and extensional stiffnesses of the reinforcing elements enter the strain energy density of the laminated medium. In the following discussion, the theory proposed by Herrmann et al [10, 11] will be followed closely but is extended to three-dimensional analysis and includes anisotropic materials.

3.3.1 Kinematics and Smoothing Operation

A stratified medium consisting of a large number of alternating plane, parallel layers of two different materials is considered (Fig. 3.3). For a general case, the following derivation of the equations of motion is based on anisotropic material. Similarly, the material constants and the thicknesses of the stiff reinforcing layers and the soft matrix layers are denoted by $(C_{11}^f, C_{12}^f, C_{13}^f, C_{22}^f, C_{23}^f, C_{33}^f, C_{44}^f, C_{55}^f, C_{66}^f, d_f)$ and $(C_{11}^m, C_{12}^m, C_{13}^m, C_{22}^m, C_{23}^m, C_{33}^m, C_{44}^m, C_{55}^m, C_{66}^m, d_m)$ respectively. Compared to the notation used in Chapter 2, $C_{ij}^f = C_{ij}^{(i)}$, $d_f = 2 h^{(i)}$, $C_{ij}^m = C_{ij}^{(i+1)}$, $d_m = 2 h^{(i+1)}$. The k^{th} pair of reinforcing and matrix layers whose midplane positions are defined by y^{fk} and y^{mk} respectively (Fig. 3.3) are considered. The displacement at the midplane of the reinforcing layer is denoted by

$$U_0^{\text{fk}}(x, y^{\text{fk}}, z, t) \text{ for component in } x \text{ direction}$$

$$V_0^{\text{fk}}(x, y^{\text{fk}}, z, t) \text{ for component in } y \text{ direction}$$

$$W_0^{\text{fk}}(x, y^{\text{fk}}, z, t) \text{ for component in } z \text{ direction}$$

For the displacement at the midplane of the matrix layer, the superscript f is changed to m .

At this point, two local coordinate systems are introduced. These two local coordinate systems (x, \bar{y}^f, z) and (x, \bar{y}^m, z) are redefined

with axes parallel to the x, y and z axes but with origins in the mid-planes of the reinforcing layer and the matrix layer respectively (Fig. 3.4).

The displacements in the k^{th} reinforcing layer ($U^{\text{fk}}, V^{\text{fk}}, W^{\text{fk}}$) and the displacements in the k^{th} matrix layer ($U^{\text{mk}}, V^{\text{mk}}, W^{\text{mk}}$) are expanded in an infinite series of Legendre polynomials [37]. For the k^{th} reinforcing layer, the displacements are written as:

$$\begin{aligned} U^{\text{fk}} &= \sum_{n=0}^{\infty} P_n \left(\frac{y}{d_f} \right) U_n^{\text{fk}}(x, y^{\text{fk}}, z, t) \\ V^{\text{fk}} &= \sum_{n=0}^{\infty} P_n \left(\frac{y}{d_f} \right) V_n^{\text{fk}}(x, y^{\text{fk}}, z, t) \\ W^{\text{fk}} &= \sum_{n=0}^{\infty} P_n \left(\frac{y}{d_f} \right) W_n^{\text{fk}}(x, y^{\text{fk}}, z, t) \end{aligned} \quad (3.15)$$

where $P_n \left(\frac{y}{d_f} \right)$ are the Legendre polynomials:

$$P_0 \left(\frac{y}{d_f} \right) = 1, P_1 \left(\frac{y}{d_f} \right) = \frac{y}{d_f}, P_2 \left(\frac{y}{d_f} \right) = \left[3 \left(\frac{y}{d_f} \right)^2 - 1 \right] / 2 \text{ etc.} \quad (3.16)$$

n is the number of terms in the polynomial

A similar expansion can be written for the matrix layer by changing superscript $^{\text{f}}$ to $^{\text{m}}$. Conceptually, a displacement approximation can achieve greater accuracy if a sufficient number of terms in the series is retained. However, with many terms, the manipulation becomes tedious and the approximation does not result in the desired simplification. In this analysis it is, therefore, stipulated that the thicknesses of the layers are sufficiently small as compared to any characteristic length of the deformation such that only linear terms in Eq. 3.16 need be retained. Thus the displacements are:

$$\begin{aligned}
 U^{fk} &= U_o^{fk} (x, y^{fk}, z, t) + \bar{y}^f \psi_{2x}^{fk} (x, y^{fk}, z, t) \\
 V^{fk} &= V_o^{fk} (x, y^{fk}, z, t) + \bar{y}^f \psi_{2y}^{fk} (x, y^{fk}, z, t) \\
 W^{fk} &= W_o^{fk} (x, y^{fk}, z, t) + \bar{y}^f \psi_{2z}^{fk} (x, y^{fk}, z, t)
 \end{aligned} \tag{3.17}$$

and

$$\begin{aligned}
 U^{mk} &= U_o^{mk} (x, y^{mk}, z, t) + \bar{y}^m \psi_{2x}^{mk} (x, y^{mk}, z, t) \\
 V^{mk} &= V_o^{mk} (x, y^{mk}, z, t) + \bar{y}^m \psi_{2y}^{mk} (x, y^{mk}, z, t) \\
 W^{mk} &= W_o^{mk} (x, y^{mk}, z, t) + \bar{y}^m \psi_{2z}^{mk} (x, y^{mk}, z, t)
 \end{aligned} \tag{3.18}$$

In Eqs. 3.17

U_o^{fk} , V_o^{fk} and W_o^{fk} represents the displacements at the median plane
of the k^{th} reinforcing layer

ψ_{2x}^{fk} and ψ_{2z}^{fk} are the antisymmetric thickness shear deformations

ψ_{2y}^{fk} represents the symmetric thickness stretch deformation

Based on compatibility, that is, the displacements at the interface of
the k^{th} reinforcing and matrix layers are continuous, the following
relation is obtained:

$$\begin{aligned}
 &U_o^{mk} (x, y^{mk}, z, t) - U_o^{fk} (x, y^{fk}, z, t) \\
 &= \frac{1}{2} d_f \psi_{2x}^{fk} (x, y^{fk}, z, t) + \frac{1}{2} d_m \psi_{2x}^{mk} (x, y^{mk}, z, t)
 \end{aligned} \tag{3.19}$$

for compatibility along the y and z axes, U_o^{mk} , U_o^{fk} , ψ_{2x}^{fk} , ψ_{2x}^{mk} , are changed
into V_o^{mk} , V_o^{fk} , ψ_{2y}^{fk} , ψ_{2y}^{mk} and W_o^{mk} , W_o^{fk} , ψ_{2z}^{fk} , ψ_{2z}^{mk} respectively.

From the displacement equations, the strain energy stored in
elements of unit surface area of the k^{th} pair of reinforcing and matrix
layers can be computed.

In an anisotropic body, the strain energy density, in the condensed
form, can be written as:

$$V_{pot} = \frac{1}{2} \int_{vol} \{\sigma_{ij}\}^T \{\epsilon_{ij}\} dV \quad i, j = x, y, \text{ or } z \tag{3.20}$$

where ϵ_{ij} is the strain tensor and summation implied.

The strain-displacement relationship, Eqs. 2.2, still holds for this case.

For the k^{th} reinforcing layer, the components of the strain tensor can be approximated by substituting the assumed displacement components, Eqs. 3.17 into Eqs. 2.2. It should be noted that the differentiation in the y-direction should be with respect to the local coordinate of the reinforcing layer \bar{y}^f . With this operation, the components of the strain tensor are found to be:

$$\epsilon_{xx}^{fk} = \frac{\partial}{\partial x} U_o^{fk} + \frac{\bar{y}^f}{y} \frac{\partial}{\partial x} \psi_{2x}^{fk} \quad (3.21a)$$

$$\epsilon_{yy}^{fk} = \frac{\partial V}{\partial \bar{y}^f} + \psi_{2y}^{fk} \quad (3.31b)$$

$$\epsilon_{zz}^{fk} = \frac{\partial}{\partial z} W_o^{fk} + \frac{\bar{y}^f}{y} \frac{\partial}{\partial z} \psi_{2z}^{fk} \quad (3.21c)$$

$$\epsilon_{xy}^{fk} = \epsilon_{yx}^{fk} = \frac{1}{2} (\psi_{2x}^{fk} + \frac{\partial}{\partial x} V_o^{fk} + \frac{\bar{y}^f}{y} \frac{\partial}{\partial x} \psi_{2y}^{fk}) \quad (3.21d)$$

$$\epsilon_{zy}^{fk} = \epsilon_{yz}^{fk} = \frac{1}{2} (\psi_{2z}^{fk} + \frac{\partial}{\partial z} V_o^{fk} + \frac{\bar{y}^f}{y} \frac{\partial}{\partial z} \psi_{2y}^{fk}) \quad (3.21e)$$

$$\epsilon_{xz}^{fk} = \epsilon_{zx}^{fk} = \frac{1}{2} (\frac{\partial}{\partial z} U_o^{fk} + \frac{\bar{y}^f}{y} \frac{\partial}{\partial z} \psi_{2x}^{fk} + \frac{\partial}{\partial x} W_o^{fk} + \frac{\bar{y}^f}{y} \frac{\partial}{\partial x} \psi_{2z}^{fk}) \quad (3.21f)$$

The corresponding expressions for the strain components in the k^{th} matrix layer can be obtained by changing the superscript f in Eqs. 3.21a-3.21f to m. For easier and clearer presentation, the following notation is adopted.

$$\partial_1 = \frac{\partial}{\partial x}, \quad \partial_2 = \frac{\partial}{\partial y}, \quad \partial_3 = \frac{\partial}{\partial z}$$

$$\partial_{13} = \frac{\partial}{\partial x \partial z}, \quad \partial_{23} = \frac{\partial}{\partial y \partial z}, \quad \text{etc.}$$

Substituting relation (2.1) and expression (3.21a-f) into the strain energy equation, (Eq. 3.20) and integrating over the thickness d_f , the strain energy stored per unit surface area of the k^{th} reinforcing layer is found to be:

$$\begin{aligned}
 V_{\text{pot}}^{\text{fk}} / \text{unit surface area} &= \frac{1}{2} \int_{-d_f/2}^{d_f/2} \{\sigma_{ij}\}^T \{\epsilon_{ij}\} d\bar{y}^f \\
 &= \frac{1}{2} C_{11}^{\text{fk}} \{d_f (\partial_1 U_o^{\text{fk}})^2 + \frac{1}{12} d_f^3 (\partial_1 \psi_{2x}^{\text{fk}})^2\} + C_{12}^{\text{fk}} d_f \psi_{2y}^{\text{fk}} (\partial_1 U_o^{\text{fk}}) \\
 &+ C_{13}^{\text{fk}} \{d_f (\partial_1 U_o^{\text{fk}}) (\partial_3 W_o^{\text{fk}}) + \frac{1}{12} d_f^3 (\partial_1 \psi_{2x}^{\text{fk}}) (\partial_3 \psi_{2z}^{\text{fk}})\} \\
 &+ \frac{1}{2} C_{22}^{\text{fk}} d_f (\psi_{2y}^{\text{fk}})^2 + C_{23}^{\text{fk}} d_f \psi_{2y}^{\text{fk}} (\partial_3 W_o^{\text{fk}}) \\
 &+ \frac{1}{2} C_{33}^{\text{fk}} \{d_f (\partial_3 W_o^{\text{fk}})^2 + \frac{1}{12} d_f^3 (\partial_3 \psi_{2z}^{\text{fk}})^2\} \\
 &+ \frac{1}{2} C_{44}^{\text{fk}} \{d_f (\psi_{2z}^{\text{fk}} + \partial_3 V_o^{\text{fk}})^2 + \frac{1}{12} d_f^3 (\partial_3 \psi_{2y}^{\text{fk}})^2\} \\
 &+ \frac{1}{2} C_{55}^{\text{fk}} \{d_f (\partial_3 U_o^{\text{fk}} + \partial_1 W_o^{\text{fk}})^2 + \frac{1}{12} d_f^3 (\partial_3 \psi_{2x}^{\text{fk}} + \partial_1 \psi_{2z}^{\text{fk}})^2\} \\
 &+ \frac{1}{2} C_{66}^{\text{fk}} \{d_f (\psi_{2x}^{\text{fk}} + \partial_1 V_o^{\text{fk}})^2 + \frac{1}{12} d_f^3 (\partial_1 \psi_{2y}^{\text{fk}})^2\} \quad (3.22)
 \end{aligned}$$

Similar computation can be carried out to derive the expression for the strain energy stored in an element of unit surface area of the k^{th} matrix layer. This expression, $V_{\text{pot}}^{\text{mk}}$, can be written by replacing in Eq. 3.22 subscripts and superscripts f by subscripts and superscripts m .

After the formulation of the strain energy density, the next step will be the formulation of the kinetic energy density. The kinetic energy of a continuum is defined by

$$T_{\text{kin}} = \frac{1}{2} \int_{\text{vol}} \rho \{ \dot{U}^2 + \dot{V}^2 + \dot{W}^2 \} dV_{\text{vol}} \quad (3.23)$$

Therefore, the kinetic energy per unit surface area of the k^{th} reinforcing layer is obtained as:

$$\begin{aligned}
 T_{\text{kin/unit area}}^{\text{fk}} &= \frac{1}{2} \rho_f d_f (\dot{U}_o^{\text{fk}})^2 + \frac{1}{24} d_f^3 \rho_f (\dot{\psi}_{2x}^{\text{fk}})^2 \\
 &+ \frac{1}{2} \rho_f d_f (\dot{V}_o^{\text{fk}})^2 + \frac{1}{24} d_f^3 \rho_f (\dot{\psi}_{2y}^{\text{fk}})^2 \\
 &+ \frac{1}{2} \rho_f d_f (\dot{W}_o^{\text{fk}})^2 + \frac{1}{24} d_f^3 \rho_f (\dot{\psi}_{2z}^{\text{fk}})^2 \quad (3.24)
 \end{aligned}$$

where ρ_f is the mass density of the reinforcing material.

$$\text{If } \eta = \frac{d_f}{(d_f + d_m)} \text{ and } I_f = \frac{1}{12} d_f^2 \eta \rho_f, \quad (3.25)$$

Eq. 3.24 can be expressed as

$$\begin{aligned} T_{\text{kin}}^{\text{fk}} = \frac{1}{2} (d_f + d_m) \{ & \eta \rho_f (\dot{U}_o^{\text{fk}})^2 + I_f (\dot{\psi}_{2x}^{\text{fk}})^2 \\ & + \eta \rho_f (\dot{V}_o^{\text{fk}})^2 + I_f (\dot{\psi}_{2y}^{\text{fk}})^2 \\ & + \eta \rho_f (\dot{W}_o^{\text{fk}})^2 + I_f (\dot{\psi}_{2z}^{\text{fk}})^2 \} \end{aligned} \quad (3.26)$$

For the k^{th} matrix layer, the kinetic energy per unit surface area is obtained by replacing in Eq. 3.24 superscripts and subscripts f by m.

This equation can then be expressed in a similar form as Eq. 3.26

$$\begin{aligned} T_{\text{kin}}^{\text{mk}} = \frac{1}{2} (d_f + d_m) \{ & (1-\eta) \rho_m (\dot{U}_o^{\text{mk}})^2 + I_m (\dot{\psi}_{2x}^{\text{mk}})^2 \\ & + (1-\eta) \rho_m (\dot{V}_o^{\text{mk}})^2 + I_m (\dot{\psi}_{2y}^{\text{mk}})^2 \\ & + (1-\eta) \rho_m (\dot{W}_o^{\text{mk}})^2 + I_m (\dot{\psi}_{2z}^{\text{mk}})^2 \} \end{aligned} \quad (3.27)$$

$$\text{where } I_m = \frac{1}{12} d_m^2 (1-\eta) \rho_m$$

Assuming that within a certain height H in the y-direction, there are n reinforcing layers and n matrix layers, then the total strain and kinetic energies stored in a rectangular parallelepiped of sides H, unity and unity, of the laminated medium are given by

$$(V_{\text{pot}})_H = \sum_{i=1}^n (V_{\text{pot}}^{\text{fk}} + V_{\text{pot}}^{\text{mk}})_i \quad (3.28)$$

$$\text{and } (T_{\text{kin}})_H = \sum_{i=1}^n (T_{\text{kin}}^{\text{fk}} + T_{\text{kin}}^{\text{mk}})_i \quad \text{respectively} \quad (3.29)$$

Based on the basic premise of the effective stiffness theory, the summation over 2n discrete points y^{fk} and y^{mk} may be approximated by a weighted integration over y thus,

$$(V_{\text{pot}})_H = \sum_{i=1}^n (V_{\text{pot}}^{\text{fk}} + V_{\text{pot}}^{\text{mk}})_i \approx \int_H \frac{1}{d_f + d_m} (V_{\text{pot}}^{\text{f}} + V_{\text{pot}}^{\text{m}}) dy \quad (3.30)$$

$$(T_{kin})_H = \sum_{i=1}^n (T_{kin}^{fk} + T_{kin}^{mk})_i \approx \int_H \frac{1}{d_f + d_m} (T_{kin}^f + T_{kin}^m) dy \quad (3.31)$$

The superscript k has been removed on the right-hand sides of Eqs. 3.30 and 3.31 to indicate that V_{pot}^f , V_{pot}^m , T_{kin}^f and T_{kin}^m are now defined for all y. By means of this "smoothing operation" the layered medium has been replaced by a homogeneous continuum whose strain and kinetic energy densities are functions of x, y, z and t, i.e.

$$V_{pot} = \frac{1}{d_f + d_m} [V_{pot}^f(x, y, z, t) + V_{pot}^m(x, y, z, t)] \quad (3.32)$$

$$T_{kin} = \frac{1}{d_f + d_m} [T_{kin}^f(x, y, z, t) + T_{kin}^m(x, y, z, t)] \quad (3.33)$$

The field variables (U_o^{fk} , V_o^{fk} , W_o^{fk} , U_o^{mk} , V_o^{mk} , W_o^{mk} , ψ_{2x}^{fk} , ψ_{2x}^{mk} , ψ_{2y}^{fk} , ψ_{2y}^{mk} , ψ_{2z}^{fk} , ψ_{2z}^{mk}) which are thus far defined only on certain discrete parallel planes, $y = y^{fk}$ and $y = y^{mk}$, have now become a function of y, and hence, the superscript k can be deleted.

Now, the state of deformation in the laminated medium can be described by twelve field variables (U_o^f , V_o^f , W_o^f , U_o^m , V_o^m , W_o^m , ψ_{2x}^f , ψ_{2x}^m , ψ_{2y}^f , ψ_{2y}^m , ψ_{2z}^f , ψ_{2z}^m) which are a function of x, y, z and t. However, by observing that U_o^f , V_o^f , W_o^f , and U_o^m , V_o^m , W_o^m should be considered as representing the same quantity, namely, the "gross displacements", the number of twelve field variables is reduced to nine. The gross displacements are then referred to as U, V and W. (ψ_{2x}^f , ψ_{2x}^m , ψ_{2y}^f , ψ_{2y}^m , ψ_{2z}^f , ψ_{2z}^m) describe the "local deformations" in the reinforcing layers and matrix layers. Therefore, they do not represent the same magnitude. The local deformations and the gradients of the gross displacements are related, however, by conditions of continuity at the interfaces of the layers. In view of Eq. 3.19, the gross displacements and the local deformations can be written as

$$\begin{aligned}
 U(x, y^{mk}, z, t) - U(x, y^{fk}, z, t) &= \frac{1}{2} d_f \psi_{2x}^f(x, y^{fk}, z, t) + \frac{1}{2} d_m \psi_{2x}^m(x, y^{mk}, z, t) \\
 V(x, y^{mk}, z, t) - V(x, y^{fk}, z, t) &= \frac{1}{2} d_f \psi_{2y}^f(x, y^{fk}, z, t) + \frac{1}{2} d_m \psi_{2y}^m(x, y^{mk}, z, t) \\
 W(x, y^{mk}, z, t) - W(x, y^{fk}, z, t) &= \frac{1}{2} d_f \psi_{2z}^f(x, y^{fk}, z, t) + \frac{1}{2} d_m \psi_{2z}^m(x, y^{mk}, z, t)
 \end{aligned} \tag{3.34}$$

$$\text{Noting that } y^{mk} = y^{fk} + \frac{1}{2} (d_m + d_f) \tag{3.35}$$

and assuming that the thicknesses of the layers are sufficiently small, the difference relation, Eq. 3.34, can be replaced by a differential relation between the local deformations and the gradients of the gross displacements:

$$\begin{aligned}
 \text{i.e. } \frac{\partial}{\partial y} U(x, y, z, t) &= \eta \psi_{2x}^f(x, y, z, t) + (1-\eta) \psi_{2x}^m(x, y, z, t) \\
 \frac{\partial}{\partial y} V(x, y, z, t) &= \eta \psi_{2y}^f(x, y, z, t) + (1-\eta) \psi_{2y}^m(x, y, z, t) \\
 \frac{\partial}{\partial y} W(x, y, z, t) &= \eta \psi_{2z}^f(x, y, z, t) + (1-\eta) \psi_{2z}^m(x, y, z, t)
 \end{aligned} \tag{3.36}$$

The continuity condition Eq. 3.19 has thus been generalized to hold at any point in the continuum. In deriving Eq. 3.36, the differences between the local deformation at y^{fk} and y^{mk} are neglected because the local deformations ($\psi_{2x}^f, \psi_{2x}^m, \psi_{2y}^f, \psi_{2y}^m, \psi_{2z}^f, \psi_{2z}^m$) had originally been defined in the domains of the reinforcing layers and the matrix layers.

In view of Eqs. 3.22 and 3.32, the approximate strain energy function of the laminated medium may now be written in terms of the derivatives of the gross displacements and of the local deformations and their derivatives. It is expressed as

$$\begin{aligned}
 V_{\text{pot}} &= \frac{1}{2} \{ \eta c_{11}^f + (1-\eta) c_{11}^m \} (\partial_1 U)^2 + \frac{1}{24} \eta d_f^2 c_{11}^f (\partial_1 \psi_{2x}^f)^2 + \eta c_{12}^f \psi_{22}^f (\partial_1 U) \\
 &+ \{ \eta c_{13}^f + (1-\eta) c_{13}^m \} (\partial_1 U) (\partial_3 W) + \frac{1}{12} \eta d_f^2 c_{13}^f (\partial_1 \psi_{2x}^f) (\partial_3 \psi_{2z}^f) \\
 &+ \frac{1}{2} \eta c_{22}^f (\psi_{22}^f)^2 + \eta c_{23}^f \psi_{22}^f (\partial_3 W) + \frac{1}{2} \{ \eta c_{33}^f + (1-\eta) c_{33}^m \} (\partial_3 W)^2 \\
 &+ \frac{1}{24} \eta d_f^2 c_{33}^f (\partial_3 \psi_{2z}^f)^2 + \frac{1}{2} \eta c_{44}^f \{ \partial_3 v + \psi_{2z}^f \}^2 + \frac{1}{24} \eta d_f^2 c_{44}^f (\partial_3 \psi_{2y}^f)^2
 \end{aligned}$$

$$\begin{aligned}
& + \frac{1}{2} \{ \eta c_{55}^f + (1-\eta) c_{55}^m \} [\partial_3 U + \partial_1 W]^2 + \frac{1}{24} \eta d_f^2 c_{55}^f [\partial_3 \psi_{2x}^f + \partial_1 \psi_{2z}^f]^2 \\
& + \frac{1}{2} \eta c_{66}^f [\partial_1 v + \psi_{2x}^f]^2 + \frac{1}{24} \eta d_f^2 c_{66}^f (\partial_1 \psi_{2y}^f)^2 \\
& + \frac{1}{24} (1-\eta) d_m^2 c_{11}^m (\partial_1 \psi_{2x}^m)^2 + (1-\eta) c_{12}^m \psi_{22}^m (\partial_1 U) \\
& + \frac{1}{12} (1-\eta) d_m^2 c_{13}^m (\partial_1 \psi_{2x}^m) (\partial_3 \psi_{2z}^m) + \frac{1}{2} (1-\eta) c_{22}^m (\psi_{2y}^m)^2 \\
& + (1-\eta) c_{22}^m \psi_{2z}^m (\partial_3 W) + \frac{1}{24} (1-\eta) d_m^2 c_{33}^m (\partial_3 \psi_{2z}^m)^2 \\
& + \frac{1}{2} (1-\eta) c_{44}^m [\partial_3 v + \psi_{2z}^m]^2 + \frac{1}{24} (1-\eta) d_m^2 c_{44}^m (\partial_3 \psi_{2y}^m)^2 \\
& + \frac{1}{24} (1-\eta) d_m^2 c_{55}^m [\partial_3 \psi_{2x}^m + \partial_1 \psi_{2z}^m]^2 + \frac{1}{2} (1-\eta) c_{66}^m [\partial_1 v + \psi_{2x}^m]^2 \\
& + \frac{1}{24} (1-\eta) d_m^2 c_{66}^m (\partial_1 \psi_{2y}^m)^2 \tag{3.37}
\end{aligned}$$

Similarly, the approximate kinetic energy can be obtained from

Eqs. 3.26, 3.27 and 3.37 as

$$\begin{aligned}
T_{kin} & = \frac{1}{2} \rho_c \dot{U}^2 + \frac{1}{2} I_f (\dot{\psi}_{2x}^f)^2 + \frac{1}{2} I_m (\dot{\psi}_{2x}^m)^2 \\
& + \frac{1}{2} \rho_c \dot{V}^2 + \frac{1}{2} I_f (\dot{\psi}_{2y}^f)^2 + \frac{1}{2} I_m (\dot{\psi}_{2y}^m)^2 \\
& + \frac{1}{2} \rho_c \dot{W}^2 + \frac{1}{2} I_f (\dot{\psi}_{2z}^f)^2 + \frac{1}{2} I_m (\dot{\psi}_{2z}^m)^2
\end{aligned}$$

in which $\rho_c = \eta \rho_f + (1-\eta) \rho_m$

$$I_f = \frac{1}{12} d_f^2 \eta \rho_f$$

$$I_m = \frac{1}{12} d_m^2 (1-\eta) \rho_m \tag{3.38}$$

3.3.2 Displacement Equations of Motion

Thus far, only the strain and kinetic energy densities of the medium have been derived. The next step will be the derivation of the displacement equations of motion. Consider a fixed regular region R of the laminated medium. Hamilton's principle for independent variations of the dependent field quantities in R at time t_0 and t_1 may be written as

$$\delta \int_{t_0}^{t_1} (T_{kin}^R - V_{pot}^R) dt + \int_{t_0}^{t_1} \delta W_1 dt = 0 \quad (3.39)$$

where δW_1 represents the variation of the work done by body forces

and T_{kin}^R and V_{pot}^R are the total kinetic and strain energies.

$$\text{i.e. } V_{pot}^R = \int_R V_{pot} dR$$

$$T_{kin}^R = \int_R T_{kin} dR \text{ in which } dR \text{ denotes the scalar volume element.}$$

In the absence of body forces, the variational problem then reduces to finding the Euler equation for

$$\delta \int_{t_0}^{t_1} \int_R (T_{kin} - V_{pot}) dt dR = 0 \quad (3.40)$$

Examination of Eq. 3.40 reveal that there are nine field variables namely $U, V, W, \psi_{2x}^f, \psi_{2x}^m, \psi_{2y}^f, \psi_{2y}^m, \psi_{2z}^f, \psi_{2z}^m$. These nine field variables can be further reduced to six by eliminating $\psi_{2x}^m, \psi_{2y}^m, \psi_{2z}^m$ by means of continuity equations 3.34. However, in order to be consistent with reference [10], a more elegant method which is to introduce the continuity conditions as subsidiary conditions through Lagrangian multiplier [34] is followed. The variational problem may be redefined as

$$\delta \int_{t_0}^{t_1} \int_R (T_{kin} - V_{pot} - \lambda_1 S_1 - \lambda_2 S_2 - \lambda_3 S_3) dt dR = 0 \quad (3.41)$$

where the Lagrangian multipliers λ_1, λ_2 and λ_3 are functions of x, y, z and t and from Eq. 3.36,

$$\begin{aligned} S_1 &= \frac{\partial}{\partial y} U - \eta \psi_{2x}^f - (1-\eta) \psi_{2x}^m \\ S_2 &= \frac{\partial}{\partial y} V - \eta \psi_{2y}^f - (1-\eta) \psi_{2y}^m \\ S_3 &= \frac{\partial}{\partial y} W - \eta \psi_{2z}^f - (1-\eta) \psi_{2z}^m \end{aligned} \quad (3.42)$$

Since $(T_{kin} - V_{pot} - \lambda_1 S_1 - \lambda_2 S_2 - \lambda_3 S_3)$ depends only on the dependent field variables and their first order derivatives, the system of Euler equations may be written as:

$$\sum_{r=1}^4 \frac{\partial}{\partial q_r} \left[\frac{\partial (T_{kin} - V_{pot} - \lambda_1 S_1 - \lambda_2 S_2 - \lambda_3 S_3)}{\partial (\partial f_s / \partial q_r)} \right] - \frac{\partial (T_{kin} - V_{pot} - \lambda_1 S_1 - \lambda_2 S_2 - \lambda_3 S_3)}{\partial f_s} = 0 \quad (3.43)$$

In Eq. 3.43, f_s represent the twelve dependent variables $(U, V, W, \psi_{2x}^f, \psi_{2y}^m, \psi_{2y}^f, \psi_{2z}^m, \psi_{2z}^f, \lambda_1, \lambda_2, \text{ and } \lambda_3)$; q_r is the spatial variables x, y, z and the time, variable t .

Substitution of the strain energy density, Eq. 3.37, and the kinetic energy density, Eq. 3.38, into Eq. 3.43 will yield a system of twelve equations. A typical computation is shown in Appendix E.

Defining the quantities

$$Q_{\ell n} = \eta C_{\ell n}^f + (1-\eta) C_{\ell n}^m, \quad n = 1, 2 \dots 6$$

$$\ell = 1, 2 \dots 6$$

and using the notation

$$\partial_{ij} U_k = \partial^2 U_k / \partial x_i \partial x_j$$

where $\partial x_1 = \partial x, \quad \partial x_2 = \partial y, \quad \partial x_3 = \partial z$

$$U_1 = U \quad U_2 = V \quad U_3 = W,$$

the twelve equations are expressed as

$$Q_{11} \partial_{11} U + Q_{55} \partial_{33} U + [Q_{55} + Q_{13}] \partial_{13} W$$

$$+ \eta C_{12}^f \partial_1 \psi_{2y}^f + (1-\eta) C_{12}^m \partial_1 \psi_{2y}^m + \partial_2 \lambda_1 = \rho_c \ddot{U} \quad (3.44)$$

$$Q_{66} \partial_{11} V + Q_{44} \partial_{33} V + \eta C_{66}^f \partial_1 \psi_{2x}^f + \eta C_{44}^f \partial_3 \psi_{2z}^f$$

$$+ (1-\eta) [C_{66}^m \partial_1 \psi_{2x}^m + C_{44}^m \partial_3 \psi_{2z}^m] + \partial_2 \lambda_2 = \rho_c \ddot{V} \quad (3.45)$$

$$Q_{33} \partial_{33} W + Q_{55} \partial_{11} W + [Q_{55} + Q_{13}] \partial_{13} U$$

$$+ \eta C_{23}^f \partial_3 \psi_{2y}^f + (1-\eta) C_{23}^m \partial_3 \psi_{2y}^m + \partial_2 \lambda_3 = \rho_c \ddot{W} \quad (3.46)$$

$$\begin{aligned} \frac{1}{12} \eta d_f^2 [C_{11}^f \partial_{11} \psi_{2x}^f + C_{13}^f \partial_{13} \psi_{2z}^f + C_{55}^f \partial_{13} \psi_{2z}^f + C_{55}^f \partial_{33} \psi_{2x}^f] \\ - \eta C_{66}^f \partial_1 v - \eta C_{66}^f \psi_{2x}^f + \eta \lambda_1 = I_f \ddot{\psi}_{2x}^f \end{aligned} \quad (3.47)$$

$$\begin{aligned} \frac{1}{12} (1-\eta) d_m^2 [C_{11}^m \partial_{11} \psi_{2x}^m + C_{13}^m \partial_{13} \psi_{2z}^m + C_{55}^m \partial_{13} \psi_{2z}^m + C_{55}^m \partial_{33} \psi_{2x}^m] \\ - (1-\eta) C_{66}^m \partial_1 v - (1-\eta) C_{66}^m \psi_{2x}^m + (1-\eta) \lambda_1 = I_m \ddot{\psi}_{2x}^m \end{aligned} \quad (3.48)$$

$$\begin{aligned} \frac{1}{12} \eta d_f^2 [C_{33}^f \partial_{33} \psi_{2z}^f + C_{13}^f \partial_{13} \psi_{2x}^f + C_{55}^f \partial_{13} \psi_{2x}^f + C_{55}^f \partial_{11} \psi_{2z}^f] \\ - \eta C_{44}^f \partial_3 v - \eta C_{44}^f \psi_{2z}^f + \eta \lambda_3 = I_f \ddot{\psi}_{2z}^f \end{aligned} \quad (3.49)$$

$$\begin{aligned} \frac{1}{12} (1-\eta) d_m^2 [C_{33}^m \partial_{33} \psi_{2z}^m + C_{13}^m \partial_{13} \psi_{2x}^m + C_{55}^m \partial_{13} \psi_{2x}^m + C_{55}^m \partial_{11} \psi_{2z}^m] \\ - (1-\eta) C_{44}^m \partial_3 v - (1-\eta) C_{44}^m \psi_{2z}^m + (1-\eta) \lambda_3 = I_m \ddot{\psi}_{2z}^m \end{aligned} \quad (3.50)$$

$$\begin{aligned} \frac{1}{12} \eta d_f^2 [C_{66}^f \partial_{11} \psi_{2y}^f + C_{44}^f \partial_{33} \psi_{2y}^f] - \eta C_{12}^f \partial_1 u - \eta C_{23}^f \partial_3 w \\ - \eta C_{22}^f \psi_{2y}^f + \eta \lambda_2 = I_f \ddot{\psi}_{2y}^f \end{aligned} \quad (3.51)$$

$$\begin{aligned} \frac{1}{12} (1-\eta) d_m^2 [C_{66}^m \partial_{11} \psi_{2y}^m + C_{44}^m \partial_{33} \psi_{2y}^m] - (1-\eta) C_{12}^m \partial_1 u - (1-\eta) C_{23}^m \partial_3 w \\ - (1-\eta) C_{22}^m \psi_{2y}^m + (1-\eta) \lambda_2 = I_m \ddot{\psi}_{2y}^m \end{aligned} \quad (3.52)$$

$$\partial_2 u - \eta \psi_{2x}^f - (1-\eta) \psi_{2x}^m = 0 \quad (3.53)$$

$$\partial_2 v - \eta \psi_{2y}^f - (1-\eta) \psi_{2y}^m = 0 \quad (3.54)$$

$$\partial_2 w - \eta \psi_{2z}^f - (1-\eta) \psi_{2z}^m = 0 \quad (3.55)$$

3.3.3 Propagation of Plane Harmonic Waves

The displacement equations of motion, Eqs. 3.44-3.55 can be used to study the propagation of plane harmonic waves in an arbitrary direction. Assuming that the variables of Eq. 3.44-3.55 have the form,

$$\bar{A} e^{ik_x x + ik_y y + ik_z z - ikct} \quad (3.56)$$

where \bar{A} is a constant amplitude

k_x, k_y, k_z are the wave numbers in the x, y and z direction respectively,

c is the phase velocity of the propagating wave and

$\omega = kc =$ angular frequencies

Eqs. 3.44 to 3.55 can be expressed as eigenvalue-eigenvector problems.

$$[A] \{x\} - \omega^2 [B] \{x\} = 0 \quad (3.57)$$

where $\{x\}^T = \langle U, V, W, \psi_{2x}^f, \psi_{2x}^m, \psi_{2z}^f, \psi_{2z}^m, \psi_{2y}^f, \psi_{2y}^m, \lambda_1, \lambda_2, \lambda_3 \rangle$

Eq. 3.57 can be expressed as

$$[S^P] \{x\} = [[A] - \omega^2[B]] \{x\} = 0$$

The explicit form of $[S^P]$ for this problem is given in Appendix F.

Similarly, the roots of this dispersion relation

$$\det [[A] - \omega^2[B]]$$

define a surface in phase-velocity vs wave-number space. A detailed discussion of these dispersion curves has been reported by Sun, Achenbach and Herrmann [11]. Their results using this effective stiffness method will be compared with those obtained using finite element method in Chapter 4.

3.3.4 Antiplane and Plane Strain Motion

Case 1: Governing equation of propagation of longitudinal waves (P waves) in the direction of the layering on x-y plane.

For waves of this type, the field variables are of the form

$$(U, \psi_{2y}^f, \psi_{2y}^m, \lambda_2) = (\bar{A}, \bar{A}_{2y}^f, \bar{A}_{2y}^m, \bar{B}_2) \exp [ik(x-ct)] \quad (3.58)$$

All other field variables vanish identically. The substitution of this governing condition into the displacement equations of motion, Eqs. 3.44-3.55 yields a system of four homogeneous equations for $\bar{A}_1, \bar{A}_{2y}^f, \bar{A}_{2y}^m$ and

\bar{B}_2 . The dispersion equation is obtained by requiring that the determinant of the coefficients vanishes. The non-dimensional form of the dispersion equation obtained is given as:

$$\begin{aligned}
& [(1-\eta) + \eta\theta]^2 \xi^2 \beta^4 - \{[(1-\eta) + \eta\theta] [(1-\eta) + \eta \delta_{66}^f + \eta \delta_{11}^f + (1-\eta) \delta_{11}^m] \xi^2 \\
& + 12\eta [(1-\eta) + \eta\theta] [\delta_{22}^f + \eta \delta_{22}^m / (1-\eta)] \beta^2 \\
& + \{[\eta \delta_{11}^f + (1-\eta) \delta_{11}^m] [(1-\eta) + \eta \delta_{66}^f] \xi^2 \\
& + 12\eta [\delta_{22}^f + \eta \delta_{22}^m / (1-\eta)] [\eta \delta_{11}^f + (1-\eta) \delta_{11}^m] - 12\eta^2 [\delta_{12}^f - \delta_{12}^m]^2 \} = 0
\end{aligned} \tag{3.59}$$

where $\beta = c / (C_{66}^m / \rho_m)^{1/2}$ is the dimensionless phase velocity
 $\xi = kd_f$ is the dimensionless wave number
 $\theta = \rho_f / \rho_m$ is the ratio of mass densities

and $\delta_{ij}^f = C_{ij}^f / C_{66}^m$
 $\delta_{ij}^m = C_{ij}^m / C_{66}^m$

If the materials of both the reinforced and matrix layers are isotropic, Eq. 3.59 degenerate to Eq. 63 of Ref. [11] in which $\delta_{66}^f = \gamma = \mu_f / \mu_m$. γ is the ratio of shear moduli of the reinforced layer, μ_f and the matrix layer, μ_m .

Case 2: Governing equation of propagation of SV waves in the direction of the layering on x-y plane.

For a shear wave, the nonvanishing field variables are V , ψ_{2x}^f , ψ_{2x}^m and λ_1 .

That is

$$(V, \psi_{2x}^f, \psi_{2x}^m, \lambda_1) = (\bar{A}_2, \bar{A}_{21}^f, \bar{A}_{21}^m, \bar{B}_1) \exp [ik(x - ct)] \tag{3.60}$$

Following the previously described procedure, the dispersion equation corresponding to the system of solutions (3.60) in nondimensional form is given as:

$$\begin{aligned}
& [(1-\eta) + \eta\theta]^2 \xi^2 \beta^4 - \{[(1-\eta) + \eta\theta] [(1-\eta) + \eta\delta_{66}^f + \eta\delta_{11}^f + (1-\eta)\delta_{11}^m] \xi^2 \\
& + 12 [(1-\eta) + \eta\theta] [(1-\eta)\delta_{66}^f + \eta] \eta/(1-\eta) \} \beta^2 \\
& + \{[(1-\eta) + \eta\delta_{66}^f] [\eta\delta_{11}^f + (1-\eta)\delta_{11}^m] \xi^2 \\
& + 12\eta \delta_{66}^f/(1-\eta) \} = 0 \tag{3.61}
\end{aligned}$$

Eq. 3.61 will degenerate to Eq. 72 of Ref. [11] if the materials of the reinforced and matrix layers are isotropic.

Case 3: Governing equation of propagation of SH waves in the direction of the layering.

For SH waves, the displacements are parallel to the z-direction while the waves propagate in the x-direction. The nonvanishing field variables are of the form

$$(W, \psi_{2z}^f, \psi_{2z}^m, \lambda_3) = (\bar{A}_3, \bar{A}_{23}^f, \bar{A}_{23}^m, \bar{B}_3) \exp [ik(x-ct)] \tag{3.62}$$

Substituting of Eq. 3.62 into Eqs. 3.44 - 3.55 will yield two uncoupled systems of equations, governing symmetric and antisymmetric motion, respectively. For symmetric motion, the field quantity is represented by

$$W = \bar{A}_3 \exp [ik(x-ct)] \tag{3.63}$$

for which the constant phase velocity is obtained as

$$\beta = \left\{ \frac{\eta\delta_{55}^f + (1-\eta)\delta_{55}^m}{[(1-\eta) + \eta\theta]} \right\}^{1/2} \tag{3.64}$$

The antisymmetric system is represented by the following solutions:

$$(\psi_{2z}^f, \psi_{2z}^m, \lambda_3) = (\bar{A}_{23}^f, \bar{A}_{23}^m, \bar{B}_3) \exp [ik(x-ct)] \tag{3.65}$$

Then, the nondimensional form of the dispersion equation obtained is given as:

$$[(1-\eta)+\eta\theta]\xi^2 \beta^2 - \{[(1-\eta)\delta_{55}^m + \eta\delta_{55}^f] \xi^2 + 12\eta [\delta_{44}^f + \eta\delta_{44}^m/(1-\eta)] \} = 0 \tag{3.66}$$

Eq. 3.64 and Eq. 3.66 are the same as Eq. 75 and Eq. 77 respectively of Ref. [11] if the material properties of the reinforced and matrix layers are isotropic.

For all the cases mentioned above, the dispersion equation can be expressed in matrix form as in Eq. 3.57. But [A] and [B] are reduced to $4n \times 4n$ for a n -layer periodicity.

For a wave propagating normal to the layering, the dispersion equation can be obtained in a similar procedure by substituting the governing displacement conditions into Eq. 3.44-3.55. It will not be discussed here. Ref. [11] provides a good discussion on the procedure.



CHAPTER 4

NUMERICAL RESULTS AND DISCUSSION

4.1 INTRODUCTION

In this Chapter, the numerical results of several examples are presented and discussed. For a two dimensional analysis of harmonic waves propagating in a periodically layered, isotropic, infinite, elastic body, Shah and Datta [33] have shown that the present finite element method gives excellent results when compared with the exact analysis proposed by Delph, Herrmann and Kaul [28, 29, 30]. For a three dimensional analysis on the same problem but using anisotropic material, Ref. [32] would be a good reference to determine the accuracy of the present analytical method outlined in Chapter 2. However, at time of writing this thesis, the detailed numerical results of Ref. [32] were not received. Therefore, comparison with their work cannot be carried out. In order to gauge the accuracy and range of applicability of this present approach, a two-layer periodic isotropic laminated medium is considered. The numerical results obtained by using this proposed finite element method are compared with those obtained by using the effective modulus method [Chapter 3.2] and the effective stiffness method [Chapter 3.3].

The second example presented considers a wave propagating through a two-layer, infinite elastic body with anisotropic material properties. The composite chosen is that of boron-fiber reinforced layers sandwiched between thin layers of aluminum. The numerical results are first compared with that obtained by extended effective modulus method and the

extended effective stiffness method. Then the behaviour of the dispersion curves for waves propagating through this media are discussed individually.

In the third example, the material considered is graphite-epoxy composite. There are two types of graphite-epoxy composites considered. A formula, outlined in Appendix G, is used to obtain their respective material constants.

For all the examples mentioned above, only a two-layer periodic medium is considered. In order to obtain better results, each layer within the unit cell is subdivided into "lamina" at mid-plane (Fig. 2.1), thus creating a four-layer periodicity. Higher layered periodicity can be created by further subdividing the lamina. However, it is shown in [33] that the numerical results for lower modes of wave propagation do not appreciably change by increasing the number of lamina. Therefore, only the results of four layered periodicity are presented here.

The numerical results presented in this Chapter are obtained from FORTRAN programs written for the extended effective modulus method, extended effective stiffness method and the finite element method. These programs are included in Appendices H, I and J.

4.2 ISOTROPIC LAMINATED MEDIUM

The dispersion curves for waves propagating through an isotropic laminated medium using the effective modulus method, effective stiffness method and the elasticity theory have been presented by Sun, Anchebach and Herrmann [11, 12]. However, their presentations are based on two dimensional analysis. For an isotropic material, the numerical results obtained by using a three dimensional analysis and those obtained using a two dimensional

analysis should be identical.

In this example, the problem is analyzed using the same material properties and parameters given in Ref. [11]. The material constants are tabulated in Table 4.1. The non-dimensional parameters used are defined as:

$$\gamma = \frac{\mu_1}{\mu_2} \quad \text{ratio of shear moduli}$$

μ_1 = shear modulus of reinforced layer
 μ_2 = shear modulus of matrix layer

$$\beta = \frac{c}{(\mu_2/\rho^{(2)})^{1/2}} \quad \text{dimensionless phase velocity}$$

c = phase velocity of propagating wave
 $\rho^{(2)}$ = density of matrix layer

$$\xi = k (2 h^{(1)}) \quad \text{dimensionless wave number}$$

$2 h^{(i)}$ = thickness of reinforced layer
 k = wave number
 $= \frac{2\pi}{\Lambda}$
 Λ = wave length of propagating wave

$$\theta = \rho^{(1)}/\rho^{(2)} \quad \text{ratio of mass densities}$$

$\rho^{(1)}$ = density of reinforced layer

To be consistent with the results presented in Ref. [11], the numerical computations are carried out for three values of γ , namely, $\gamma = 100, 50$ and 10 , and for $\eta = 0.8, \theta = 3$. η is shown in Eq. 3.25. The Poisson ratio of the reinforced layer and the matrix layer are 0.3 and 0.35 , respectively.

Based on these material properties and parameters and using the effective modulus and effective stiffness method, the curves presented in Ref. [11] are reproduced. The results obtained by using the finite

element method based on the same material properties and parameters are then plotted on the graphs. These graphs are shown in Fig. 4.1 to Fig. 4.4. It is found that the results using the finite element method coincide with the results obtained by using theory of elasticity for $\gamma = 10, 50$ and 100 . This proves the validity of the proposed finite element method and with this observation, the proposed method can be applied to the analysis of harmonic waves propagating in anisotropic composites, with confidence.

4.3 FIBER-REINFORCED BORON-ALUMINIUM COMPOSITE

Datta and Ledbetter [39] have computed the elastic constants for the fiber-reinforced boron-aluminium composite. This composite is a heat resistance material and is used mainly for aerospace structures such as space shuttles. Shah and Datta then used the same elastic constants and geometric parameters to perform a plane-strain analysis to derive the dispersion characteristics of harmonic waves propagating in the composite [33]. For analytical purpose, the composite is modelled as a two-layer medium. The first layer is the boron-fiber reinforced layer with anisotropic material properties while the second layer is the thin layer of aluminium. In the following discussion, the method outlined in Chapter 2 is used to determine the dispersion characteristics in this two-layer medium. The material constants for the fiber reinforced layer are slightly different (about 6% smaller) than those presented in Ref. [39], and are listed in Table 4.2. The reason for the slight difference in values is that more experimental works have been carried out to determine the properties of the composite. The new set of material constants, provided by Datta, are presumably a better representation of the composite. The parameters used in the discussion are:

$\Omega = \frac{\omega}{\omega_s}$ Dimensionless frequency of waves

$$\omega_s = \frac{\pi}{2h^{(2)}} \cdot \sqrt{\frac{\mu_2}{\rho^{(2)}}}$$

ω = frequency of waves

$\bar{\eta} = \frac{2h^{(2)}}{\pi} k_y$ Dimensionless y-component of wave number

k_y = y-component of wave number

$\bar{k} = \frac{2h^{(2)}}{\pi} k$ Dimensionless wave number

$$k = \text{wave number} = \frac{2\pi}{\Lambda}$$

$\bar{d} = \frac{2h^{(1)}}{2h^{(2)}}$ Ratio of thickness of reinforced layer and the thickness of matrix layer

α Horizontal angle made by propagating wave on x-z plane with respect to x-axis

ϕ Vertical angle made by propagating wave with respect to x-z plane

For comparison with the effective modulus and the effective stiffness method, a β vs ξ plot for waves propagating parallel and normal to the layering is first considered. \bar{d} is taken to be 12.

For waves propagating parallel to the layering and along the global x-axis ($\alpha = 0^\circ$, $\phi = 0^\circ$), the results are presented in Fig. 4.5. It is shown that for small wave numbers ($\xi < 2$), the quasi-longitudinal mode (P-wave) is in agreement with the effective modulus and the effective stiffness method. As the wave number increases, the results obtained using finite element

method departs substantially from those obtained by using the other two methods. This dispersive behaviour is similar to that observed for the isotropic case presented in Fig. 4.3. It has been summarized in Ref. [24] that for large γ ($\gamma = 50, 100$), there should be a rapid decrease of the phase velocity of the lowest longitudinal mode (P-wave). This is because there is a shift of the participation in the motion of both reinforcing and matrix layers to the matrix layer only. For both isotropic and anisotropic materials, only the finite element method shows this behaviour (Fig. 4.3 and 4.5). As for the quasi-transverse mode (SV-wave), there is no remarkable difference between the three methods.

For waves propagating normal to the layering, ($\alpha = 0^\circ$, $\phi = 90^\circ$), the results are presented in Fig. 4.6. In this figure, there is a remarkable variation between the three methods, especially for higher wave number. For isotropic material, Ref [11] shows that the effective stiffness method and effective modulus method is comparable to the exact method only for small value of ξ ($\xi < 1$) for both P-waves and SV-waves. The results are shown in Fig. 4.4. However, the results obtained using finite element method still coincides with that obtained from the theory of elasticity. For plane-strain analysis of a laminated boron-aluminium composite, Ref. [37] concluded that the dispersive behaviour of wave propagating normal to the layering agrees with experimental observations. This verifies the validity of the finite element method. However, due to the lack of numerical results in the three dimensional analysis of harmonic waves propagating through anisotropic media, Fig. 4.6 can only be shown but can not be compared with those obtained using the theory of elasticity.

For the rest of the graphical presentation in this section, the numerical results will be presented using the material properties in Table 4.2 but the frequency of the propagating wave is determined, instead of the phase velocity. Ω , the dimensionless frequency, is obtained by normalizing the roots of the dispersion relation in Eq. 2.13.

Figs. 4.7 to 4.18 show the dispersion curves for the lowest longitudinal (P), lowest transverse (SV) and the lowest symmetric SH mode propagating in the x-y, y-z and x-z plane. It can be concluded that for small magnitude of \bar{k} where \bar{k} is the nondimensional wave number, say $\bar{k} \leq 0.07$, the frequency, Ω , for the three modes is directly proportional to \bar{k} . This agrees with the actual behaviour as stated in Ref. [40]. One disadvantage of this Ω vs \bar{k} plot is that for $\bar{k} = 0$, the phase velocity of the waves cannot be determined. Comparing the 3-sets of graphs, namely Figs. 4.7-4.10 for waves on the x-y plane, Figs. 4.11-4.14 for waves on the y-z plane and Figs. 4.15-4.18 for waves on the x-z planes, it is observed that the waves are less dispersed when they travel along the x-z plane. This is due to the fact that they are travelling along the matrix layer which is the homogeneous isotropic layer. Greater dispersion is observed for the waves travelling along the x-y and y-z planes because for these two planes, the reinforcing layer and the matrix layer are involved. The dispersion is the greatest for waves propagating normal to the layering ($\alpha = 0^\circ, \phi = 90^\circ$ or $\alpha = 90^\circ, \phi = 90^\circ$) due to the maximum participation of both layers in vibrating the particles.

Figs. 4.19-4.27 are plots showing the variation of frequencies with respect to the directions of propagation on the plane for a particular \bar{k} . Similar observations, as described above, are obtained.

Instead of examining the variation in frequencies with respect to angular changes in the direction of propagating waves, the computer program listed in Appendix J is capable of handling the analysis by treating the y-component of the nondimensional wave number, $\bar{\eta}$ as a known quantity. These Ω vs. $\bar{\eta}$ plots are presented in Figs. 4.28 to 4.32. The SH mode can be easily determined from the output. However, the longitudinal and transverse modes cannot be distinguished. Therefore, the lowest five branches, regardless of modes, are plotted. It is observed that for large values of \bar{k} (0.5, 1.0) there is very little variation in the frequencies as $\bar{\eta}$ changes correspondingly. This is due to the fact that, for small $\bar{\eta}$ and large magnitudes in \bar{k} , the waves are travelling along the matrix layer only.

Similar plots are carried out for the Ω vs \bar{k} plot for a different $\bar{\eta}$ and at a horizontal angle of 0° and 45° . The results of the lowest 5 branches are shown in Figs. 4.33 to 4.38. Only the lowest out-of plane, (SH) mode can be identified.

4.4 GRAPHITE-EPOXY FIBER REINFORCED COMPOSITE

In this section, the behaviour of dispersion curves for waves propagating through two types of graphite-epoxy composites will be considered. Graphite-epoxy composite has high strength and high electrical resistance and it can be used as thermal insulation in nuclear power plants. Since the material constants change when the percentage of fibre in the composite differ, a formula is provided by Datta [42], and is listed in Appendix G,

to calculate the material constants for the two types of composites used in this analysis. The value of \bar{c} in the formula is used as a control. If \bar{c} is different, other material constants for that type of graphite epoxy composite can be calculated. The following discussion will be based on two different values of \bar{c} , namely, when $\bar{c} = 0.3$ and $\bar{c} = 0.668$. Similar to the second example, the composite is modelled to be a two layer medium. The first layer is the graphite fiber reinforced layer while the second layer is the thin layer of epoxy.

4.4.1 Graphite-Epoxy Composite (i)

For $\bar{c} = 0.3$, the material constants are calculated according to the formula in Appendix G. For convenience, these values have been tabulated in Table 4.3. In this section, two different ratios of thicknesses between the reinforcing layer and the matrix layer are considered. The two ratios are

$$\bar{d} = 4.0 \text{ and } \bar{d} = 9.0$$

The parameters used in Section 4.3 are used here for graphical presentation. For $\bar{d} = 4.0$, the frequencies are proportional to \bar{k} from 0 to as far as 0.09 which is equivalent to a wave length of $44.4 h^{(2)}$ (Fig. 4.39-4.42). In these figures, attempts to differentiate the propagating waves into SH, SV or P modes are not carried out. Therefore, only the lowest 3 branches, irrespective of modes, are plotted. For the waves travelling on each plane, only one representative direction of

propagation will be considered. For example, when waves are propagating on the x-y plane, the direction of propagation is taken to be 45° with respect to the x-axis [$\alpha = 0^\circ$, $\phi = 45^\circ$]. This is shown in Fig. 4.39. In Fig. 4.42, the arbitrary direction of the propagating waves through the medium is chosen to be at $\alpha = 45^\circ$, $\phi = 45^\circ$.

Fig. 4.43 ($\alpha = 0^\circ$), Fig. 4.44 ($\alpha = 45^\circ$) and Fig. 4.45 ($\alpha = 90^\circ$) shows the lowest 3 branches plot for the variation of frequencies with respect to the value of $\bar{\eta}$ for a constant value of \bar{k} . It is shown in these three graphs that for $\bar{k} = 1.0$, the frequencies of the lowest three branches are independent of $\bar{\eta}$. This is due to the fact that the waves are propagating along the epoxy layer which is the isotropic layer.

Fig. 4.46 ($\alpha = 45^\circ$) shows the characteristic variation of Ω with respect to \bar{k} for this graphite-epoxy composite.

For $\bar{d} = 9.0$, Figs. 4.47 to 4.50 show that Ω is proportional to \bar{k} if \bar{k} is smaller than 0.04. This shows that when the thickness of the reinforcing layer increases, greater dispersion of the propagating waves is observed.

Figs. 4.51 to 4.54 are similar plots to Figs. 4.43 to 4.46 for $\bar{d} = 9$. Similar behaviour is observed.

4.4.2 Graphite-Epoxy Composite (ii)

For $\bar{c} = 0.668$, the material constants are calculated and tabulated in Table 4.4. Two ratios of thicknesses $\bar{d} = 4.0$ and $\bar{d} = 9.0$ are considered. The parameters used in the graphical presentations are similar to that of Section 4.4.1. Figs. 4.55 to 4.70 plotted using the same parameters as in Figs. 4.39 to 4.54 correspondingly. The general behaviour of the dispersion curves are the same as in Section 4.4.1. The only difference is that the waves are travelling with a higher frequency.

4.5 COMPARISON OF THE THREE METHODS:

(Effective Modulus, Effective Stiffness and Finite Element Method.)

In analyzing for the first branch of the frequency spectrum using three layered transversely isotropic sphere, Fyre [41] compared his results using the finite element method, with that obtained by the Shell theory. He showed that for a soft middle layer, the shell theory produce much higher values than the finite element method. To verify this point, the same material properties he used have been reproduced here. They are listed in Table 4.5. Three types of matrix layer will be used. The first type is a very soft layer whose material constants are about ten times smaller than the reinforcing layer. It is designated as 2-i. The material constants, for the second type designated as 2-ii, are about half of that of the reinforcing layer. For the third type, 2-iii, it is of the same material as the reinforcing layer. Only two-layer periodic medium similar to those in Chapter 2 and Chapter 3 is considered here.

\bar{d} is taken to be 0.6 and the periodicity is equal to 4 for all three cases. The results of the dispersion relation using the effective modulus [Chapter 3.2], effective stiffness [Chapter 3.3] and finite element [Chapter 2] method are obtained with the aid of the computer programs in Appendix H, I and J. The phase velocity, β , vs wave number, ξ , plots of the results are shown in Figs. 4.71 and 4.72.

Fig. 4.71 shows the SV mode for waves propagating along the x-axis. It is shown that when using matrix layer 2-i, there is a large discrepancy between the three methods. The effective stiffness method produces a higher value than the other two methods, even for a small wave number. This discrepancy decreases when matrix layer 2-ii is used. For matrix layer 2-iii, there is no difference in the results obtained by the three

methods. This is because for the effective modulus and effective stiffness method, the dispersion relations are formulated by applying an averaging or smoothing operation through the media. This operation has been discussed in Chapter 3. As the difference between the layer stiffnesses increases, it is understandable that the first two approximate methods will yield a result that is farther away from the exact value. Finite element method is subdividing the media into smaller laminae without averaging the material properties of the laminae. Interpolation functions (Eq. 2.6) are used to ensure compatibility of the laminae. Therefore, it is reasonable to assume that it should yield a better approximation to the exact value. In Ref. [33], it is shown that for isotropic material, the present finite element method is in agreement with the results obtained using the theory of elasticity. Therefore, it can be concluded that the finite element method should be used instead of the other two methods if the matrix layer is too soft when compared with the reinforced layer ($\gamma > 10$).

Fig. 4.72 shows a similar plot but for the SH mode. The same conclusion can be deduced.

4.6 CONCLUSION

A finite element method has been presented in this thesis for the study of harmonic waves propagating in a layered composite medium. This approximate method utilizes the interpolation functions, satisfying the continuity of displacements and tractions at the interfaces of a periodically laminated composite medium, and Floquet's theory. The formulation of the dispersion relations is based on a three-dimensional analysis of the harmonic waves propagating in a periodically layered, anisotropic, infinite body. However, the method can be readily applied to any two-dimensional analysis. Two-

dimensional analysis is applicable only to harmonic waves travelling in isotropic or transversely anisotropic media where the plane-strain and antiplane strain motions are not coupled. However, the composites for practical applications can seldom be modified to be transversely anisotropic materials. Therefore, the proposed three-dimensional analysis should be used. To assess the accuracy of this proposed method, comparison to the effective modulus and the stiffness method were carried out. It is shown that the finite element yields better approximations than the other two methods (Fig. 4.1 to Fig. 4.6). For two-dimensional analysis on isotropic materials, the present method yields excellent results when compared with that obtained by using the theory of elasticity (Fig. 4.1 to Fig. 4.4).

The dispersive behaviour of harmonic waves propagating through fiber-reinforced boron-aluminium composite and graphite epoxy composite are also presented (Fig. 4.7 to 4.70). Both composites are modelled as a layer of anisotropic reinforced material and a layer of isotropic matrix material. Ref. [37] has shown that for the plane-strain analysis of a wave propagating in fiber-reinforced boron-aluminium composite, the analytical results obtained from the present finite element formulation agree with the experimental observations.

At present an analytical solution for waves propagating through an anisotropic laminate is not available. Therefore, an approximate method (finite element method) to solve such problems is proposed. Due to the lack of numerical results in the same research area in literature, it is hoped that the results presented in this thesis can serve as a bench mark for further approximate theories.

REFERENCES

REFERENCES

1. Pinstler, K.S., and Dong, S.B., 'Elastic Bending of Layered Plates', Journal of the Engineering Mechanics Division, ASCE, Vol. 85 #EM4, 1959, pp. 7-10.
2. Reissner, E., and Stavsky, Y., 'Bending and Stretching of Certain Types of Heterogeneous Anisotropic Elastic Plates', Journal of Applied Mechanics, Vol. 28 #3, Trans. ASME, Vol. 83, Series E, Sept. 1961, pp. 402-408.
3. Dong, S.B., Pister, K.S., and Taylor, R.L., 'On the Theory of Laminated Anisotropic Shells and Plates', Journal of Aerospace Sciences, Vol. 29, No. 8, 1962, pp. 969-975.
4. Ambartsumyan, S.A., 'Contributions to the Theory of Anisotropic Layered Shells', Applied Mechanics Review, Vol. 15 #4, 1962, pp. 245-249.
5. Sun, C.T., and Whitney, J.M., 'On Theories for the Dynamic Responses of Laminated Plates', Proceeding AIAA/ASME/SAE 13th Structural Dynamics and Material Conference, AIAA Paper No. 72-398, 1972.
6. Nelson, R.B., and Lorch, D.R., 'A Refined Theory for Laminated Orthotropic Plates', Journal of Applied Mechanics, Vol. 96, March 1974, pp. 177-183.
7. Postma, G.W., 'Wave Propagation in a Stratified Medium', Geophysics, Vol. 20 #4, 1955, pp. 780-806.
8. Rytov, S.M., 'The Acoustical Properties of a Thinly Laminated Medium', Soviet Physics Acoustic, Vol. 2, 1956, pp. 68-80.
9. White, J.E., and Angona, F.A., 'Elastic Wave Velocity in Laminated Media', Journal of the Acoustical Society of America, Vol. 27, 1955, pp. 311-317.
10. Herrmann, G., and Achenbach, J.D., 'On Dynamic Theories of Fiber Reinforced Composites', Proceedings of the AIAA/ASME 8th Structures, Structural Dynamics and Materials Conference, March 29-31, 1967, Palm Springs, California.
11. Sun, C.T., Achenbach, J.D., and Herrmann, G., 'Continuum Theory for a Laminated Medium', Journal of Applied Mechanics, Vol. 35, Trans, ASME, Vol. 90, Series E, 1968, pp. 467-475.
12. Achenbach, J.D., Sun, C.T., and Herrmann, G., 'On the Vibrations of a Laminated Body', Journal of Applied Mechanics, Vol. 90, Dec. 1968, pp. 689-696.
13. Sun, C.T., 'Theory of Laminated Plates', Journal of Applied Mechanics, Vol. 93, March 1971, pp. 235-238.

14. Drumheller, D.S., and Bedford, A., 'On a Continuum Theory for a Laminated Medium', *Journal of Applied Mechanics*, Vol. 95, June 1973, pp. 527-532.
15. Jones, J.P., 'Wave Propagation in a Two-Layered Medium', *Journal of Applied Mechanics*, Vol. 23, #2, *Trans. ASME*, Vol. 86, Series E, June 1964, pp. 213-222.
16. Bedford, A., and Stern, M., 'Toward a Diffusing Continuum Theory of Composite Materials', *Journal of Applied Mechanics*, Vol. 38, 1971, p. 8.
17. Bedford, A., and Stern, M., 'A Multicontinuum Theory of Composite Materials', *Acta Mechanica*, Vol. 14, 1972, p. 85.
18. McNiven, H.D., and Mengi, Y., 'A Mixture Theory for Elastic Laminated Composites', *Int. Journal of Solid Structures*, Vol. 15, 1979, p. 281.
19. Hegemier, G.A., 'On a Theory of Interacting Continua for Wave Propagation in Composites', *Dynamics of Composite Materials*, p. 70, *The American Society of Mechanical Engineers* (1972).
20. Hegemier, G.A., and Bache, T.C., 'A General Continuum Theory with Microstructure for Wave Propagation in Elastic Laminated Composites', *Journal of Applied Mechanics*, Vol. 41, 1974, p. 101.
21. Nemat-Nasser, S., 'General Variational Method for Elastic Waves in Composites', *Journal of Elasticity*, Vol. 2, 1972, pp. 79-90.
22. Minagawa, S., and Nemat-Nasser, S., 'On Harmonic Waves in Layered Composites', *Journal of Applied Mechanics*, Vol. 44, 1977, pp. 689-695.
23. Mengi, Y., Birlik, G., and McNiven, H.D., 'A New Approach for Developing Dynamic Theories for Structural Elements. Part 2: Application to Thermoelastic Layered Composites', *Int. Journal of Solids Structures*, Vol. 16, 1980, p. 1169.
24. Sun, C.T., Achenbach, J.D., and Herrmann, G., 'Time-harmonic Waves in a Stratified Medium Propagating in the Direction of the Layering', *Journal of Applied Mechanics* Vol. 35, 1968, p. 408.
25. Lee, E.H., and Yang, W.H., 'On Waves in Composite Materials with Periodic Structures', *SIAM, Journal of Applied Mathematics*, Vol. 25, 1973, p. 492.
26. Robinson, C.W., 'Shear Waves in Layered Composites', Report No. SCL-RR-720351, Sandia Laboratories, Livermore, California, 1972.
27. Sve, C., 'Time-harmonic Waves Travelling Obliquely in a Periodically Laminated Medium', *Journal of Applied Mechanics*, Vol. 38, 1971, p. 477.

28. Delph, T.J., Herrmann, G., and Kual, R.K., 'Harmonic Waves Propagation in a Periodically Layered, Infinite Elastic Body: Antiplane Strain', *Journal of App. Mech.*, Vol. 45, 1978, p. 343.
29. Delph, T.J., Herrmann, G., and Kual, R.K., 'Harmonic Waves Propagation in a Periodically Layered, Infinite Elastic Body: Plane Strain, Analytical Results', *Journal of App. Mech.*, Vol. 46, 1979, p. 113.
30. Delph, T.J., Herrmann, G., and Kual, R.K., 'Harmonic Waves Propagation in a Periodically Layered, Infinite Elastic Body: Plane Strain, Numerical Results', *Journal of App. Mech.*, Vol. 47, 1980, p. 531.
31. Kulkarni, S.V., and Pagano, N.J., 'Dynamic Characteristic of Composite Laminates', *Journal of Sound Vibration*, Vol. 23, 1972, pp. 127-143.
32. Yamada, M., and Nemat-Nasser, S., 'Harmonic Waves with Arbitrary Propagation Direction in Layered Orthotropic Elastic Composites', *Journal of Composites Material*, Vol. 15, 1981.
33. Shah, A.H., and Datta, S.K., 'Harmonic Waves in a Periodically Laminated Media', *Int. Journal of Sound and Structures*, Vol. 18, 1982, pp. 397-410.
34. Desai, C.S., and Abel, J.F., 'Introduction to Finite Element Method', VNR, New York, 1972.
35. Ince, E.I., 'Ordinary Differential Equations', Dover Publications, New York, 1956.
36. Christensen, R.M., 'Mechanics of Composite Materials', Willy Interscience Publications, 1977.
37. Datta, S.K., Shah, A.H., and Ledbetter, H.M., 'Harmonic Waves in a Periodically Laminated Medium', IUTAM Symposium on Mechanics of Composite Materials, Virginia Polytechnic Institute and State University, Blacksburg, Virginia, U.S.A. Aug. 16-19, 1982.
38. Spiegel, M.R., 'Applied Differential Equation', 2nd edition, Prentice-Hall, 1967.
39. Datta, S.K., and Ledbetter, H.M., 'Anisotropic Elastic Constants of a fiber-reinforced Boron-Aluminium Composite', *Mech. of Nondestructive Testing*, Ed. W.W. Stinchcomb, Plenum Press, New York, 1980.
40. Hearmon, R.F.S., 'An Introduction to Applied Anisotropic Elasticity', Oxford University Press, 1961.
41. Frye, J., 'Some Problems in the Dynamics of Layered Spherical Shells', Ph.D. Thesis, University of Manitoba, 1969.
42. Datta, S.K., Ledbetter, H.M., Kriz, R.D., 'Calculated Elastic Constants of Composites Containing Anisotropic Fibers', *Int. Journal of Solids and Structures*, 1983 (to appear).
43. Lo, P.L.Y., 'Harmonic Wave Propagation in Periodically Layered Materials', B.Sc. Thesis, University of Manitoba, 1981.

A P P E N D I X A

DERIVATION OF THE INTERPOLATION FUNCTION

APPENDIX A

By using third degree approximation and interpolation, the functions U_I , V_I and W_I can be derived. This is done in order to satisfy the stress and strain continuity.

Using the interpolation functions, U_I , V_I and W_I can be expressed as:

$$\begin{aligned}U_I &= f_1(\eta_i)u_1 + f_2(\eta_i)u_2 + f_3(\eta_i)u_3 + f_4(\eta_i)u_4 \\V_I &= f_1(\eta_i)v_1 + f_2(\eta_i)v_2 + f_3(\eta_i)v_3 + f_4(\eta_i)v_4 \\W_I &= f_1(\eta_i)w_1 + f_2(\eta_i)w_2 + f_3(\eta_i)w_3 + f_4(\eta_i)w_4\end{aligned}\tag{A-1}$$

$$\begin{aligned}\text{where } f_1(\eta_i) &= \frac{1}{4} (2-3\eta_i + \eta_i^3) \\f_2(\eta_i) &= \frac{1}{4} (2-3\eta_i - \eta_i^3) \\f_3(\eta_i) &= \frac{h^{(i)}}{4} (1-\eta_i - \eta_i^2 + \eta_i^3) \\f_4(\eta_i) &= \frac{h^{(i)}}{4} (-1-\eta_i + \eta_i^2 + \eta_i^3)\end{aligned}$$

in which η_i is the vertical local coordinates with the property

$$-h^{(i)} \leq y_{(i)} \leq h^{(i)}; \quad -1 \leq \eta_i \leq 1. \quad \text{or } \eta_i = \frac{y_i}{h^{(i)}}.$$

u , v and w are function of x and z and are the nodal displacements of the i , $i+1$ node [Fig. 2.1].

The derivation of $f_1(\eta_i)$, $f_2(\eta_i)$, $f_3(\eta_i)$, and $f_4(\eta_i)$, is given in most finite element textbooks. It is also derived in Ref. [43].

For a particular lamina, the relevant stress-strain relations are

$$\begin{Bmatrix} \sigma_{xx}^{(i)} \\ \sigma_{yy}^{(i)} \\ \sigma_{zz}^{(i)} \end{Bmatrix} = \begin{bmatrix} C_{11}^{(i)} & C_{12}^{(i)} & C_{13}^{(i)} \\ C_{12}^{(i)} & C_{22}^{(i)} & C_{23}^{(i)} \\ C_{13}^{(i)} & C_{23}^{(i)} & C_{33}^{(i)} \end{bmatrix} \begin{Bmatrix} \epsilon_{xx}^{(i)} \\ \epsilon_{yy}^{(i)} \\ \epsilon_{zz}^{(i)} \end{Bmatrix}$$

$$\sigma_{yz}^{(i)} = C_{44}^{(i)} \gamma_{yz}^{(i)}$$

$$\sigma_{xz}^{(i)} = C_{55}^{(i)} \gamma_{xz}^{(i)}$$

$$\sigma_{xy}^{(i)} = C_{66}^{(i)} \gamma_{xy}^{(i)}$$

where $C_{ij}^{(i)}$ is the elastic constant of the $(i)^{th}$ layer

$\epsilon_{kk}^{(i)}$ is the normal strain in k-k plane

$\gamma_{mn}^{(i)}$ is the shear strain in m-n plane.

It is known from the theory of linear elasticity that

$$\epsilon_{xx}^{(i)} = \frac{\partial U_I}{\partial x} \quad ; \quad \gamma_{xy}^{(i)} = \frac{\partial V_I}{\partial x} + \frac{\partial U_I}{\partial y}$$

$$\epsilon_{yy}^{(i)} = \frac{\partial V_I}{\partial y} \quad ; \quad \gamma_{yz}^{(i)} = \frac{\partial W_I}{\partial y} + \frac{\partial V_I}{\partial z}$$

$$\epsilon_{zz}^{(i)} = \frac{\partial W_I}{\partial z} \quad ; \quad \gamma_{zx}^{(i)} = \frac{\partial U_I}{\partial z} + \frac{\partial W_I}{\partial x}$$

$$\text{let } \sigma_{yy}^{(i)} \Big|_{\eta=-1} = \sigma_i \quad ;$$

$$\sigma_{yx}^{(i)} \Big|_{\eta=-1} = \chi_i \quad ;$$

$$\text{and } \sigma_{yz}^{(i)} \Big|_{\eta=-1} = \tau_i$$

$$\begin{aligned} \text{Then } \sigma_{yy}^{(i)} &= C_{12}^{(i)} \frac{\partial U_I}{\partial x} + C_{22}^{(i)} \frac{\partial V_I}{\partial y} + C_{23}^{(i)} \frac{\partial W_I}{\partial z} \\ \sigma_{yx}^{(i)} &= C_{66}^{(i)} \left(\frac{\partial U_I}{\partial z} + \frac{\partial W_I}{\partial x} \right) \\ \sigma_{yz}^{(i)} &= C_{44}^{(i)} \left(\frac{\partial W_I}{\partial y} + \frac{\partial V_I}{\partial z} \right) \end{aligned}$$

In order to satisfy the stress continuity at the interface between two consecutive layers, the evaluation of σ_{yx} , σ_{yz} and σ_{yy} at the boundary nodes is required. With reference to Fig. 2.1, the boundary nodes are at $\eta_i = -1$ and $\eta_i = +1$.

For the I (superscript (i)) lamina and the i node

$$\begin{aligned} \sigma_{yx}^{(i)} \Big|_{\eta_i = -1} &= C_{66}^{(i)} \left[f_3'(-1) u_3 + \frac{\partial v_1}{\partial x} \right] \\ &= C_{66}^{(i)} \left[u_3 + \frac{\partial v_1}{\partial x} \right] = \chi_i \end{aligned}$$

$$\text{thus } u_3 = \left(\frac{\chi_i}{C_{66}^{(i)}} - \frac{\partial v_1}{\partial x} \right)$$

$$\sigma_{yx}^{(i)} \Big|_{\eta_i = +1} = C_{66}^{(i)} \left[u_4 + \frac{\partial v_2}{\partial x} \right] = \chi_{i+1}$$

$$\text{thus } u_4 = \left(\frac{\chi_{i+1}}{C_{66}^{(i)}} - \frac{\partial v_2}{\partial x} \right)$$

Similarly,

$$\sigma_{yy}^{(i)} \Big|_{\eta_i = -1} = C_{12}^{(i)} \frac{\partial u_1}{\partial x} + C_{22}^{(i)} v_3 + C_{23}^{(i)} \frac{\partial w_1}{\partial z} = \sigma_i$$

$$\text{thus, } v_3 = \frac{1}{C_{22}^{(i)}} \left[\sigma_i - C_{12}^{(i)} \frac{\partial u_1}{\partial x} - C_{23}^{(i)} \frac{\partial w_1}{\partial z} \right]$$

$$\sigma_{yy}^{(i)} \Big|_{\eta_i=+1} = C_{12}^{(i)} \frac{\partial u_2}{\partial x} + C_{22}^{(i)} v_4 + C_{23}^{(i)} \frac{\partial w_2}{\partial z} = \sigma_{i+1}$$

$$v_4 = \frac{1}{C_{22}^{(i)}} \left[\sigma_{i+1} - C_{12}^{(i)} \frac{\partial u_2}{\partial x} - C_{23}^{(i)} \frac{\partial w_2}{\partial z} \right]$$

and

$$\sigma_{yz}^{(i)} \Big|_{\eta_i=-1} = C_{44}^{(i)} \left(w_3 + \frac{\partial v_1}{\partial z} \right) = \tau_i$$

$$\text{thus, } w_3 = \left(\frac{\tau_i}{C_{44}^{(i)}} - \frac{\partial v_1}{\partial z} \right)$$

$$\sigma_{yz}^{(i)} \Big|_{\eta_i=+1} = C_{44}^{(i)} \left(w_4 + \frac{\partial v_2}{\partial z} \right) = \tau_{i+1}$$

$$w_4 = \left(\frac{\tau_{i+1}}{C_{44}^{(i)}} - \frac{\partial v_2}{\partial z} \right)$$

Realizing that subscript 2 above is referring to the i+1 node and by letting i+1 = j, the components of displacement equations become

$$U_I = f_1(\eta_i) u_i + f_2(\eta_i) u_j + f_3(\eta_i) \left[\frac{\chi_i}{C_{66}^{(i)}} - \frac{\partial v_i}{\partial x} \right] + f_4(\eta_i) \left[\frac{\chi_j}{C_{66}^{(i)}} - \frac{\partial v_j}{\partial x} \right]$$

$$V_I = f_1(\eta_i) v_i + f_2(\eta_i) v_j + f_3(\eta_i) \left[\frac{1}{C_{22}^{(i)}} \left(\sigma_i - C_{12}^{(i)} \frac{\partial u_i}{\partial x} - C_{23}^{(i)} \frac{\partial w_i}{\partial z} \right) \right] + f_4(\eta_i) \left[\frac{1}{C_{22}^{(i)}} \left(\sigma_j - C_{12}^{(i)} \frac{\partial u_j}{\partial x} - C_{23}^{(i)} \frac{\partial w_j}{\partial z} \right) \right]$$

$$W_I = f_1(\eta_i) w_i + f_2(\eta_i) w_j + f_3(\eta_i) \left[\frac{\tau_i}{C_{44}^{(i)}} - \frac{\partial v_i}{\partial z} \right] + f_4(\eta_i) \left[\frac{\tau_{i+1}}{C_{44}^{(i)}} - \frac{\partial v_j}{\partial z} \right]$$

A P P E N D I X B
INTEGRATION OF INTERPOLATION FUNCTION

APPENDIX B

In the derivation of the potential and kinetic energy (see Appendix C) several integrations involving the interpolation functions are considered. These integrals will be summarized below.

(A) The evaluation of the integral $\int_{-1}^1 \{f\} \{f\}^T d\eta$ can be given by the symmetric matrix [A], as shown:

$$\begin{aligned} A_{11} &= 78/105 & ; & & A_{12} &= 9/35 \\ A_{13} &= 22h/105 & ; & & A_{14} &= -13h/105 \\ A_{22} &= 78/105 & ; & & A_{23} &= 13h/105 \\ A_{24} &= -22h/105 & ; & & A_{33} &= 8h^2/105 \\ A_{34} &= -6h^2/105 & ; & & A_{44} &= 8h^2/105 \end{aligned}$$

(B) The evaluation of the integral $\int_{-1}^1 \{f'\} \{f'\}^T d\eta$ can be given by the symmetric matrix [B] as shown:

$$\begin{aligned} B_{11} &= 3/5 & ; & & B_{12} &= -3/5 \\ B_{13} &= h/10 & ; & & B_{14} &= h/10 \\ B_{22} &= 3/5 & ; & & B_{23} &= -h/10 \\ B_{24} &= -h/10 & ; & & B_{33} &= 4h^2/15 \\ B_{34} &= -h^2/15 & ; & & B_{44} &= 4h^2/15 \end{aligned}$$

(C) The evaluation of the integral $\int_{-1}^1 \{f\} \{f'\}^T d\eta$ can be given by the skew-symmetric matrix [D] as shown:

$$\begin{aligned} D_{11} &= -1/2 & ; & & D_{12} &= 1/2 \\ D_{13} &= h/5 & ; & & D_{14} &= -h/5 \\ D_{22} &= 1/2 & ; & & D_{23} &= -h/5 \\ D_{24} &= h/5 & ; & & D_{33} &= 0 \\ D_{34} &= -h^2/15 & ; & & D_{44} &= 0 \end{aligned}$$

A P P E N D I X C

EVALUATION OF THE INTEGRAL IN ENERGY EQUATION

(EQ. 2.10 OF CHAPTER 2)

APPENDIX C

(A) The evaluation of the integral $\int_{-1}^1 U \bar{U} d\eta_i$ can be given by the matrix [U] whose coefficients are:

$$\begin{aligned}
 U_{1,1} &= A_{11}^* & ; & & U_{1,2} &= A_{13}/C_{66} \\
 U_{1,3} &= -ik_x A_{13} & ; & & U_{1,7} &= A_{12} \\
 U_{1,8} &= A_{14}/C_{66} & ; & & U_{1,9} &= -ik_x A_{14} \\
 U_{2,2} &= A_{33}/C_{66}^2 & ; & & U_{2,3} &= -ik_x A_{33}/C_{66}^2 \\
 U_{2,7} &= A_{23}/C_{66} & ; & & U_{2,8} &= A_{34}/C_{66}^2 \\
 U_{2,9} &= -ik_x A_{34}/C_{66} & ; & & & \\
 U_{3,3} &= k_x^2 A_{33} & ; & & U_{3,7} &= ik_x A_{23} \\
 U_{3,8} &= ik_x A_{34}/C_{66} & ; & & U_{3,9} &= k_x^2 A_{34} \\
 U_{7,7} &= A_{22} & ; & & U_{7,8} &= A_{24}/C_{66} \\
 U_{7,9} &= -ik_x A_{24} & ; & & & \\
 U_{8,8} &= A_{44}/C_{66}^2 & ; & & U_{8,9} &= -ik_x A_{44}/C_{66} \\
 U_{9,9} &= k_x^2 A_{44} & & & &
 \end{aligned}$$

Notes: For the above coefficients of [U]

i) $i = \sqrt{-1}$

ii) [U] is a Hermitian matrix

iii) the rest of the coefficients that are not listed above are all equal to zero.

The notes applied to all other integrals unless specified otherwise.

(B) For the evaluation of the integral $\int_{-1}^1 U' \bar{U}' d\eta_i$ change $[A]_{ij}$ of U to $[B]_{ij}$.

*Matrix [A], [B] and [D] are given in Appendix B.

(C) The evaluation of the integral $\int_{-1}^1 V \bar{V} d\eta_1$, can be given by the matrix [V] where

$$\begin{aligned}
 V_{1,1} &= k_x^2 A_{33} C_{12}^2 / C_{22}^2 & ; & & V_{1,3} &= ik_x A_{13} C_{12} / C_{22} \\
 V_{1,4} &= ik_x A_{33} C_{12} / C_{22}^2 & ; & & V_{1,5} &= k_x k_z A_{33} C_{12} C_{23} / C_{22}^2 \\
 V_{1,7} &= k_x^2 A_{34} C_{12}^2 / C_{22}^2 & ; & & V_{1,9} &= ik_x A_{23} C_{12} / C_{22} \\
 V_{1,10} &= ik_x A_{34} C_{12} / C_{22}^2 & ; & & V_{1,11} &= k_x k_z A_{34} C_{12} C_{23} / C_{22}^2 \\
 V_{3,3} &= A_{11} & ; & & V_{3,4} &= A_{13} / C_{22} \\
 V_{3,5} &= -ik_z A_{13} C_{23} / C_{22} & ; & & V_{3,7} &= -ik_x A_{14} C_{12} / C_{22} \\
 V_{3,9} &= A_{12} & ; & & V_{3,10} &= A_{14} / C_{22} \\
 V_{3,11} &= -ik_z A_{14} C_{23} / C_{22} & ; & & & \\
 V_{4,4} &= A_{33} / C_{22}^2 & ; & & V_{4,5} &= -ik_z A_{33} C_{23} / C_{22}^2 \\
 V_{4,7} &= -ik_x A_{34} C_{12} / C_{22}^2 & ; & & V_{4,9} &= A_{23} / C_{22} \\
 V_{4,10} &= A_{34} / C_{22}^2 & ; & & V_{4,11} &= -ik_z A_{34} C_{23} / C_{22}^2 \\
 V_{5,5} &= k_z^2 A_{33} C_{23}^2 / C_{22}^2 & ; & & V_{5,7} &= k_x k_z A_{34} C_{12} C_{23} / C_{22}^2 \\
 V_{5,9} &= ik_z A_{23} C_{23} / C_{22} & ; & & V_{5,10} &= ik_z A_{34} C_{23} / C_{22}^2 \\
 V_{5,11} &= k_z^2 A_{34} C_{23}^2 / C_{22}^2 & ; & & & \\
 V_{7,7} &= k_x^2 A_{44} C_{12}^2 / C_{22}^2 & ; & & V_{7,9} &= ik_x A_{24} C_{12} / C_{22} \\
 V_{7,10} &= ik_x A_{44} C_{12} / C_{22}^2 & ; & & V_{7,11} &= k_x k_z A_{44} C_{12} C_{23} / C_{22}^2
 \end{aligned}$$

$$\begin{aligned}
 V_{9,9} &= A_{22} & ; & & V_{9,10} &= A_{24}/C_{22} \\
 V_{9,11} &= -ik_z A_{24} C_{23}/C_{22} & ; & & & \\
 V_{10,10} &= A_{44}/C_{22}^2 & ; & & V_{10,11} &= -ik_z A_{44} C_{23}/C_{22}^2 \\
 V_{11,11} &= k_z^2 A_{44} C_{23}^2/C_{22}^2 & & & &
 \end{aligned}$$

(D) For the evaluation of the integral $\int_{-1}^1 V' \bar{V}' d\eta_i$, change $[A]_{ij}$ of $[V]$ to $[B]_{ij}$

(E) The evaluation of the integral $\int_{-1}^1 W \bar{W} d\eta_i$, can be given by the matrix $[W]$ where

$$\begin{aligned}
 W_{3,3} &= k_z^2 A_{33} & ; & & W_{3,5} &= ik_z A_{13} \\
 W_{3,6} &= ik_z A_{33}/C_{44} & ; & & W_{3,9} &= k_z^2 A_{34} \\
 W_{3,11} &= ik_z A_{23} & ; & & W_{3,12} &= ik_z A_{34}/C_{44} \\
 W_{5,5} &= A_{11} & ; & & W_{5,6} &= A_{13}/C_{44} \\
 W_{5,9} &= -ik_z A_{14} & ; & & A_{5,11} &= A_{12} \\
 W_{5,12} &= A_{14}/C_{44} & ; & & & \\
 W_{6,6} &= A_{33}/C_{44}^2 & ; & & W_{6,9} &= -ik_z A_{34}/C_{44} \\
 W_{6,11} &= A_{23}/C_{44} & ; & & W_{6,12} &= A_{34}/C_{44}^2 \\
 W_{9,9} &= k_z^2 A_{44} & ; & & W_{9,11} &= ik_z A_{24} \\
 W_{9,12} &= ik_z A_{44}/C_{44} & ; & & & \\
 W_{11,11} &= A_{22} & ; & & W_{11,12} &= A_{24}/C_{44} \\
 W_{12,12} &= A_{44}/C_{44}^2 & & & &
 \end{aligned}$$

(F) For the evaluation of the integral $\int_{-1}^1 W' \bar{W}' d\eta_i$, change $[A]_{ij}$ of $[W]$ to $[B]_{ij}$.

(G) The evaluation of $\int_{-1}^1 (U \bar{V}' - V' \bar{U}) d\eta_i$ can be given by the matrix $[UV]$ as shown

$$\begin{aligned}
 UV_{1,1} &= 2 ik_x D_{13} C_{12}/C_{22} \\
 UV_{1,2} &= ik_x D_{33} C_{12} T_1 / (C_{22} C_{66}) \\
 UV_{1,3} &= (k_x^2 D_{33} C_{12}/C_{22} - D_{11}) T_1 \\
 UV_{1,4} &= -D_{13}/C_{22} \\
 UV_{1,5} &= ik_z D_{13} C_{23}/C_{22} \\
 UV_{1,7} &= ik_x D_{23} C_{12}/C_{22} + ik_x D_{14} C_{12}/C_{22} \\
 UV_{1,8} &= -ik_x D_{34} C_{12}/(C_{22} C_{66}) \\
 UV_{1,9} &= -k_x^2 D_{34} C_{12}/C_{22} - D_{12} \\
 UV_{1,10} &= -D_{14}/C_{22} \\
 UV_{1,11} &= ik_z D_{14} C_{23}/C_{22} \\
 UV_{2,3} &= D_{13}/C_{66} \\
 UV_{2,4} &= -D_{33} T_1 / (C_{22} C_{66}) \\
 UV_{2,5} &= ik_z D_{33} C_{23} T_1 / (C_{22} C_{66}) \\
 UV_{2,7} &= ik_x D_{34} C_{12}/(C_{22} C_{66}) \\
 UV_{2,9} &= D_{23}/C_{66} \\
 UV_{2,10} &= -D_{34}/(C_{22} C_{66}) \\
 UV_{2,11} &= ik_z D_{34} C_{23}/(C_{22} C_{66})
 \end{aligned}$$

$$\begin{aligned}
 UV_{3,3} &= 2 ik_x D_{13} \\
 UV_{3,4} &= -ik_x D_{33} T_1 / C_{22} \\
 UV_{3,5} &= -k_x k_z D_{33} C_{23} T_1 / C_{22} \\
 UV_{3,7} &= -D_{12} - k_x^2 D_{34} C_{12} / C_{22} \\
 UV_{3,8} &= -D_{14} / C_{66} \\
 UV_{3,9} &= ik_x D_{14} + ik_x D_{23} \\
 UV_{3,10} &= -ik_x D_{34} / C_{22} \\
 UV_{3,11} &= -k_x k_z D_{34} C_{23} / C_{22} \\
 UV_{4,7} &= D_{23} / C_{22} \\
 UV_{4,8} &= -D_{34} / (C_{22} C_{66}) \\
 UV_{4,9} &= ik_x D_{34} / C_{22} \\
 UV_{5,7} &= ik_z D_{23} C_{23} / C_{22} \\
 UV_{5,8} &= -ik_z D_{34} C_{23} / (C_{22} C_{66}) \\
 UV_{5,9} &= -k_x k_z D_{34} C_{23} / C_{22} \\
 UV_{7,7} &= 2 ik_x D_{24} C_{12} / C_{22} \\
 UV_{7,8} &= ik_x D_{44} C_{12} T_1 / (C_{22} C_{66}) \\
 UV_{7,9} &= (k_x^2 D_{44} C_{12} / C_{22} - D_{22}) T_1 \\
 UV_{7,10} &= -D_{24} / C_{22}
 \end{aligned}$$

$$\begin{aligned}
 UV_{7,11} &= ik_z D_{24} C_{23} / C_{22} \\
 UV_{8,9} &= D_{24} / C_{66} \\
 UV_{8,10} &= -D_{44} T_1 / (C_{22} C_{66}) \\
 UV_{8,11} &= ik_z D_{44} C_{23} T_1 / (C_{22} C_{66}) \\
 UV_{9,9} &= 2 ik_x D_{24} \\
 UV_{9,10} &= -ik_x D_{44} T_1 / C_{22} \\
 UV_{9,11} &= -k_x k_z D_{44} C_{23} T_1 / C_{22}
 \end{aligned}$$

where $T_1 = 1.0$

and $[UV]_{ji}$ is the negative of the conjugate of $[UV]_{ij}$

(H) For the evaluation of $\int_{-1}^1 (\bar{U}' - U'\bar{V}) d\eta_i$, set $T_1 = -1.0$ for $[UV]$.

(I) The evaluation of $\int_{-1}^1 (\bar{W}U + U\bar{W}) d\eta_i$ can be given by the matrix $[UW]$ as:

$$\begin{aligned}
 UW_{1,3} &= -ik_z A_{13} & ; & & UW_{1,5} &= A_{11} \\
 UW_{1,6} &= A_{13} / C_{44} & ; & & UW_{1,9} &= -ik_z A_{14} \\
 UW_{1,11} &= A_{12} & ; & & UW_{1,12} &= A_{14} / C_{44} \\
 UW_{2,3} &= -ik_z A_{33} / C_{66} & ; & & UW_{2,5} &= A_{13} / C_{66} \\
 UW_{2,6} &= A_{33} / (C_{44} C_{66}) & ; & & UW_{2,9} &= -ik_z A_{34} / C_{66} \\
 UW_{2,11} &= A_{23} / C_{66} & ; & & UW_{2,12} &= A_{34} / (C_{44} C_{66}) \\
 UW_{3,3} &= 2 k_x k_z A_{33} & ; & & UW_{3,5} &= ik_x A_{13} \\
 UW_{3,6} &= ik_x A_{33} / C_{44} & ; & & UW_{3,7} &= ik_z A_{23} \\
 UW_{3,8} &= ik_z A_{34} / C_{66} & ; & & UW_{3,9} &= k_x k_z A_{34}
 \end{aligned}$$

$$\begin{aligned}
 UW_{3,11} &= ik_x A_{23} & ; & & UW_{3,12} &= ik_x A_{34}/C_{44} \\
 UW_{5,7} &= A_{12} & ; & & UW_{5,8} &= A_{14}/C_{66} \\
 UW_{5,9} &= -ik_x A_{14} & ; & & & \\
 UW_{6,7} &= A_{23}/C_{44} & ; & & UW_{6,8} &= A_{34}/(C_{44} C_{66}) \\
 UW_{6,9} &= -ik_x A_{34}/C_{44} & ; & & & \\
 UW_{7,9} &= -ik_z A_{24} & ; & & UW_{7,11} &= A_{22} \\
 UW_{7,12} &= A_{24}/C_{44} & & & & \\
 UW_{8,9} &= -ik_z A_{44}/C_{66} & ; & & UW_{8,11} &= A_{24}/C_{66} \\
 UW_{8,12} &= A_{44}/(C_{44} C_{66}) & & & & \\
 UW_{9,9} &= 2k_x k_z A_{44} & ; & & UW_{9,11} &= ik_x A_{24} \\
 UW_{9,12} &= ik_x A_{44}/C_{44} & & & &
 \end{aligned}$$

(J) The evaluation of $\int_{-1}^1 (W \bar{V}' - V' \bar{W}) d\eta_i$ can be given by the matrix [WV] as shown

$$\begin{aligned}
 WV_{1,3} &= k_x k_z D_{33} C_{12} T_1 / C_{22} & ; & & & \\
 WV_{1,5} &= ik_x D_{13} C_{12} / C_{22} & ; & & WV_{1,6} &= ik_x D_{33} C_{21} T_1 / (C_{22} C_{44}) \\
 WV_{1,9} &= -k_x k_z D_{34} C_{12} / C_{22} & ; & & WV_{1,11} &= ik_x D_{23} C_{12} / C_{22} \\
 WV_{1,12} &= -ik_x D_{34} C_{12} / (C_{22} C_{44}) & ; & & & \\
 WV_{3,3} &= 2ik_z D_{13} & ; & & WV_{3,4} &= ik_z D_{33} T_1 / C_{22} \\
 WV_{3,5} &= (D_{11} - k_z^2 D_{33} C_{23} / C_{22}) T_1 & & & &
 \end{aligned}$$

$$WV_{3,6} = -D_{13}/C_{44}$$

$$WV_{3,7} = -k_x k_z D_{34} C_{12}/C_{22}$$

$$WV_{3,10} = -ik_z D_{34}/C_{22}$$

$$WV_{3,12} = -D_{14}/C_{44}$$

$$WV_{4,5} = D_{13}/C_{22}$$

$$WV_{4,9} = ik_z D_{34}/C_{22}$$

$$WV_{4,12} = -D_{34}/(C_{22} C_{44})$$

$$WV_{5,5} = 2ik_z D_{13} C_{23}/C_{22}$$

$$WV_{5,6} = ik_z D_{33} C_{23} T_1/(C_{22} C_{44})$$

$$WV_{5,7} = ik_x D_{14} C_{12}/C_{22}$$

$$WV_{5,10} = -D_{14}/C_{22}$$

$$WV_{5,11} = ik_z D_{23} C_{23}/C_{22} + ik_z D_{14} C_{23}/C_{22}$$

$$WV_{5,12} = -ik_z D_{34} C_{23}/(C_{22} C_{44})$$

$$WV_{6,7} = ik_x D_{34} C_{12}/(C_{22} C_{44})$$

$$WV_{6,10} = -D_{34}/(C_{22} C_{44})$$

$$WV_{7,9} = k_x k_z D_{44} C_{12} T_1/C_{22}$$

$$WV_{7,11} = ik_x D_{24} C_{12}/C_{22}$$

$$WV_{9,9} = 2ik_z D_{24}$$

$$WV_{9,11} = (D_{22} - k_z^2 D_{44} C_{23}/C_{22}) T_1$$

$$WV_{9,12} = -D_{24}/C_{44}$$

$$; \quad WV_{3,9} = ik_z D_{14} + ik_z D_{23}$$

$$; \quad WV_{3,11} = -D_{12} - k_z^2 D_{34} C_{23}/C_{22}$$

$$; \quad WV_{4,6} = D_{33} T_1/(C_{22} C_{44})$$

$$; \quad WV_{4,11} = D_{23}/C_{22}$$

$$; \quad WV_{5,9} = D_{12} - k_z^2 D_{34} C_{23}/C_{22}$$

$$; \quad WV_{6,9} = D_{23}/C_{44}$$

$$; \quad WV_{6,11} = ik_z D_{34} C_{23}/(C_{22} C_{44})$$

$$; \quad WV_{7,12} = ik_x D_{44} C_{12} T_1/(C_{22} C_{44})$$

$$; \quad WV_{9,10} = -ik_z D_{44} T_1/C_{22}$$

$$WV_{10,11} = D_{24}/C_{22} \quad ; \quad WV_{10,12} = +D_{44}T_1/(C_{22}C_{44})$$

$$WV_{11,11} = 2ik_x D_{24}C_{23}/C_{22}$$

$$WV_{11,12} = ik_z D_{44}C_{23}T_1/(C_{22}C_{44})$$

where $T_1 = 1.0$

and $[WV]_{ji}$ is the negative of the conjugate of $[WV]_{ij}$.

(K) For the evaluation of $\int_{-1}^1 (\bar{W}' - W\bar{V}') d\eta_1$, set $T_1 = -1.0$ for $[WV]$.

A P P E N D I X D

ASSEMBLY PROCESS OF STIFFNESS MATRIX

Using Floquet's Theory, we obtain $u_3 = u_1 * E$

$$u_4 = u_2 * E$$

where $E = e^{iky}$ is a constant.

Substituting these values of u_3 and u_4 into Eqs. D-3 and D-4, we obtain:

$$S_{21}^{(1)} u_1 + [S_{22}^{(1)} + S_{11}^{(2)}] u_2 + S_{12}^{(2)} (E u_1) = 0 \quad (D-5)$$

$$S_{21}^{(2)} u_2 + [S_{22}^{(2)} + S_{11}^{(3)}] (E u_1) + S_{12}^{(3)} (E u_2) = 0 \quad (D-6)$$

After rearranging Eqs. D-5 and D-6 can be written as

$$\begin{aligned} [S_{21}^{(1)} + ES_{12}^{(2)}] u_1 + [S_{22}^{(1)} + S_{11}^{(2)}] u_2 &= 0 \\ E [S_{22}^{(2)} + S_{11}^{(3)}] u_1 + [S_{21}^{(2)} + ES_{12}^{(3)}] u_2 &= 0 \end{aligned}$$

Thus, by this assembly process, the same number of equations as the number of unknowns can be obtained.

A P P E N D I X E
EVALUATION OF EULER EQUATION
(EQ. 3.43 OF CHAPTER 3)

APPENDIX E

In the effective stiffness method, the 12 dependent variables can be derived by coordinatizing a system of Euler equations which were written as

$$\sum_{r=1}^4 \frac{\partial}{\partial q_r} \left[\frac{\partial (T_k - V_p - \lambda_1 S_1 - \lambda_2 S_2 - \lambda_3 S_3)}{\partial (\partial f_s / \partial q_r)} \right] - \frac{\partial (T_k - V_p - \lambda_1 S_1 - \lambda_2 S_2 - \lambda_3 S_3)}{\partial f_s} = 0 \quad (E-1)$$

where f_s represent the twelve dependent variables

$(U, V, W, \psi_{2x}^f, \psi_{2x}^m, \psi_{2y}^f, \psi_{2y}^m, \psi_{2z}^f, \psi_{2z}^m, \lambda_1, \lambda_2, \lambda_3)$

and q_r are the spatial variables x, y, z , and time t

(I) For $f_s = U$, the Euler Equation become:

$$\frac{\partial}{\partial x} \left[\frac{\partial F}{\partial (\partial U / \partial x)} \right] - \frac{\partial F}{\partial U} + \frac{\partial}{\partial y} \left[\frac{\partial F}{\partial (\partial U / \partial y)} \right] - \frac{\partial F}{\partial U} + \frac{\partial}{\partial z} \left[\frac{\partial F}{\partial (\partial U / \partial z)} \right] - \frac{\partial F}{\partial U} + \frac{\partial}{\partial t} \left[\frac{\partial F}{\partial (\partial U / \partial t)} \right] - \frac{\partial F}{\partial U} = 0$$

$$\text{where } F = T_k - V_p - \lambda_1 S_1 - \lambda_2 S_2 - \lambda_3 S_3$$

$\frac{\partial F}{\partial U} = 0$, using the notation $\frac{\partial}{\partial x} = \partial_1, \frac{\partial}{\partial y} = \partial_2, \frac{\partial}{\partial z} = \partial_3$, the equation

$$\text{become: } \partial_1 \left[\frac{\partial F}{\partial (\partial_1 U)} \right] + \partial_2 \left[\frac{\partial F}{\partial (\partial_2 U)} \right] + \partial_3 \left[\frac{\partial F}{\partial (\partial_3 U)} \right] + \frac{\partial}{\partial t} \left[\frac{\partial F}{\partial \dot{U}} \right] = 0$$

$$\partial_1 \left\{ \begin{aligned} \frac{\partial T_k}{\partial (\partial_1 U)} &= 0 \\ \frac{\partial V_p}{\partial (\partial_1 U)} &= \{ n c_{11}^f + (1-n) c_{11}^m \} (\partial_1 U) + n c_{12}^f \psi_{2y}^f + \{ n c_{13}^f + (1-n) c_{13}^m \} \partial_3 W \\ &\quad + (1-n) c_{12}^m \psi_{2y}^m \\ \frac{\partial \lambda_1 S_1}{\partial (\partial_1 U)} &= \frac{\partial \lambda_2 S_2}{\partial (\partial_1 U)} = \frac{\partial \lambda_3 S_3}{\partial (\partial_1 U)} = 0 \\ \frac{\partial F}{\partial U} &= 0 \end{aligned} \right.$$

$$\partial_2 \begin{cases} \frac{\partial T_k}{\partial(\partial_2 U)} = 0 \\ \frac{\partial V_f}{\partial(\partial_2 U)} = 0 \\ \frac{\partial \lambda_1 s_1}{\partial(\partial_2 U)} = \lambda_1, \frac{\partial \lambda_2 s_2}{\partial(\partial_2 U)} = \frac{\partial \lambda_3 s_3}{\partial(\partial_2 U)} = 0 \end{cases}$$

$$\partial_3 \begin{cases} \frac{\partial T_k}{\partial(\partial_3 U)} = 0 \\ \frac{\partial V_p}{\partial(\partial_3 U)} = \{n c_{55}^f + (1-n) c_{55}^m\} \{ \partial_3 U + \partial_1 W \} \\ \frac{\partial \lambda_1 s_1}{\partial(\partial_3 U)} = \frac{\partial \lambda_2 s_2}{\partial(\partial_3 U)} = \frac{\partial \lambda_3 s_3}{\partial(\partial_3 U)} = 0 \end{cases}$$

$$\frac{\partial}{\partial t} \begin{cases} \frac{\partial T_k}{\partial \dot{U}} = \rho_c \dot{U} \\ \frac{\partial V_p}{\partial \dot{U}} = \frac{\partial \lambda_1 s_1}{\partial \dot{U}} = \frac{\partial \lambda_2 s_2}{\partial \dot{U}} = \frac{\partial \lambda_3 s_3}{\partial \dot{U}} = 0 \end{cases}$$

Then, the Euler equation becomes

$$-\{n c_{11}^f + (1-n) c_{11}^m\} \partial_{11} U - n c_{12}^f \partial_1 \psi_{2y}^f - \{n c_{13}^f + (1-n) c_{13}^m\} \partial_{13} W - (1-n) c_{12}^m \partial_1 \psi_{2y}^m - \partial_2 \lambda_1 - \{n c_{55}^f + (1-n) c_{55}^m\} \{ \partial_{33} U + \partial_{31} W \} + \rho_c \ddot{U} = 0$$

or

$$\begin{aligned} & \{n c_{11}^f + (1-n) c_{11}^m\} \partial_{11} U + \{n c_{55}^f + (1-n) c_{55}^m\} \partial_{33} U + \{[n c_{13}^f + (1-n) c_{13}^m] \\ & + [n c_{55}^f + (1-n) c_{55}^m]\} \partial_{13} W + n c_{12}^f \partial_1 \psi_{2y}^f + (1-n) c_{12}^m \partial_1 \psi_{2y}^m \\ & + \partial_2 \lambda_1 = \rho_c \ddot{U} \end{aligned} \tag{E-2}$$

The other 11 equations can be derived in a similar way.

A P P E N D I X F
ELEMENTS OF THE IMPEDANCE MATRIX

APPENDIX F

Omitting the superscript (i) for the (i)th lamina and defining

$$Q_n = \eta C_{nn}^f + (1 - \eta) C_{nn}^m \quad \text{where } n = 1, 2, \dots, 6$$

$$Q_7 = \eta C_{13}^f + (1 - \eta) C_{13}^m$$

[S^P] is a 12 x 12 Hermitian matrix whose non-zero elements are given by:

$$S_{1,1}^P = -k_x^2 Q_1 - k_z^2 Q_5 - \rho_c \omega^2$$

$$S_{1,3}^P = -k_x k_z Q_5 Q_7$$

$$S_{1,8}^P = ik_x \eta C_{12}^f$$

$$S_{1,9}^P = ik_x (1 - \eta) C_{12}^m$$

$$S_{1,10}^P = S_{2,11}^P = S_{3,12}^P = -ik_y$$

$$S_{2,2}^P = -k_x^2 Q_6 - k_z^2 Q_4 - \rho_c \omega^2$$

$$S_{2,4}^P = ik_x \eta C_{66}^f$$

$$S_{2,5}^P = ik_x (1 - \eta) C_{66}^m$$

$$S_{2,6}^P = ik_z \eta C_{44}^f$$

$$S_{2,7}^P = ik_z (1 - \eta) C_{44}^m$$

$$S_{3,3}^P = -k_x^2 Q_5 - k_z^2 Q_3 - \rho_c \omega^2$$

$$S_{3,8}^P = ik_z \eta C_{23}^f$$

$$S_{3,9}^P = ik_z (1 - \eta) C_{23}^m$$

$$S_{4,4}^P = -\frac{1}{12} \eta d_f^2 [k_x^2 C_{11}^f + k_z^2 C_{55}^f] - \eta C_{66}^f - \rho_c \omega^2$$

$$S_{4,6}^P = -\frac{1}{12} \eta d_f^2 k_x k_z [C_{13}^f + C_{55}^f]$$

$$S_{4,10}^P = S_{6,12}^P = S_{8,11}^P = -\eta$$

$$S_{5,5}^p = -\frac{1}{12} (1 - \eta) d_m^2 [k_x^2 C_{11}^m + k_z^2 C_{55}^m] - (1 - \eta) C_{66}^m - \rho_c \omega^2$$

$$S_{5,7}^p = -\frac{1}{12} (1 - \eta) d_m^2 k_x k_z [C_{13}^m + C_{55}^m]$$

$$S_{5,10}^p = S_{7,12}^p = S_{9,11}^p = -(1 - \eta)$$

$$S_{6,6}^p = -\frac{1}{12} \eta d_f^2 [k_x^2 C_{55}^f + k_z^2 C_{33}^f] - \eta C_{44}^f - \rho_c \omega^2$$

$$S_{7,7}^p = -\frac{1}{12} (1 - \eta) d_m^2 [k_x^2 C_{55}^m + k_z^2 C_{33}^m] - (1 - \eta) C_{44}^m - \rho_c \omega^2$$

$$S_{8,8}^p = -\frac{1}{12} \eta d_f^2 [k_x^2 C_{66}^f + k_z^2 C_{44}^f] - \eta C_{22}^f - \rho_c \omega^2$$

$$S_{9,9}^p = -\frac{1}{12} (1 - \eta) d_m^2 [k_x^2 C_{66}^m + k_z^2 C_{44}^m] - (1 - \eta) C_{22}^m - \rho_c \omega^2$$

f denotes the reinforced layer

m is the matrix layer

C_{ij} is the material constants of the layer

k_x, k_y, k_z are the components of wave number in the x, y and z-direction

ω is the angular frequency

η is defined in Eq. 3.25 ; $\eta = \frac{d_f}{d_f + d_m}$

ρ_c is defined in Eq. 3.38 ; $\rho_c = \eta \rho_f + (1 - \eta) \rho_m$

A P P E N D I X G

FORMULA TO CALCULATE THE MATERIAL CONSTANTS

OF GRAPHITE-EPOXY FIBER-REINFORCED COMPOSITE

APPENDIX G

The material constants of graphite-epoxy fiber-reinforced composite are given as:

$$\begin{aligned} C_{11} &= E_L + 2 \nu_{LT} C_{13} \\ C_{13} &= C_{12} = 2 \nu_{LT} K_T \\ C_{22} &= C_{33} = K_T + \mu_{TT} \\ C_{23} &= K_T - \mu_{TT} \\ C_{44} &= \mu_{TT} = \frac{1}{2} (C_{33} - C_{23}) \\ C_{55} &= C_{66} = \mu_{LT} \end{aligned}$$

where

- E_L = lateral modulus of elasticity
- ν_{LT} = Poission's ratio
- K_T = Bulk's modulus
- μ_{TT} = transverse shear modulus
- μ_{LT} = lateral shear modulus

The constants E_L , K_T , μ_{LT} , μ_{TT} and ν_{LT} are determined from the properties of graphite and epoxy.

Epoxy matrix is isotropic with properties denoted by subscript m.

Its material properties are given as:

$$\begin{aligned} E_m &= 5.35 * 10^9 \text{ N/m}^2 \\ K_m &= 6.06 * 10^9 \text{ N/m}^2 \\ \mu_m &= 1.95 * 10^9 \text{ N/m}^2 \\ \nu_m &= 0.353 \end{aligned}$$

The graphite fibers layer are transversely isotropic with properties given by the primed quantities.

$$\begin{aligned} E'_L &= 2.32 * 10^{11} \text{ N/m}^2 \\ K'_T &= 15.0 * 10^9 \text{ N/m}^2 \\ \mu'_{LT} &= 24.0 * 10^9 \text{ N/m}^2 \\ \mu'_{TT} &= 5.02 * 10^9 \text{ N/m}^2 \\ \nu'_{LT} &= 0.290 \end{aligned}$$

With these properties of graphite and epoxy, E_L , K_T , μ_{LT} , μ_{TT} and ν_{LT} can be obtained using the following relations.

$$\begin{aligned} D_1 &= \frac{1 - \bar{c}}{K'} + \frac{\bar{c}}{K_m} + \frac{1}{\mu_m} \\ E_L &= E_m (1 - \bar{c}) + \bar{c} E'_L + \frac{4\bar{c}(1-\bar{c}) (\nu'_{LT} - \nu_m)^2}{D_1} \\ \nu_{LT} &= \nu_m (1-\bar{c}) + \bar{c} \nu'_{LT} + \frac{\bar{c}(1-\bar{c}) (\nu'_{LT} - \nu_m) \left(\frac{1}{K_m} - \frac{1}{K'_T}\right)}{D_1} \\ K_T &= K_m + \frac{\bar{c}(K_m + \mu_m) (K'_T - K_m)}{(1-\bar{c}) K'_T + \bar{c}K_m + \mu_m} \\ \frac{\mu_{TT}}{\mu_m} &= 1 + \frac{2\bar{c} (K_m + \mu_m) (\mu'_{TT} - \mu_m)}{K_m \mu_m + (K_m + 2\mu_m) [\bar{c}\mu_m + (1-\bar{c}) \mu'_{TT}]} \\ n &= \mu'_{LT} / \mu_m \\ \frac{\mu_{LT}}{\mu_m} &= \frac{1 + \bar{c}(n-1)/(n+1)}{1 - \bar{c}(n-1)/(n+1)} \end{aligned}$$

In the above relations, \bar{c} is a constant value that can be chosen to determine the various material constants for different types of graphite epoxy fiber reinforced composite. \bar{c} is chosen to be 0.3 and 0.668 for the two cases of presentation mentioned in Chapter 4. The computed material constants are shown in Table 4.3 and Table 4.4 respectively.

A P P E N D I X H

FORTRAN PROGRAM FOR THE EFFECTIVE MODULUS METHOD

```

10. C
20. C *****
30. C *
40. C *           EFFECTIVE MODULIS METHOD           *
50. C *           PROGRAMMED BY                     *
60. C *           JOHNNY K.T. YEO                   *
70. C *           THE UNIVERSITY OF MANITOBA         *
80. C *           DECEMBER, 1982                     *
90. C *
100. C *****

```

```

110. C
120. C NOTES :
130. C 1) ALL INPUTS ARE FORMAT-FREE.
140. C 2) NLayer, IPRINT, NKBAR, NPHI, NALFA ARE INTEGER VALUES
150. C 3) H, C, RHO, KBAR ARE REAL
160. C

```

```

170. C .....
180. C

```

```

190. C           INPUT DESCRIPTION
200. C

```

```

210. C .....
220. C

```

- 230. C A. START CARD - ONE CARD FOR NLayer AND IPRINT.
- 240. C * NLayer = NUMBER OF LAYERS
- 250. C * IPRINT = NUMBER OF SETS OF VECTORS AS OUTPUT
- 260. C
- 270. C B. MATERIAL PROPERTIES CARD - NLayer OF CARDS FOR :
- 280. C H(I), C11(I), C12(I), C13(I), C22(I), C23(I),
- 290. C C33(I), C44(I), C55(I), C66(I), RHO(I)
- 300. C * H(I) = LAYER THICKNESS
- 310. C * CJK(I) = MATERIAL CONSTANTS OF THE LAYER
- 320. C * RHO(I) = DENSITY OF THE MATERIAL
- 330. C * I = 1 TO NLayer
- 340. C
- 350. C C. BASIC CONTROL CARD - ONE CARD FOR NKBAR.
- 360. C * NKBAR = NUMBER OF WAVE NUMBER TO BE EVALUATED
- 370. C
- 380. C D. WAVE NUMBER CARD - AS MANY CARDS AS REQUIRED FOR KBAR.
- 390. C * KBAR(J) = VALUE OF WAVE NUMBER
- 400. C * J = 1 TO NKBAR
- 410. C
- 420. C E. ANGLE CONTROL CARD - ONE CARD FOR NPHI
- 430. C * NPHI = NUMBER OF VERTICAL ANGLES
- 440. C
- 450. C F. VERTICAL ANGLE CARD - AS MANY CARDS AS REQUIRED FOR PHI.
- 460. C * PHI(K) = VERTICAL ANGLES IN DEGREE.
- 470. C * K = 1 TO NPHI
- 480. C
- 490. C G. ANGLE CONTROL CARD - ONE CARD FOR NALFA
- 500. C * NALFA = NUMBER OF HORIZONTAL ANGLES
- 510. C
- 520. C H. HORIZONTAL ANGLES CARD - AS MANY CARDS AS REQUIRED FOR ALFA.
- 530. C * ALFA(L) = HORIZONTAL ANGLE IN DEGREE
- 540. C * L = 1 TO NALFA
- 550. C

```

560. C .....
570. C

```

```

580. C           OUTPUT DESCRIPTION
590. C

```

```

600. C .....
610. C

```

```

620. C
630. C ZETA = DIMENSIONLESS WAVE NUMBER
640. C OM(M) = PHASE VELOCITY OF PROPAGATING WAVE

```

```
650. C
660. C .....
670. C .....
680. C
690. C          SAMPLE DATA
700. C .....
710. C .....
720. C CARD A : 2 1
730. C CARD B :
740. C      8.0 2.56 0.583 0.583 1.797 0.745 1.797 0.526 0.559 0.559 2.534
750. C      0.5 1.107 0.573 0.573 1.107 0.573 1.107 0.267 0.267 0.267 2.702
760. C CARD C : 1
770. C CARD D : 0.0
780. C CARD E : 1
790. C CARD F : 45
800. C CARD G : 1
810. C CARD H : 45
820. C
830. C .....
840. C .....
850. C .....
860. C .....
870. C **** DECLARATION ****
880. C
890. C      INTEGER L1,L2,L3,N1,N2,N3
900. C      REAL*8 PI,H(2),C11(2),C12(2),C13(2),C22(2),C23(2),
910. C      C33(2),C44(2),C55(2),C66(2),RHO(2),ZETA(20)
920. C      REAL*8 KHBAR,XK,XK2,ZK,ZK2,YK,YK2,KBAR(20),PHI(10),ALFA(10)
930. C      COMPLEX*16 A(3,3),B(3,3),EIGA(3),EIGB(3),OM(3),
940. C      OMSQ(3),Z(3,3),WK(3,6),CIMGG,ZERO
950. C
960. C      ZERO=(0.0,0.0)
970. C      CIMGG=(0.0,1.0)
980. C      PI=4.*ATAN(1.0)
990. C
1000. C ***** MAIN LINE PROGRAM *****
1010. C
1020. C      CALL TRAPS(99999, 99999, 99999, 99999, 99999)
1030. C
1040. C THIS SUBROUTINE WILL TRAPS ANY NUMBER APPROACHING ZERO
1050. C
1060. C
1070. C      READ IN NUMBER OF LAYERS
1080. C
1090. C      READ, N LAYER , IPRINT
1100. C
1110. C      READ IN PROPERTIES OF EACH LAYER
1120. C
1130. C      READ, (H(1),C11(1),C12(1),C13(1),C22(1),C23(1),C33(1),
1140. C      C44(1),C55(1),C66(1),RHO(1),I=1,N LAYER)
1150. C      PRINT 10, N LAYER
1160. C 10 FORMAT ('1'////,40X,'NUMBER OF LAYERS =',3X,12'////,1X,
1170. C      ' LAYER PROPERTIES *'//)
1180. C      DO 20 I=1,N LAYER
1190. C          PRINT 30, I,H(1),C11(1),C12(1),C13(1),C22(1)
1200. C          PRINT 31,C23(1),C33(1),C44(1),C55(1),C66(1),RHO(1)
1210. C 30 FORMAT ('-',' LAYER=',12,2X,'H =',G16.9,'C11=',G16.9,
1220. C      'C12=',G16.9,'C13=',G16.9,'C22=',G16.9)
1230. C 31 FORMAT ('0',9X,'C23=',G16.9,'C33=',G16.9,'C44=',G16.9,
1240. C      'C55=',G16.9,'C66=',G16.9,'RHO=',G16.9)
1250. C 20 CONTINUE
1260. C
1270. C      DBAR = H(1)/H(2)
1280. C      C11BAR=((DBAR*C11(1)+C11(2))*C22(1)+DBAR*C22(2))
```

```
1290. .      -DBAR*(C12(1)-C12(2))**2)/((1+DBAR)*(C22(1)
1300. .      +DBAR*C22(2)))
1310. C12BAR=(C22(1)*C12(2)+DBAR*C12(1)*C22(2))/
1320. .      (C22(1)+DBAR*C22(2))
1330. C13BAR=((DBAR*C13(1)+C13(2))*(C22(1)+DBAR*C22(2))
1340. .      +(C23(2)-C23(1))*DBAR*(C12(1)-C12(2)))
1350. .      /((1+DBAR)*(C22(1)+DBAR*C22(2)))
1360. C
1370. C22BAR=((1+DBAR)*C22(1)*C22(2))/((C22(1)+DBAR*C22(2)))
1380. C23BAR=(DBAR*C23(1)*C22(2)+C23(2)*C22(1))/(C22(1)+DBAR*C22(2))
1390. C
1400. C33BAR=((DBAR*C33(1)+C33(2))*(C22(1)+DBAR*C22(2))
1410. .      -DBAR*(C23(1)-C23(2))**2)/
1420. .      ((1+DBAR)*(C22(1)+DBAR*C22(2)))
1430. C
1440. C44BAR=(1+DBAR)*C44(1)*C44(2)/(DBAR*C44(2)+C44(1))
1450. C55BAR=(DBAR*C55(1)+C55(2))/(DBAR+1)
1460. C66BAR=((1+DBAR)*C66(1)*C66(2))/(DBAR*C66(2)+C66(1))
1470. C
1480. RHOBAR=(RHO(2)+DBAR*RHO(1))/(1.+DBAR)
1490. C
1500. C
1510. NUM =1
1520. PRINT 40
1530. 40  FORMAT ('0'///,5X,'THE EFFECTIVE MODULUS OF THE TWO LAYERS IS '/')
1540. PRINT 30,NUM,H(1)+H(2),C11BAR,C12BAR,C13BAR,C22BAR
1550. PRINT 31, C23BAR,C33BAR,C44BAR,C55BAR,C66BAR,RHOBAR
1560. C
1570. C
1580. READ, NKBAR
1590. DO 50 L1=1,NKBAR
1600. READ, KBAR(L1)
1610. ZETA(L1) = H(1)*KBAR(L1)
1620. 50  CONTINUE
1630. C
1640. C ***** READ PHI IN DEGREE *****
1650. C
1660. READ, NPHI
1670. DO 60 L2=1,NPHI
1680. READ, PHI(L2)
1690. 60  CONTINUE
1700. C
1710. C ***** READ ALFA IN DEGREE *****
1720. C
1730. READ, NALFA
1740. DO 65 L3=1,NALFA
1750. READ, ALFA(L3)
1760. 65  CONTINUE
1770. C
1780. C
1790. DO 70 N1=1,NKBAR
1800. PRINT 75, KBAR(N1), ZETA(N1)
1810. 75  FORMAT ('-' ,///,10X,'KBAR =',F12.8,5X,'ZETA=',F12.8//)
1820. DO 80 N2=1,NPHI
1830. ANGLE = PHI(N2)*PI/180.
1840. KHBAR = KBAR(N1)*COS(ANGLE)
1850. YK = KBAR(N1)*SIN(ANGLE)
1860. DO 90 N3=1,NALFA
1870. ROT =ALFA(N3)*PI/180
1880. XK =KHBAR*COS(ROT)
1890. ZK = KHBAR*SIN(ROT)
1900. PRINT 100,PHI(N2),YK,ALFA(N3),XK,ZK
1910. 100  FORMAT (' ',3X,'PHI =',F8.5,3X,'KAPAY =',F10.7,3X,
1920. .      'ALFA =',F8.5,3X,'KAPAX =',F10.7,3X,
```

```
1930.      'KAPAZ =',F10.7)
1940.      DO 11 JJ=1,3
1950.      DO 22 KK=1,3
1960.      A (JJ, KK) =ZERO
1970.      B (JJ, KK) =ZERO
1980. 22    CONTINUE
1990. 11    CONTINUE
2000. C
2010.      XK2 = XK*XK
2020.      YK2 = YK*YK
2030.      ZK2 = ZK*ZK
2040. C
2050. C ***** FORMULATION OF THE A MATRIX *****
2060. C
2070.      A (1, 1) =-C11BAR*XK2-C66BAR*YK2-C55BAR*ZK2
2080.      A (1, 2) =-XK*YK*(C12BAR+C66BAR)
2090.      A (1, 3) =-XK*ZK*(C13BAR+C55BAR)
2100. C
2110.      A (2, 1) = A (1, 2)
2120.      A (2, 2) =-C66BAR*XK2-C22BAR*YK2-C44BAR*ZK2
2130.      A (2, 3) =-YK*ZK*(C23BAR+C44BAR)
2140. C
2150.      A (3, 1) = A (1, 3)
2160.      A (3, 2) = A (2, 3)
2170.      A (3, 3) =-C55BAR*XK2-C44BAR*YK2-C33BAR*ZK2
2180. C
2190. C ***** FORMULATION OF B MATRIX
2200. C
2210.      B (1, 1) =-RHOBAR
2220.      B (2, 2) =-RHOBAR
2230.      B (3, 3) =-RHOBAR
2240. C
2250. C
2260.      IJOB=1
2270.      IA =3
2280.      IB =3
2290.      IZ =3
2300.      N =3
2310.      CALL EIGZC (A, IA, B, IB, N, IJOB, EIGA, EIGB, Z, IZ, WK
2320.      , INFER, IER)
2330.      DO 120 M=1,3
2340.      OMSQ (M) =EIGA (M) /EIGB (M)
2350.      OM (M) =CDSQRT (OMSQ (M)) / (C44 (2) /RHO (2)) **0.5
2360.      OM (M) =OM (M) /KBAR (N1)
2370.      PRINT 125, M, OM (M)
2380. 125    FORMAT ('0', 1X, 12, 5X, 2G16.9)
2390. 120    CONTINUE
2400.      IF (IPRINT .GT. 0) THEN DO
2410.      IV=1
2420.      PRINT 140, IV
2430. 140    FORMAT ('0'//, 1X, 'M', 10X, 'THE CORRESPONDING Z MATRIX'
2440.      ' OF CELL ', 11, 1X, 'IS :'//)
2450.      DO 150 K=1,3
2460.      PRINT 160, K, (Z (L, K), L=1, 3)
2470. 160    FORMAT ('0', 12, 1X, 3 (2F10.6, 1X))
2480. 150    CONTINUE
2490.      IPRINT=IPRINT-1
2500.      END IF
2510. C
2520. 90      CONTINUE
2530. 80      CONTINUE
2540. 70      CONTINUE
2550.      STOP
2560.      END
```

A P P E N D I X I

FORTRAN PROGRAM FOR THE EFFECTIVE STIFFNESS METHOD

10. C
20. C *****
30. C *
40. C * EFFECTIVE STIFFNESS METHOD *
50. C * PROGRAMMED BY *
60. C * JOHNNY K.T. YEO *
70. C * UNIVERSITY OF MANTIBA *
80. C *
90. C *****

100. C
110. C NOTES :
120. C 1) ALL INPUTS ARE FORMAT-FREE.
130. C 2) NLayer, IPRINT, NKBAR, NPHI, NALFA ARE INTEGER VALUES
140. C 3) H, C, RHO, KBAR ARE REAL
150. C

160. C

170. C
180. C INPUT DESCRIPTION
190. C
200. C

210. C
220. C A. START CARD - ONE CARD FOR NLayer AND IPRINT.
230. C * NLayer = NUMBER OF LAYERS
240. C * IPRINT = NUMBER OF SETS OF VECTORS AS OUTPUT
250. C
260. C B. MATERIAL PROPERTIES CARD - NLayer OF CARDS FOR :
270. C H(I), C11(I), C12(I), C13(I), C22(I), C23(I),
280. C C33(I), C44(I), C55(I), C66(I), RHO(I)
290. C * H(I) = LAYER THICKNESS
300. C * CJK(I) = MATERIAL CONSTANTS OF THE LAYER
310. C * RHO(I) = DENSITY OF THE MATERIAL
320. C * I = 1 TO NLayer
330. C
340. C C. BASIC CONTROL CARD - ONE CARD FOR NKBAR.
350. C * NKBAR = NUMBER OF WAVE NUMBER TO BE EVALUATED
360. C
370. C D. WAVE NUMBER CARD - AS MANY CARDS AS REQUIRED FOR KBAR.
380. C * KBAR(J) = VALUE OF WAVE NUMBER
390. C * J = 1 TO NKBAR
400. C
410. C E. ANGLE CONTROL CARD - ONE CARD FOR NPHI
420. C * NPHI = NUMBER OF VERTICAL ANGLES
430. C
440. C F. VERTICAL ANGLE CARD - AS MANY CARDS AS REQUIRED FOR PHI.
450. C * PHI(K) = VERTICAL ANGLES IN DEGREE.
460. C * K = 1 TO NPHI
470. C
480. C G. ANGLE CONTROL CARD - ONE CARD FOR NALFA
490. C * NALFA = NUMBER OF HORIZONTAL ANGLES
500. C
510. C H. HORIZONTAL ANGLES CARD - AS MANY CARDS AS REQUIRED FOR ALFA.
520. C * ALFA(L) = HORIZONTAL ANGLE IN DEGREE
530. C * L = 1 TO NALFA
540. C
550. C

560. C

570. C
580. C OUTPUT DESCRIPTION
590. C
600. C

610. C
620. C ZETA = DIMENSIONLESS WAVE NUMBER
630. C OM(M) = PHASE VELOCITY OF PROPAGATING WAVE
640. C

```
650. C .....
660. C
670. C          SAMPLE DATA
680. C
690. C .....
700. C
710. C CARD A : 2   1
720. C CARD B :
730. C      8.0 2.56 0.583 0.583 1.797 0.745 1.797 0.526 0.559 0.559 2.534
740. C      0.5 1.107 0.573 0.573 1.107 0.573 1.107 0.267 0.267 0.267 2.702
750. C CARD C : 1
760. C CARD D : 0.0
770. C CARD E : 1
780. C CARD F : 45
790. C CARD G : 1
800. C CARD H : 45
810. C
820. C .....
830. C
840. C
850. C
860. C **** DECLARATION      ****
870. C
880. C      INTEGER L1,L2,L3,N1,N2,N3
890. C      REAL*8  PI,H(2),C11(2),C12(2),C13(2),C22(2),C23(2),
900. C      .      C33(2),C44(2),C55(2),C66(2),RHO(2)
910. C      REAL*8  ETA,DF,DM,RHOF,RHOM,RHOC,IFF,IMM,KHBAR,
920. C      .      XK,XK2,ZK,ZK2,YK,KBAR(20),PHI(10),ALFA(10),ZETA(20)
930. C      COMPLEX*16 A(12,12),B(12,12),EIGA(12),EIGB(12),OM(12),
940. C      .      OMSQ(12),Z(12,12),WK(12,24),CIMGG,ZERO
950. C
960. C      ZERO=(0.0,0.0)
970. C      CIMGG=(0.0,1.0)
980. C      PI  =4.*ATAN(1.0)
990. C
1000. C ***** MAIN LINE PROGRAM *****
1010. C
1020. C      CALL TRAPS(99999, 99999, 99999, 99999, 99999)
1030. C
1040. C THIS SUBROUTINE WILL TRAPS ANY NUMBER APPROACHING ZERO
1050. C
1060. C
1070. C      READ IN NUMBER OF LAYERS
1080. C
1090. C      READ, N LAYER , IPRINT
1100. C
1110. C      READ IN PROPERTIES OF EACH LAYER
1120. C
1130. C      READ, (H(I),C11(I),C12(I),C13(I),C22(I),C23(I),C33(I),
1140. C      .      C44(I),C55(I),C66(I),RHO(I),I=1,N LAYER)
1150. C      PRINT 10, N LAYER
1160. C 10  FORMAT ('1'////,40X,'NUMBER OF LAYERS =',3X,12////,1X,
1170. C      .      'LAYER PROPERTIES *'//)
1180. C      DO 20 I=1,N LAYER
1190. C          PRINT 30, I,H(I),C11(I),C12(I),C13(I),C22(I)
1200. C          PRINT 31,C23(I),C33(I),C44(I),C55(I),C66(I),RHO(I)
1210. C 30  FORMAT ('-', 'LAYER=', I :, 2X, 'H =', G16.9, 'C11=', G16.9,
1220. C      .      'C12=', G16.9, 'C13=', G16.9, 'C22=', G16.9)
1230. C 31  FORMAT ('0', 9X, 'C23=', G16.9, 'C33=', G16.9, 'C44=', G16.9,
1240. C      .      'C55=', G16.9, 'C66=', G16.9, 'RHO=', G16.9)
1250. C 20  CONTINUE
1260. C
1270. C      READ, NKBAR
1280. C      DO 50 L1=1,NKBAR
```

```

1290.      READ, KBAR (L1)
1300.      ZETA (L1) = H(1)*KBAR (L1)
1310. 50   CONTINUE
1320. C
1330. C ***** READ PHI IN DEGREE *****
1340. C
1350.      READ, NPHI
1360.      DO 60 L2=1,NPHI
1370.      READ, PHI (L2)
1380. 60   CONTINUE
1390. C
1400. C ***** READ ALFA IN DEGREE *****
1410. C
1420.      READ, NALFA
1430.      DO 65 L3=1,NALFA
1440.      READ, ALFA (L3)
1450. 65   CONTINUE
1460. C
1470. C
1480.      DO 70 N1=1,NKBAR
1490.      PRINT 75, KBAR (N1), ZETA (N1)
1500. 75   FORMAT ('-',////,10X,'KBAR =',F12.8,5X,'ZETA =',F12.8//)
1510.      DO 80 N2=1,NPHI
1520.      ANGLE = PHI (N2)*PI/180.
1530.      KHBAR = KBAR (N1)*COS (ANGLE)
1540.      YK    = KBAR (N1)*SIN (ANGLE)
1550.      DO 90 N3=1,NALFA
1560.      ROT =ALFA (N3)*PI/180
1570.      XK  =KHBAR*COS (ROT)
1580.      ZK  =KHBAR*SIN (ROT)
1590.      PRINT 100,PHI (N2),YK,ALFA (N3),XK,ZK
1600. 100  FORMAT (' ',3X,'PHI =',F8.5,3X,'KAPAY =',F10.7,3X,
1610.      'ALFA =',F8.5,3X,'KAPAX =',F10.7,3X,
1620.      'KAPAZ =',F10.7)
1630.      DO 11 JJ=1,12
1640.      DO 22 KK=1,12
1650.      A (JJ, KK)=ZERO
1660.      B (JJ, KK)=ZERO
1670. 22   CONTINUE
1680. 11   CONTINUE
1690. C
1700. C
1710.      DF = H (1)
1720.      DM = H (2)
1730.      ETA= DF / (DF+DM)
1740.      RHOF = RHO (1)
1750.      RHOM = RHO (2)
1760.      RHOC = ETA*RHOF + (1-ETA)*RHOM
1770.      IFF = DF*DF*RHOF*ETA/12.0
1780.      IMM = DM*DM*RHOM*(1-ETA)/12.0
1790.      XK2 = XK*XK
1800.      ZK2 = ZK*ZK
1810. C
1820. C ***** FORMATION OF A MATRIX *****
1830. C
1840.      A ( 1, 1)=-XK2*(ETA*C11 (1)+(1-ETA)*C11 (2))
1850.      -ZK2*(ETA*C55 (1)+(1-ETA)*C55 (2))
1860.      A ( 1, 3)=-XK*ZK*((ETA*C55 (1)+(1-ETA)*C55 (2))
1870.      +(ETA*C13 (1)+(1-ETA)*C13 (2)))
1880.      A ( 1, 8) = XK*ETA*C12 (1)*CIMGG
1890.      A ( 1, 9) = XK*(1.-ETA)*C12 (2)*CIMGG
1900.      A ( 1,10)=-YK*CIMGG
1910. C
1920.      A ( 2, 2)=-XK2*(ETA*C66 (1)+(1.-ETA)*C66 (2))

```

1930. $-ZK2*(ETA*C44(1)+(1.-ETA)*C44(2))$
 1940. $A(2,4) = XK*ETA*C66(1)*CIMGG$
 1950. $A(2,5) = XK*(1.-ETA)*C66(2)*CIMGG$
 1960. $A(2,6) = ZK*ETA*C44(1)*CIMGG$
 1970. $A(2,7) = ZK*(1.-ETA)*C44(2)*CIMGG$
 1980. $A(2,11) = -YK*CIMGG$
 1990. C
 2000. $A(3,1) = A(1,3)$
 2010. $A(3,3) = -XK2*(ETA*C55(1)+(1.-ETA)*C55(2))$
 2020. $-ZK2*(ETA*C33(1)+(1.-ETA)*C33(2))$
 2030. $A(3,8) = ZK*ETA*C23(1)*CIMGG$
 2040. $A(3,9) = ZK*(1.-ETA)*C23(2)*CIMGG$
 2050. $A(3,12) = -YK*CIMGG$
 2060. C
 2070. $A(4,2) = -A(2,4)$
 2080. $A(4,4) = -XK2*ETA*DF*DF*C11(1)/12.0$
 2090. $-ZK2*ETA*DF*DF*C55(1)/12.0 - ETA*C66(1)$
 2100. $A(4,6) = -XK*ZK*(ETA*DF*DF*C13(1)/12.0$
 2110. $+ ETA*DF*DF*C55(1)/12.0)$
 2120. $A(4,10) = -ETA$
 2130. C
 2140. $A(5,2) = -A(2,5)$
 2150. $A(5,5) = -XK2*(1.-ETA)*DM*DM*C11(2)/12.0$
 2160. $-ZK2*(1.-ETA)*DM*DM*C55(2)/12.0 - (1.-ETA)*C66(2)$
 2170. $A(5,7) = -XK*ZK*(1.-ETA)*DM*DM*(C13(2)+C55(2))/12.0$
 2180. $A(5,10) = -(1.-ETA)$
 2190. C
 2200. $A(6,2) = -A(2,6)$
 2210. $A(6,4) = A(4,6)$
 2220. $A(6,6) = -XK2*ETA*DF*DF*C55(1)/12.0$
 2230. $-ZK2*ETA*DF*DF*C33(1)/12.0 - ETA*C44(1)$
 2240. $A(6,12) = -ETA$
 2250. C
 2260. $A(7,2) = -A(2,7)$
 2270. $A(7,5) = A(5,7)$
 2280. $A(7,7) = -XK2*(1.-ETA)*DM*DM*C55(2)/12.0$
 2290. $-ZK2*(1.-ETA)*DM*DM*C33(2)/12.0 - (1.-ETA)*C44(2)$
 2300. $A(7,12) = -(1.-ETA)$
 2310. C
 2320. $A(8,1) = -A(1,8)$
 2330. $A(8,3) = -A(3,8)$
 2340. $A(8,8) = -XK2*ETA*DF*DF*C66(1)/12.0$
 2350. $-ZK2*ETA*DF*DF*C44(1)/12.0 - ETA*C22(1)$
 2360. $A(8,11) = -ETA$
 2370. C
 2380. $A(9,1) = -A(1,9)$
 2390. $A(9,3) = -A(3,9)$
 2400. $A(9,9) = -XK2*(1.-ETA)*DM*DM*C66(2)/12.0$
 2410. $-ZK2*(1.-ETA)*DM*DM*C44(2)/12.0 - (1.-ETA)*C22(2)$
 2420. $A(9,11) = -(1.-ETA)$
 2430. C
 2440. $A(10,1) = -A(1,10)$
 2450. $A(10,4) = A(4,10)$
 2460. $A(10,5) = A(5,10)$
 2470. C
 2480. $A(11,2) = -A(2,11)$
 2490. $A(11,8) = A(8,11)$
 2500. $A(11,9) = A(9,11)$
 2510. C
 2520. $A(12,3) = -A(3,12)$
 2530. $A(12,6) = A(6,12)$
 2540. $A(12,7) = A(7,12)$
 2550. C
 2560. C ***** FORMULATION OF THE B MATRIX *****

```
2570. C
2580.          B( 1, 1)--RHOC
2590.          B( 2, 2)--RHOC
2600.          B( 3, 3)--RHOC
2610.          B( 4, 4)--IFF
2620.          B( 5, 5)--IMM
2630.          B( 6, 6)--IFF
2640.          B( 7, 7)--IMM
2650.          B( 8, 8)--IFF
2660.          B( 9, 9)--IMM
2670. C
2680. C
2690. C
2700.          IJOB=1
2710.          IA =12
2720.          IB =12
2730.          IZ =12
2740.          N  =12
2750.          CALL EIGZC(A, IA, B, IB, N, IJOB, EIGA, EIGB, Z, IZ, WK
2760.                  , INFER, IER)
2770.          DO 120 M=1, 12
2780.              OMSQ(M)=EIGA(M)/EIGB(M)
2790.              OM(M)  =CDSQRT(OMSQ(M))/((C44(2)/RHOM)**0.5)
2800.              OM(M)  =OM(M)/KBAR(N1)
2810.              PRINT 125, M, OM(M)
2820. 125       FORMAT ('0', 1X, 12, 5X, 2G16.9)
2830. 120       CONTINUE
2840.          IF (IPRINT .GT. 0) THEN DO
2850.              IV=1
2860.              PRINT 140, IV
2870. 140       FORMAT ('0'//, 1X, 'M', 10X, 'THE CORRESPONDING Z MATRIX'
2880.                  ' OF CELL ', 11, 1X, 'IS :')//)
2890.              DO 150 K=1, 12
2900.                  PRINT 160, K, (Z(L,K), L=1, 12)
2910.                  FORMAT ('0', 12, 1X, 6(2F10.6, 1X) /, 4X, 6(2F10.6, 1X))
2920. 150       CONTINUE
2930.              IPRINT=IPRINT-1
2940.          END IF
2950. C
2960. 90         CONTINUE
2970. 80         CONTINUE
2980. 70         CONTINUE
2990.          STOP
3000.          END
3010. $ENTRY
```

A P P E N D I X J

FORTRAN PROGRAM FOR THE FINITE ELEMENT METHOD

There are two main line computer programs written for the finite element method outlined in Chapter 2. The first program read the value of \bar{k} travelling in any arbitrary direction that make a horizontal angle, α , with the x-axis and a vertical angle, ϕ , with respect to the x-z plane. The components of \bar{k} are calculated by taking sine and cosine of the angles. The other main line program will read in \bar{k} and the y-component, $\bar{\eta}$ and angle, α , it makes with respect to the x-axis in (x-z) plane. Only the second program will be listed in this Appendix. However, it does not cause much difficulties in converting one program to the other. The procedure of modification will be to read the vertical angle, ϕ , as input and y-component of \bar{k} is calculated by taking the sine of angle ϕ .

```

10. C
20. C *****
30. C *
40. C * HARMONIC WAVE PROPAGATION ANALYSIS PROGRAM *
50. C * BY *
60. C * JOHNNY K.T. YEO *
70. C * THE UNIVERSITY OF MANITOBA *
80. C * DECEMBER, 1982 *
90. C *
100. C *****
110. C

```

```

120. C NOTES :
130. C 1) ALL INPUTS ARE FORMAT-FREE EXCEPT FOR ETA.
140. C 2) NP, IPRINT, NKHBAR, NALFA, NETA ARE INTEGER VALUES
150. C 3) H, C, RHO, KHBAR ARE REAL
160. C

```

```

170. C .....
180. C
190. C INPUT DESCRIPTION
200. C
210. C .....
220. C

```

- A. START CARD - ONE CARD FOR NP AND IPRINT.
 - * NP = NUMBER OF PERIODICITY
 - * IPRINT = NUMBER OF SETS OF VECTORS AS OUTPUT
- B. MATERIAL PROPERTIES CARD - (NP+1) OF CARDS FOR :
 - H(I), C11(I), C12(I), C13(I), C22(I), C23(I),
 - C33(I), C44(I), C55(I), C66(I), RHO(I)
 - * H(I) = LAYER THICKNESS
 - * C(I) = MATERIAL CONSTANTS OF THE LAYER
 - * RHO(I) = DENSITY OF THE MATERIAL
 - * I = 1 TO (NP+1)
- C. BASIC CONTROL CARD - ONE CARD FOR NKHBAR.
 - * NKHBAR = NUMBER OF HORIZONTAL WAVE NUMBER TO BE EVALUATED
- D. WAVE NUMBER CARD - AS MANY CARDS AS REQUIRED FOR KHBAR.
 - * KBAR(J) = VALUE OF WAVE NUMBER
 - J = 1 TO NKHBAR
- E. ANGLE CONTROL CARD - ONE CARD FOR NALFA
 - * NALFA = NUMBER OF HORIZONTAL ANGLES
- F. HORIZONTAL ANGLE CARD - AS MANY CARDS AS REQUIRED FOR ALFA.
 - * ALFA(K) = HORIZONTAL ANGLES IN DEGREE.
 - * K = 1 TO NALFA
- G. VERTICAL COMPONENT CONTROL CARD - ONE CARD FOR NETA
 - * NETA = NUMBER OF VERTICAL COMPONENT OF WAVE NUMBER
- H. VERTICAL COMPONENT CARD - AS MANY CARDS AS REQUIRED FOR ETA.
 - * ETA(L) = VERTICAL DIMENSIONLESS WAVE NUMBER
 - L = 1 TO NETA

```

590. C FORMAT (2F10.7)
600. C
610. C .....
620. C
630. C OUTPUT DESCRIPTION
640. C

```

```
650. C .....
660. C
670. C     ZETA = DIMENSIONLESS WAVE NUMBER
680. C     OM(M) = ANGULAR FREQUENCY OF PROPAGATING WAVE
690. C
700. C .....
710. C
720. C           SAMPLE DATA
730. C
740. C .....
750. C
760. C     CARD A : 4   1
770. C     CARD B :
780. C         4.0 2.56 0.583 0.583 1.797 0.745 1.797 0.526 0.559 0.559 2.534
790. C         4.0 2.56 0.583 0.583 1.797 0.745 1.797 0.526 0.559 0.559 2.534
800. C         0.5 1.107 0.573 0.573 1.107 0.573 1.107 0.267 0.267 0.267 2.702
810. C         0.5 1.107 0.573 0.573 1.107 0.573 1.107 0.267 0.267 0.267 2.702
820. C         4.0 2.56 0.583 0.583 1.797 0.745 1.797 0.526 0.559 0.559 2.534
830. C     CARD C : 1
840. C     CARD D : 2.0
850. C     CARD E : 1
860. C     CARD F : 45
870. C     CARD G : 1
880. C     CARD H : 2   (FORMAT 2F10.7)
890. C
900. C .....
910. C
920. C
930. C
940. C
950. C     ***** DECLARATION *****
960. C
970. C     INTEGER NP1, NP2, IC2
980. C     REAL *8   H(5), C11(5), C12(5), C13(5), C22(5), C23(5), C33(5),
990. C               C44(5), C55(5), C66(5), RHO(5), ALFA(15), DEPTH
1000. C     REAL *8   A(4,4), B(4,4), D(4,4), KHBAR(45), XK, ZK, PI, KAPPA
1010. C     COMPLEX *16 AK(36,36), BK(36,36), CK(36,36), DK(36,36),
1020. C     &         AM(36,36), BM(36,36), DZ(36,36), EIGA(36),
1030. C     &         EIGB(36), OMSQ(36), OM(36), ETA(50),
1040. C     &         WK(24,48), E, YK, Z(36,36), CIMGG, ZERO
1050. C
1060. C
1070. C     COMMON/BLK1/ NP1, NP2, IC2
1080. C     COMMON/BLK2/ CIMGG, ZERO
1090. C     COMMON/BLK3/ PI
1100. C
1110. C
1120. C     ZERO=(0.0 ,0.0)
1130. C     CIMGG=(0.0, 1.0)
1140. C     PI=4. * ATAN(1.0)
1150. C
1160. C
1170. C     ***** MAIN LINE PROGRAM *****
1180. C
1190. C     CALL TRAPS(99999, 99999, 99999, 99999, 99999)
1200. C
1210. C THIS SUBROUTINE WILL TRAPS ANY NUMBER APPROACHING ZERO
1220. C
1230. C **** READ IN NUMBER OF PERIODICITY ****
1240. C
1250. C **** IPRINT IS THE NUMBER OF EIGENVECTORS TO BE PRINTED ****
1260. C
1270. C     READ, NP , IPRINT
1280. C     NP1= NP + 1
```

```
1290.      NP2= NP + 2
1300.      IC2= 6 * NP2
1310. C
1320. C READ IN PROPERTIES OF NP + 1 LAYERS.
1330. C
1340.      READ, (H(I),C11(I),C12(I),C13(I),C22(I),C23(I),C33(I),
1350.      .      C44(I),C55(I),C66(I),RHO(I),I=1,NP1)
1360.      PRINT 30, NP
1370.      30 FORMAT('1'///// ' ', 40X, 'PERIODICITY =', 3X, 12/////
1380.      *      ' ', 1X, 'LAYER PROPERTIES : '//)
1390. C
1400. C
1410.      X1 = RHO(NP) / C55(NP)
1420.      XMULT= SQRT(X1)
1430.      DO 40 I=1, NP1
1440.      PRINT 50, I,H(I),C11(I),C12(I),C13(I),C22(I)
1450.      PRINT 51, C23(I),C33(I),C44(I),C55(I),C66(I),RHO(I)
1460.      50 FORMAT('-','LAYER=',12,2X,'H =',G16.9,
1470.      .      'C11=',G16.9,'C12=',G16.9,'C13=',G16.9,
1480.      .      'C22=',G16.9)
1490.      51 FORMAT('0',9X,'C23=',G16.9,'C33=',G16.9,'C44=',G16.9,
1500.      .      'C55=',G16.9,'C66=',G16.9,'RHO=',G16.9)
1510.      40 CONTINUE
1520. C
1530.      ICOUNT = 6 * NP
1540.      DEPTH = 0.0
1550.      DO 10 I=1, NP
1560.      DEPTH = DEPTH + H(I)
1570.      10 CONTINUE
1580. C
1590. C READ IN KAPPABAR
1600. C
1610.      READ, NKHBAR
1620.      DO 35 J=1, NKHBAR
1630.      READ, KHBAR(J)
1640.      35 CONTINUE
1650. C
1660. C READ ALFA IN DEGREE
1670. C
1680.      READ, NALFA
1690.      DO 37 J=1, NALFA
1700.      READ, ALFA(J)
1710.      37 CONTINUE
1720. C
1730. C READ IN ETA (KAPPAY)
1740. C
1750.      READ, NETA
1760.      DO 52 J=1, NETA
1770.      READ 55, ETA(J)
1780.      55  FORMAT (2F10.7)
1790.      52 CONTINUE
1800. C
1810. C      READ, NCELL
1820. C
1830.      CALL INFORM(A, B, D)
1840. C
1850. C
1860. C
1870.      DO 60 L1=1, NKHBAR
1880.      KAPPA = KHBAR(L1) * PI / 2.
1890. C
1900.      DO 70 L2=1, NALFA
1910.      ANGLE = ALFA(L2) * PI / 180.
1920.      XK = KHBAR(L1)*COS(ANGLE)*PI/2.
```

```
1930.      ZK   = KHBAR(L1)*SIN(ANGLE)*PI/2.
1940.      PRINT 66,KAPPA, ALFA(L2), XK, ZK ,KHBAR(L1)
1950.      66   FORMAT ('-'/'-',5X,'KAPPA=',F10.5,3X,'ANGLE =',F10.5,
1960.      .     3X,'KAPAX=',F10.5,3X,'KAPAZ=',F10.5,3X,
1970.      .     '( KAPPABAR=',F10.5,3X,' ) ')
1980. C
1990.      DO 11 JJ=1, IC2
2000.      DO 22 KK=1, IC2
2010.      AK(JJ, KK) = ZERO
2020.      BK(JJ, KK) = ZERO
2030.      CK(JJ, KK) = ZERO
2040.      DK(JJ, KK) = ZERO
2050.      AM(JJ, KK) = ZERO
2060.      BM(JJ, KK) = ZERO
2070.      22   CONTINUE
2080.      11   CONTINUE
2090. C
2100. C      **** FIRST FORM THE MATRICES INVOLVING UUBAR ****
2110. C
2120.      CALL UUBAR(NP,H,C11,C55,C66,RHO,XK,ZK,A,1,AK)
2130. C
2140. C
2150.      CALL UUBAR(NP,H,C11,C55,C66,RHO,XK,ZK,A,2,BK)
2160. C
2170.      CALL ADDING(NP,AK,BK)
2180. C
2190. C
2200.      CALL UUBAR(NP,H,C11,C55,C66,RHO,XK,ZK,B,3,BK)
2210. C
2220.      CALL ADDING(NP, AK, BK)
2230. C
2240. C
2250.      CALL UUBAR(NP,H,C11,C55,C66,RHO,XK,ZK,A,4,AM)
2260. C
2270. C
2280. C
2290. C ***** THEN FORM THE MATRICES INVOLVING VVBAR *****
2300. C
2310.      CALL VVBAR(NP,H,C12,C22,C23,C44,C66,RHO,XK,ZK,B,1,BK)
2320. C
2330.      CALL ADDING(NP, AK, BK)
2340. C
2350.      CALL VVBAR(NP,H,C12,C22,C23,C44,C66,RHO,XK,ZK,A,2,BK)
2360. C
2370.      CALL ADDING(NP, AK, BK)
2380. C
2390.      CALL VVBAR(NP,H,C12,C22,C23,C44,C66,RHO,XK,ZK,A,3,BK)
2400. C
2410.      CALL ADDING(NP, AK, BK)
2420. C
2430.      CALL VVBAR(NP,H,C12,C22,C23,C44,C66,RHO,XK,ZK,A,4,BM)
2440. C
2450.      CALL ADDING(NP, AM, BM)
2460. C
2470. C      **** FORM THE MATRICES INVOLVING WWBAR ****
2480. C
2490.      CALL WWBAR(NP,H,C33,C44,C55,RHO,XK,ZK,A,1,BK)
2500. C
2510.      CALL ADDING(NP, AK, BK)
2520. C
2530.      CALL WWBAR(NP,H,C33,C44,C55,RHO,XK,ZK,B,2,BK)
2540. C
2550.      CALL ADDING(NP, AK, BK)
2560. C
```

```

2570. CALL WUBAR (NP, H, C33, C44, C55, RHO, XK, ZK, A, 3, BK)
2580. C
2590. CALL ADDING (NP, AK, BK)
2600. C
2610. CALL WUBAR (NP, H, C33, C44, C55, RHO, XK, ZK, A, 4, BM)
2620. C
2630. CALL ADDING (NP, AM, BM)
2640. C
2650. C **** FORM THE MATRICES INVOLVING UVBAR DOING : ****
2660. C **** (UVBAR' - V'UBAR) & (VUBAR' - U'VBAR) ****
2670. C
2680. CALL UVBAR (NP, H, C12, C22, C23, C66, XK, ZK, D, 1, BK)
2690. C
2700. CALL ADDING (NP, AK, BK)
2710. C
2720. CALL UVBAR (NP, H, C12, C22, C23, C66, XK, ZK, D, 2, BK)
2730. C
2740. CALL ADDING (NP, AK, BK)
2750. C
2760. C **** FORM THE MATRICES INVOLVING WUBAR DOING : ****
2770. C **** (WUBAR + UWBAR) ****
2780. C
2790. CALL WUBAR (NP, H, C13, C44, C55, C66, XK, ZK, A, 1, BK)
2800. C
2810. CALL ADDING (NP, AK, BK)
2820. C
2830. CALL WUBAR (NP, H, C13, C44, C55, C66, XK, ZK, A, 2, BK)
2840. C
2850. CALL ADDING (NP, AK, BK)
2860. C
2870. C **** FORM THE MATRICES INVOLVING WVBAR DOING ****
2880. C **** (WVBAR' - V'WBAR) & (VWBAR' - W'VBAR) ****
2890. C
2900. CALL WVBAR (NP, H, C12, C22, C23, C44, XK, ZK, D, 1, BK)
2910. C
2920. CALL ADDING (NP, AK, BK)
2930. C
2940. CALL WVBAR (NP, H, C12, C22, C23, C44, XK, ZK, D, 2, BK)
2950. C
2960. CALL ADDING (NP, AK, BK)
2970. C
2980. C
2990. C ***** TO SHIFT UP AK AND AM BY 6 ROWS *****
3000. C
3010. NP6 = 6 * NP
3020. NPSQ = 6 * NP2
3030. C
3040. DO 33 I=1, NP6
3050. IR = I + 6
3060. DO 44 J=1, NPSQ
3070. AK(I, J) = AK(IR, J)
3080. AM(I, J) = AM(IR, J)
3090. 44 CONTINUE
3100. 33 CONTINUE
3110. C
3120. C
3130. C *** THE FOLLOWING WILL FORM THE 'D' MATRIX (WHICH IS PART OF THE
3140. C THE ASSEMBLY MATRIX AND TO BE MODIFIED) . THE D MATRIX OF
3150. C THE K MATRIX IS STORED IN BK, WHILE THAT OF THE M MATRIX IS
3160. C STORED IN BM. ***
3170. C
3180. C
3190. CALL FORMDD (NP, AK, AM, BK, BM)
3200. C

```

```

3210. C
3220. DO 77 J=1, NETA
3230. YK = PI / 2. * ETA(J)
3240. E = CDEXP(YK * 2. * DEPTH * CIMGG)
3250. DO 80 K=1, ICOUNT
3260. DO 90 L=1, ICOUNT
3270. CK(K, L) = AK(K, L) + E * BK(K, L)
3280. DK(K, L) = - ( AM(K, L) + E * BM(K, L) )
3290. 90 CONTINUE
3300. 80 CONTINUE
3310. C
3320. C
3330. IJOB = 1
3340. IA = IC2
3350. IB = IC2
3360. IZ = IC2
3370. N = ICOUNT
3380. CALL EIGZC (CK, IA, DK, IB, N, IJOB, EIGA, EIGB, Z,
3390. * IZ, WK, INFER, IER)
3400. C
3410. C
3420. PRINT 100, ETA(J)
3430. 100 FORMAT('-', 44X, 'ETA =', 3X, 2G16.9/)
3440. PRINT 105
3450. 105 FORMAT('O', T4, 'M', T25, 'OMEGA(M)', T65, 'EIGA(M)',
3460. * T109, 'EIGB(M)')
3470. C
3480. DO 110 M=1, ICOUNT
3490. OMSQ(M) = EIGA(M) / EIGB(M)
3500. OM(M) = CDSQRT( OMSQ(M) ) * 2.DO / PI
3510. OM(M) = OM(M) * XMULT
3520. PRINT 120, M, OM(M), EIGA(M), EIGB(M)
3530. 120 FORMAT('O', 1X, 12, 6(5X, G16.9))
3540. 110 CONTINUE
3550. C
3560. IF (IPRINT .GT. 0) THEN DO
3570. C DO 503 IN=1, ICOUNT
3580. C DO 504 JN=1, ICOUNT
3590. C DZ(IN, JN) = Z(IN, JN)
3600. C504 CONTINUE
3610. C503 CONTINUE
3620. C
3630. C ** DZ IS USED TO CALCULATE THE MODULI **
3640. C
3650. IV=1
3660. PRINT 140, IV
3670. 140 FORMAT('-', 1X, 'M', 10X, 'THE CORRESPONDING Z MATRIX OF'
3680. * ' CELL ', 11, 1X, 'IS :')
3690. DO 151 K=1, ICOUNT
3700. PRINT 161, K, (Z(L, K), L=1, ICOUNT)
3710. 161 FORMAT ('O', 12, 1X, 6(2F10.6, 1X) /, 4X, 6(2F10.6, 1X) /,
3720. 4X, 6(2F10.6, 1X) /, 4X, 6(2F10.6, 1X) /)
3730. 151 CONTINUE
3740. C
3750. C THE FOLLOWING SHOULD BE INCLUDED IF MORE THAN 1 UNIT CELL IS USED.
3760. C NCELL IS THE NUMBER OF UNIT CELL USED
3770. C
3780. C
3790. C DO 141 IV=2, NCELL
3800. C PRINT 140, IV
3810. C DO 142 JJ=1, ICOUNT
3820. C DO 143 KK=1, ICOUNT
3830. C Z(JJ, KK) = Z(JJ, KK) * E
3840. C143 CONTINUE

```

```
3850. C          PRINT 161, JJ, (Z(LL,JJ),LL=1,ICOUNT)
3860. C142          CONTINUE
3870. C141          CONTINUE
3880. C
3890. C
3900. C
3910. C THE ABOVE PROCEDURE EVALUATES ALL THE Z MATRICES OF NCELL
3920. C
3930. C THE SAME PROCEDURE IS EMPLOYED TO EVALUATE THE CORRESPONDING
3940. C MODULI OF THESE Z MATRICES
3950. C
3960. C          IV=1
3970. C          PRINT 170, IV
3980. C170          FORMAT('-'//',1X,'M',10X,'THE CORRESPONDING MODULI OF Z'
3990. C          ., ' MATRIX OF CELL ',11,1X,' IS :')
4000. C          DO 180 K=1,ICOUNT
4010. C          PRINT 190,K,(CDABS(DZ(L,K)),L=1,ICOUNT)
4020. C190          FORMAT('0',12,5X,6(F10.6,2X)/,8X,6(F10.6,2X)/,
4030. C          ., 8X,6(F10.6,2X)/,8X,6(F10.6,2X)/)
4040. C          ., 8X,6(F10.6,2X)/,8X,6(F10.6,2X))
4050. C180          CONTINUE
4060. C          DO 1300 IV=2,NCELL
4070. C          PRINT 170, IV
4080. C          DO 1400 JJ=1,ICOUNT
4090. C          DO 1500 KK=1,ICOUNT
4100. C          DZ(JJ,KK)=DZ(JJ,KK)*E
4110. C1500          CONTINUE
4120. C          PRINT 190, JJ, (CDABS(DZ(LL, JJ)), LL=1, ICOUNT)
4130. C1400          CONTINUE
4140. C1300          CONTINUE
4150. C506          CONTINUE
4160. C
4170. C
4180. C          IPRINT=IPRINT-1
4190. C          END IF
4200. C          77          CONTINUE
4210. C          70          CONTINUE
4220. C          60          CONTINUE
4230. C          STOP
4240. C          END
10. C
20. C
30. C
40. C*****
50. C
60. C          SUBROUTINE INFORM          *
70. C          *
80. C*****
90. C
100. C
110. C          SUBROUTINE INFORM(A, B, D)
120. C
130. C
140. C          REAL*8 A(4,4), B(4,4), D(4,4)
150. C
160. C          ***** TO FORM THE MATRICES A, B AND D *****
170. C
180. C          A(1, 1) = 78. / 105.
190. C          A(2, 1) = A(1, 2) = 9. / 35.
200. C          A(3, 1) = A(1, 3) = 22. / 105.
210. C          A(4, 1) = A(1, 4) = - 13. / 105.
220. C
230. C          A(2, 2) = 78. / 105.
240. C          A(3, 2) = A(2, 3) = 13. / 105.
```

```
250.      A(4, 2) = A(2, 4) = - 22. / 105.
260. C
270.      A(3, 3) = 8. / 105.
280.      A(4, 3) = A(3, 4) = - 6. / 105.
290. C
300.      A(4, 4) = 8. / 105.
310. C
320. C
330.      B(1, 1) = 3. / 5.
340.      B(2, 1) = B(1, 2) = - 3. / 5.
350.      B(3, 1) = B(1, 3) = 1. / 10.
360.      B(4, 1) = B(1, 4) = 1. / 10.
370. C
380.      B(2, 2) = 3. / 5.
390.      B(3, 2) = B(2, 3) = - 1. / 10.
400.      B(4, 2) = B(2, 4) = - 1. / 10.
410. C
420.      B(3, 3) = 4. / 15.
430.      B(4, 3) = B(3, 4) = - 1. / 15.
440. C
450.      B(4, 4) = 4. / 15.
460. C
470. C
480.      D(1, 1) = - 1. / 2.
490.      D(1, 2) = 1. / 2.
500.      D(1, 3) = 1. / 5.
510.      D(1, 4) = - 1. / 5.
520. C
530.      D(2, 1) = - D(1, 2)
540.      D(2, 2) = 1. / 2.
550.      D(2, 3) = - 1. / 5.
560.      D(2, 4) = 1. / 5.
570. C
580.      D(3, 1) = - D(1, 3)
590.      D(3, 2) = - D(2, 3)
600.      D(3, 3) = 0.000
610.      D(3, 4) = - 1. / 15.
620. C
630.      D(4, 1) = - D(1, 4)
640.      D(4, 2) = - D(2, 4)
650.      D(4, 3) = - D(3, 4)
660.      D(4, 4) = 0.000
670. C
680.      RETURN;END
690. C
700. C
710. C
720. C
730. C
740. C*****
750. C
760. C          SUBROUTINE  UUBAR          *
770. C
780. C*****
790. C
800. C
810.      SUBROUTINE UUBAR (NP,H,C11,C55,C66,RHO,XK,ZK,AB,N,AKNAM)
820. C
830. C
840.      COMMON/BLK1/NP1, NP2, IC2
850.      COMMON/BLK2/CIMGG, ZERO
860.      REAL *8          H(NP1),C11(NP1),C55(NP1),C66(NP1),RHO(NP1),
870.      *                AB(4, 4), XK, XK2, ZK, ZK2
880.      COMPLEX *16      AKNAM(IC2,IC2), U(12,12), CONST ,CIMGG, ZERO
```

```
890. C
900.   XK2 = XK * XK
910.   ZK2 = ZK * ZK
920.   DO 1000 JJ=1, IC2
930.     DO 1050 KK=1, IC2
940.       AKNAM(JJ, KK) = ZERO
950.   1050 CONTINUE
960.   1000 CONTINUE
970. C
980.   DO 991 L1=1, 12
990.     DO 992 L2=1, 12
1000.       U(L1,L2) = ZERO
1010.   992 CONTINUE
1020.   991 CONTINUE
1030.   DO 10 I=1, NP1
1040. C
1050.   U(1, 1) = AB(1, 1)
1060.   U(1, 2) = AB(1, 3) * H(1) / C66(1)
1070.   U(2, 1) = U(1, 2)
1080.   U(1, 3) = - AB(1, 3) * H(1) * XK * CIMGG
1090.   U(3, 1) = - U(1, 3)
1100.   U(1, 4) = U(4, 1) = ZERO
1110.   U(1, 7) = AB(1, 2)
1120.   U(7, 1) = U(1, 7)
1130.   U(1, 8) = AB(1, 4) * H(1) / C66(1)
1140.   U(8, 1) = U(1, 8)
1150.   U(1, 9) = - AB(1, 4) * H(1) * XK * CIMGG
1160.   U(9, 1) = - U(1, 9)
1170.   U(1,10) = U(10,1) = ZERO
1180. C
1190.   U(2, 2) = AB(3, 3) * H(1) * H(1) / C66(1) / C66(1)
1200.   U(2, 3) = -AB(3, 3)*H(1)*H(1)*XK*CIMGG/C66(1)
1210.   U(3, 2) = - U(2, 3)
1220.   U(2, 7) = AB(2, 3) * H(1) / C66(1)
1230.   U(7, 2) = U(2, 7)
1240.   U(2, 8) = AB(3, 4) * H(1) * H(1) / C66(1) / C66(1)
1250.   U(8, 2) = U(2, 8)
1260.   U(2, 9) = - AB(3, 4) * H(1) * H(1) * XK * CIMGG / C66(1)
1270.   U(9, 2) = - U(2, 9)
1280. C
1290.   U(3, 3) = AB(3, 3) * H(1) * H(1) * XK2
1300.   U(3, 4) = U(4, 3) = ZERO
1310.   U(3, 7) = AB(2, 3) * H(1) * XK * CIMGG
1320.   U(7, 3) = - U(3, 7)
1330.   U(3, 8) = AB(3, 4) * H(1) * H(1) * XK * CIMGG / C66(1)
1340.   U(8, 3) = - U(3, 8)
1350.   U(3, 9) = AB(3, 4) * H(1) * H(1) * XK2
1360.   U(9, 3) = U(3, 9)
1370. C
1380. C
1390.   U(7, 7) = AB(2, 2)
1400.   U(7, 8) = AB(2, 4) * H(1) / C66(1)
1410.   U(8, 7) = U(7, 8)
1420.   U(7, 9) = - AB(2, 4) * H(1) * XK * CIMGG
1430.   U(9, 7) = - U(7, 9)
1440. C
1450.   U(8, 8) = AB(4, 4) * H(1) * H(1) / C66(1) / C66(1)
1460.   U(8, 9) = -AB(4, 4)*H(1)*H(1)*XK*CIMGG/C66(1)
1470.   U(9, 8) = - U(8, 9)
1480. C
1490.   U(9, 9) = AB(4, 4) * H(1) * H(1) * XK2
1500. C
1510. C
1520. C
PRINT, ((U(L1,L2), L1=1,12), L2=1,12)
```

```
1530. C
1540.     IF ( N .EQ. 1 ) THEN DO
1550.         CONST = C11(I) * XK2 * H(I)
1560.     ELSE DO
1570.         IF ( N .EQ. 2 ) THEN DO
1580.             CONST = C55(I) * H(I) *ZK2
1590.         ELSE DO
1600.             IF ( N .EQ. 3 ) THEN DO
1610.                 CONST = C66(I) / H(I)
1620.             ELSE DO
1630.                 CONST = -RHO(I) * H(I)
1640.             END IF
1650.         END IF
1660.     END IF
1670. C
1680. C
1690.     ITIME = I - 1
1700.     DO 20 J=1, 12
1710.         IR = J + 6 * ITIME
1720.         DO 30 K=1, 12
1730.             IC = K + 6 * ITIME
1740.             AKNAM(IR, IC) = AKNAM(IR, IC) + CONST * U(J, K)
1750.         30 CONTINUE
1760.     20 CONTINUE
1770. 10 CONTINUE
1780. C
1790.     RETURN;END
1800. C
1810. C
1820. C
1830. C
1840. C*****
1850. C
1860. C     SUBROUTINE VVBAR
1870. C
1880. C*****
1890. C
1900. C
1910.     SUBROUTINE VVBAR (NP,H,C12,C22,C23,C44,C66,RHO,XK,ZK,AB,N,BKNBM)
1920. C
1930.     COMMON/BLK1/ NP1, NP2, IC2
1940.     COMMON/BLK2/ CIMGG, ZERO
1950.     REAL *8     H(NP1),C12(NP1),C22(NP1),C23(NP1),C44(NP1),
1960.     *          C66(NP1), RHO(NP1), XK, XK2, ZK, ZK2, AB(4, 4)
1970.     COMPLEX *16 BKNBM(IC2,IC2), V(12,12), CONST, CIMGG, ZERO
1980. C
1990.     XK2 = XK * XK
2000.     ZK2 = ZK * ZK
2010. C
2020.     DO 1000 JJ=1, IC2
2030.         DO 1050 KK=1, IC2
2040.             BKNBM(JJ, KK) = ZERO
2050.         1050 CONTINUE
2060.     1000 CONTINUE
2070. C
2080.     DO 991 L1=1, 12
2090.         DO 992 L2=1, 12
2100.             V(L1,L2) = ZERO
2110.     992 CONTINUE
2120. 991 CONTINUE
2130. C
2140.     DO 10 I=1, NP1
2150. C
2160.         V(1, 1) = AB(3, 3) * H(I) * H(I) * XK2 * C12(I) * C12(I)
```

```

2170.
2180. * / C22 (1) / C22 (1)
2190. V (1, 2) = V (2, 1) = ZERO
2200. V (1, 3) = AB (1, 3) * H (1) * XK * C12 (1) * CIMGG / C22 (1)
2210. V (3, 1) = - V (1, 3)
2220. V (1, 4) = AB (3, 3) * H (1) * H (1) * C12 (1) * XK * CIMGG / C22 (1) / C22 (1)
2230. V (4, 1) = - V (1, 4)
2240. V (1, 5) = AB (3, 3) * ZK * XK * H (1) * H (1) * C12 (1) * C23 (1) / C22 (1) / C22 (1)
2250. V (5, 1) = V (1, 5)
2260. * V (1, 7) = AB (3, 4) * H (1) * H (1) * XK2 * C12 (1) * C12 (1)
      / C22 (1) / C22 (1)
2270. V (7, 1) = V (1, 7)
2280. V (1, 8) = V (8, 1) = ZERO
2290. V (1, 9) = AB (2, 3) * H (1) * XK * C12 (1) * CIMGG / C22 (1)
2300. V (9, 1) = - V (1, 9)
2310. * V (1, 10) = AB (3, 4) * H (1) * H (1) * XK * C12 (1) * CIMGG
      / C22 (1) / C22 (1)
2320.
2330. V (10, 1) = - V (1, 10)
2340. V (1, 11) = AB (3, 4) * ZK * XK * H (1) * H (1) * C12 (1) * C23 (1) / C22 (1) / C22 (1)
2350. V (11, 1) = V (1, 11)
2360. C
2370. C
2380.
2390. V (3, 3) = AB (1, 1)
2400. V (3, 4) = AB (1, 3) * H (1) / C22 (1)
2410. V (4, 3) = V (3, 4)
2420. V (3, 5) = - AB (1, 3) * ZK * H (1) * C23 (1) * CIMGG / C22 (1)
2430. V (5, 3) = - V (3, 5)
2440. V (3, 7) = - AB (1, 4) * H (1) * XK * C12 (1) * CIMGG / C22 (1)
2450. V (7, 3) = - V (3, 7)
2460. V (3, 8) = V (8, 3) = ZERO
2470. V (3, 9) = AB (1, 2)
2480. V (9, 3) = V (3, 9)
2490. V (3, 10) = AB (1, 4) * H (1) / C22 (1)
2500. V (10, 3) = V (3, 10)
2510. V (3, 11) = - AB (1, 4) * ZK * H (1) * C23 (1) * CIMGG / C22 (1)
2520. C V (11, 3) = - V (3, 11)
2530.
2540. V (4, 4) = AB (3, 3) * H (1) * H (1) / C22 (1) / C22 (1)
2550. V (4, 5) = - AB (3, 3) * H (1) * H (1) * ZK * C23 (1) * CIMGG / C22 (1) / C22 (1)
2560. V (5, 4) = - V (4, 5)
2570. * V (4, 7) = - AB (3, 4) * H (1) * H (1) * XK * C12 (1) * CIMGG
      / C22 (1) / C22 (1)
2580. V (7, 4) = - V (4, 7)
2590. V (4, 8) = V (8, 4) = ZERO
2600. V (4, 9) = AB (2, 3) * H (1) / C22 (1)
2610. V (9, 4) = V (4, 9)
2620. V (4, 10) = AB (3, 4) * H (1) * H (1) / C22 (1) / C22 (1)
2630. V (10, 4) = V (4, 10)
2640. V (4, 11) = - AB (3, 4) * H (1) * H (1) * ZK * C23 (1) * CIMGG / C22 (1) / C22 (1)
2650. V (11, 4) = - V (4, 11)
2660. C
2670. V (5, 5) = AB (3, 3) * H (1) * H (1) * ZK2 * C23 (1) * C23 (1) / C22 (1) / C22 (1)
2680. V (5, 7) = AB (3, 4) * H (1) * H (1) * ZK * XK * C12 (1) * C23 (1)
      / C22 (1) / C22 (1)
2690.
2700. V (7, 5) = V (5, 7)
2710. V (5, 9) = AB (2, 3) * H (1) * ZK * C23 (1) * CIMGG / C22 (1)
2720. V (9, 5) = - V (5, 9)
2730. V (5, 10) = AB (3, 4) * H (1) * H (1) * ZK * C23 (1) * CIMGG / C22 (1) / C22 (1)
2740. V (10, 5) = - V (5, 10)
2750. V (5, 11) = AB (3, 4) * H (1) * H (1) * ZK2 * C23 (1) * C23 (1) / C22 (1) / C22 (1)
2760. V (11, 5) = V (5, 11)
2770. C
2780.
2790. * V (7, 7) = AB (4, 4) * H (1) * H (1) * XK2 * C12 (1) * C12 (1)
      / C22 (1) / C22 (1)
2800. V (7, 8) = V (8, 7) = ZERO

```

```

2810.      V(7, 9) = AB(2, 4) * H(1) * XK * C12(1) * CIMGG / C22(1)
2820.      V(9, 7) = - V(7, 9)
2830.      V(7, 10) = AB(4, 4) * H(1) * H(1) * XK * CIMGG * C12(1) / C22(1) / C22(1)
2840.      V(10, 7) = -V(7, 10)
2850.      V(7, 11) = AB(4, 4) * H(1) * H(1) * ZK * XK * C12(1) * C23(1) / C22(1) / C22(1)
2860.      V(11, 7) = V(7, 11)
2870. C
2880. C
2890.      V(9, 9) = AB(2, 2)
2900.      V(9, 10) = AB(2, 4) * H(1) / C22(1)
2910.      V(10, 9) = V(9, 10)
2920.      V(9, 11) = -AB(2, 4) * H(1) * ZK * C23(1) * CIMGG / C22(1)
2930.      V(11, 9) = -V(9, 11)
2940. C
2950.      V(10, 10) = AB(4, 4) * H(1) * H(1) / C22(1) / C22(1)
2960.      V(10, 11) = -AB(4, 4) * H(1) * H(1) * ZK * C23(1) * CIMGG / C22(1) / C22(1)
2970.      V(11, 10) = -V(10, 11)
2980.      V(11, 11) = AB(4, 4) * H(1) * H(1) * ZK * C23(1) * C23(1) / C22(1) / C22(1)
2990. C
3000. C
3010.      IF ( N .EQ. 1 ) THEN DO
3020.          CONST = C22(1) / H(1)
3030.      ELSE DO
3040.          IF ( N .EQ. 2 ) THEN DO
3050.              CONST = C44(1) * ZK2 * H(1)
3060.          ELSE DO
3070.              IF ( N .EQ. 3 ) THEN DO
3080.                  CONST = C66(1) * XK2 * H(1)
3090.              ELSE DO
3100.                  CONST = -RHO(1) * H(1)
3110.              END IF
3120.          END IF
3130.      END IF
3140. C
3150.      ITIME = I - 1
3160.      DO 20 J=1, 12
3170.          IR = J + 6 * ITIME
3180.          DO 30 K=1, 12
3190.              IC = K + 6 * ITIME
3200.              BKNBM(IR, IC) = BKNBM(IR, IC) + CONST * V(J, K)
3210.          30 CONTINUE
3220.      20 CONTINUE
3230.      10 CONTINUE
3240. C
3250.      RETURN; END
3260. C
3270. C*****
3280. C
3290. C          SUBROUTINE WBAR          *
3300. C          *
3310. C*****
3320. C
3330. C
3340.      SUBROUTINE WBAR(NP, H, C33, C44, C55, RHO, XK, ZK, AB, N, CKNCM)
3350. C
3360. C
3370.      COMMON/BLK1/NP1, NP2, IC2
3380.      COMMON/BLK2/CIMGG, ZERO
3390.      REAL*8      H(NP1), C33(NP1), C44(NP1), C55(NP1), RHO(NP1),
3400.      @          AB(4, 4), XK, XK2, ZK, ZK2
3410.      COMPLEX*16  CKNCM(IC2, IC2), W(12, 12), CONST, CIMGG, ZERO
3420. C
3430.      XK2=XK*XK
3440.      ZK2=ZK*ZK

```

```
3450.      DO 1000 JJ=1,1C2
3460.          DO 1050 KK=1,1C2
3470.              CKNCM(JJ, KK) = ZERO
3480. 1050      CONTINUE
3490. 1000      CONTINUE
3500. C
3510.      DO 991 L1=1, 12
3520.          DO 992 L2=1, 12
3530.              W(L1, L2) = ZERO
3540. 992      CONTINUE
3550. 991      CONTINUE
3560.      DO 10 I=1, NP1
3570.          W(3, 3) = AB(3, 3)*ZK2*H(1)*H(1)
3580.          W(3, 5) = AB(1, 3)*ZK*H(1)*CIMGG
3590.          W(5, 3) = -W(3, 5)
3600.          W(3, 6) = AB(3, 3)*H(1)*H(1)*ZK*CIMGG/C44(1)
3610.          W(6, 3) = -W(3, 6)
3620.          W(3, 9) = AB(3, 4)*H(1)*H(1)*ZK2
3630.          W(9, 3) = W(3, 9)
3640.          W(3, 11) = AB(2, 3)*H(1)*ZK*CIMGG
3650.          W(11, 3) = -W(3, 11)
3660.          W(3, 12) = AB(3, 4)*H(1)*H(1)*ZK*CIMGG/C44(1)
3670.          W(12, 3) = -W(3, 12)
3680. C
3690.          W(5, 5) = AB(1, 1)
3700.          W(5, 6) = AB(1, 3)*H(1)/C44(1)
3710.          W(6, 5) = W(5, 6)
3720.          W(5, 9) = -AB(1, 4)*H(1)*ZK*CIMGG
3730.          W(9, 5) = -W(5, 9)
3740.          W(5, 11) = AB(1, 2)
3750.          W(11, 5) = W(5, 11)
3760.          W(5, 12) = AB(1, 4)*H(1)/C44(1)
3770.          W(12, 5) = W(5, 12)
3780. C
3790.          W(6, 6) = AB(3, 3)*H(1)*H(1)/C44(1)/C44(1)
3800.          W(6, 9) = -AB(3, 4)*H(1)*H(1)*ZK*CIMGG/C44(1)
3810.          W(9, 6) = -W(6, 9)
3820.          W(6, 11) = AB(2, 3)*H(1)/C44(1)
3830.          W(11, 6) = W(6, 11)
3840.          W(6, 12) = AB(3, 4)*H(1)*H(1)/C44(1)/C44(1)
3850.          W(12, 6) = W(6, 12)
3860. C
3870.          W(9, 9) = AB(4, 4)*H(1)*H(1)*ZK2
3880.          W(9, 11) = AB(2, 4)*H(1)*ZK*CIMGG
3890.          W(11, 9) = -W(9, 11)
3900.          W(9, 12) = AB(4, 4)*H(1)*H(1)*ZK*CIMGG/C44(1)
3910.          W(12, 9) = -W(9, 12)
3920. C
3930.          W(11, 11) = AB(2, 2)
3940.          W(11, 12) = AB(2, 4)*H(1)/C44(1)
3950.          W(12, 11) = W(11, 12)
3960. C
3970.          W(12, 12) = AB(4, 4)*H(1)*H(1)/C44(1)/C44(1)
3980. C
3990.          IF (N .EQ. 1) THEN DO
4000.              CONST = C33(1)*ZK2*H(1)
4010.          ELSE DO
4020.              IF (N .EQ. 2) THEN DO
4030.                  CONST = C44(1)/H(1)
4040.              ELSE DO
4050.                  IF (N .EQ. 3) THEN DO
4060.                      CONST = C55(1)*XK2*H(1)
4070.                  ELSE DO
4080.                      CONST = -RHO(1)*H(1)
```

```
4090.          END IF
4100.          END IF
4110.          END IF
4120. C
4130.          ITIME = I - 1
4140.          DO 20 J=1, 12
4150.              IR = J + 6 * ITIME
4160.          DO 30 K=1, 12
4170.              IC = K + 6 * ITIME
4180.              CKNCM(IR, IC) = CKNCM(IR, IC) + CONST * W(J, K)
4190.          30 CONTINUE
4200.          20 CONTINUE
4210.          10 CONTINUE
4220. C
4230. C
4240.          RETURN;END
4250. C
4260. C
4270. C
4280. C*****
4290. C
4300. C          SUBROUTINE UVBAR
4310. C
4320. C*****
4330. C
4340. C
4350.          SUBROUTINE UVBAR (NP,H,C12,C22,C23,C66,XK,ZK,D,N,DK12)
4360. C
4370.          COMMON/BLK1/ NP1, NP2, IC2
4380.          COMMON/BLK2/ CIMGG, ZERO
4390.          REAL *8      H(NP1),C12(NP1),C22(NP1),C23(NP1),C66(NP1),
4400.          *          D(4,4),CHSIGN, XK, XK2, ZK, ZK2
4410.          COMPLEX *16 DK12(IC2,IC2), UV(12,12), CONST, CIMGG, ZERO
4420. C
4430.          DO 1000 JJ=1, IC2
4440.              DO 1050 KK=1, IC2
4450.                  DK12(JJ, KK) = ZERO
4460.          1050 CONTINUE
4470.          1000 CONTINUE
4480. C
4490.          DO 991 L1=1, 12
4500.              DO 992 L2=1, 12
4510.                  UV(L1,L2) = ZERO
4520.          992 CONTINUE
4530.          991 CONTINUE
4540. C
4550.          XK2 = XK * XK
4560.          ZK2 = ZK * ZK
4570.          IF ( N .EQ. 1 ) THEN DO
4580.              CHSIGN = 1.0D0
4590.          ELSE DO
4600.              CHSIGN = - 1.0D0
4610.          END IF
4620. C
4630.          DO 10 I=1, NP1
4640. C
4650.              UV(1, 1) = 2. * D(1, 3) * H(I) * XK * C12(I) * CIMGG / C22(I)
4660.              UV(1, 2) = UV(2, 1) = ZERO
4670.              UV(1, 3) = - D(1, 1) * CHSIGN
4680.              UV(3, 1) = - UV(1, 3)
4690.              UV(1, 4) = - D(1, 3) * H(I) / C22(I)
4700.              UV(4, 1) = - UV(1, 4)
4710.              UV(1, 5) = D(1, 3)*ZK*C23(I)*H(I)*CIMGG/C22(I)
4720.              UV(5, 1) = UV(1, 5)
```

4730. UV(1, 7) = D(2, 3) * H(1) * XK * C12(1) * CIMGG / C22(1)
4740. * + D(1, 4) * H(1) * XK * C12(1) * CIMGG / C22(1)
4750. UV(7, 1) = UV(1, 7)
4760. UV(1, 8) = - D(3, 4) * H(1) * H(1) * XK * C12(1) * CIMGG
4770. * / C22(1) / C66(1)
4780. UV(8, 1) = UV(1, 8)
4790. UV(1, 9) = (- D(3, 4) * H(1) * H(1) * XK2 * C12(1) / C22(1))
4800. * - D(1, 2)
4810. UV(9, 1) = - UV(1, 9)
4820. UV(1, 10) = - D(1, 4) * H(1) / C22(1)
4830. UV(10, 1) = - UV(1, 10)
4840. UV(1, 11) = UV(11, 1) = D(1, 4) * H(1) * ZK * C23(1) * CIMGG / C22(1)
4850. C
4860. UV(2, 2) = ZERO
4870. UV(2, 3) = D(1, 3) * H(1) / C66(1)
4880. UV(3, 2) = - UV(2, 3)
4890. UV(2, 7) = D(3, 4) * H(1) * H(1) * XK * C12(1) * CIMGG
4900. * / C22(1) / C66(1)
4910. UV(7, 2) = UV(2, 7)
4920. UV(2, 8) = UV(8, 2) = ZERO
4930. UV(2, 9) = D(2, 3) * H(1) / C66(1)
4940. UV(9, 2) = - UV(2, 9)
4950. UV(2, 10) = - D(3, 4) * H(1) * H(1) / C22(1) / C66(1)
4960. UV(10, 2) = - UV(2, 10)
4970. UV(2, 11) = UV(11, 2) = D(3, 4) * H(1) * H(1) * ZK * C23(1) * CIMGG /
4980. C22(1) / C66(1)
4990. C
5000. UV(3, 3) = 2. * D(1, 3) * H(1) * XK * CIMGG
5010. UV(3, 4) = UV(4, 3) = ZERO
5020. UV(3, 7) = (- D(1, 2)) - D(3, 4) * H(1) * H(1) * XK2
5030. * C12(1) / C22(1)
5040. UV(7, 3) = - UV(3, 7)
5050. UV(3, 8) = - D(1, 4) * H(1) / C66(1)
5060. UV(8, 3) = - UV(3, 8)
5070. UV(3, 9) = D(1, 4) * H(1) * XK * CIMGG
5080. * + D(2, 3) * H(1) * XK * CIMGG
5090. UV(9, 3) = UV(3, 9)
5100. UV(3, 10) = - D(3, 4) * H(1) * H(1) * XK * CIMGG / C22(1)
5110. UV(10, 3) = UV(3, 10)
5120. UV(3, 11) = - D(3, 4) * H(1) * H(1) * ZK * C23(1) / C22(1)
5130. UV(11, 3) = - UV(3, 11)
5140. C
5150. UV(4, 4) = ZERO
5160. UV(4, 7) = D(2, 3) * H(1) / C22(1)
5170. UV(7, 4) = - UV(4, 7)
5180. UV(4, 8) = - D(3, 4) * H(1) * H(1) / C22(1) / C66(1)
5190. UV(8, 4) = - UV(4, 8)
5200. UV(4, 9) = D(3, 4) * H(1) * H(1) * XK * CIMGG / C22(1)
5210. UV(9, 4) = UV(4, 9)
5220. C
5230. UV(5, 7) = D(2, 3) * H(1) * ZK * C23(1) * CIMGG / C22(1)
5240. UV(7, 5) = UV(5, 7)
5250. UV(5, 8) = - D(3, 4) * H(1) * H(1) * ZK * C23(1) * CIMGG / C22(1) / C66(1)
5260. UV(8, 5) = UV(5, 8)
5270. UV(5, 9) = - D(3, 4) * H(1) * H(1) * ZK * C23(1) / C22(1)
5280. UV(9, 5) = - UV(5, 9)
5290. C
5300. UV(7, 7) = 2. * D(2, 4) * H(1) * XK * CIMGG * C12(1) / C22(1)
5310. UV(7, 9) = - D(2, 2) * CHSIGN
5320. UV(9, 7) = - UV(7, 9)
5330. UV(7, 10) = - D(2, 4) * H(1) / C22(1)
5340. UV(10, 7) = - UV(7, 10)
5350. UV(7, 11) = UV(11, 7) = D(2, 4) * H(1) * ZK * C23(1) * CIMGG / C22(1)
5360. C

```
5370.      UV(8, 8) = ZERO
5380.      UV(8, 9) = D(2, 4) * H(1) / C66(1)
5390.      UV(9, 8) = - UV(8, 9)
5400.      UV(9, 9) = 2. *D(2, 4) * H(1) * XK * CIMGG
5410. C
5420. C
5430.      IF (N .EQ. 1) THEN DO
5440.          CONST = C12(1) *XK * CIMGG
5450.      ELSE DO
5460.          CONST = C66(1) *XK *CIMGG
5470.      END IF
5480. C
5490.      ITIME = I - 1
5500.      DO 20 J=1, 12
5510.          IR = J + 6 * ITIME
5520.          DO 30 K=1, 12
5530.              IC = K + 6 * ITIME
5540.              DK12(IR, IC) = DK12(IR, IC) + CONST * UV(J, K)
5550.          30 CONTINUE
5560.      20 CONTINUE
5570.      10 CONTINUE
5580. C
5590.      RETURN;END
5600. C
5610. C
5620. C
5630. C*****
5640. C
5650. C          SUBROUTINE WUBAR DOING WU + UW          *
5660. C
5670. C*****
5680. C
5690. C
5700.      SUBROUTINE WUBAR(NP,H,C13,C44,C55,C66,XK,ZK,AB,N,EK12)
5710. C
5720. C
5730.      COMMON/BLK1/ NP1, NP2, IC2
5740.      COMMON/BLK2/ CIMGG, ZERO
5750.      REAL *8      H(NP1),C13(NP1),C44(NP1),C55(NP1),C66(NP1),
5760.      *            XK, XK2, ZK, ZK2, AB(4, 4)
5770.      COMPLEX *16  EK12(IC2,IC2),WU(12,12), CONST, CIMGG, ZERO
5780. C
5790.      XK2 = XK * XK
5800.      ZK2 = ZK * ZK
5810. C
5820.      DO 1000 JJ=1, IC2
5830.          DO 1050 KK=1, IC2
5840.              EK12(JJ, KK) = ZERO
5850.      1050 CONTINUE
5860.      1000 CONTINUE
5870. C
5880.      DO 991 L1=1, 12
5890.          DO 992 L2=1, 12
5900.              WU(L1,L2) = ZERO
5910.      992 CONTINUE
5920.      991 CONTINUE
5930. C
5940.      DO 10 I=1, NP1
5950. C
5960.          WU(1, 3)=-AB(1,3)*H(1)*ZK*CIMGG
5970.          WU(3, 1)=-WU(1, 3)
5980.          WU(1, 5)= AB(1,1)
5990.          WU(5, 1)= WU(1, 5)
6000.          WU(1, 6)= AB(1,3)*H(1)/C44(1)
```

6010. WU(6, 1) = WU(1, 6)
6020. WU(1, 9) = -AB(1, 4) * H(1) * ZK * CIMGG
6030. WU(9, 1) = -WU(1, 9)
6040. WU(1, 11) = AB(1, 2)
6050. WU(11, 1) = WU(1, 11)
6060. WU(1, 12) = AB(1, 4) * H(1) / C44(1)
6070. WU(12, 1) = WU(1, 12)
6080. C
6090. WU(2, 3) = -AB(3, 3) * H(1) * H(1) * ZK * CIMGG / C66(1)
6100. WU(3, 2) = -WU(2, 3)
6110. WU(2, 5) = AB(1, 3) * H(1) / C66(1)
6120. WU(5, 2) = WU(2, 5)
6130. WU(2, 6) = AB(3, 3) * H(1) * H(1) / C44(1) / C66(1)
6140. WU(6, 2) = WU(2, 6)
6150. WU(2, 9) = -AB(3, 4) * H(1) * H(1) * ZK * CIMGG / C66(1)
6160. WU(9, 2) = -WU(2, 9)
6170. WU(2, 11) = AB(2, 3) * H(1) / C66(1)
6180. WU(11, 2) = WU(2, 11)
6190. WU(2, 12) = AB(3, 4) * H(1) * H(1) / C44(1) / C66(1)
6200. WU(12, 2) = WU(2, 12)
6210. C
6220. WU(3, 3) = 2 * AB(3, 3) * H(1) * H(1) * ZK * XK
6230. WU(3, 5) = AB(1, 3) * H(1) * XK * CIMGG
6240. WU(5, 3) = -WU(3, 5)
6250. WU(3, 6) = AB(3, 3) * H(1) * H(1) * XK * CIMGG / C44(1)
6260. WU(6, 3) = -WU(3, 6)
6270. WU(3, 7) = AB(2, 3) * H(1) * ZK * CIMGG
6280. WU(7, 3) = -WU(3, 7)
6290. WU(3, 8) = AB(3, 4) * H(1) * H(1) * ZK * CIMGG / C66(1)
6300. WU(8, 3) = -WU(3, 8)
6310. WU(3, 9) = 2 * AB(3, 4) * H(1) * H(1) * ZK * XK
6320. WU(9, 3) = WU(3, 9)
6330. WU(3, 11) = AB(2, 3) * H(1) * XK * CIMGG
6340. WU(11, 3) = -WU(3, 11)
6350. WU(3, 12) = AB(3, 4) * H(1) * H(1) * XK * CIMGG / C44(1)
6360. WU(12, 3) = -WU(3, 12)
6370. C
6380. WU(5, 7) = AB(1, 2)
6390. WU(7, 5) = WU(5, 7)
6400. WU(5, 8) = AB(1, 4) * H(1) / C66(1)
6410. WU(8, 5) = WU(5, 8)
6420. WU(5, 9) = -AB(1, 4) * H(1) * XK * CIMGG
6430. WU(9, 5) = -WU(5, 9)
6440. C
6450. WU(6, 7) = AB(2, 3) * H(1) / C44(1)
6460. WU(7, 6) = WU(6, 7)
6470. WU(6, 8) = AB(3, 4) * H(1) * H(1) / C44(1) / C66(1)
6480. WU(8, 6) = WU(6, 8)
6490. WU(6, 9) = -AB(3, 4) * H(1) * H(1) * XK * CIMGG / C44(1)
6500. WU(9, 6) = -WU(6, 9)
6510. C
6520. WU(7, 9) = -AB(2, 4) * H(1) * ZK * CIMGG
6530. WU(9, 7) = -WU(7, 9)
6540. WU(7, 11) = AB(2, 2)
6550. WU(11, 7) = WU(7, 11)
6560. WU(7, 12) = AB(2, 4) * H(1) / C44(1)
6570. WU(12, 7) = WU(7, 12)
6580. r
6590. WU(8, 9) = -AB(4, 4) * H(1) * H(1) * ZK * CIMGG / C66(1)
6600. WU(9, 8) = -WU(8, 9)
6610. WU(8, 11) = AB(2, 4) * H(1) / C66(1)
6620. WU(11, 8) = WU(8, 11)
6630. WU(8, 12) = AB(4, 4) * H(1) * H(1) / C44(1) / C66(1)
6640. WU(12, 8) = WU(8, 12)

```

6650. C
6660.      WU(9,9) = 2.*AB(4,4)*H(1)*H(1)*ZK*XK
6670.      WU(9,11) = AB(2,4)*XK*H(1)*CIMGG
6680.      WU(11,9) = -WU(9,11)
6690.      WU(9,12) = AB(4,4)*H(1)*H(1)*XK*CIMGG/C44(1)
6700.      WU(12,9) = -WU(9,12)
6710. C
6720.      IF (N.EQ. 1) THEN DO
6730.          CONST = C13(1)*H(1)*XK*ZK
6740.      ELSE DO
6750.          CONST = C55(1)*H(1)*XK*ZK
6760.      END IF
6770. C
6780. C
6790.      ITIME = I - 1
6800.      DO 20 J=1, 12
6810.          IR = J + 6 * ITIME
6820.          DO 30 K=1, 12
6830.              IC = K + 6 * ITIME
6840.              EK12(IR, IC) = EK12(IR, IC) + CONST *WU(J, K)
6850.          30 CONTINUE
6860.          20 CONTINUE
6870.      10 CONTINUE
6880. C
6890. C
6900.      RETURN;END
6910. C
6920. C
6930. C*****
6940. C
6950. C          SUBROUTINE WVBAR DOING WVBAR'-V'WBAR AND          *
6960. C          VWBAR'-W'VBAR          *
6970. C          *
6980. C*****
6990. C
7000. C
7010.      SUBROUTINE WVBAR(NP,H,C12,C22,C23,C44,XK,ZK,D,N,FK12)
7020. C
7030. C
7040.      COMMON/BLK1/NP1,NP2,IC2
7050.      COMMON/BLK2/CIMGG,ZERO
7060.      REAL*8 H(NP1),C12(NP1),C22(NP1),C23(NP1),C44(NP1),
7070.      @ D(4,4),XK,XK2,ZK,ZK2
7080.      COMPLEX*16 FK12(IC2,IC2),WV(12,12),CONST,CIMGG,ZERO
7090. C
7100.      XK2=XK*XK
7110.      ZK2=ZK*ZK
7120.      DO 1000 JJ=1,IC2
7130.          DO 1050 KK=1,IC2
7140.              FK12(JJ,KK) = ZERO
7150.          1050 CONTINUE
7160.      1000 CONTINUE
7170. C
7180.      DO 991 L1=1, 12
7190.          DO 992 L2=1, 12
7200.              WV(L1,L2) = ZERO
7210.          992 CONTINUE
7220.      991 CONTINUE
7230. C
7240.      IF (N.EQ. 1) THEN DO
7250.          CHSIGN = 1.0D0
7260.      ELSE DO
7270.          CHSIGN = -1.0D0
7280.      END IF

```

```
7290. C
7300. DO 10 I=1,NP1
7310. WV(1, 5) = D(1,3)*H(1)*XK*C12(1)*CIMGG/C22(1)
7320. WV(5, 1) = WV(1, 5)
7330. WV(1, 9) = -D(3,4)*H(1)*H(1)*XK*XK*C12(1)/C22(1)
7340. WV(9, 1) = -WV(1, 9)
7350. WV(1,11) = D(2,3)*H(1)*XK*C12(1)*CIMGG/C22(1)
7360. WV(11,1) = WV(1,11)
7370. WV(1,12) = D(3,4)*H(1)*H(1)*XK*C12(1)*CIMGG/C22(1)/C44(1)
7380. WV(12,1) = WV(1,12)
7390. C
7400. WV(3, 3) = 2.*D(1,3)*H(1)*ZK*CIMGG
7410. WV(3, 5) = D(1,1)*CHSIGN
7420. WV(5, 3) = -WV(3, 5)
7430. WV(3, 6) = -D(1,3)*H(1)/C44(1)
7440. WV(6, 3) = -WV(3, 6)
7450. WV(3, 7) = -D(3,4)*H(1)*H(1)*ZK*XK*C12(1)/C22(1)
7460. WV(7, 3) = -WV(3, 7)
7470. WV(3, 9) = D(1,4)*H(1)*ZK*CIMGG
7480. +D(2,3)*H(1)*ZK*CIMGG
7490. WV(9, 3) = WV(3, 9)
7500. WV(3,10) = -D(3,4)*H(1)*H(1)*ZK*CIMGG/C22(1)
7510. WV(10,3) = WV(3,10)
7520. WV(3,11) = (-D(1,2)) -D(3,4)*H(1)*H(1)*ZK2*C23(1)/C22(1)
7530. WV(11,3) = -WV(3,11)
7540. WV(3,12) = -D(1,4)*H(1)/C44(1)
7550. WV(12,3) = -WV(3,12)
7560. C
7570. WV(4, 5) = D(1,3)*H(1)/C22(1)
7580. WV(5, 4) = -WV(4, 5)
7590. WV(4, 9) = D(3,4)*H(1)*H(1)*ZK*CIMGG/C22(1)
7600. WV(9, 4) = WV(4, 9)
7610. WV(4,11) = D(2,3)*H(1)/C22(1)
7620. WV(11,4) = -WV(4,11)
7630. WV(4,12) = -D(3,4)*H(1)*H(1)/C22(1)/C44(1)
7640. WV(12,4) = -WV(4,12)
7650. C
7660. WV(5, 5) = 2.*D(1,3)*ZK*H(1)*CIMGG*C23(1)/C22(1)
7670. WV(5, 7) = D(1,4)*H(1)*XK*C12(1)*CIMGG/C22(1)
7680. WV(7, 5) = WV(5, 7)
7690. WV(5, 9) = (-D(1,2)) -D(3,4)*H(1)*H(1)*ZK2*C23(1)/C22(1)
7700. WV(9, 5) = -WV(5, 9)
7710. WV(5,10) = -D(1,4)*H(1)/C22(1)
7720. WV(10,5) = -WV(5,10)
7730. WV(5,11) = D(1,4)*H(1)*ZK*CIMGG*C23(1)/C22(1)
7740. +D(2,3)*H(1)*ZK*CIMGG*C23(1)/C22(1)
7750. WV(11,5) = WV(5,11)
7760. WV(5,12) = -D(3,4)*ZK*H(1)*H(1)*C23(1)*CIMGG/C22(1)/C44(1)
7770. WV(12,5) = WV(5,12)
7780. C
7790. WV(6, 7) = D(3,4)*H(1)*H(1)*XK*C12(1)*CIMGG/C22(1)/C44(1)
7800. WV(7, 6) = WV(6, 7)
7810. WV(6, 9) = D(2,3)*H(1)/C44(1)
7820. WV(9, 6) = -WV(6, 9)
7830. WV(6,10) = -D(3,4)*H(1)*H(1)/C22(1)/C44(1)
7840. WV(10,6) = -WV(6,10)
7850. WV(6,11) = D(3,4)*H(1)*H(1)*ZK*C23(1)*CIMGG/C22(1)/C44(1)
7860. WV(11,6) = WV(6,11)
7870. C
7880. WV(7,11) = D(2,4)*H(1)*XK*C12(1)*CIMGG/C22(1)
7890. WV(11,7) = WV(7,11)
7900. C
7910. WV(9, 9) = 2.*D(2,4)*H(1)*ZK*CIMGG
7920. WV(9,11) = D(2,2)*CHSIGN
```

```
7930.      WV(11,9)=-WV(9,11)
7940.      WV(9,12)=-D(2,4)*H(1)/C44(1)
7950.      WV(12,9)=-WV(9,12)
7960. C
7970.      WV(10,11) = D(2,4)*H(1)/C22(1)
7980.      WV(11,10)=-WV(10,11)
7990. C
8000.      WV(11,11) = 2.*D(2,4)*H(1)*ZK*C23(1)*CIMGG/C22(1)
8010. C
8020.      IF (N.EQ. 1) THEN DO
8030.          CONST = C23(1) * ZK* CIMGG
8040.      ELSE DO
8050.          CONST = C44(1) * ZK * CIMGG
8060.      END IF
8070. C
8080.      ITIME = 1 - 1
8090.      DO 20 J=1, 12
8100.          IR = J + 6 * ITIME
8110.          DO 30 K=1, 12
8120.              IC = K + 6 * ITIME
8130.              FK12(IR, IC) = FK12(IR, IC) + CONST *WV(J, K)
8140.          30 CONTINUE
8150.          20 CONTINUE
8160.          10 CONTINUE
8170. C
8180. C
8190.      RETURN;END
8200. C
8210. C
8220. C*****
8230. C
8240. C          SUBROUTINE ADDING          *
8250. C          *
8260. C*****
8270. C
8280. C
8290.      SUBROUTINE ADDING (NP, SK, MK)
8300. C
8310.      COMMON/BLK1/NP1, NP2, IC2
8320.      COMMON/BLK2/ CIMGG, ZERO
8330.      COMPLEX *16  SK(IC2,IC2), MK(IC2,IC2), CIMGG, ZERO
8340. C
8350.      NP6 = 6 * NP
8360.      NPSQ = 6 * ( NP + 2 )
8370.      NPSQM6 = NPSQ - 6
8380. C
8390. C      FIRST, ADD UP ALL THE MATRICES AND STORE THE RESULT IN AK
8400. C
8410.      DO 10 I=7, NPSQM6
8420.          DO 20 J=1, NPSQ
8430.              SK(I, J) = SK(I, J) + MK(I, J)
8440.          20 CONTINUE
8450.          10 CONTINUE
8460. C
8470.      RETURN;END
8480. C
8490. C
8500. C
8510. C
8520. C
8530. C*****
8540. C
8550. C          SUBROUTINE FORMDD          *
8560. C          *
      *
```

```
8570. C*****
8580. C
8590. C
8600. SUBROUTINE FORMDD (NP, AK, AM, BK, BM)
8610. C
8620. COMMON/BLK1/ NP1, NP2, IC2
8630. COMMON/BLK2/ CIMGG, ZERO
8640. COMPLEX *16 AK(IC2,IC2), AM(IC2,IC2), BK(IC2,IC2), BM(IC2,IC2)
8650. *          ,CIMGG, ZERO
8660. C
8670. DO 1000 JJ=1, IC2
8680. DO 1050 KK=1, IC2
8690. BK(JJ, KK) = ZERO
8700. BM(JJ, KK) = ZERO
8710. 1050 CONTINUE
8720. 1000 CONTINUE
8730. C
8740. NP6 = 6 * NP
8750. DO 10 I=1, NP6
8760. DO 20 J=1, 12
8770. IC = J + NP6
8780. BK(I, J) = AK(I, IC)
8790. BM(I, J) = AM(I, IC)
8800. 20 CONTINUE
8810. 10 CONTINUE
8820. C
8830. RETURN;END
8840. C
8850. $ENTRY
```

T A B L E S

$$\text{PERIODICITY} = 4, \bar{d} = 4$$

	Thickness ($2h^{(i)}$)	C_{11}	C_{12}	C_{13}	C_{22}	C_{23}	C_{33}	C_{44}	C_{55}	C_{66}	Density ($\rho^{(i)}$)
$\gamma = 10$	4.0	35	15	15	35	15	35	10	10	10	3.0
	1.0	4.333	2.333	2.333	4.333	2.333	4.333	1.0	1.0	1.0	1.0
$\gamma = 50$	4.0	175	75	75	175	75	175	50	50	50	3.0
	1.0	4.333	2.333	2.333	4.333	2.333	4.333	1.0	1.0	1.0	1.0
$\gamma = 100$	4.0	350	150	150	350	150	350	100	100	100	3.0
	1.0	4.333	2.333	2.333	4.333	2.333	4.333	1.0	1.0	1.0	1.0

Table 4.1: Material constants of composites for different isotropic lamina.

NOTE: To achieve a periodicity of 4, the properties of 5 layers are required as input. The first and second layers are subdivided into two layers each. The fifth layer is the same as the first sub-divided layer.

PERIODICITY = 4 , $\bar{d} = 12$

$$C_{ij} = C_{ij} * 10^{11} \text{N/m}^2$$

ρ is in g/cm

Layer	Thickness $h^{(i)}$	C_{11}	C_{12}	C_{13}	C_{22}	C_{23}	C_{33}	C_{44}	C_{55}	C_{66}	Density
1	6.0	2.6907	0.5850	0.5850	1.8860	0.7634	1.8860	0.5613	0.6019	0.6019	2.5200
2	6.0	2.6907	0.5850	0.5850	1.8860	0.7634	1.8860	0.5613	0.6019	0.6019	2.5200
3	0.5	1.1070	0.5730	0.5730	1.1070	0.5730	1.1070	0.2670	0.2670	0.2670	2.7020
4	0.5	1.1070	0.5730	0.5730	1.1070	0.5730	1.1070	0.2670	0.2670	0.2670	2.7020
5	6.0	2.6907	0.5850	0.5850	1.8860	0.7634	1.8860	0.5613	0.6019	0.6019	2.5200

Table 4.2: Material constants for fiber-reinforced Boron-Aluminium Composite.

NOTE: 5 layer as input

PERIODICITY = 4 , $\bar{d} = 4$

Units: $C_{ij} : * 10^{11} \text{N/m}^2$

$\rho : \text{g/cm}$

Layer	Thickness $h(i)$	C_{11}	C_{12}	C_{13}	C_{22}	C_{23}	C_{33}	C_{44}	C_{55}	C_{66}	Density
1	2.0	0.7669	0.0503	0.0503	0.1007	0.0507	0.1007	0.0250	0.0328	0.0328	1.200
2	2.0	0.7669	0.0503	0.0503	0.1007	0.0507	0.1007	0.0250	0.0328	0.0328	1.200
3	0.5	0.0865	0.0475	0.0475	0.0865	0.0475	0.0865	0.0195	0.0195	0.0195	1.800
4	0.5	0.0865	0.0475	0.0475	0.0865	0.0475	0.0865	0.0195	0.0195	0.0195	1.800
5	2.0	0.7669	0.0503	0.0503	0.1007	0.0507	0.1007	0.0250	0.0328	0.0328	1.200

Table 4.3: Material constants for graphite-epoxy composite (i).

PERIODICITY = 4 , $\bar{d} = 9$

Units: C_{ij} : 10^{11} N/m^2
 ρ : g/cm

Layer	Thickness $h^{(i)}$	C_{11}	C_{12}	C_{13}	C_{22}	C_{23}	C_{33}	C_{44}	C_{55}	C_{66}	Density
1	4.50	1.6073	0.0644	0.0644	0.1392	0.0692	0.1392	0.0350	0.0707	0.0707	1.20
2	4.50	1.6073	0.0644	0.0644	0.1392	0.0692	0.1392	0.0350	0.0707	0.0707	1.20
3	0.50	0.0865	0.0475	0.0475	0.0865	0.0475	0.0865	0.0195	0.0195	0.0195	1.80
4	0.50	0.0865	0.0475	0.0475	0.0865	0.0475	0.0865	0.0195	0.0195	0.0195	1.80
5	4.50	1.6073	0.0644	0.0644	0.1392	0.0692	0.1392	0.0350	0.0707	0.0707	1.20

Table 4.4: Material constants for graphite-epoxy composite (ii).

$$\text{PERIODICITY} = 4 : \bar{d} = 0.6$$

Layer	Thickness $z_h^{(i)}$	C_{11}	C_{12}	C_{13}	C_{22}	C_{23}	C_{33}	C_{44}	C_{55}	C_{66}	DENSITY	
1	0.6	7.000	0.300	3.000	0.700	3.000	7.000	2.000	2.000	2.000	1.000	
2-	i	1.0	0.700	0.300	0.300	0.700	0.300	0.700	0.200	0.020	0.020	1.000
	ii	1.0	3.850	0.300	1.650	0.700	1.650	3.850	1.100	1.010	1.010	1.000
	iii	1.0	7.000	0.300	3.000	0.700	3.000	7.000	2.000	2.000	2.000	1.000

Table 4.5: Material constants of transversely isotropic laminae

NOTE: Same as the note in Table 4.1. Layer 2 denotes the three types of matrix layers to be considered. Only one of these should be used at one consideration.

F I G U R E S

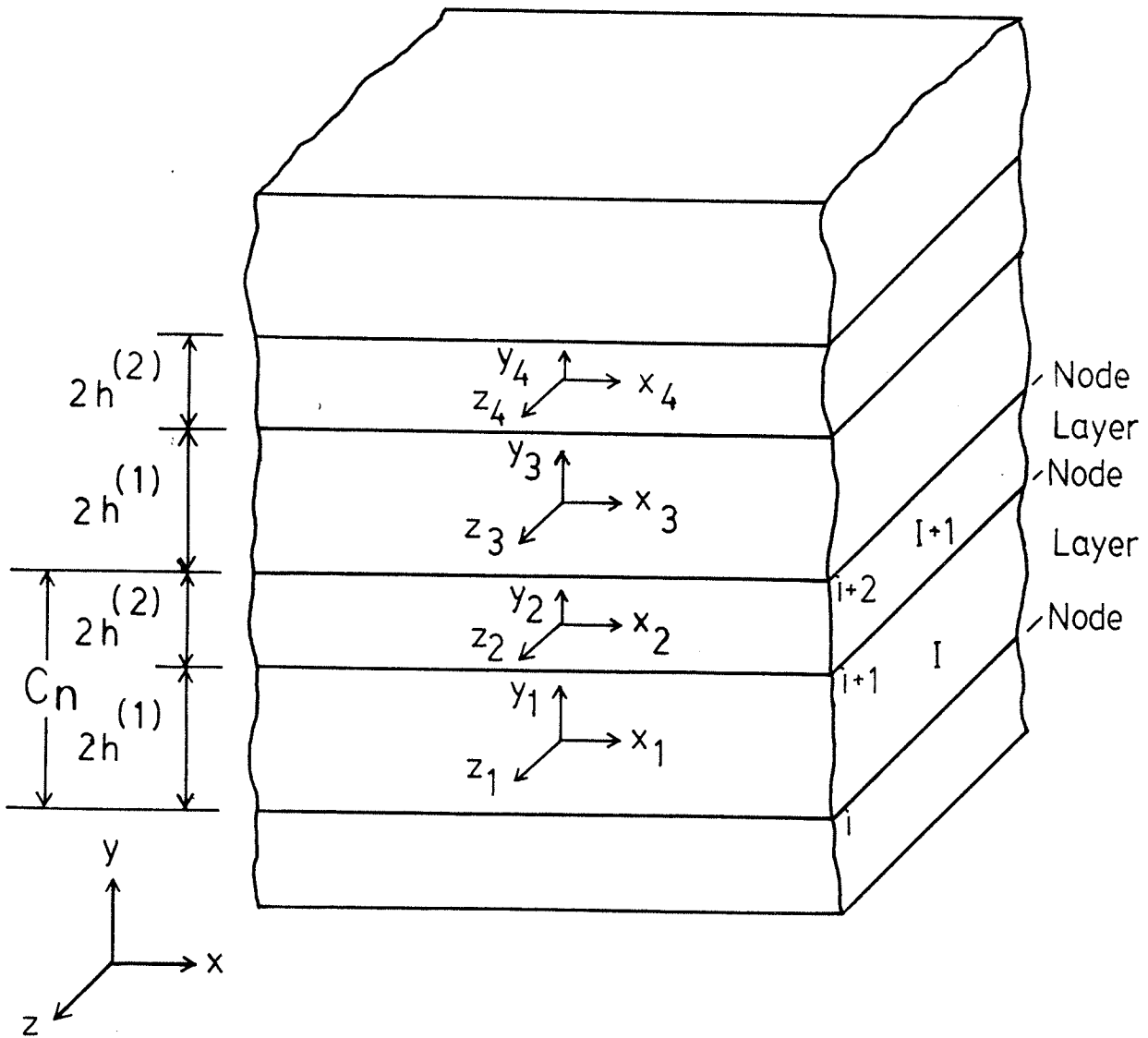


Fig. 2.1 Geometry of periodically laminated infinite medium.

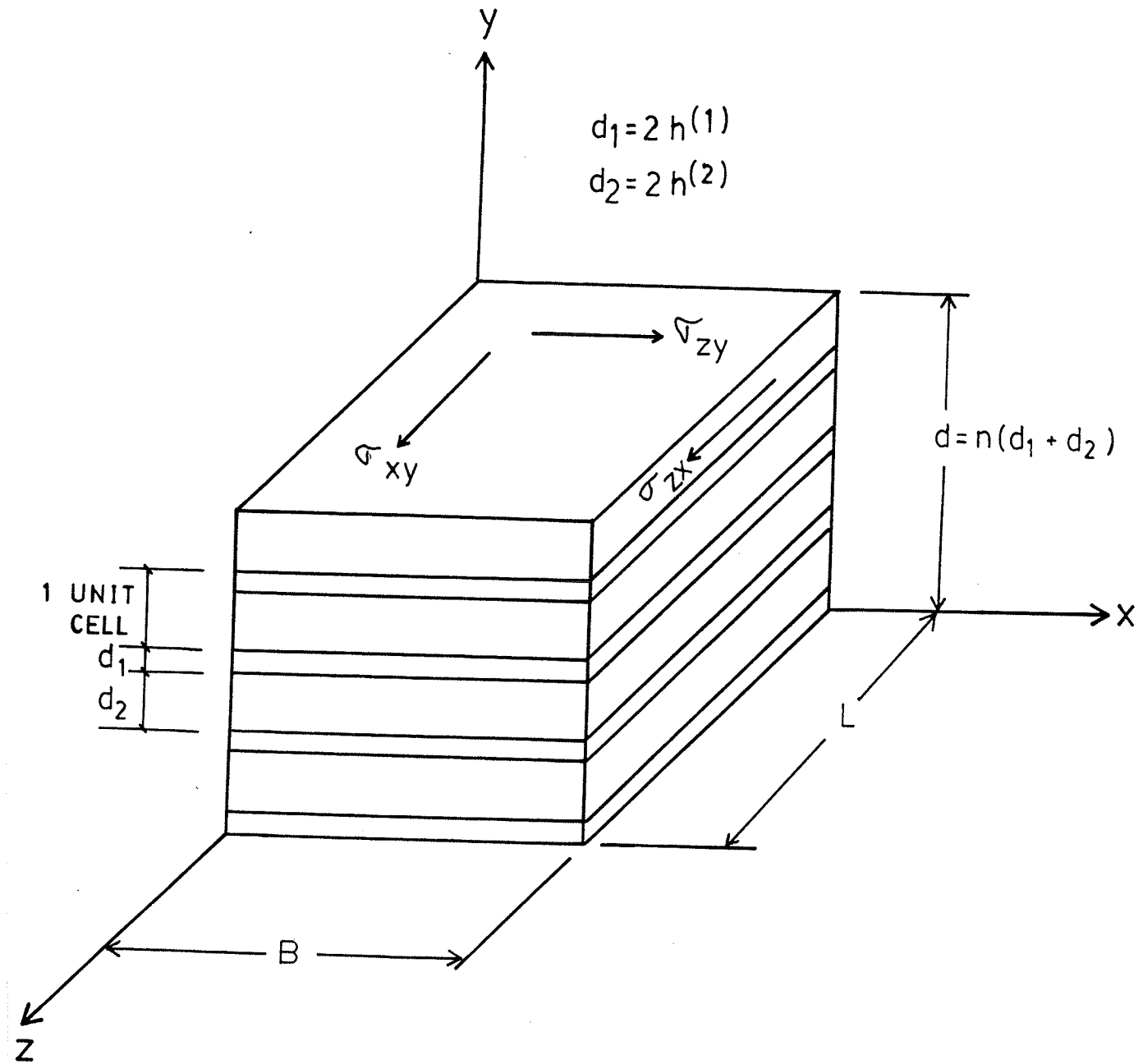


Fig. 3.1 Typical finite laminated medium showing shear stresses acting on the surface of the medium.

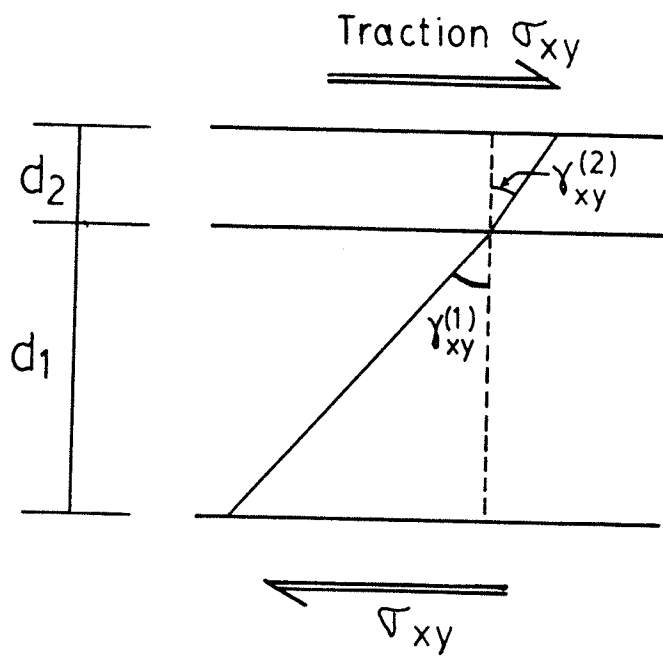


Fig. 3.2 Laminated layers subjected to tangential traction.

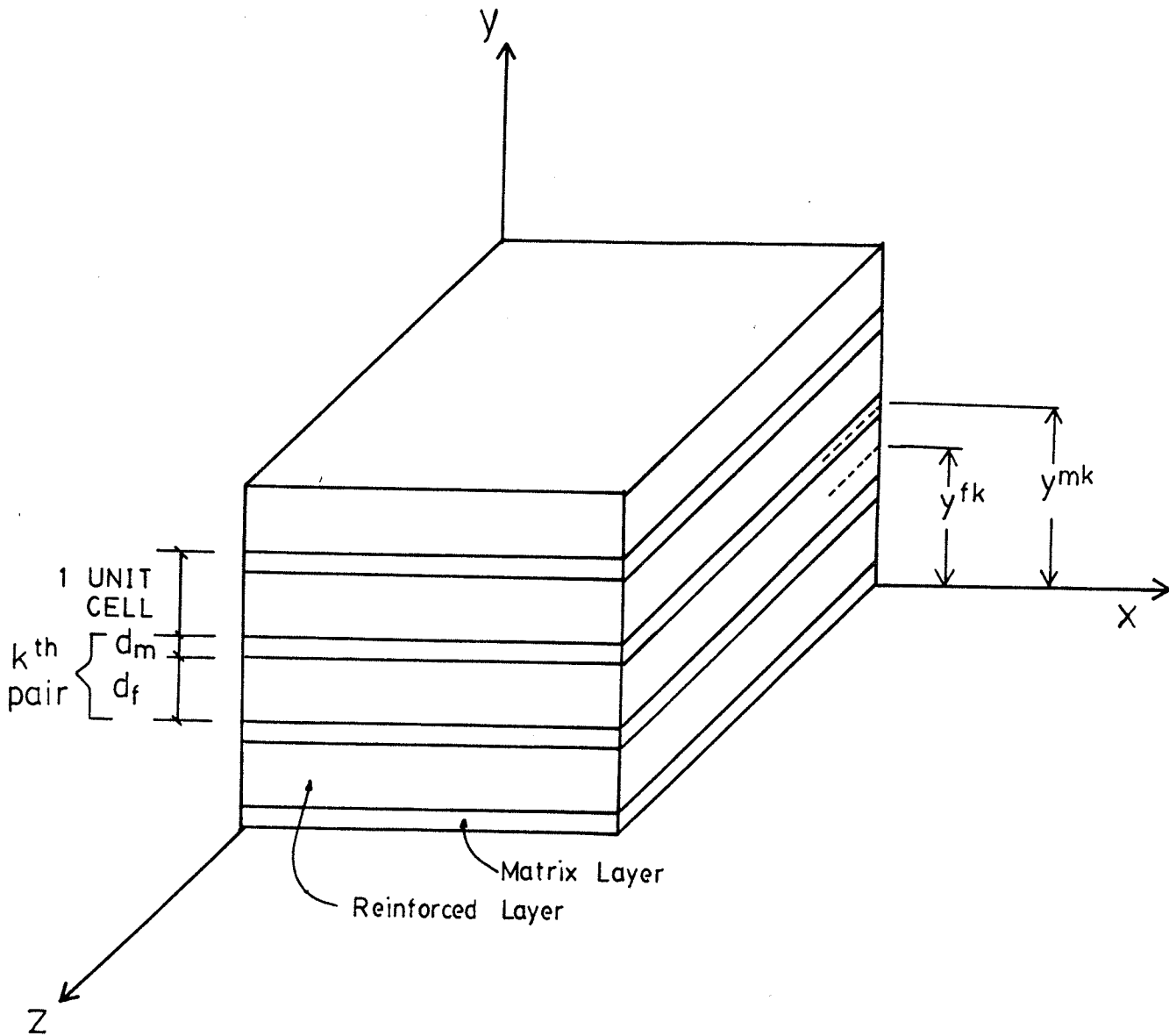


Fig. 3.3 Laminated medium used for the Effective Stiffness Method showing the layer properties and local coordinates.

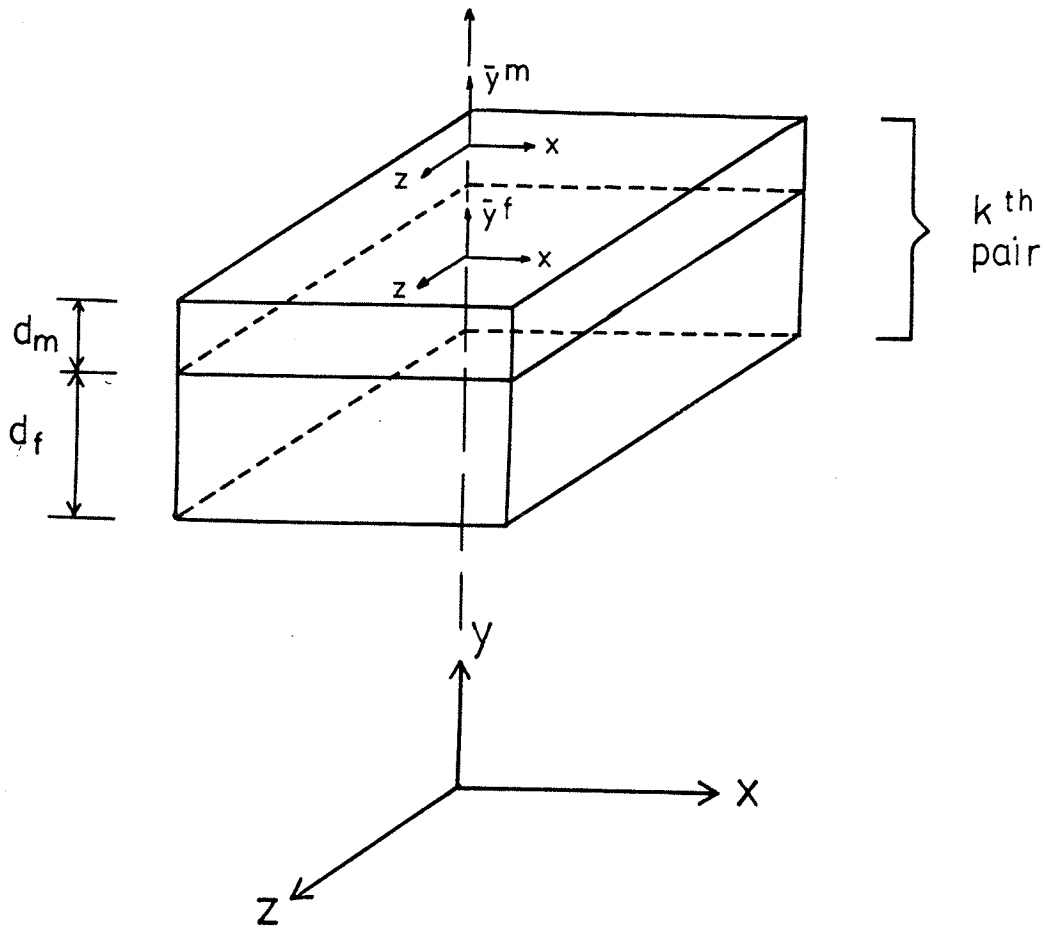


Fig. 3.4 Pair of reinforcing and matrix layers.

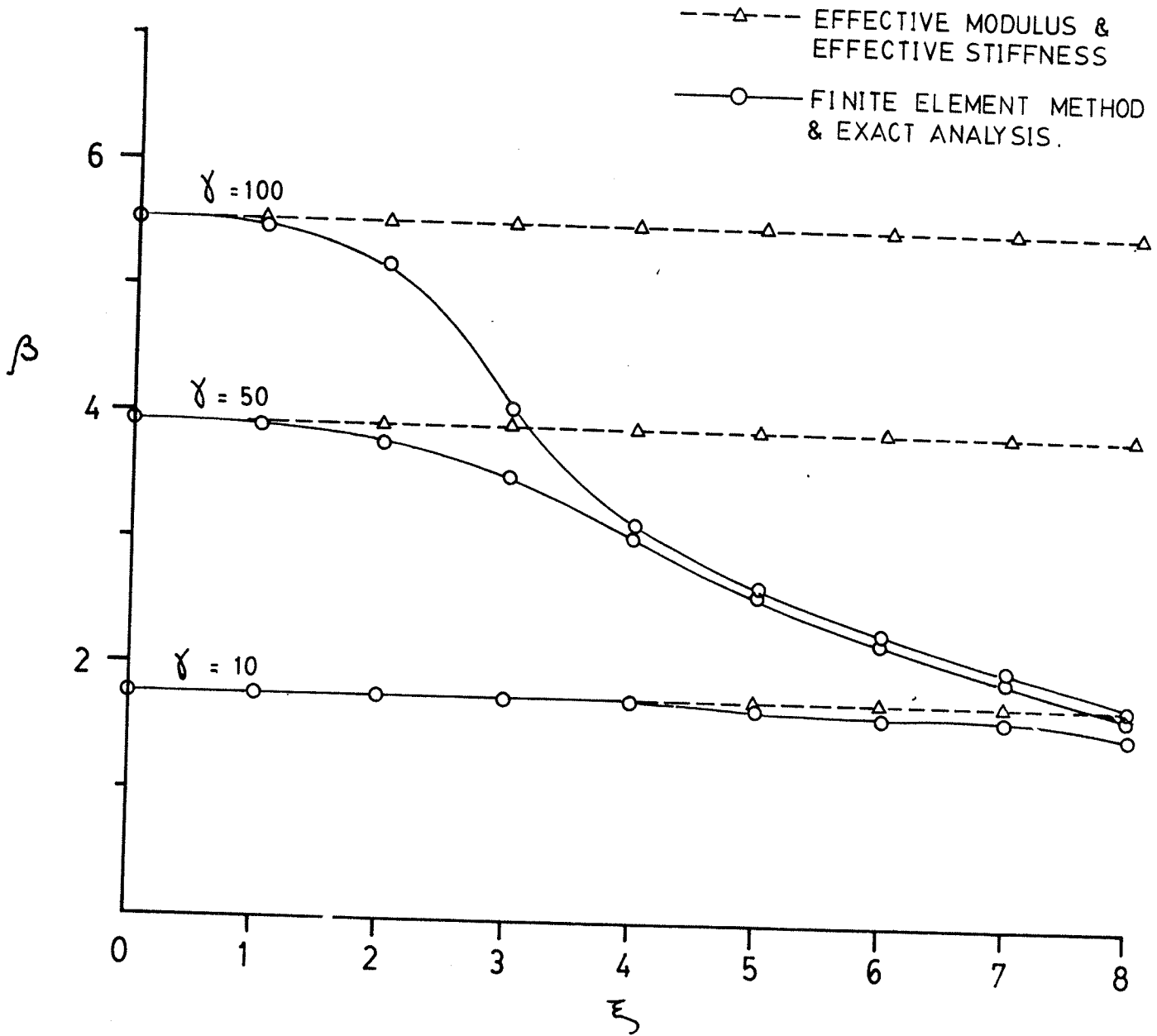


Fig. 4.1 Lowest symmetric SH mode propagating in the direction of the layering for isotropic material.

Fig. 4.2 Phase velocity vs. wave number plot for the lowest anti-symmetric mode (SV) propagating in the direction of the layering.

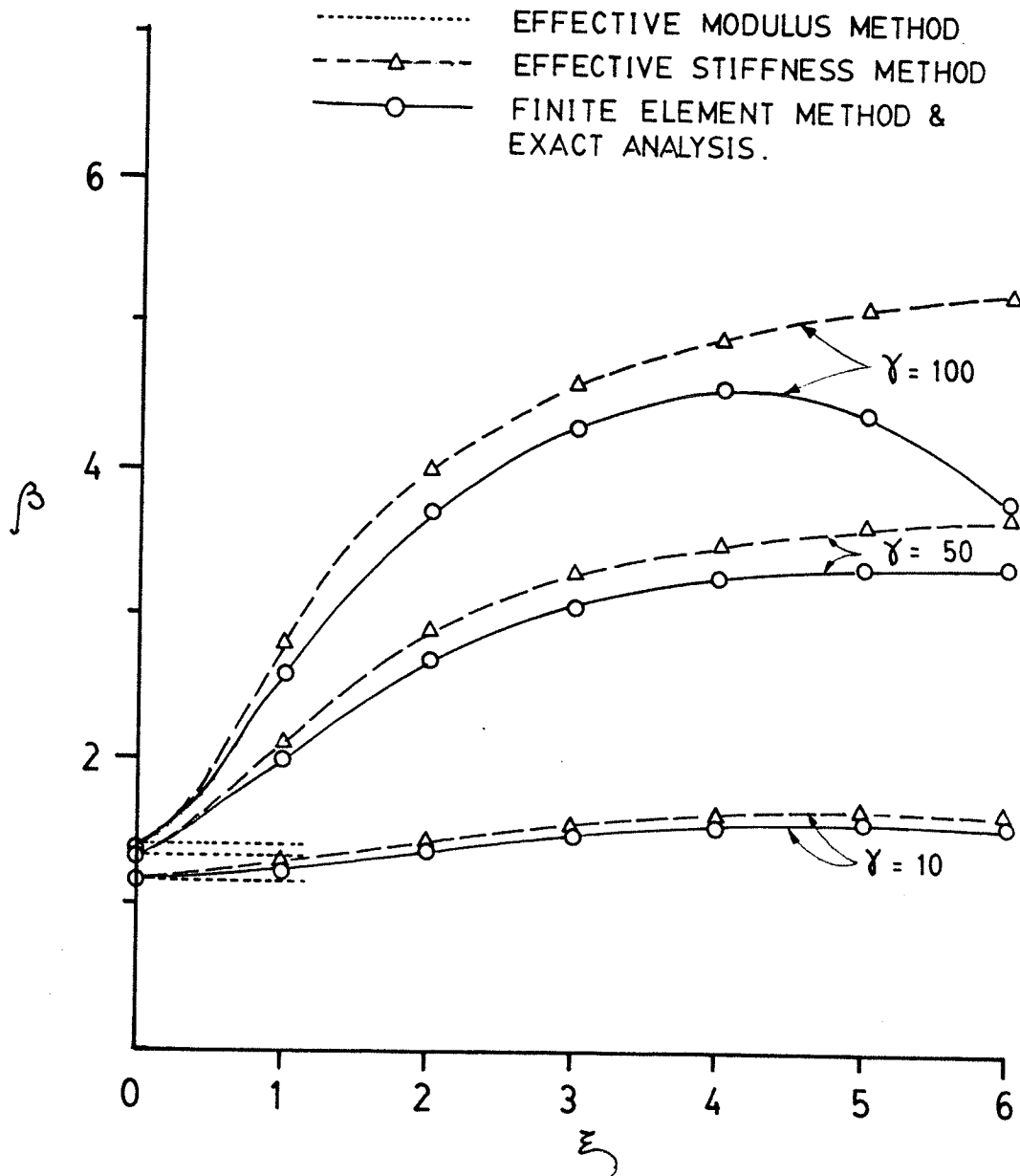


Fig. 4.3 Lowest symmetric P mode propagating in the direction of the layering.

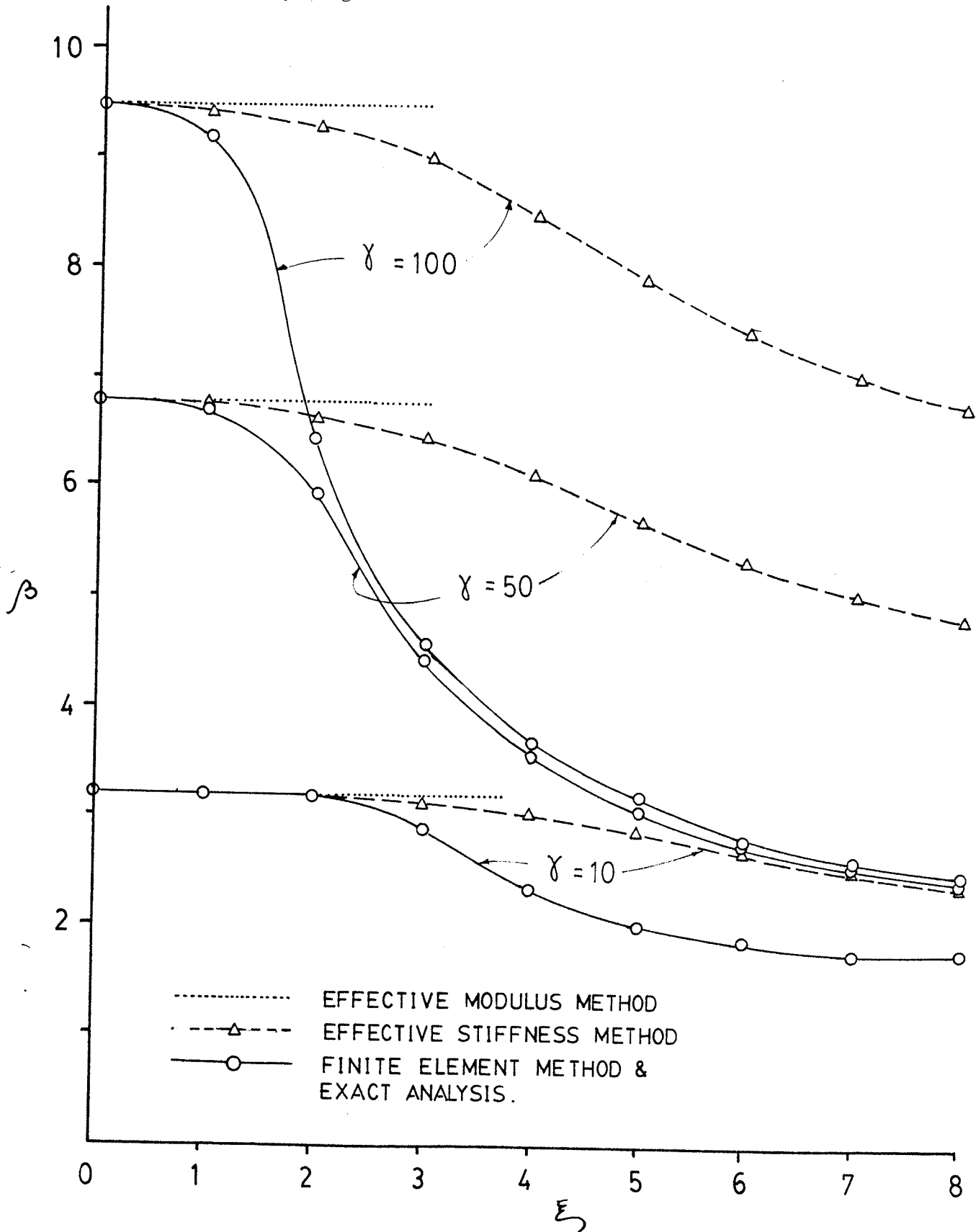


Fig. 4.4 Lowest transverse (SV) and longitudinal (P) mode propagating normal to the layering.

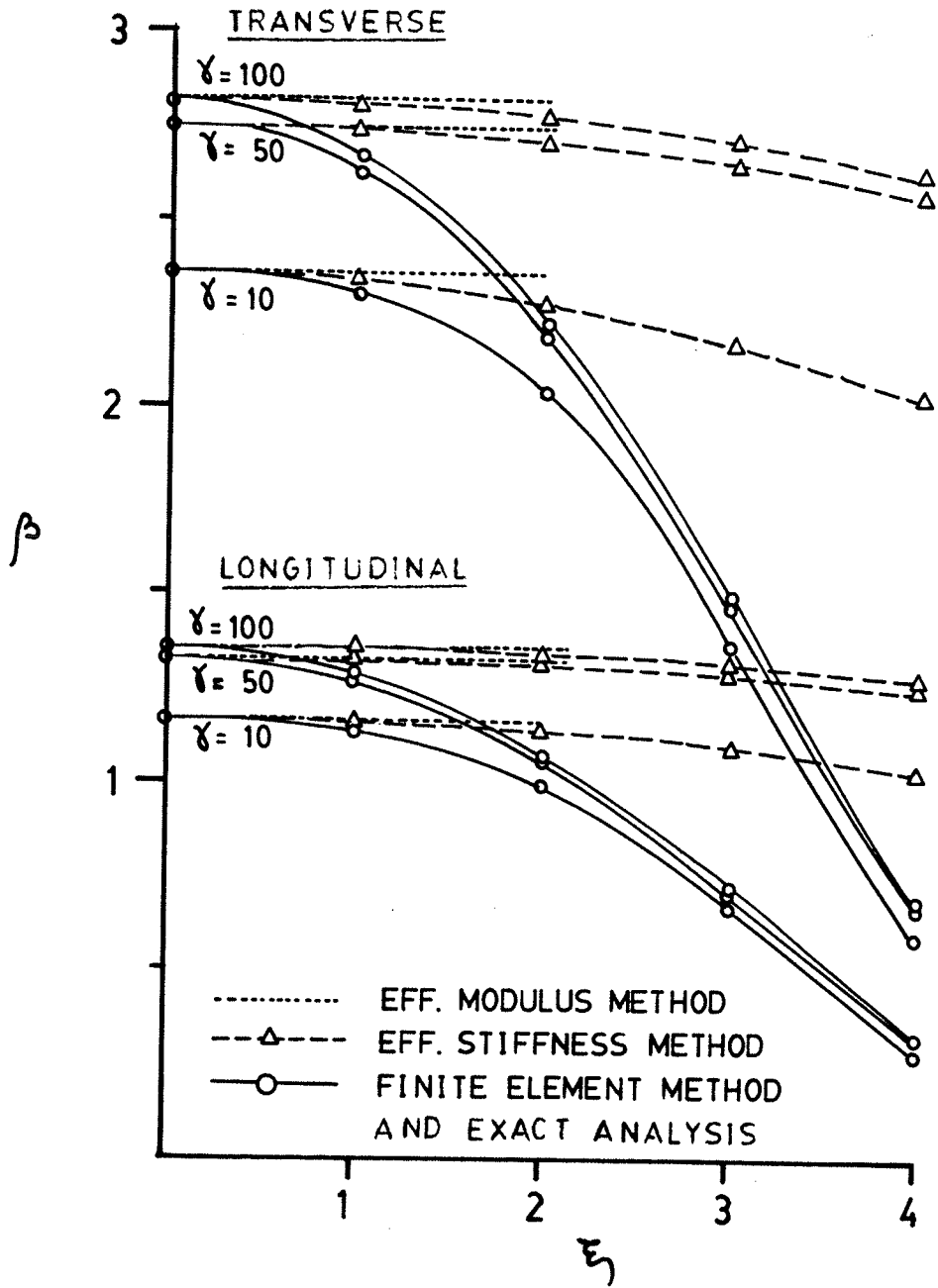


Fig. 4.5 Lowest transverse (SV) and longitudinal (P) mode propagating in the direction of the layering for anisotropic material.

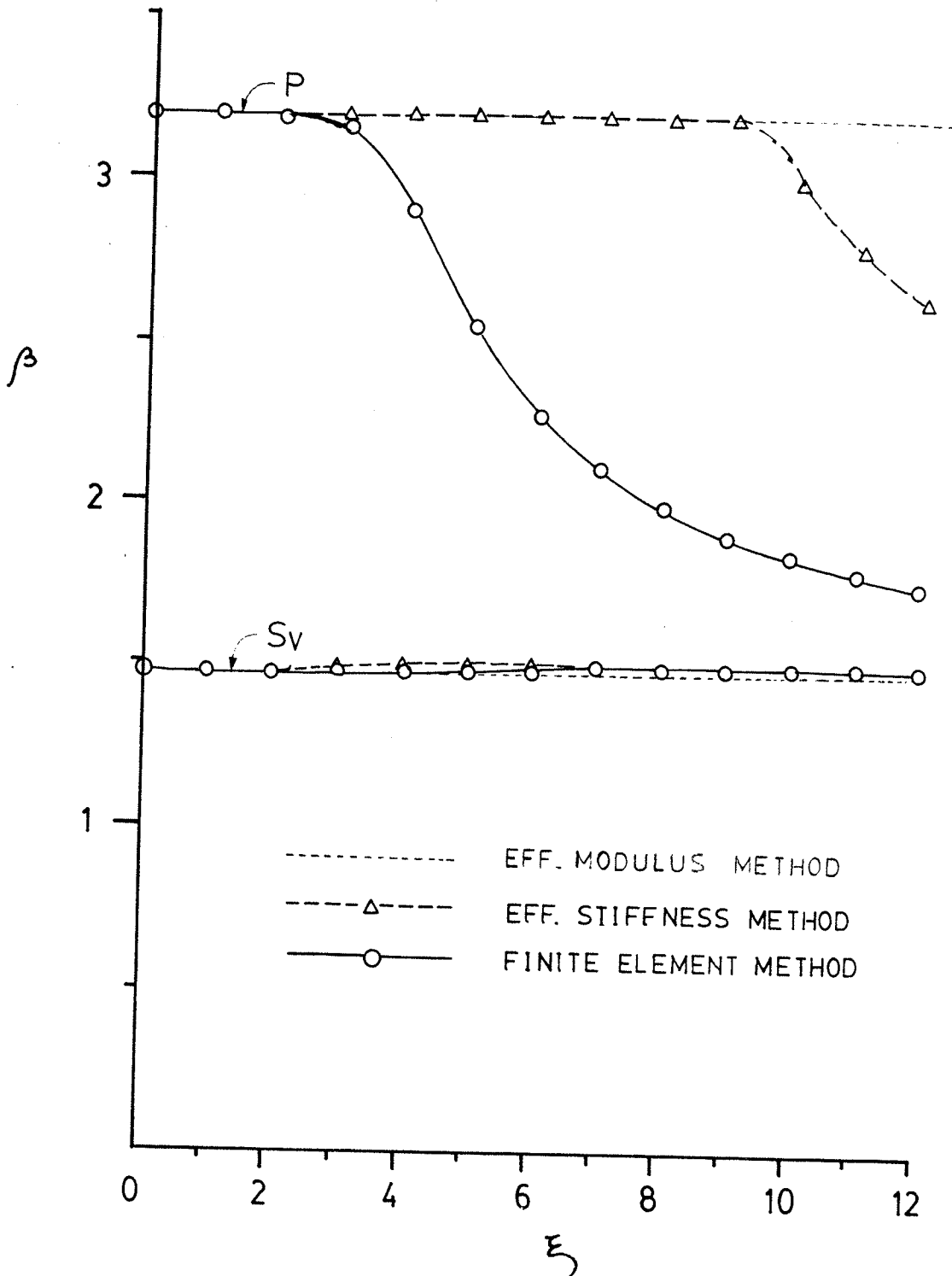


Fig. 4.6 Lowest SH, SV and P mode propagating normal to the layering for anisotropic material, $\alpha = 0^\circ$, $\phi = 90^\circ$.

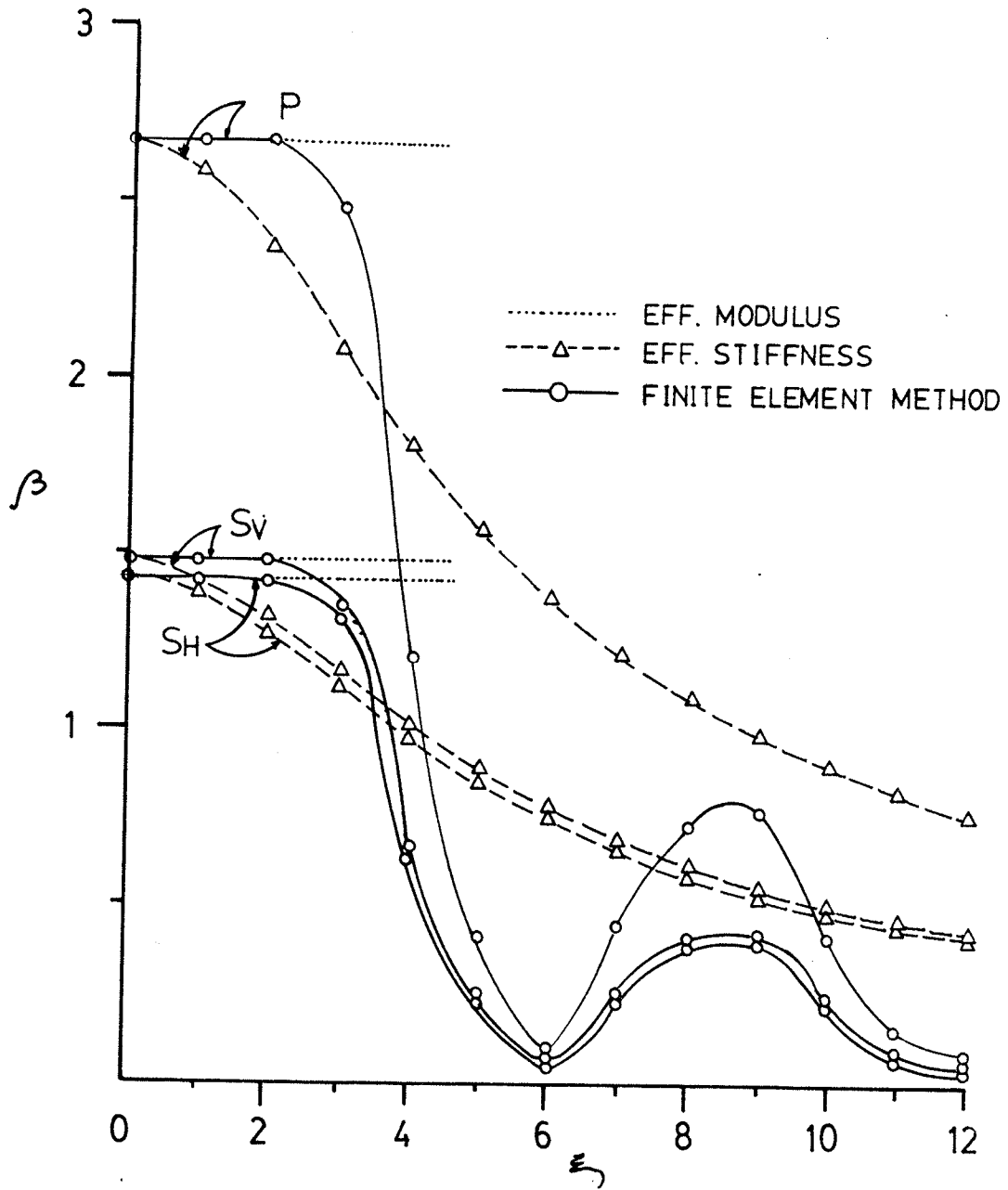


Fig. 4.7 Lowest SH, SV and P mode propagating along x-y plane, $\phi = 0^\circ$.

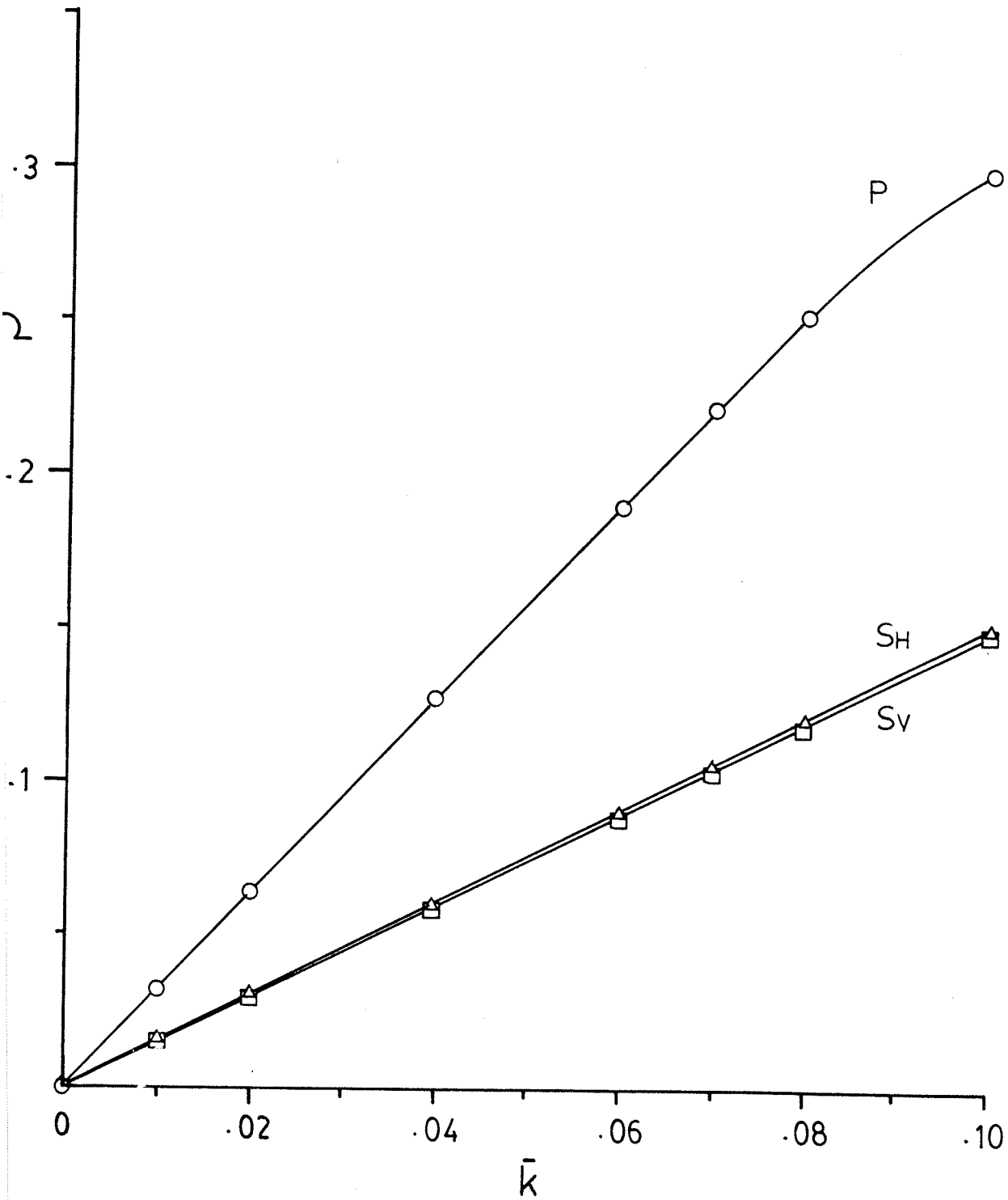


Fig. 4.8 Lowest SH, SV and P mode propagating along x-y plane, $\phi = 30^\circ$.

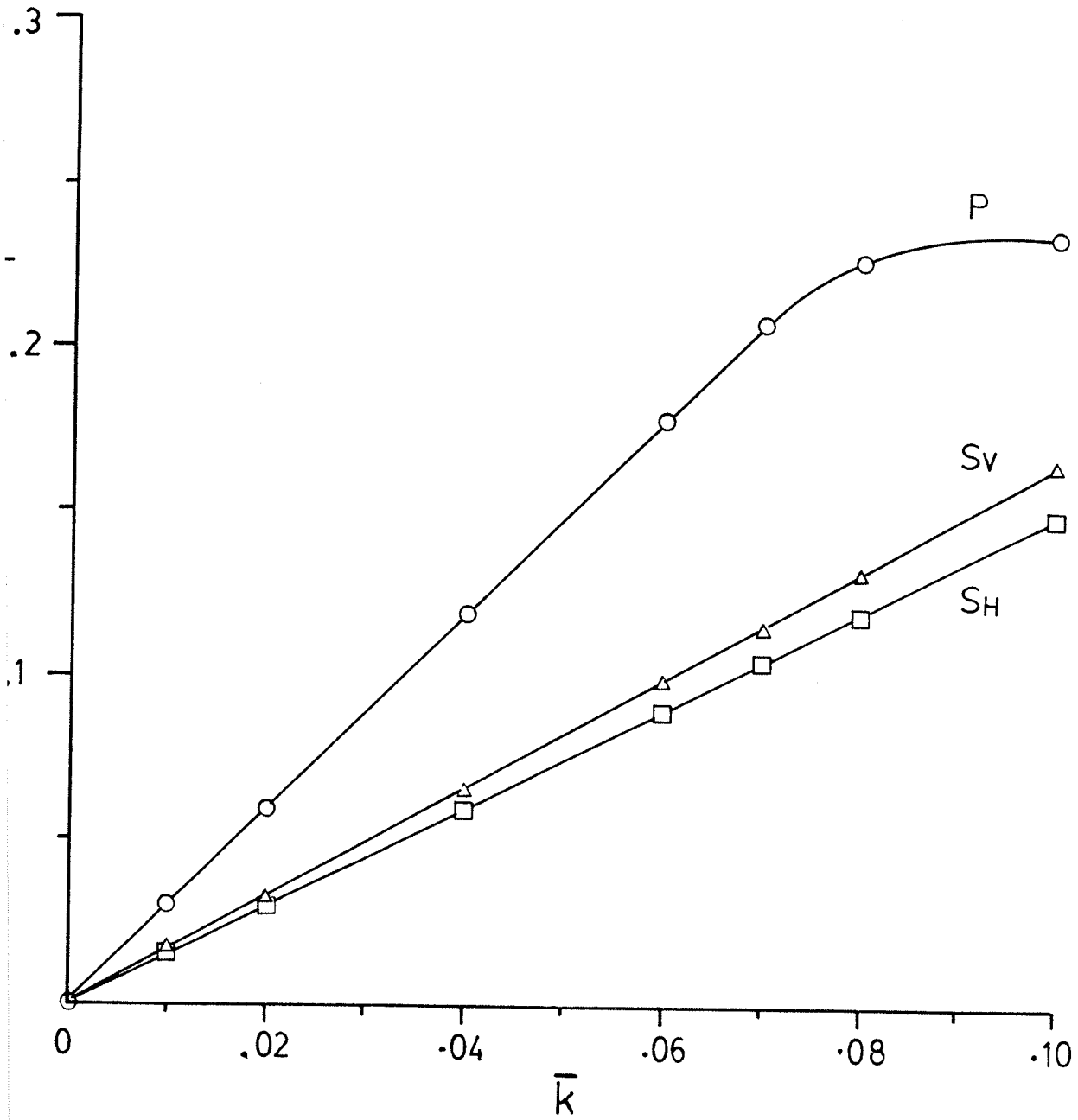


Fig. 4.9 Lowest SH, SV and P mode propagating along x-y plane, $\phi = 60^\circ$.

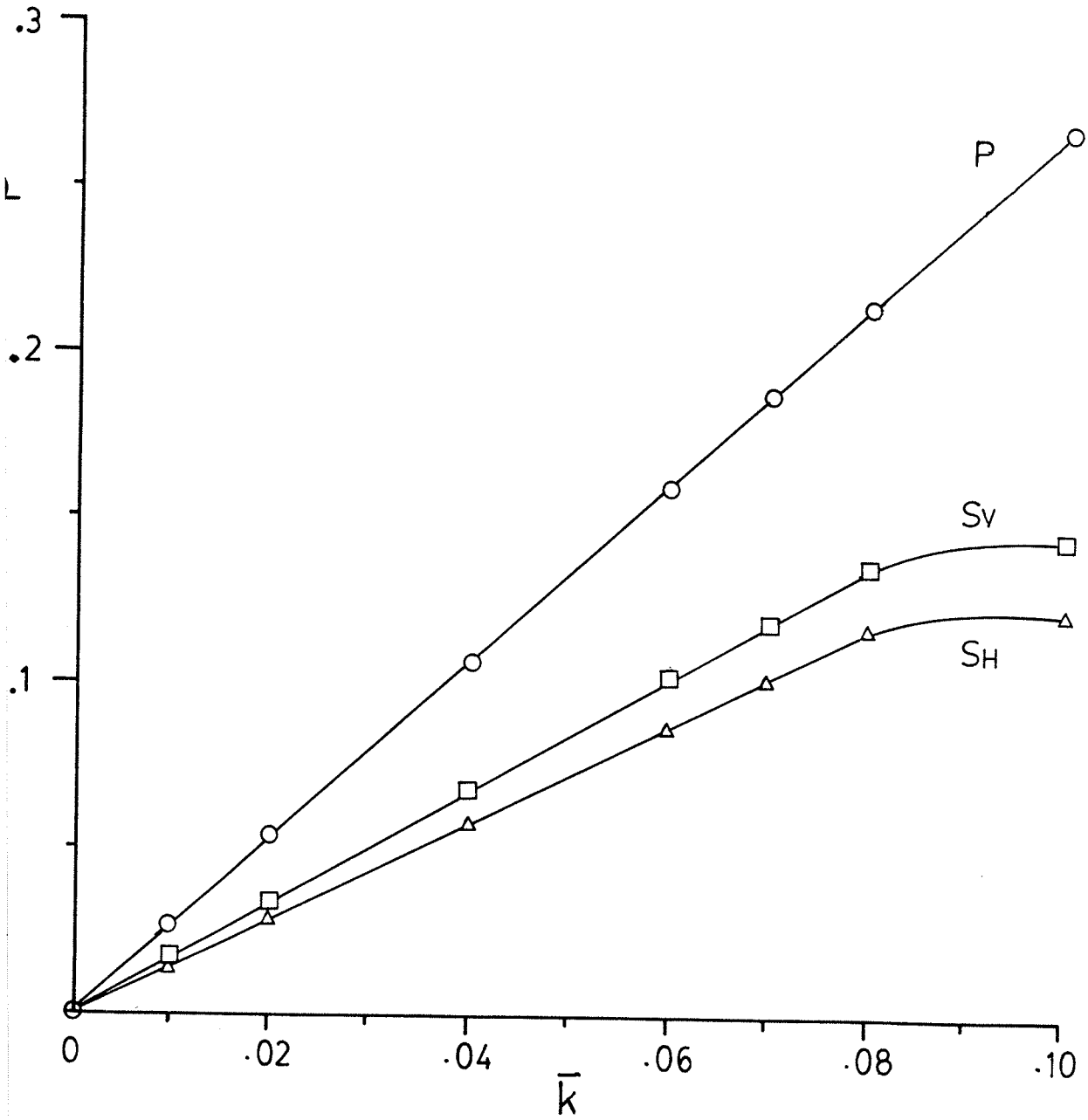


Fig. 4.10 Lowest SH, SV and P mode propagating along x-y plane, $\phi = 90^\circ$.

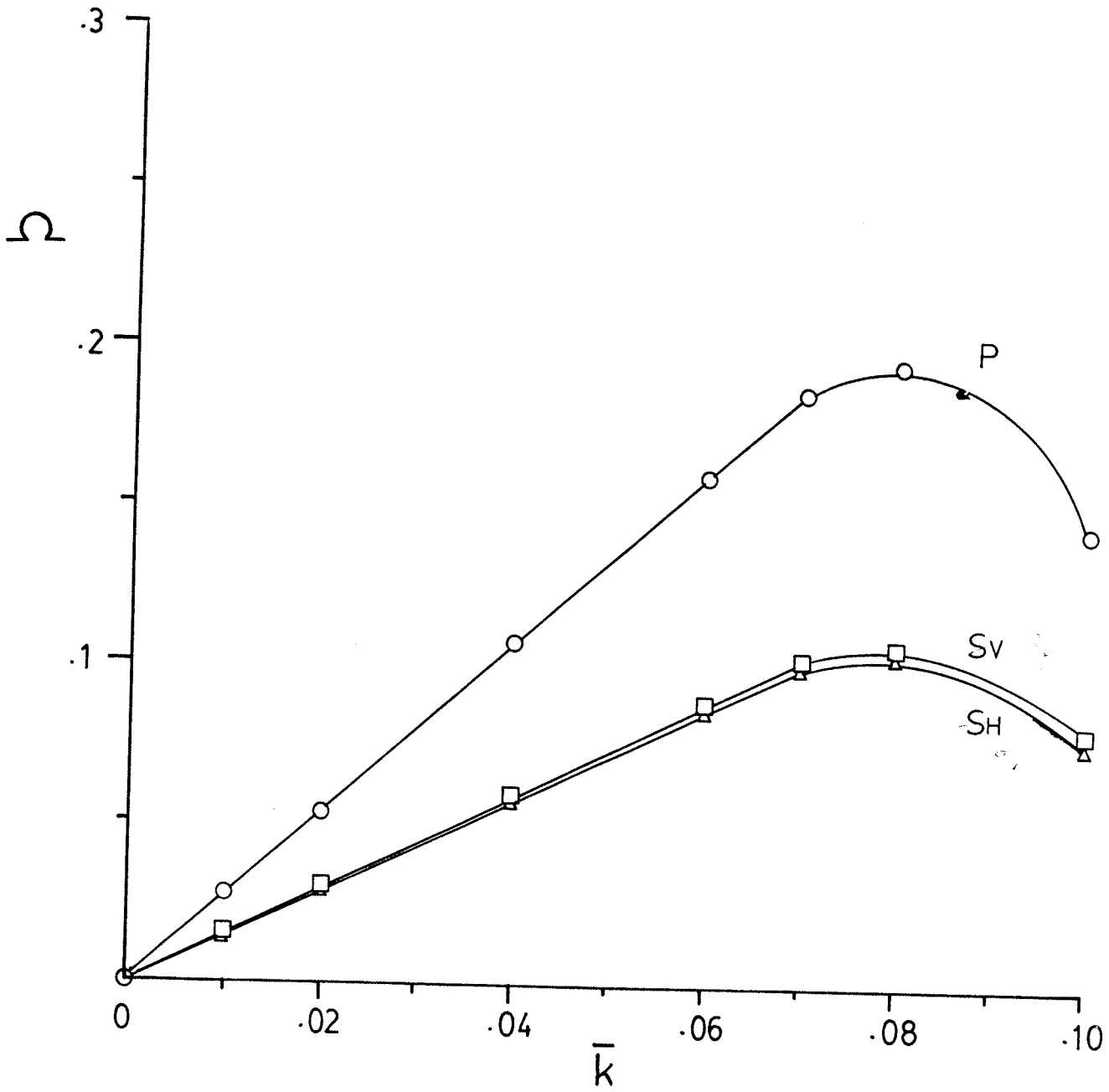


Fig. 4.11 Lowest SH, SV and P mode propagating along y-z plane, $\phi = 0^\circ$, $\alpha = 90^\circ$.

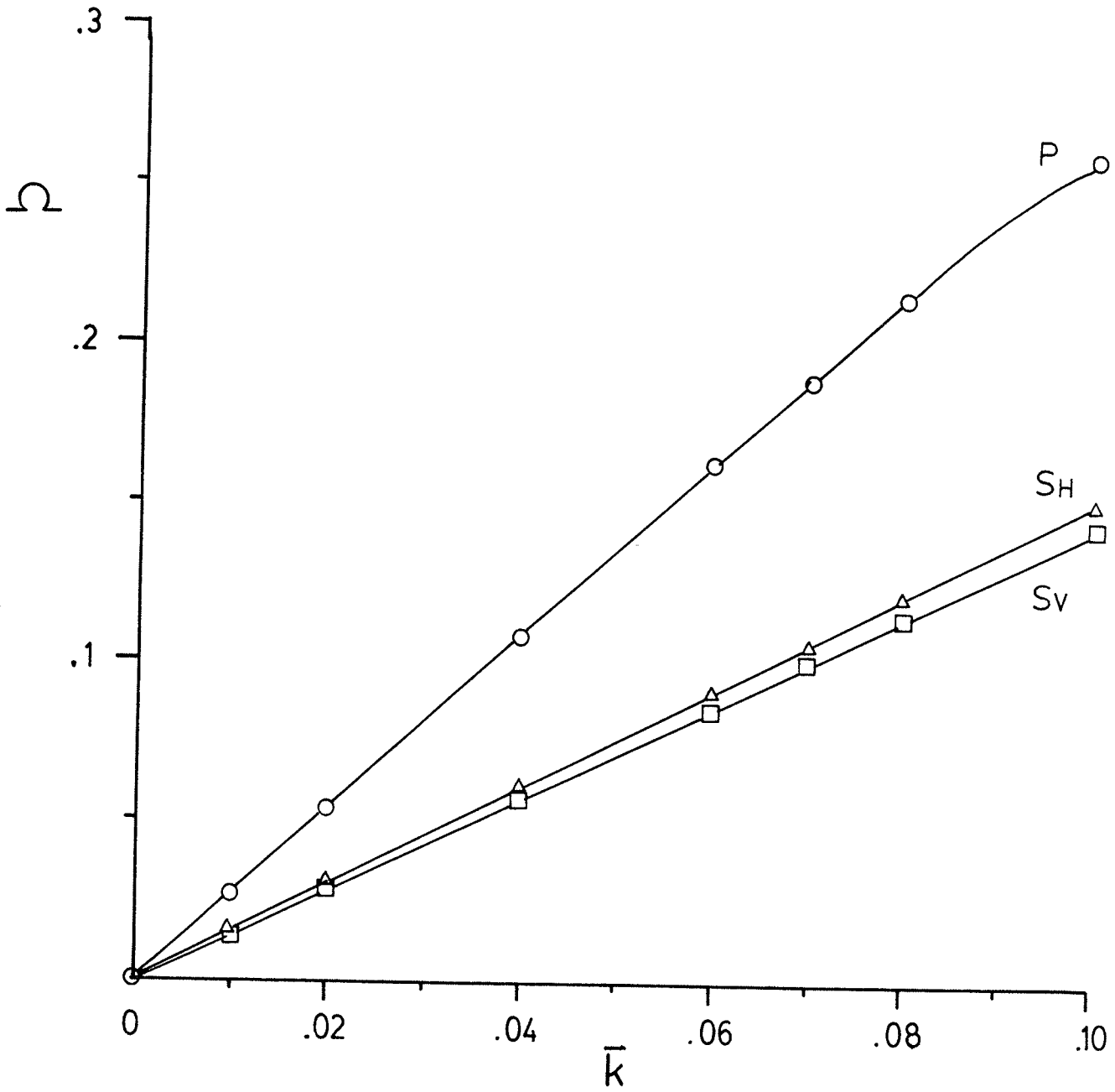


Fig. 4.12 Lowest SH, SV and P mode propagating along y-z plane, $\phi = 30^\circ$.

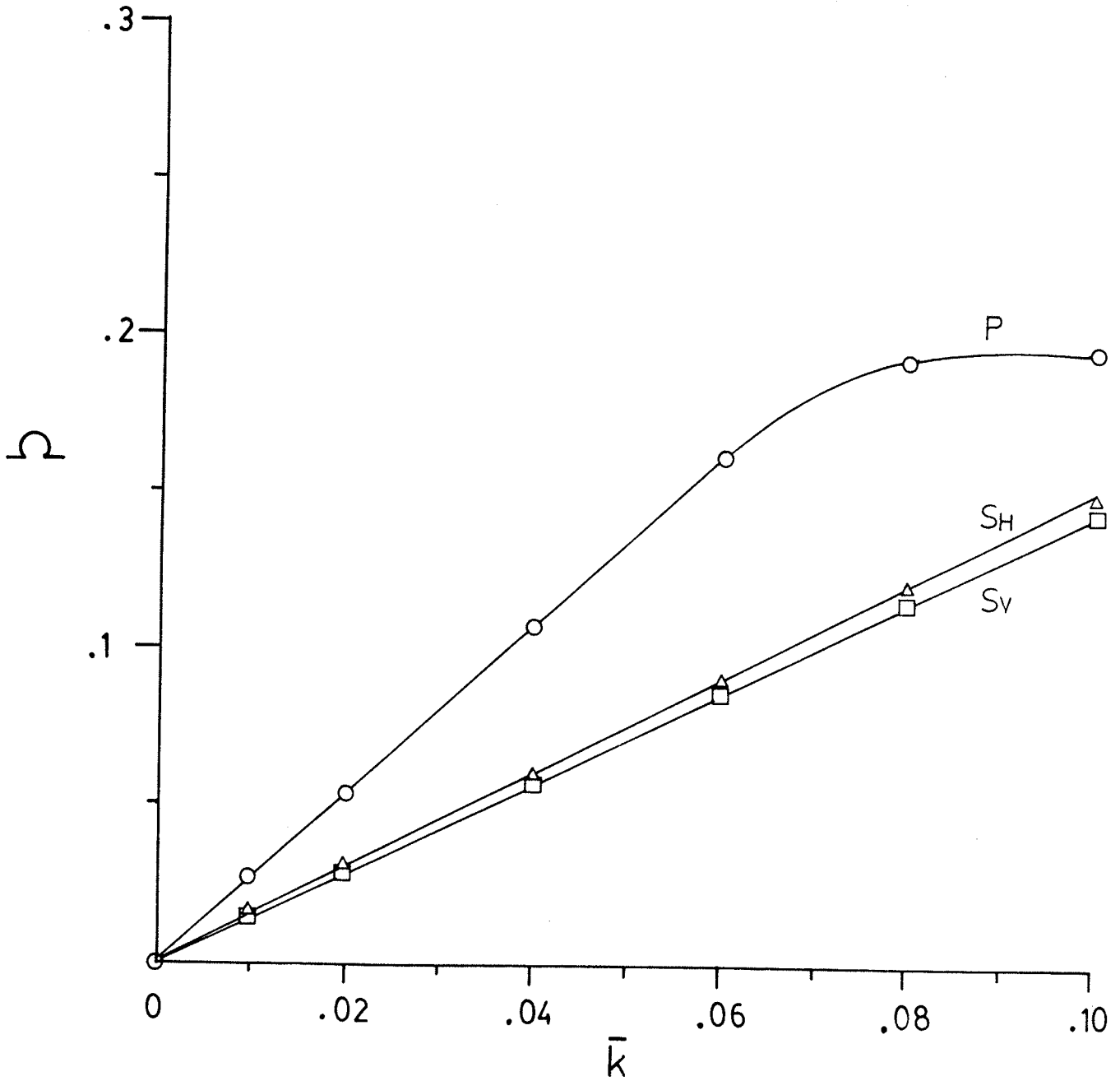


Fig. 4.13 Lowest SH, SV and P mode propagating along y-z plane, $\phi = 60^\circ$.

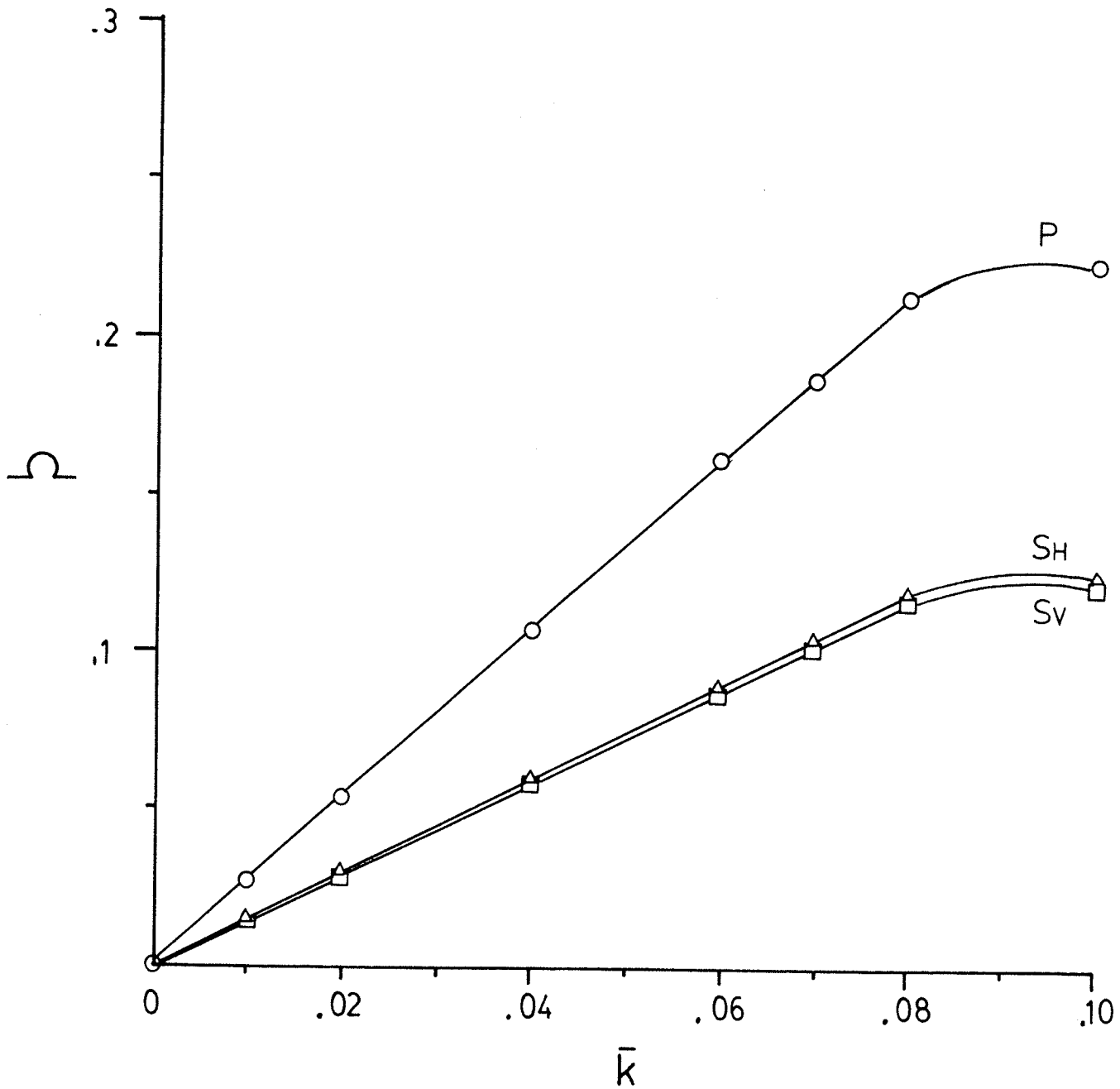


Fig. 4.14 Lowest SH, SV and P mode propagating along y-z plane, $\phi = 90^\circ$.
(This figure is the same as Fig. 4.10)

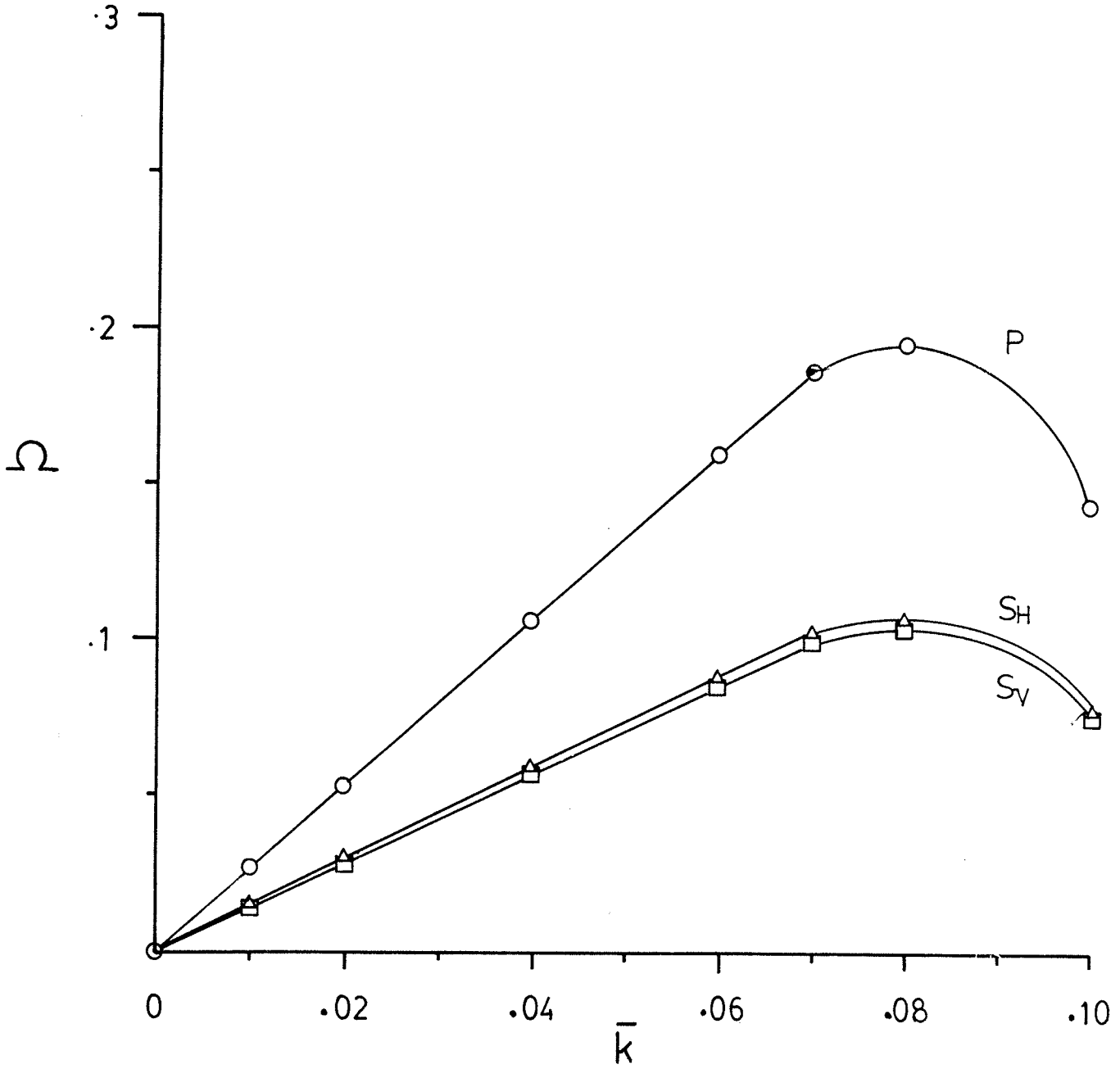


Fig. 4.15 Lowest SH, SV and P mode propagating along x-z plane, $\alpha = 0^\circ$.
(This figure is the same as Fig. 4.7)

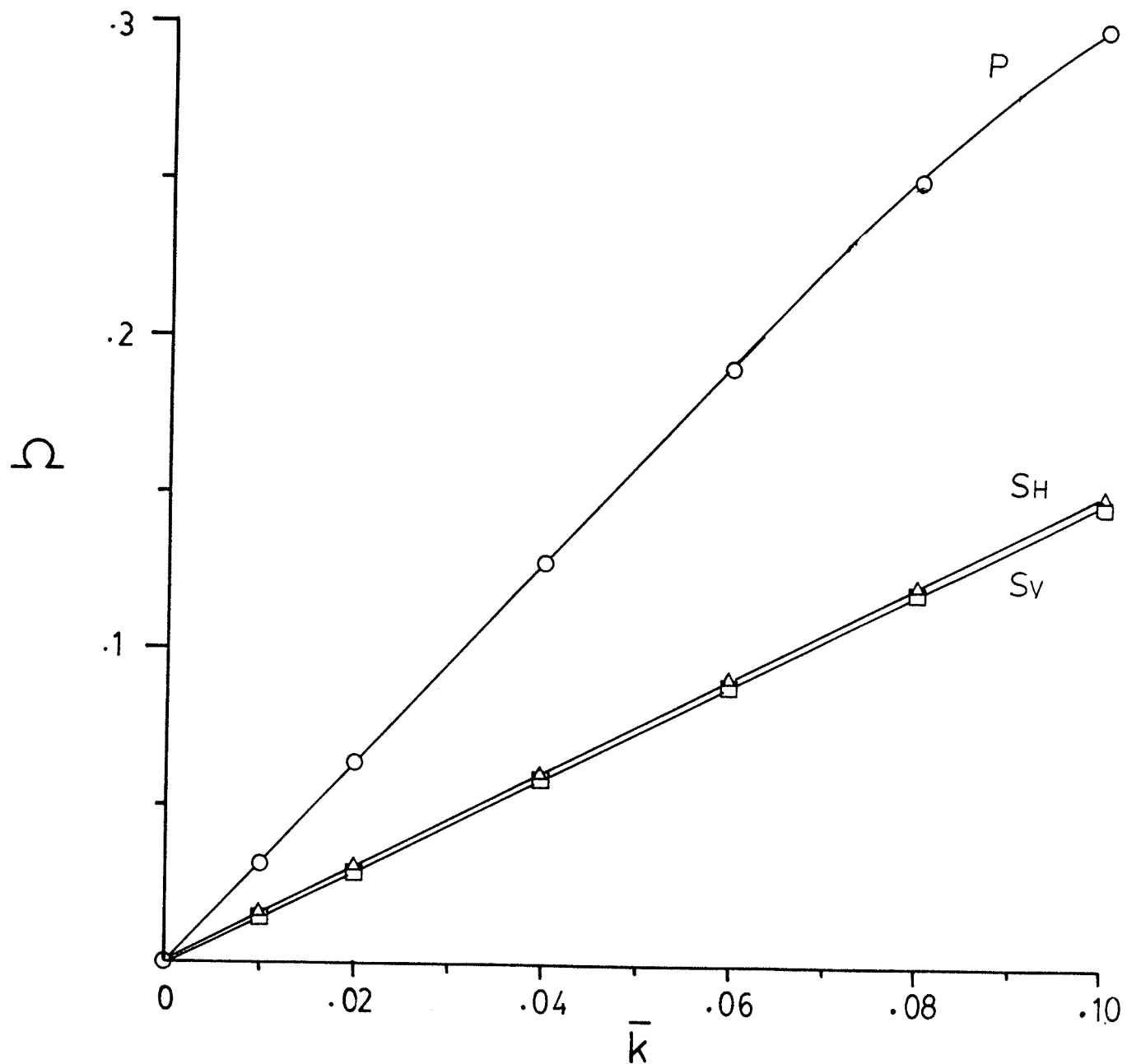


Fig. 4.16 Lowest SH, SV and P mode propagating along x-z plane, $\alpha = 30^\circ$.

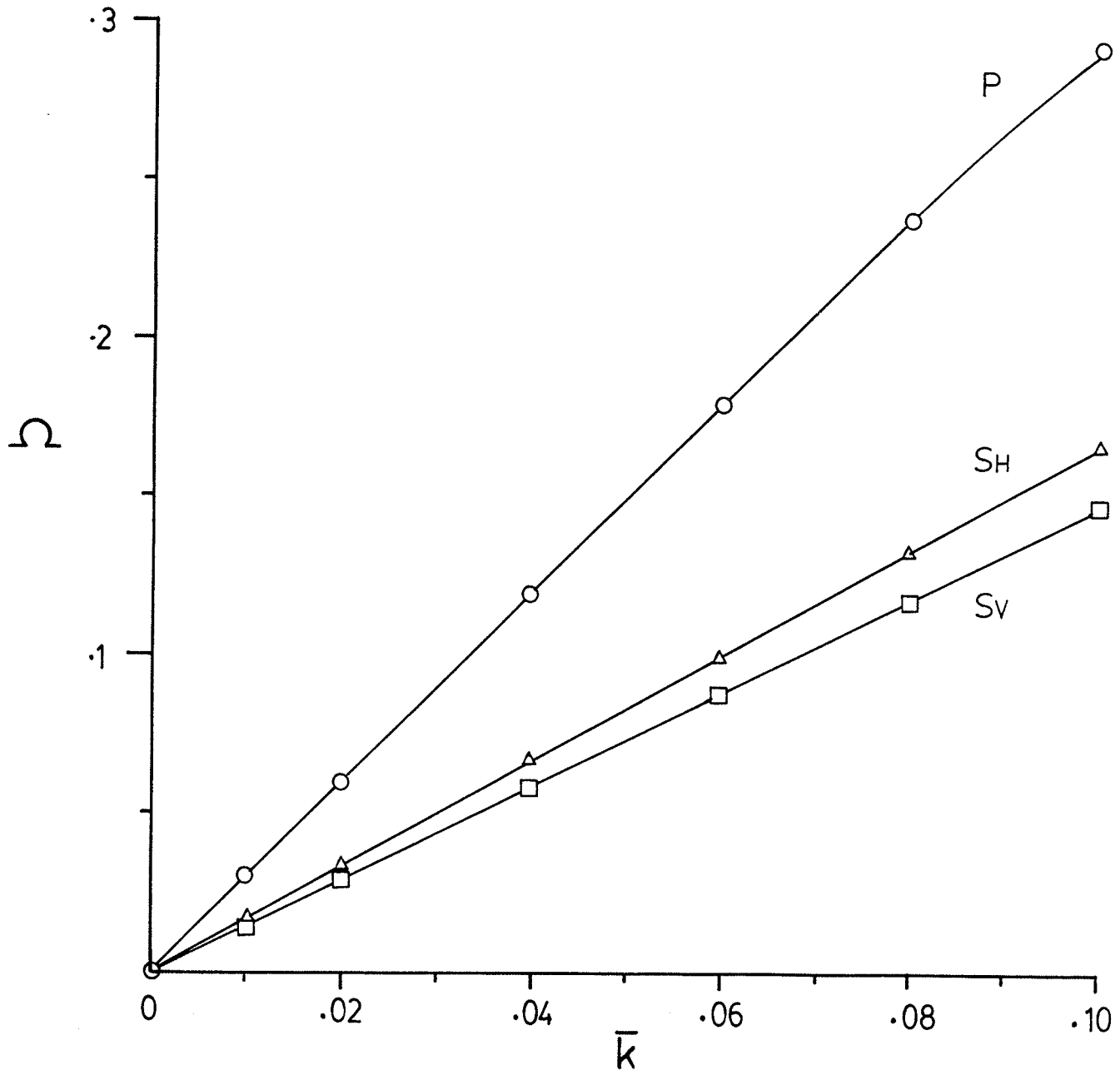


Fig. 4.17 Lowest SH, SV and P mode propagating along x-z plane, $\alpha = 60^\circ$.

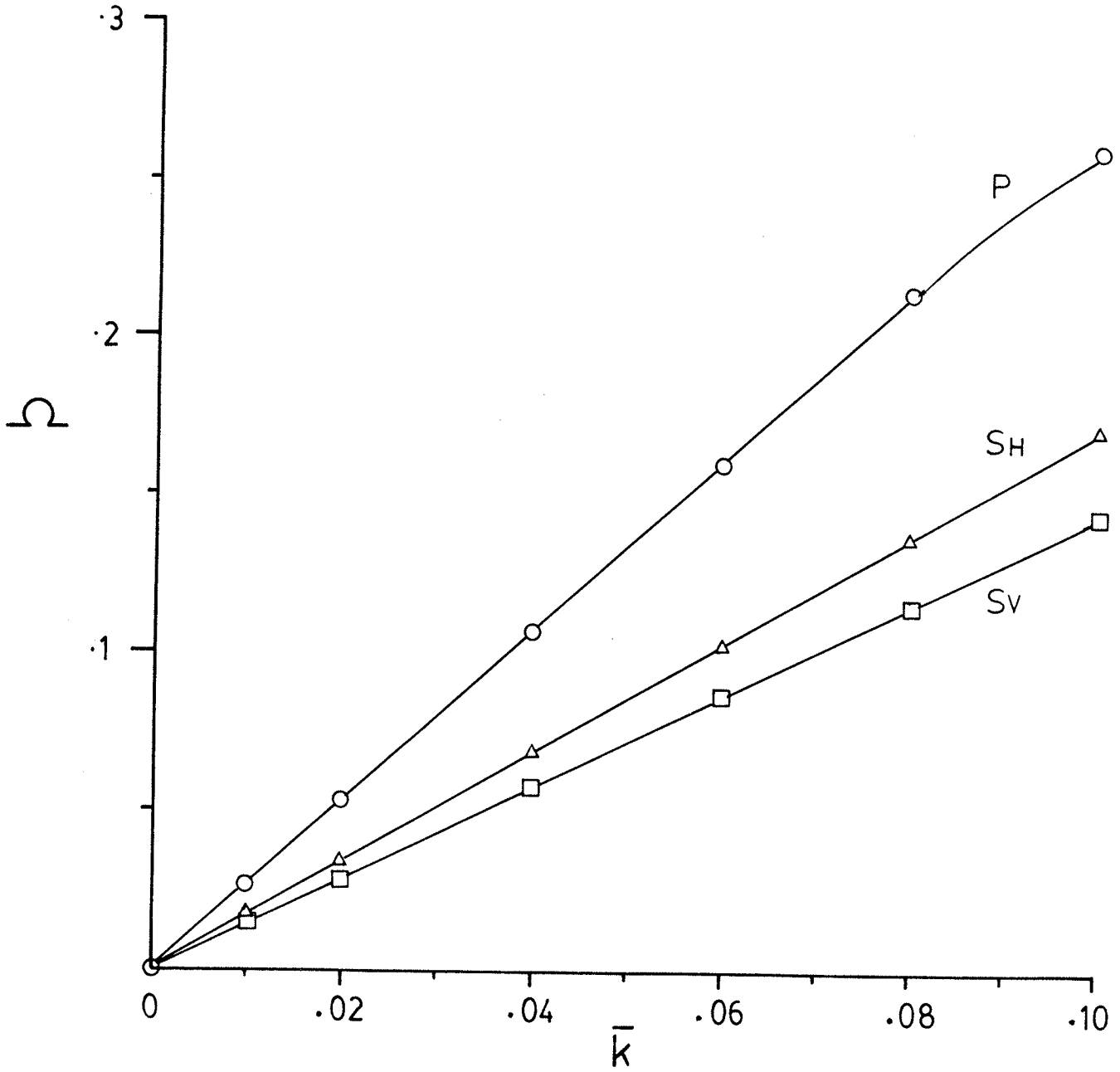


Fig. 4.18 Lowest SH, SV and P mode propagating along x-z plane, $\alpha = 90^\circ$.
(This figure is the same as Fig. 4.11)

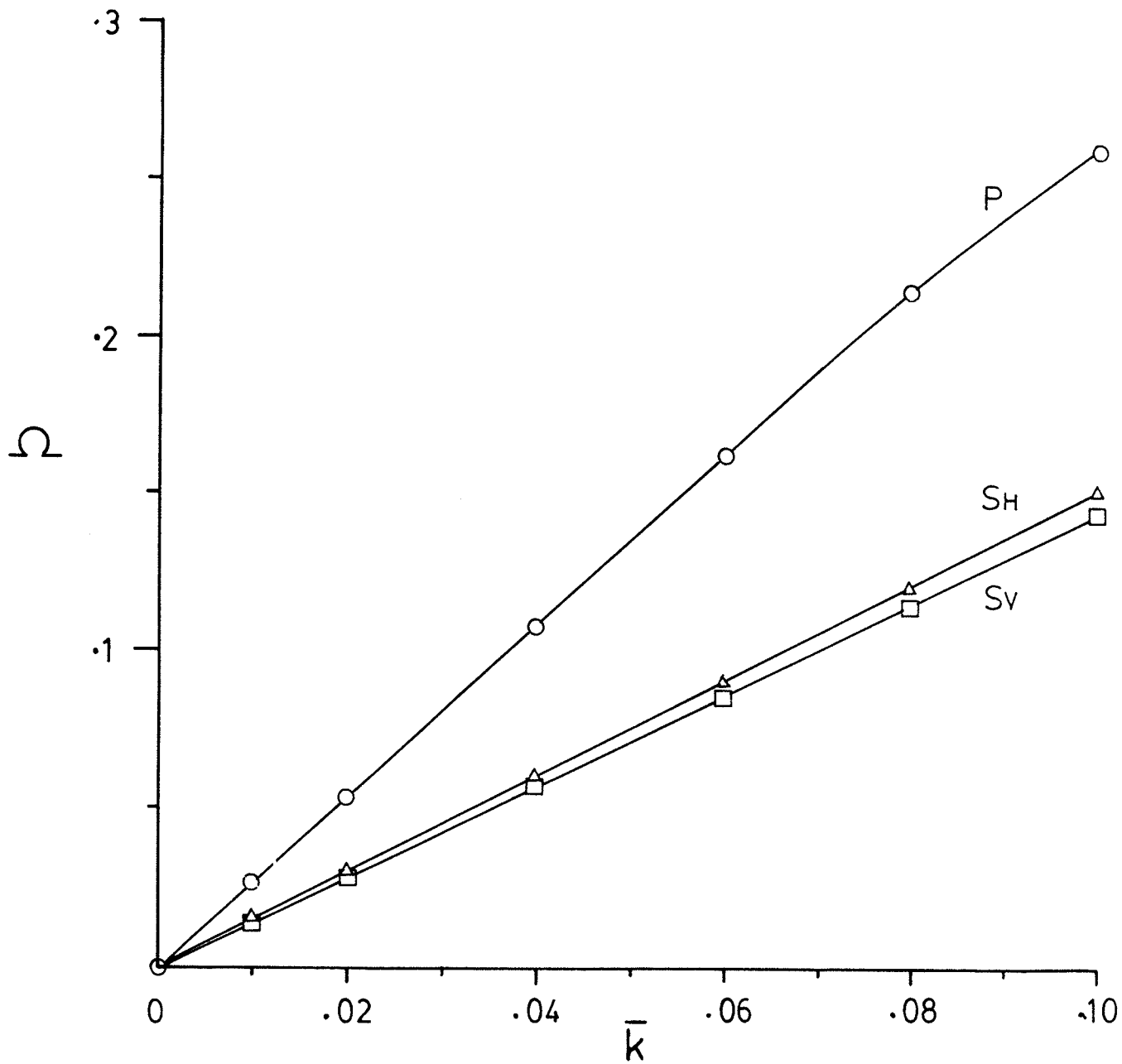


Fig. 4.19 Frequency vs. vertical angle plot for SH mode propagating on x-y plane.

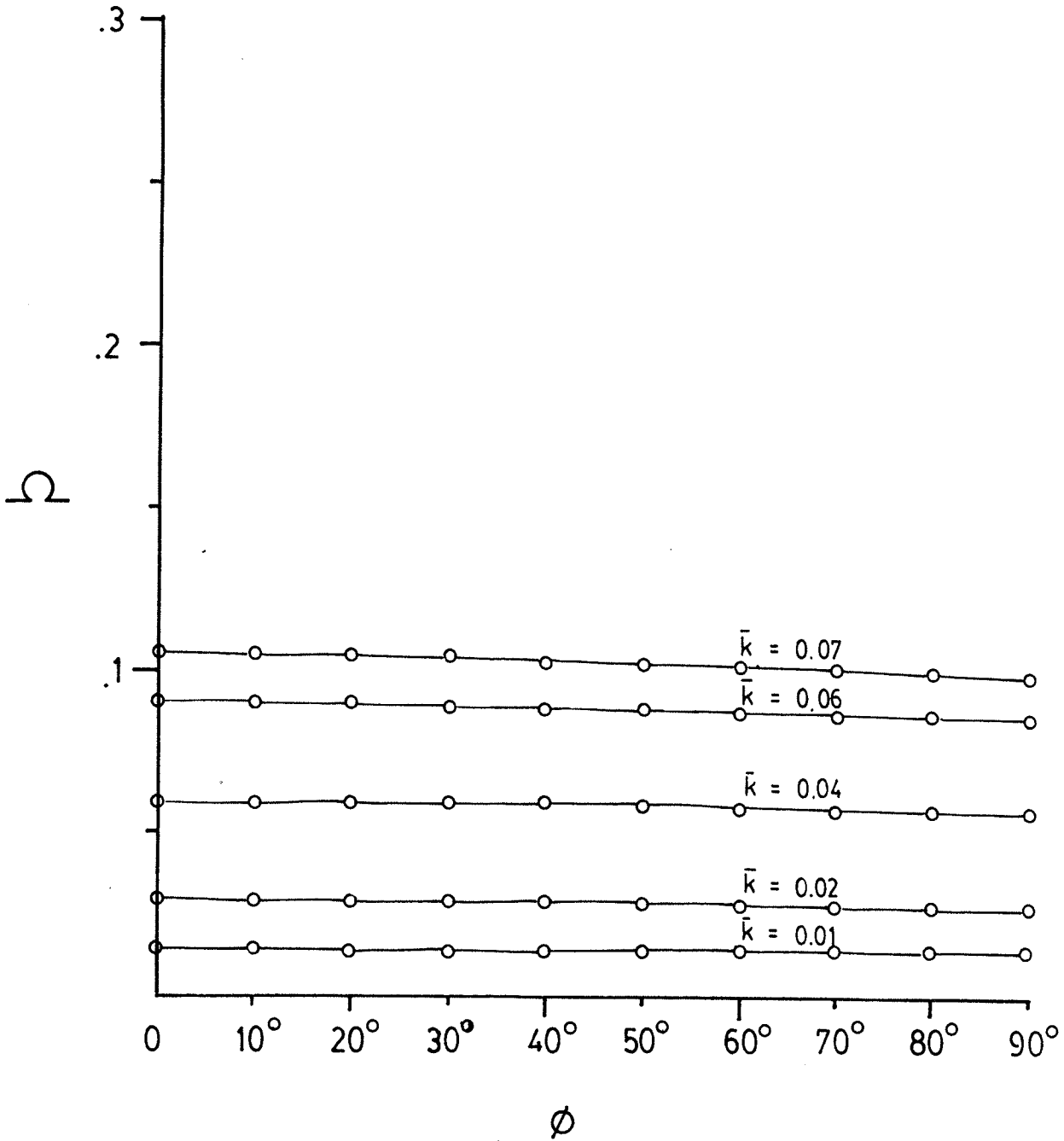


Fig. 4.20 Frequency vs. vertical angle plot for SV mode propagating on x-y plane.

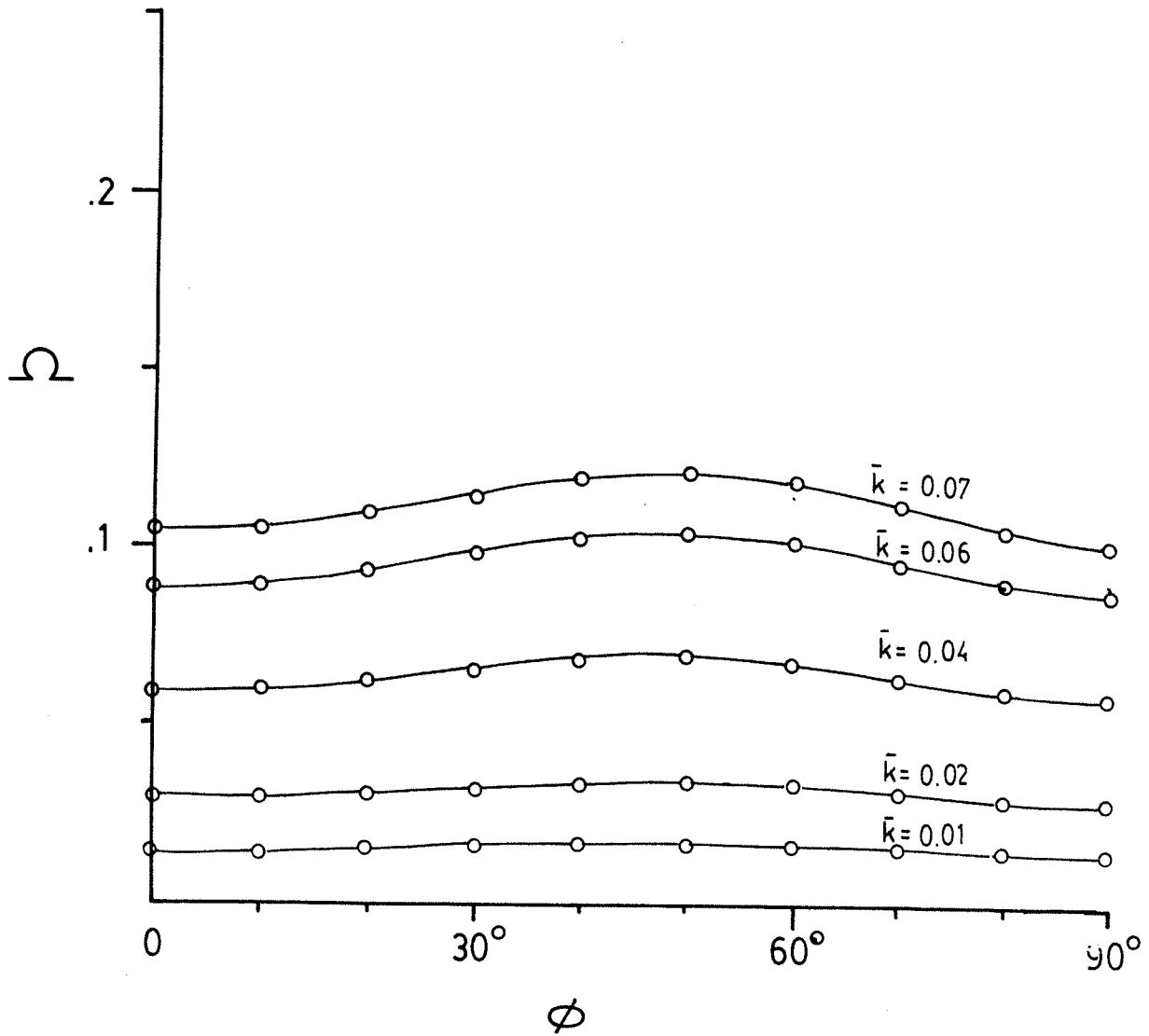


Fig. 4.21 Frequency vs. vertical angle plot for P mode propagating on x-y plane.

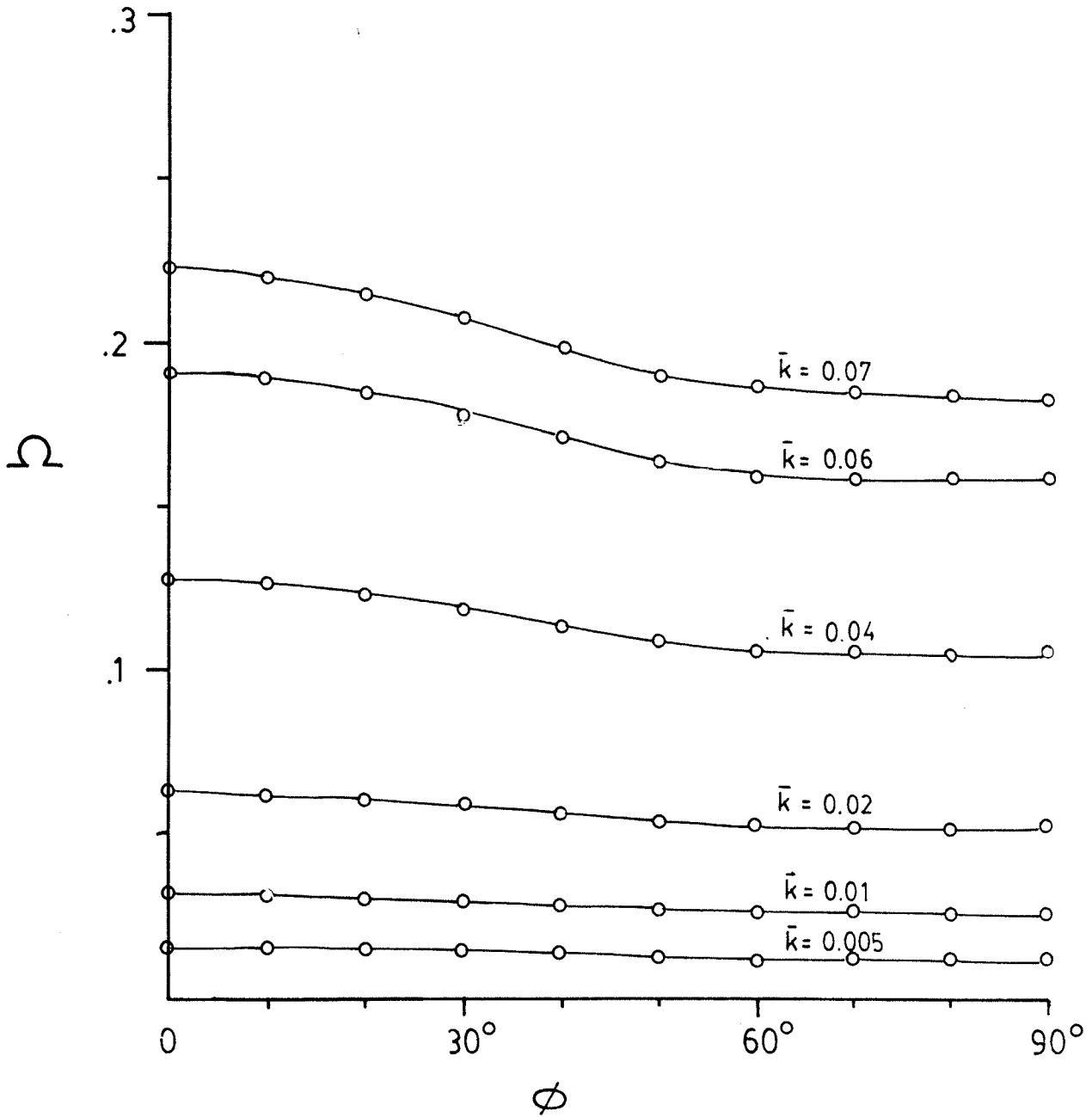


Fig. 4.22 Frequency vs. vertical angle plot for lowest SH mode propagating on y-z plane.

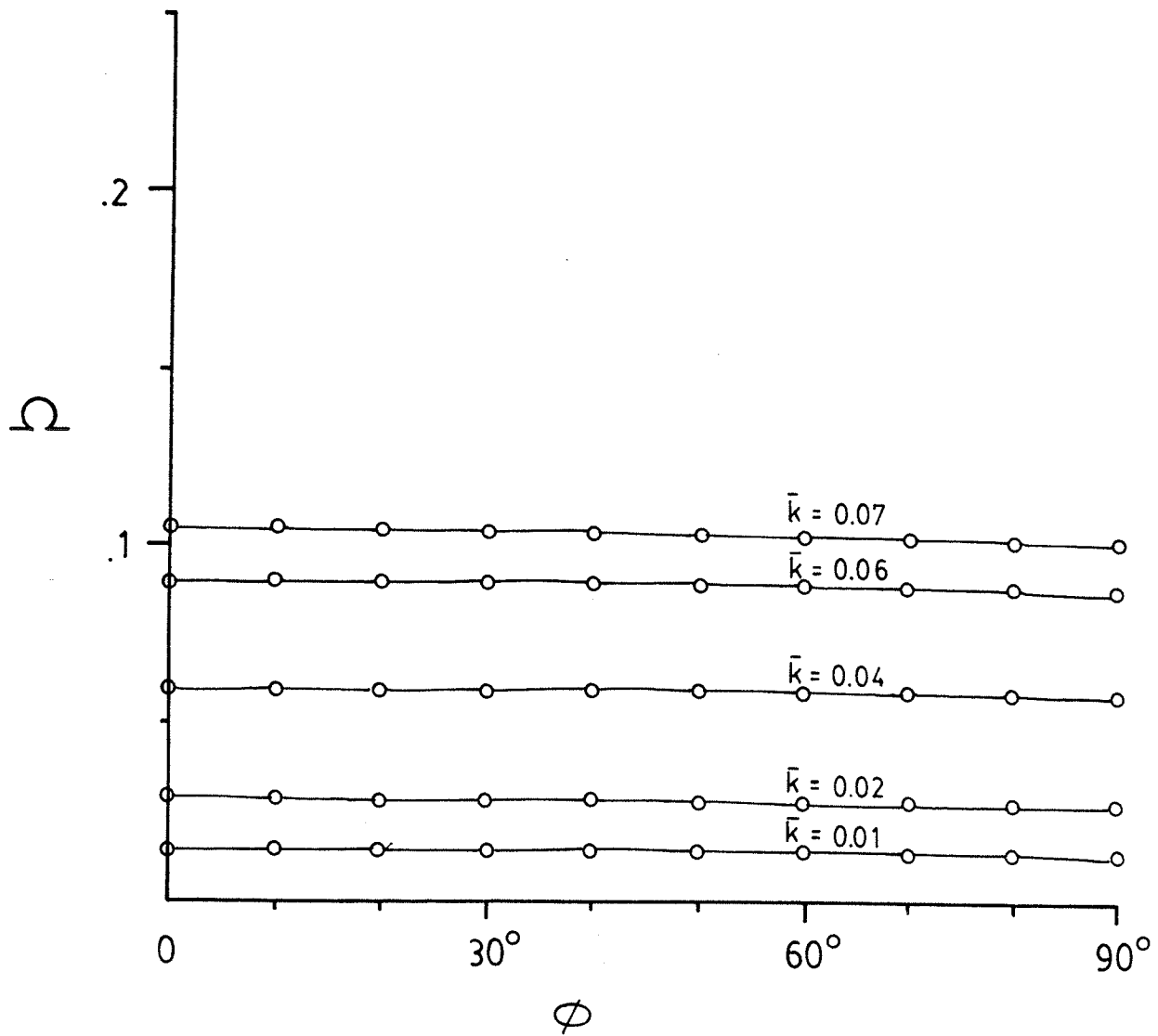


Fig. 4.23 Frequency vs. vertical angle plot for lowest SV mode propagating on y-z plane.

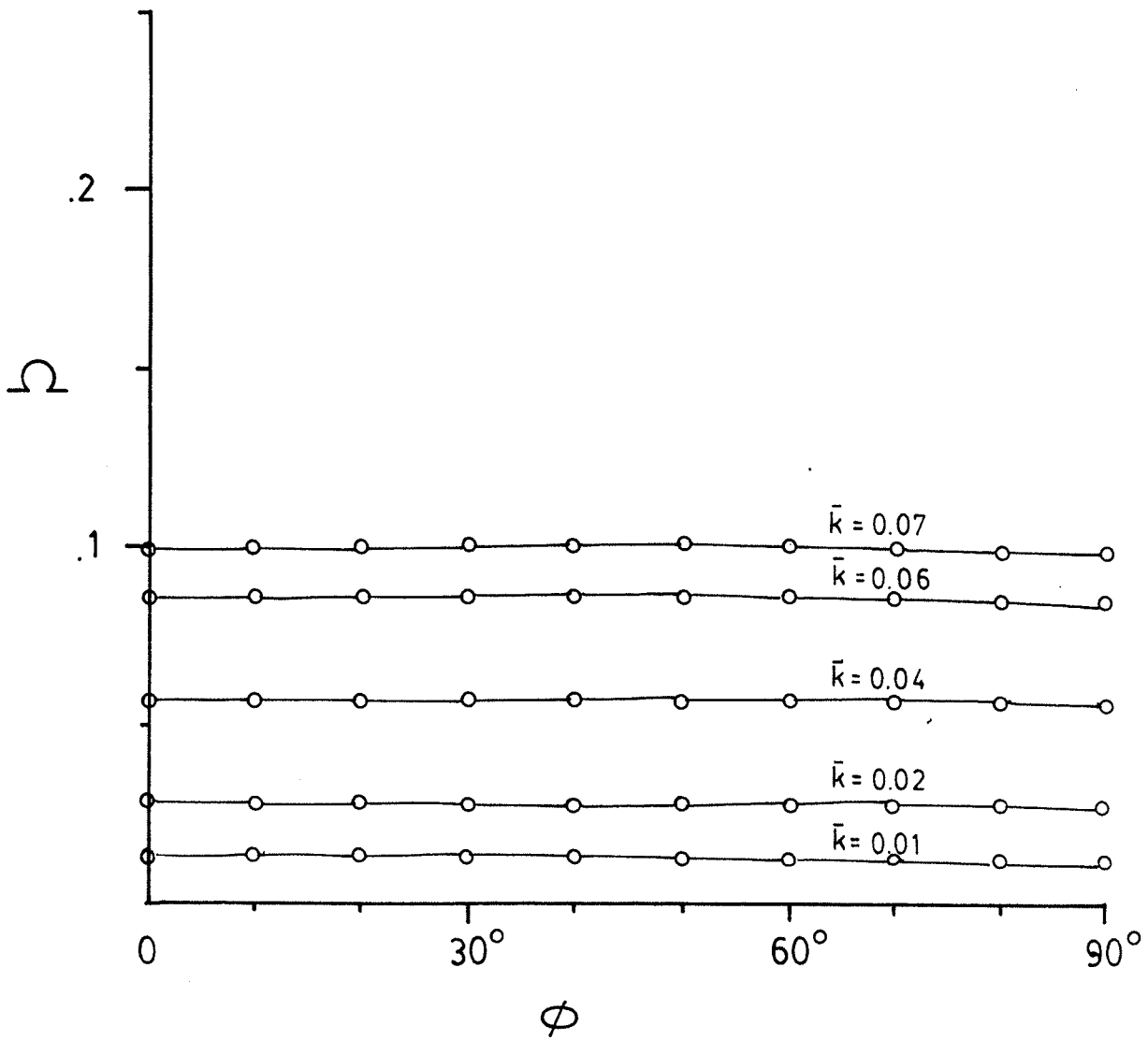


Fig. 4.24 Frequency vs. vertical angle plot for lowest P mode propagating on y-z plane.

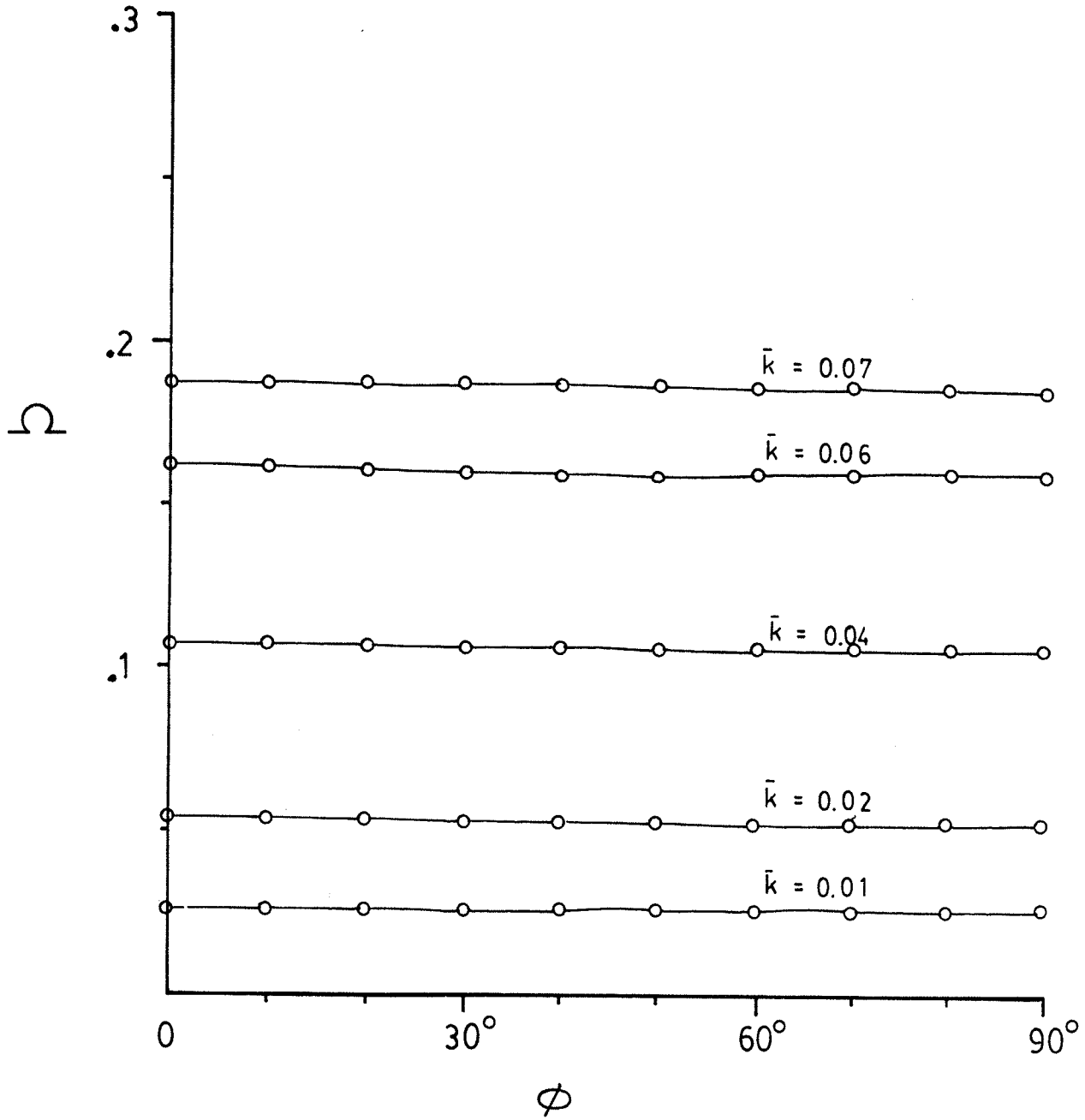


Fig. 4.25 Frequency vs. horizontal plane plot for lowest SH mode propagating on x-z plane.

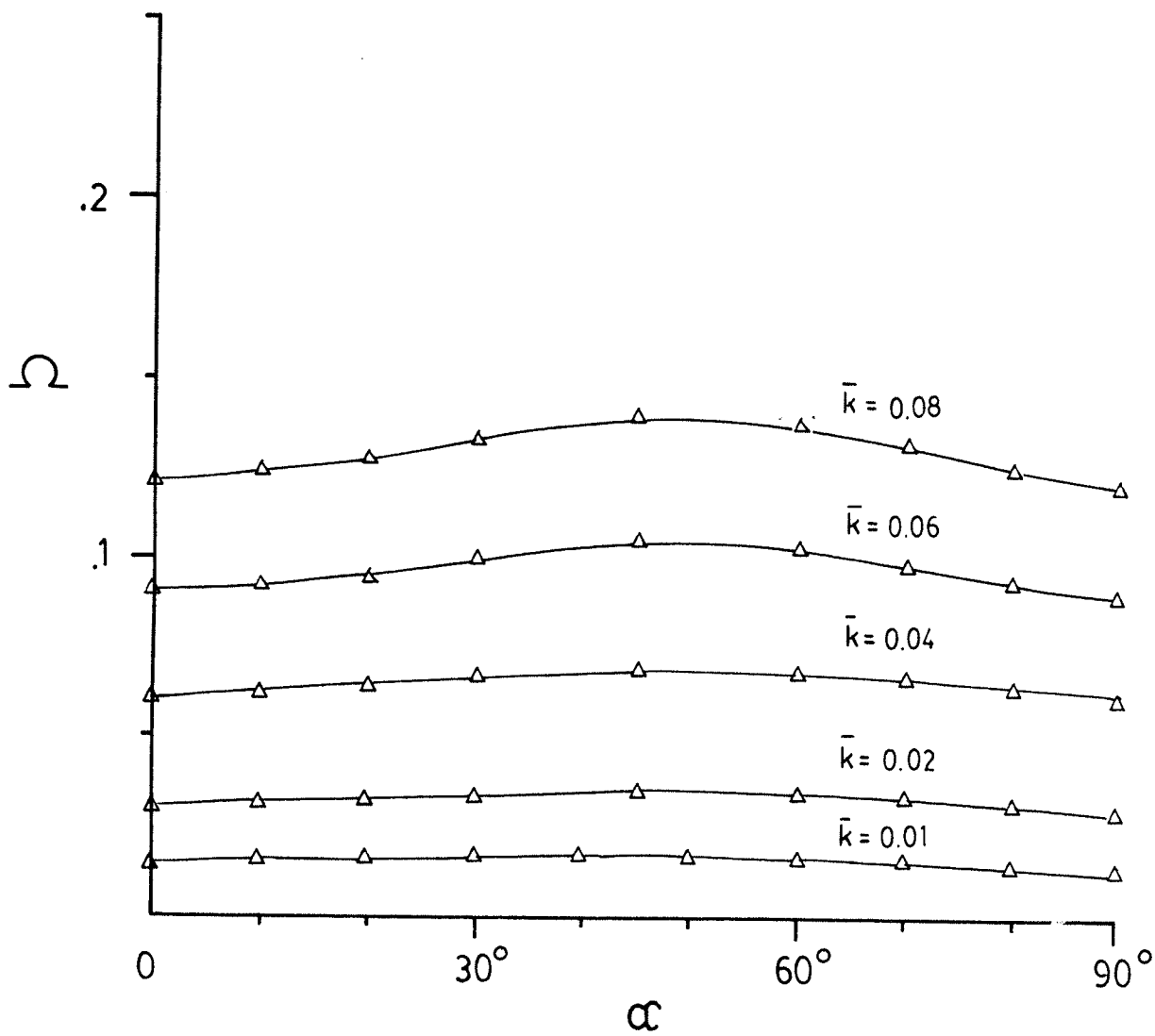


Fig. 4.26 Frequency vs. horizontal angle plot for lowest SV mode propagating on x-z plane.

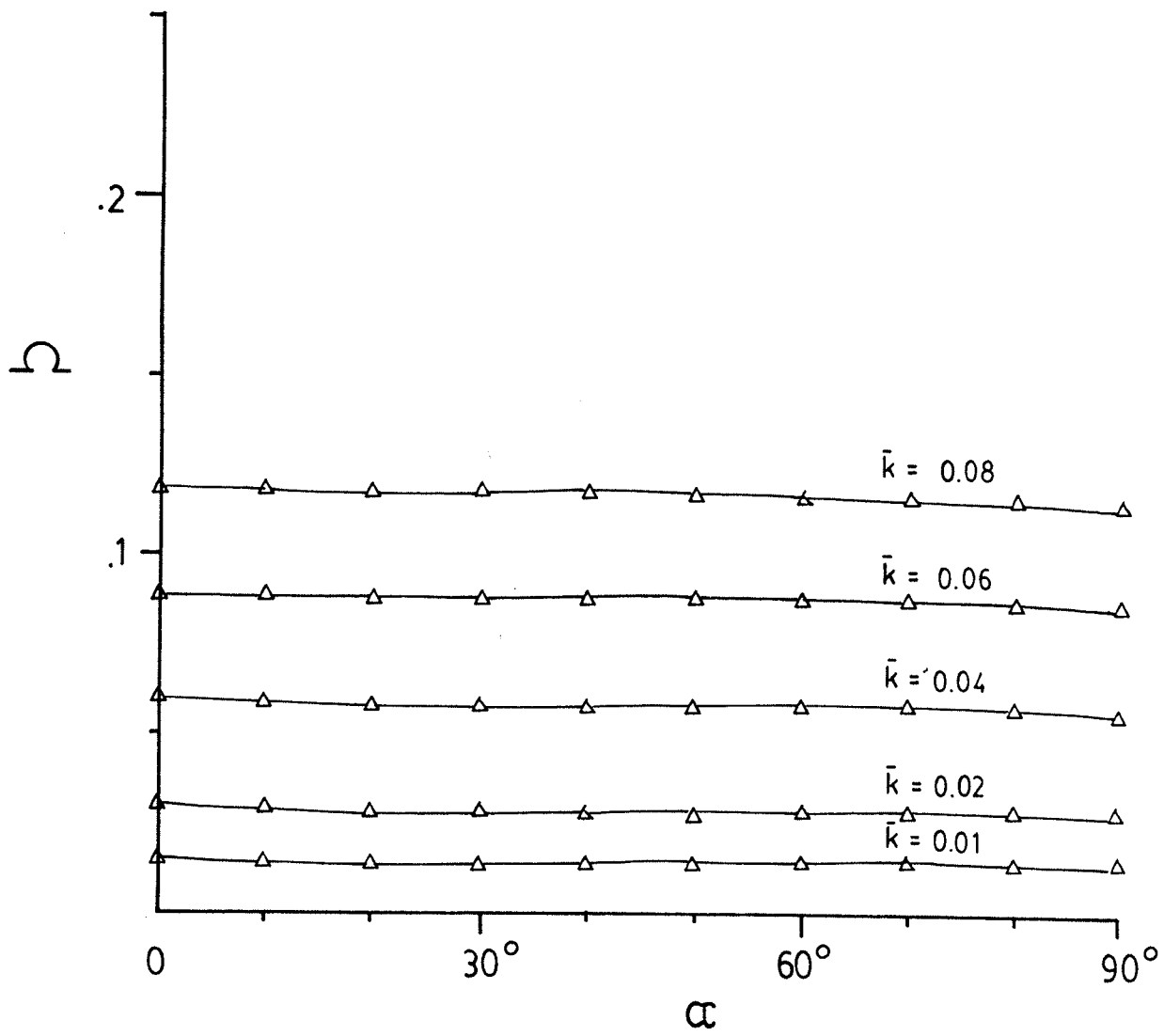
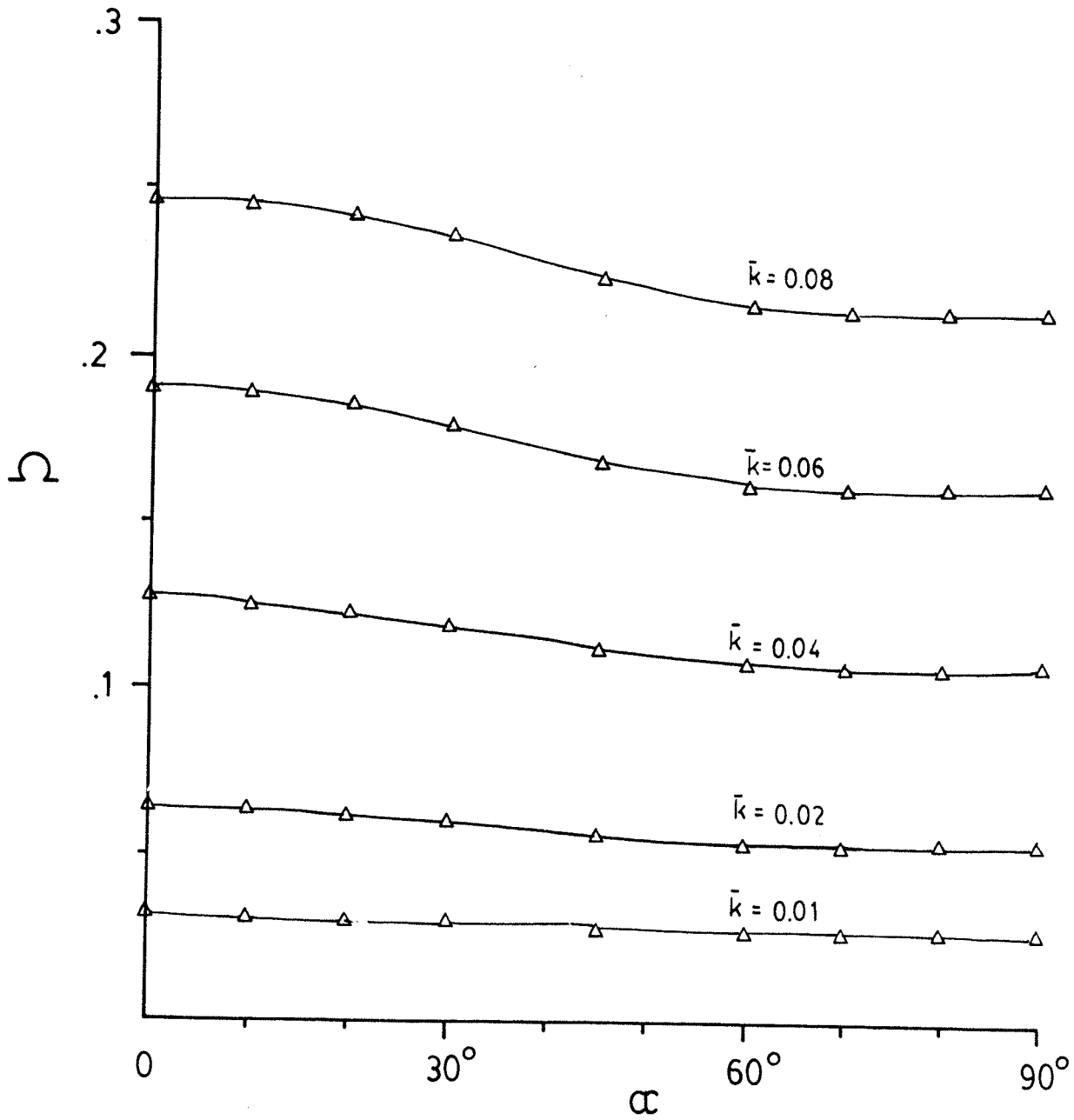


Fig. 4.27 Frequency vs. horizontal angle plot for lowest P mode propagating on x-z plane.



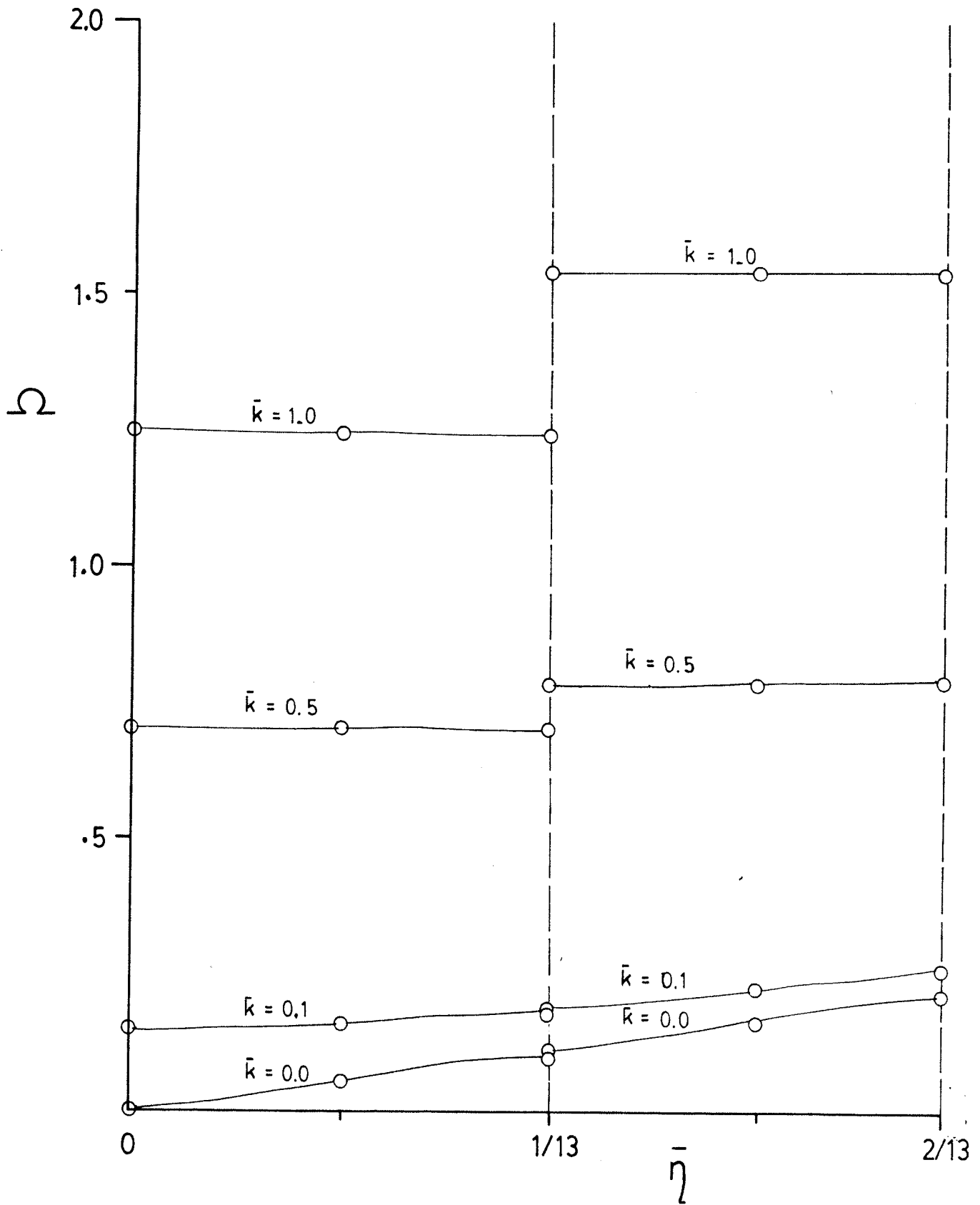


Fig. 4.28 Curves of constant \bar{k} for lowest SH mode, $\alpha = 0^\circ$.

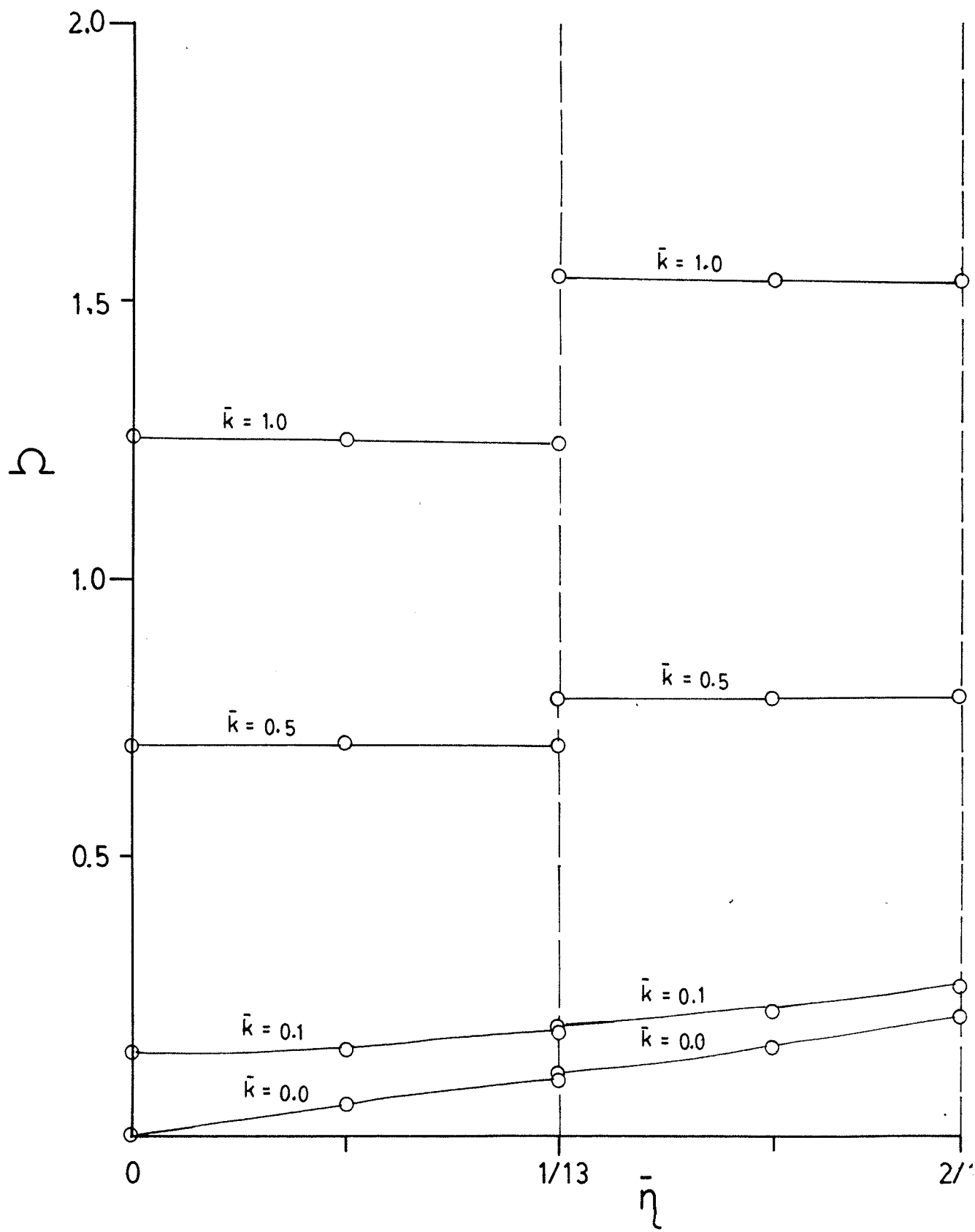


Fig. 4.29 Curves of constant \bar{k} for lowest SH mode, $\alpha = 90^\circ$.

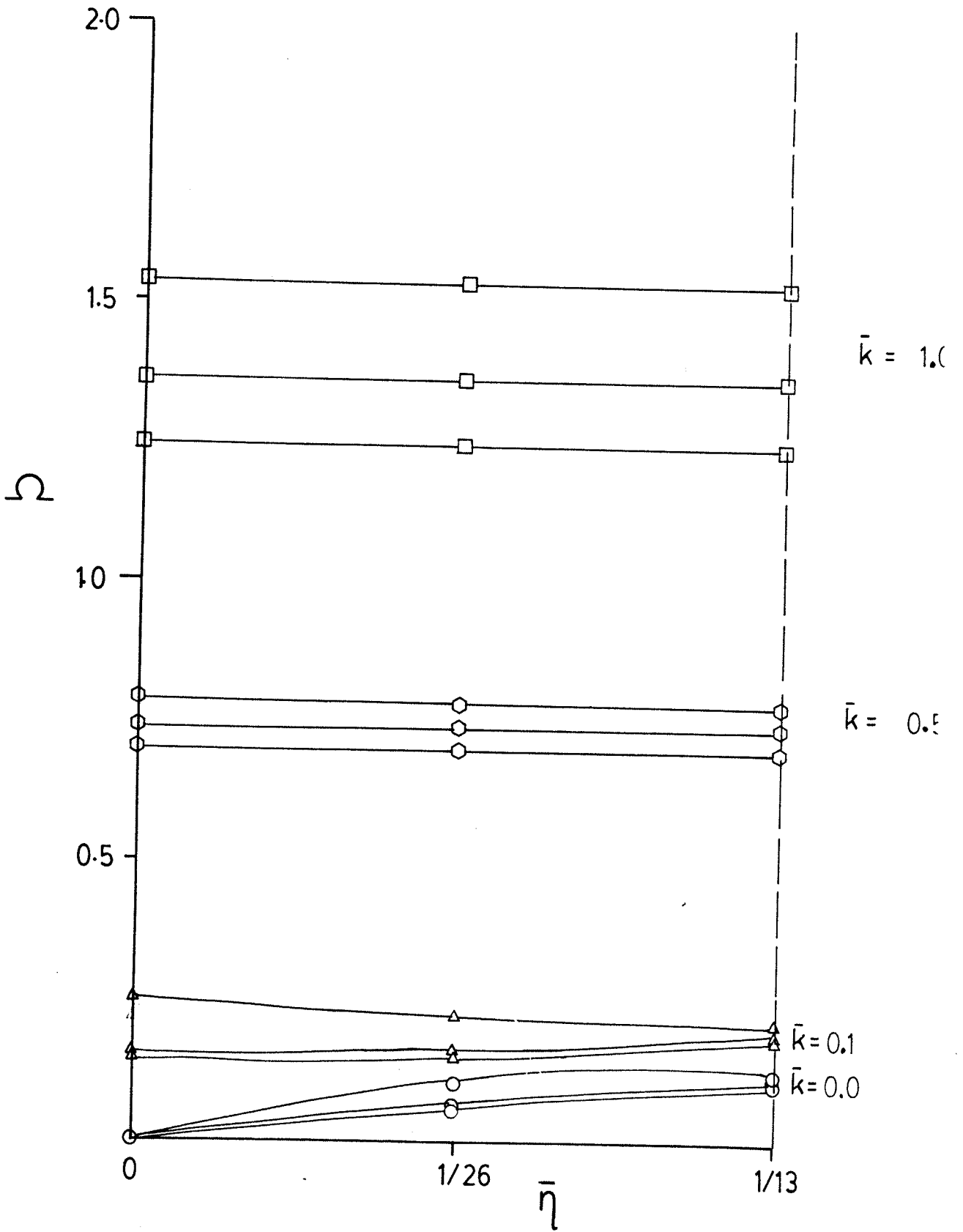


Fig. 4.30 Curves of constant \bar{k} on x-y plane, $\alpha = 0^\circ$.

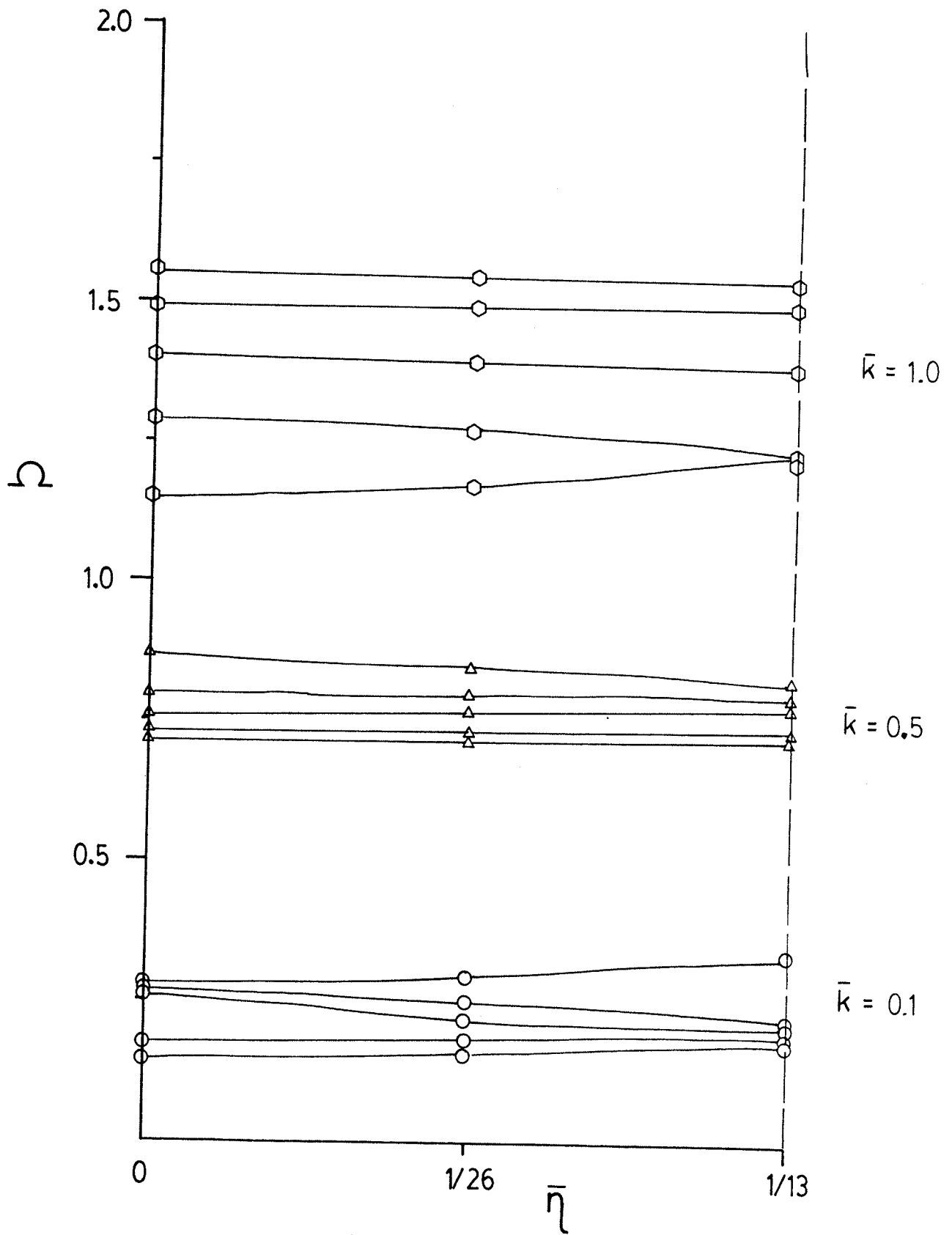


Fig. 4.31 Lowest 5 branches for curves of constant \bar{k} on x-y plane, $\alpha = 45^\circ$.

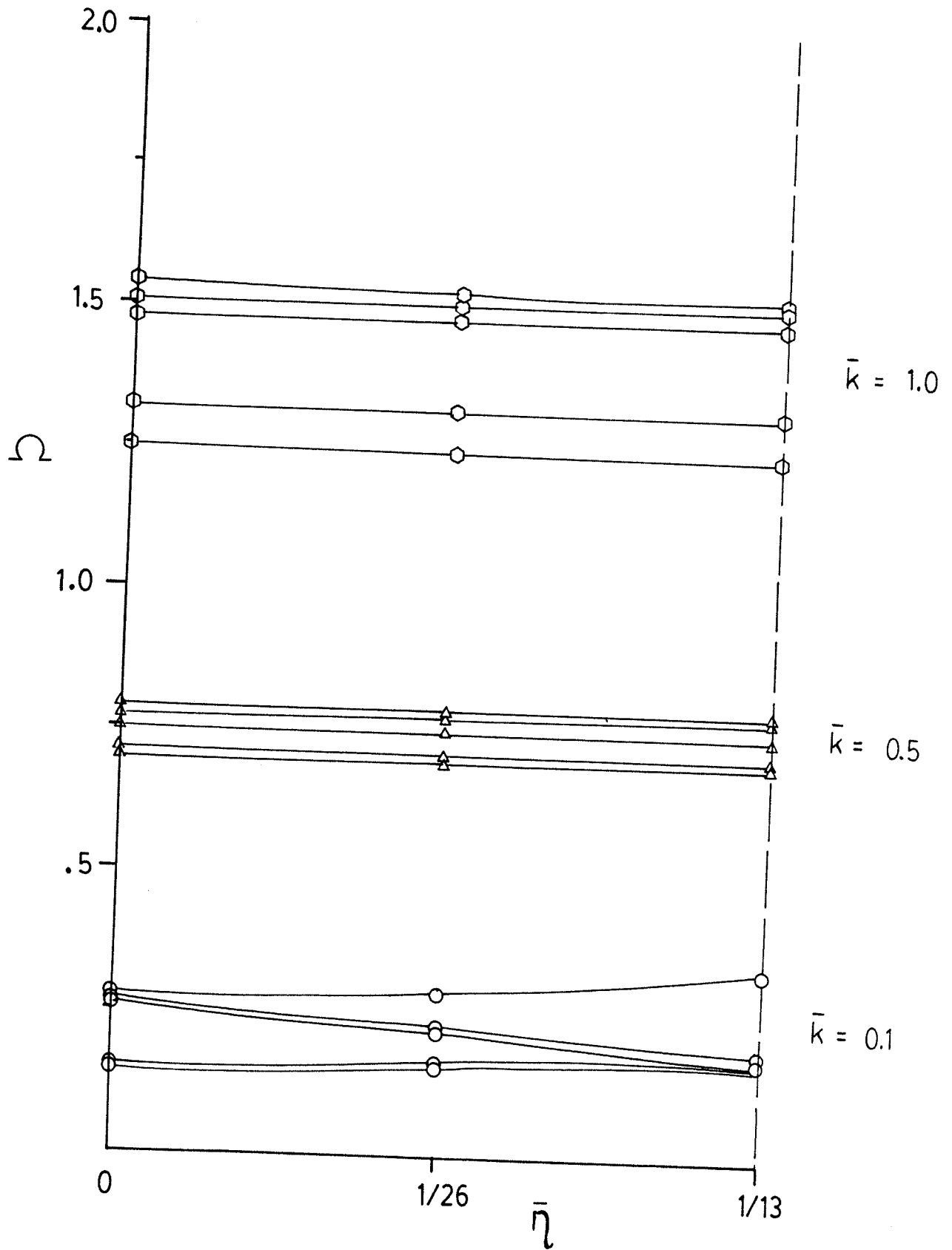


Fig. 4.32 Lowest 5 branches for curves of constant \bar{k} on y-z plane, $\alpha = 90^\circ$.

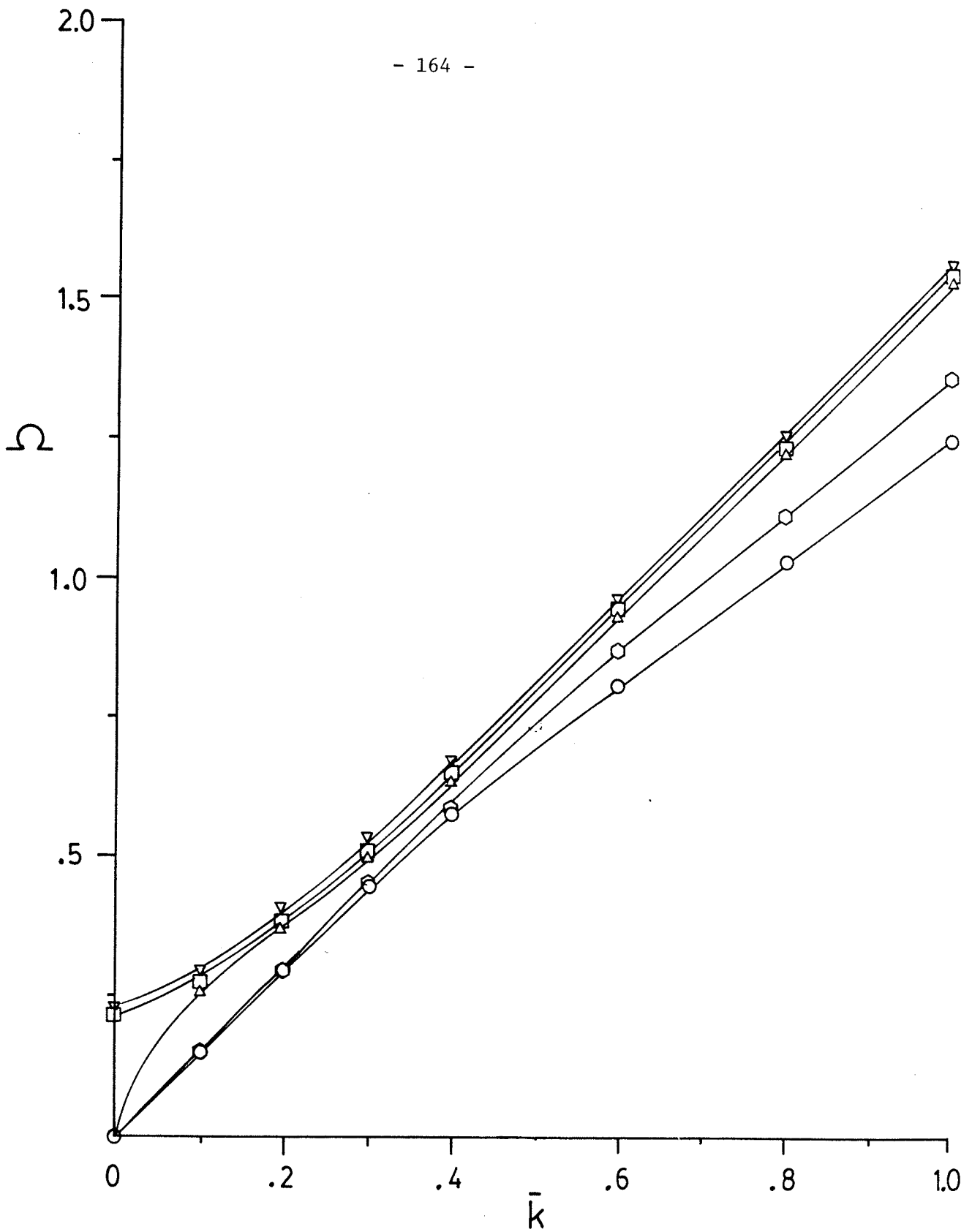


Fig. 4.33 Lowest 5 branches for $\alpha = 0^\circ$, $\bar{\eta} = 0.0$.

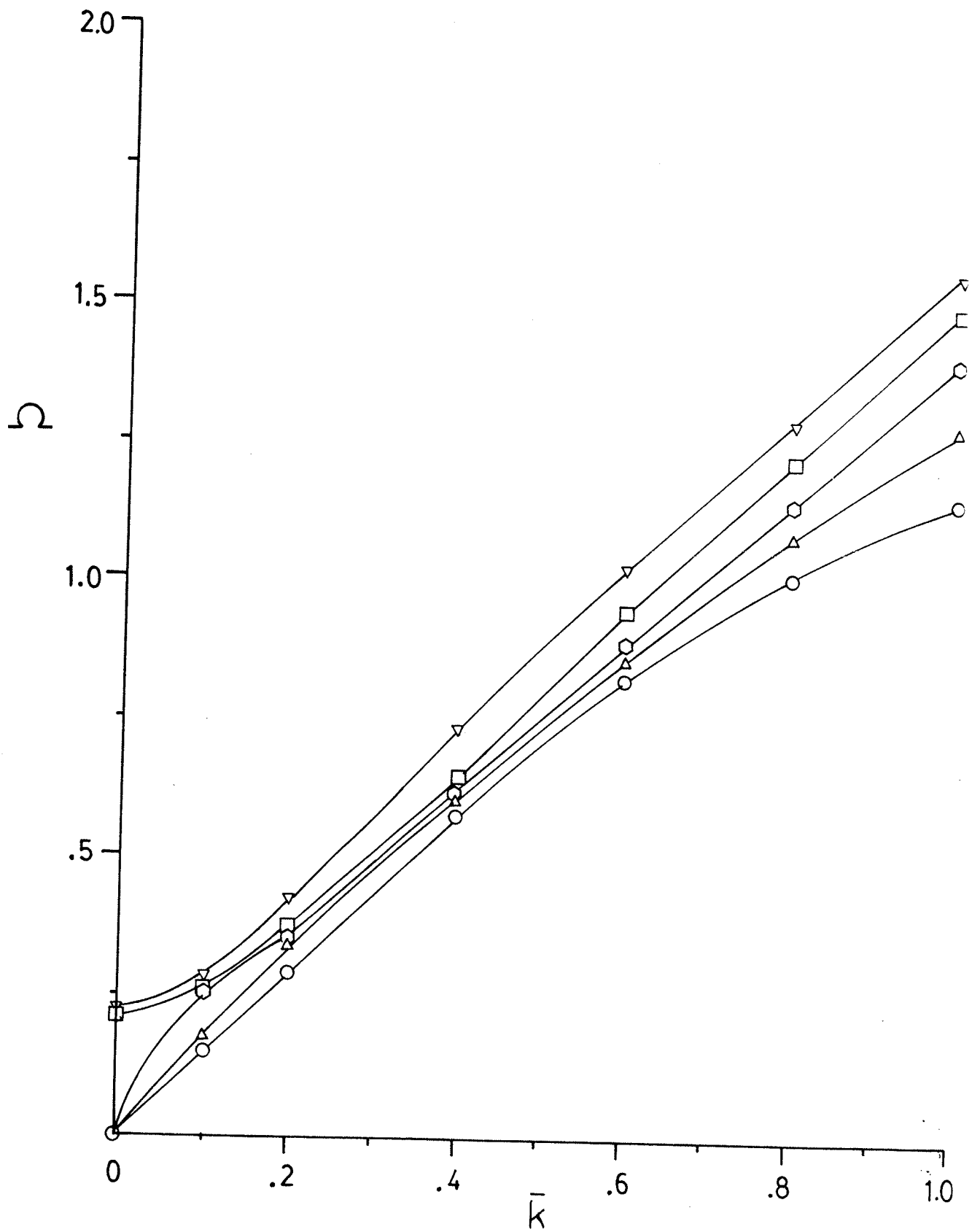


Fig. 4.34 Lowest 5 branches for $\alpha = 45^\circ$, $\bar{\eta} = 0.0$.

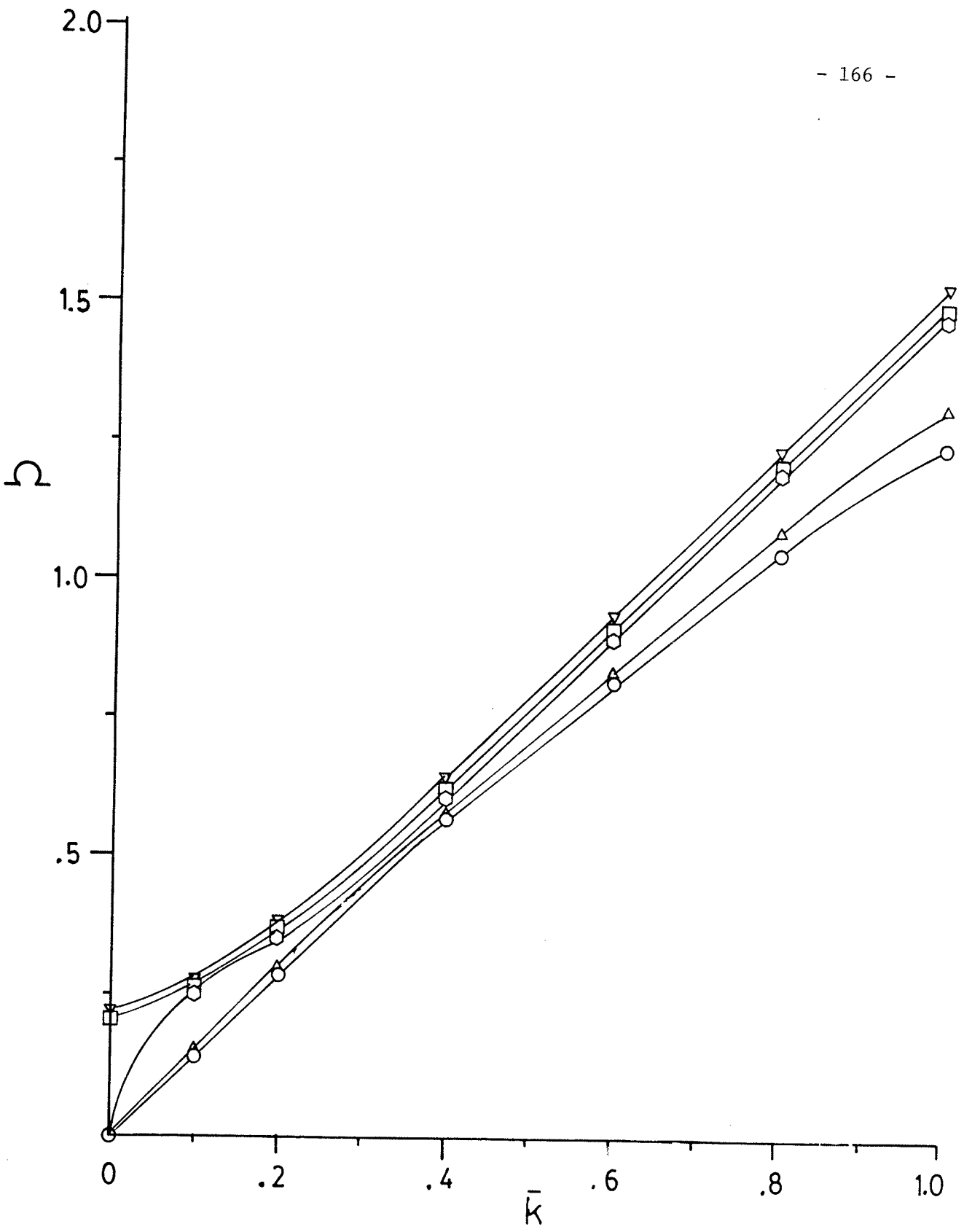
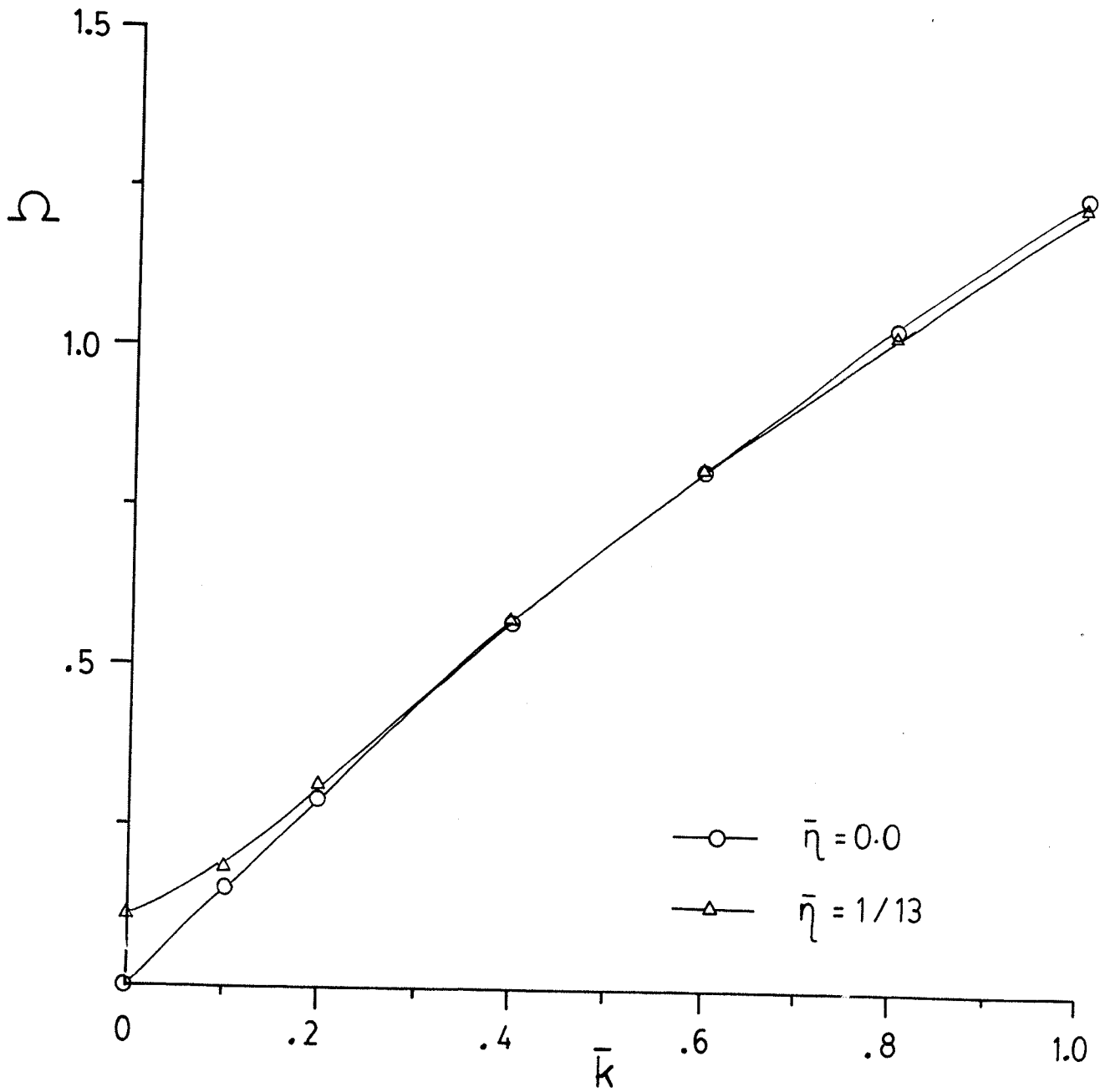


Fig. 4.35 Lowest 5 branches for $\alpha = 90^\circ$, $\bar{\eta} = 0.0$.

Fig. 4.36 Frequency vs. wave number plot for lowest SH mode, $\eta = 0.0$ and $\bar{\eta} = 1/13$.



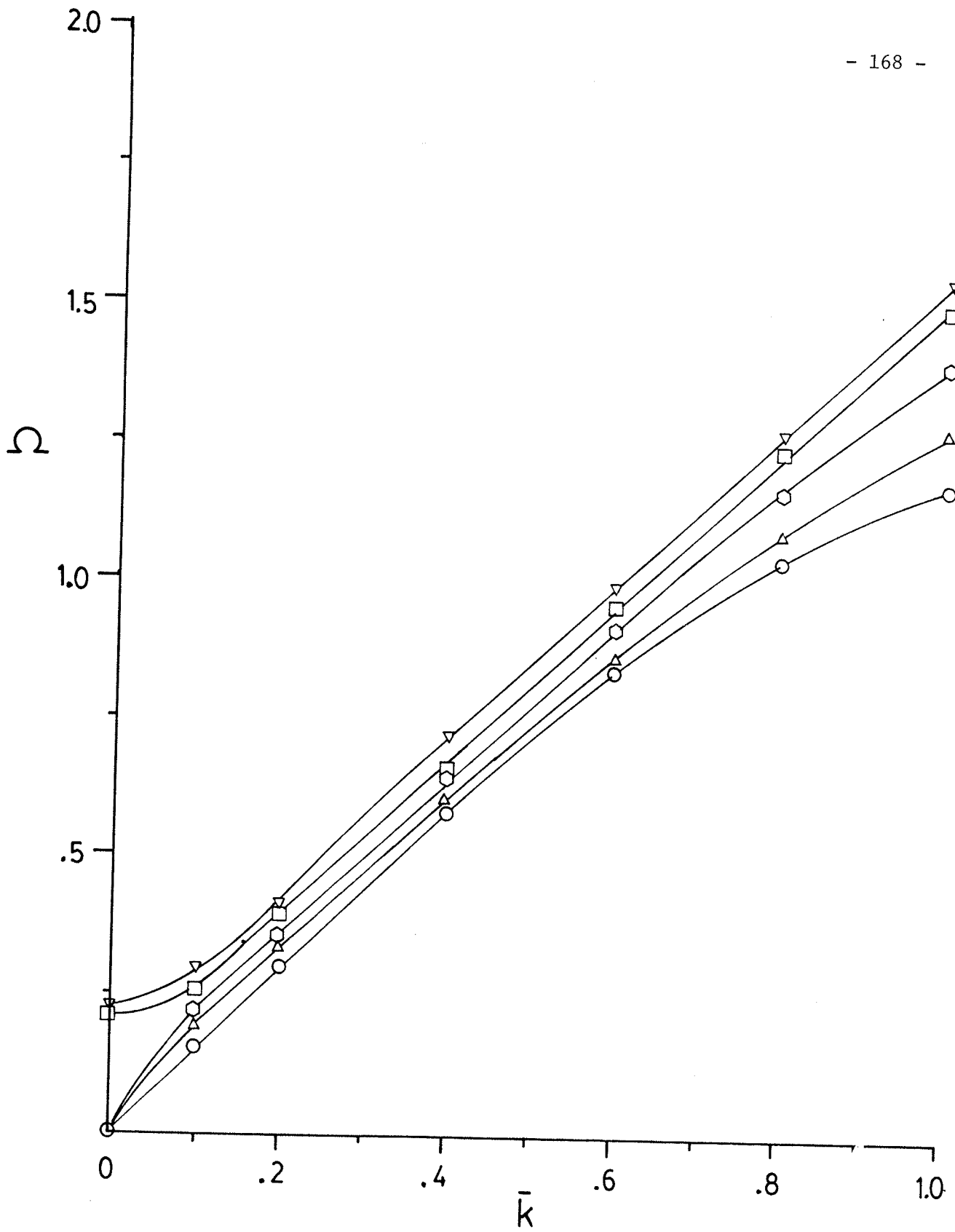


Fig. 4.37 Lowest 5 branches for $\alpha = 45^\circ$, $\bar{\eta} = 1/26$.

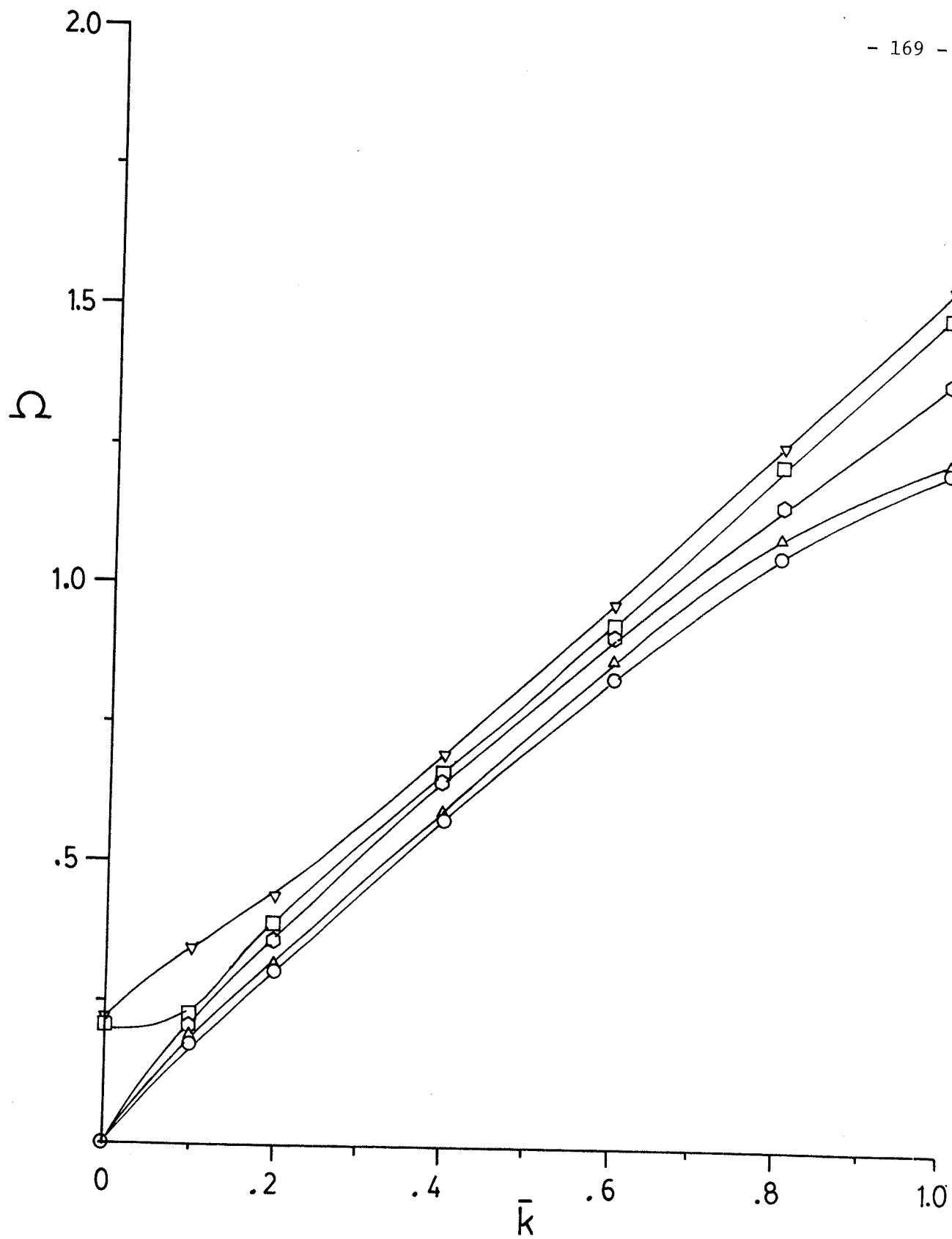
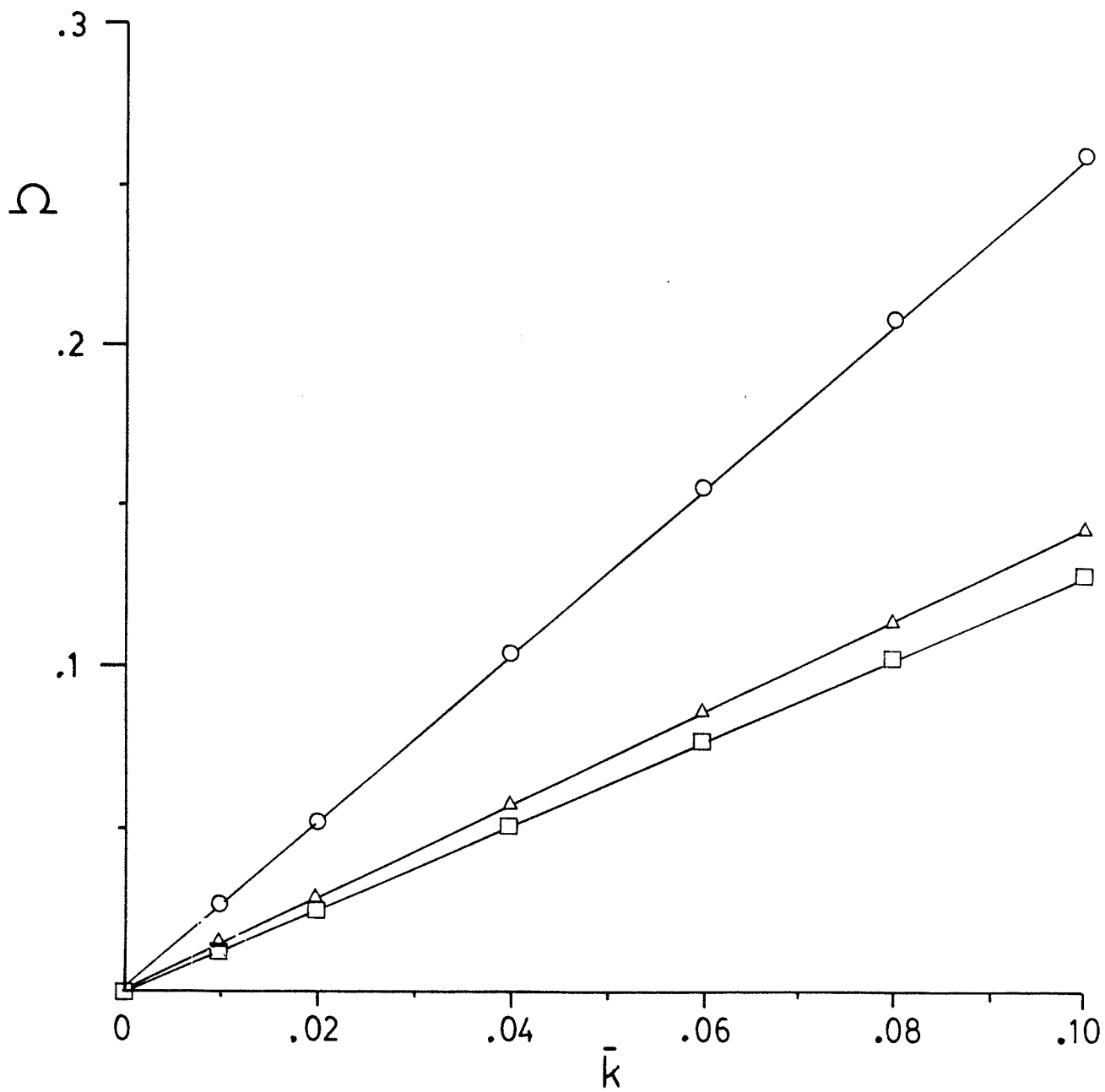


Fig. 4.38 Lowest 5 branches for $\alpha = 45^\circ$, $\bar{\eta} = 1/13$.

Fig. 4.39 Lowest 3 branches for wave propagating on x-y plane,
 $\alpha = 0^\circ$, $\phi = 45^\circ$.



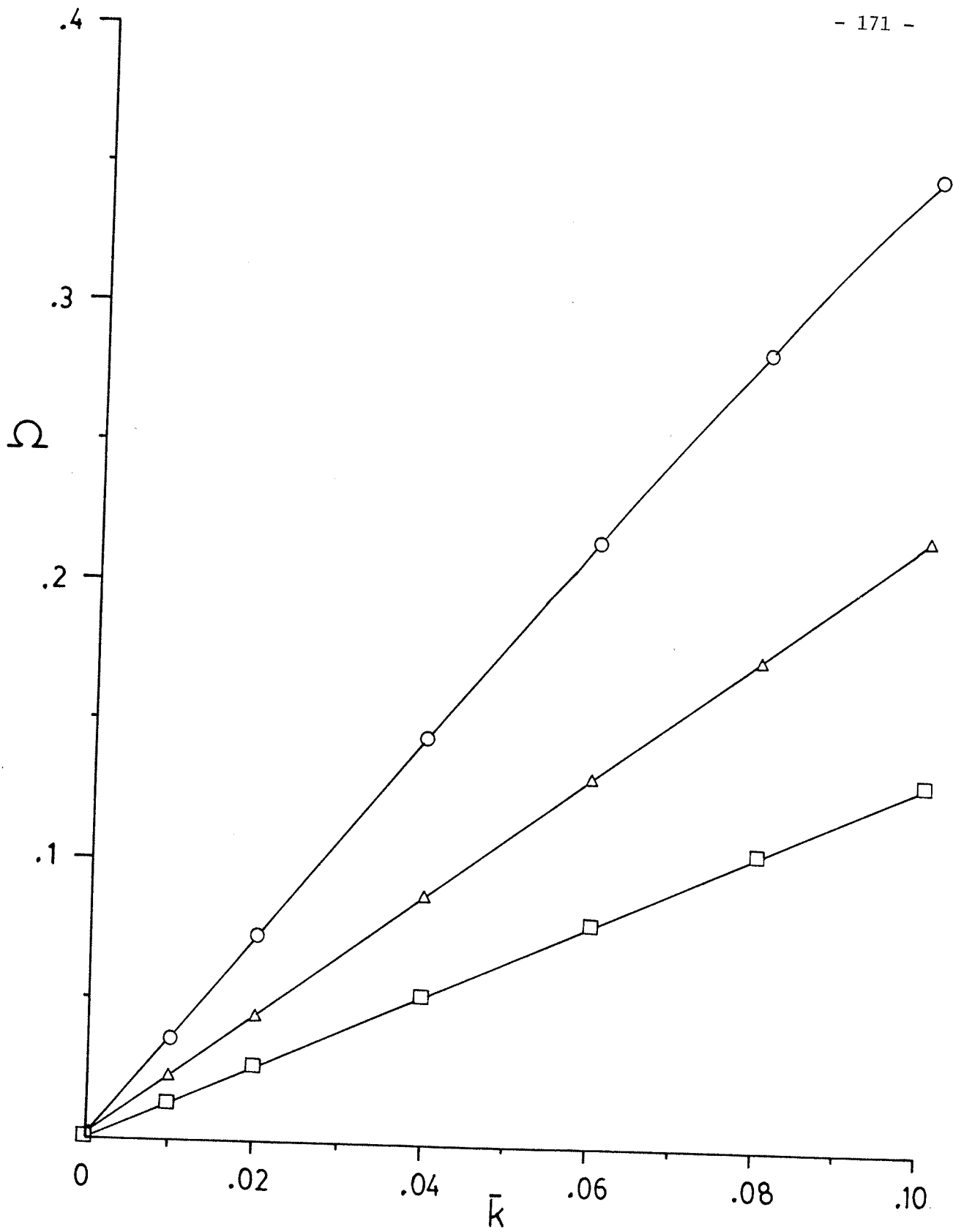


Fig. 4.40 Lowest 3 branches for wave propagating on y-z plane, $\alpha = 90^\circ$, $\phi = 45^\circ$.

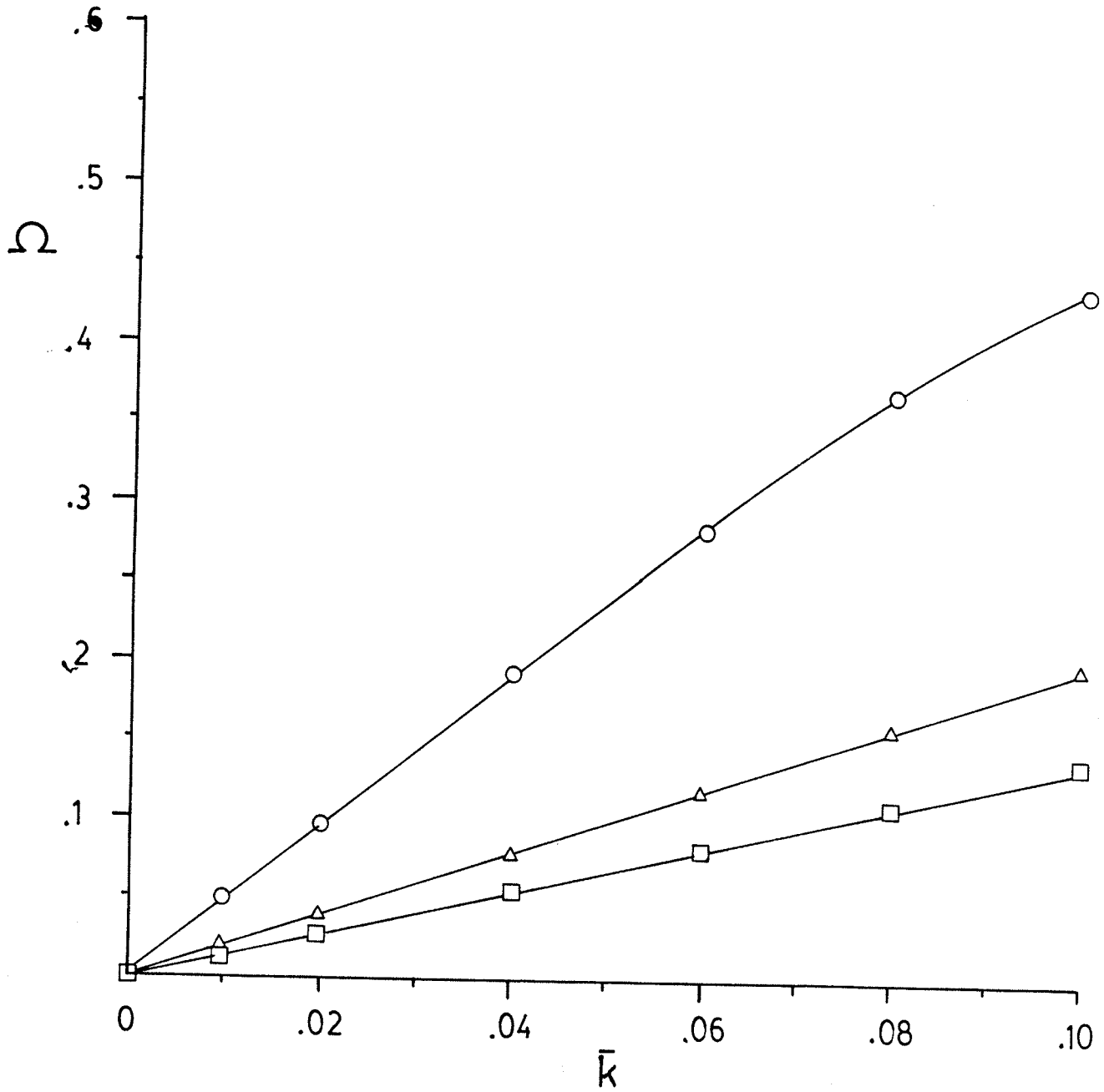


Fig. 4.41 Lowest 3 branches for wave propagating on x-z plane, $\alpha = 45^\circ$, $\phi = 0^\circ$.

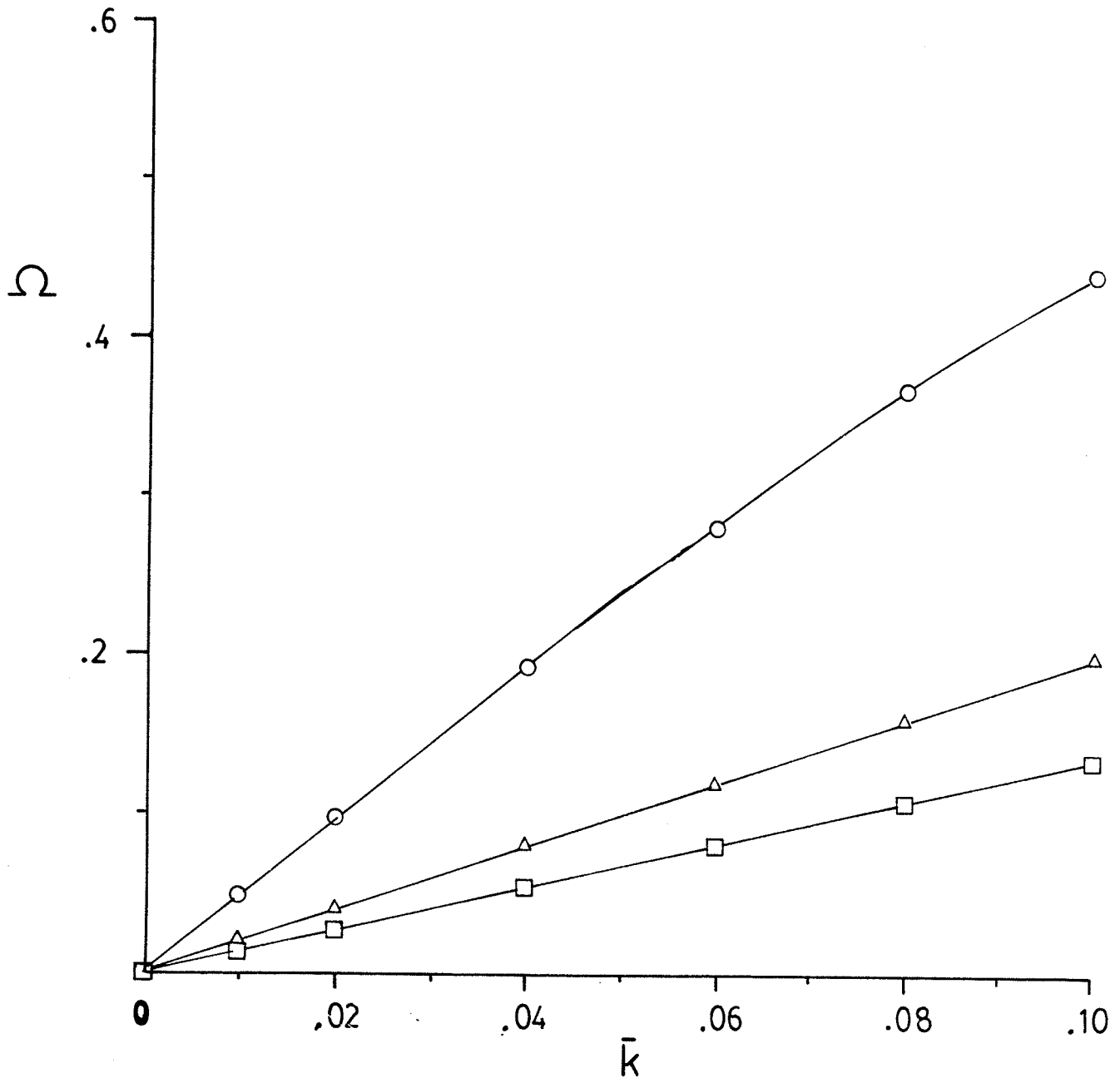


Fig. 4.42 Lowest 3 branches for wave propagating at $\alpha = 45^\circ$, $\phi = 45^\circ$.

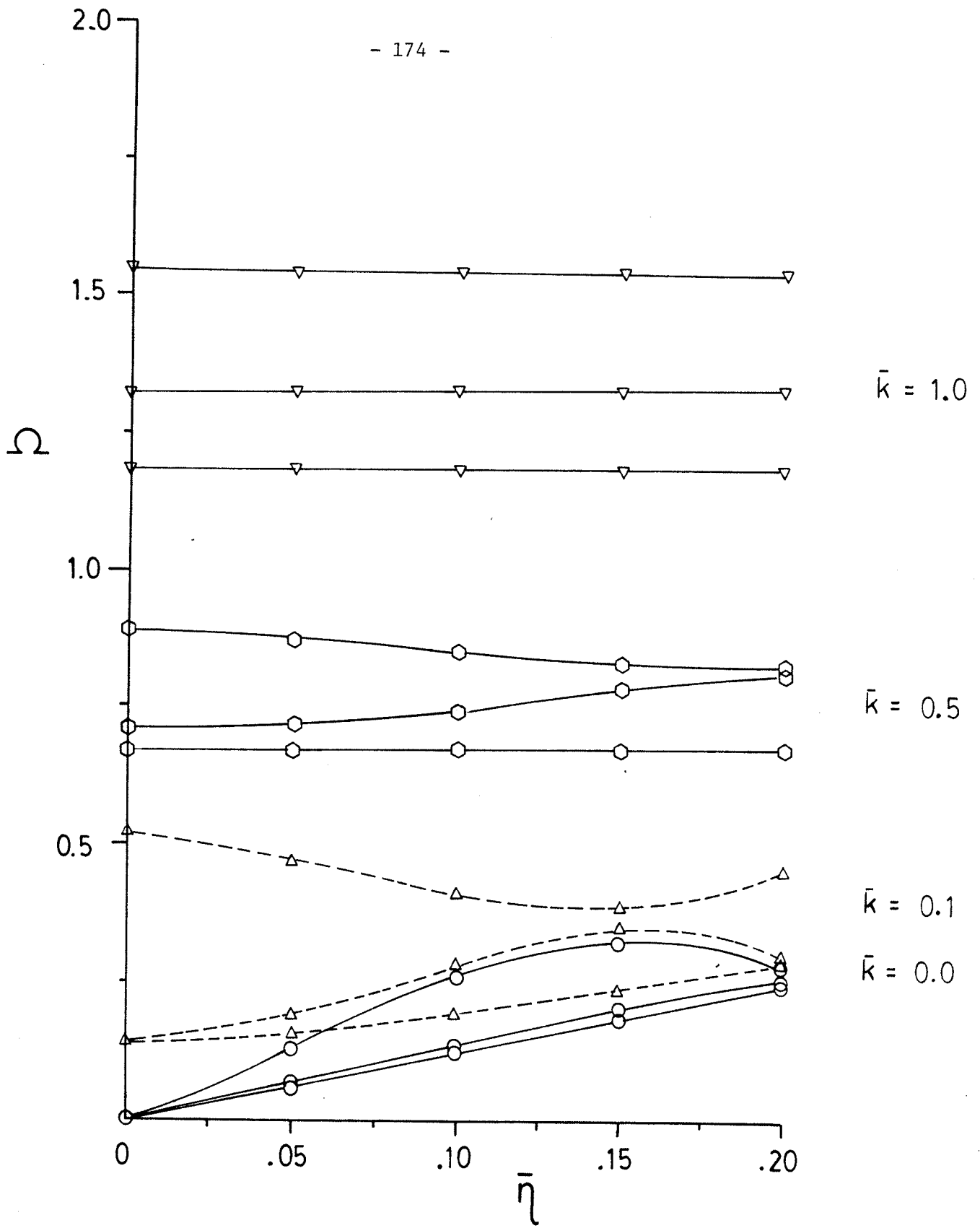


Fig. 4.43 Lowest 3 branches for curves of constant \bar{k} , $\alpha = 0^\circ$.

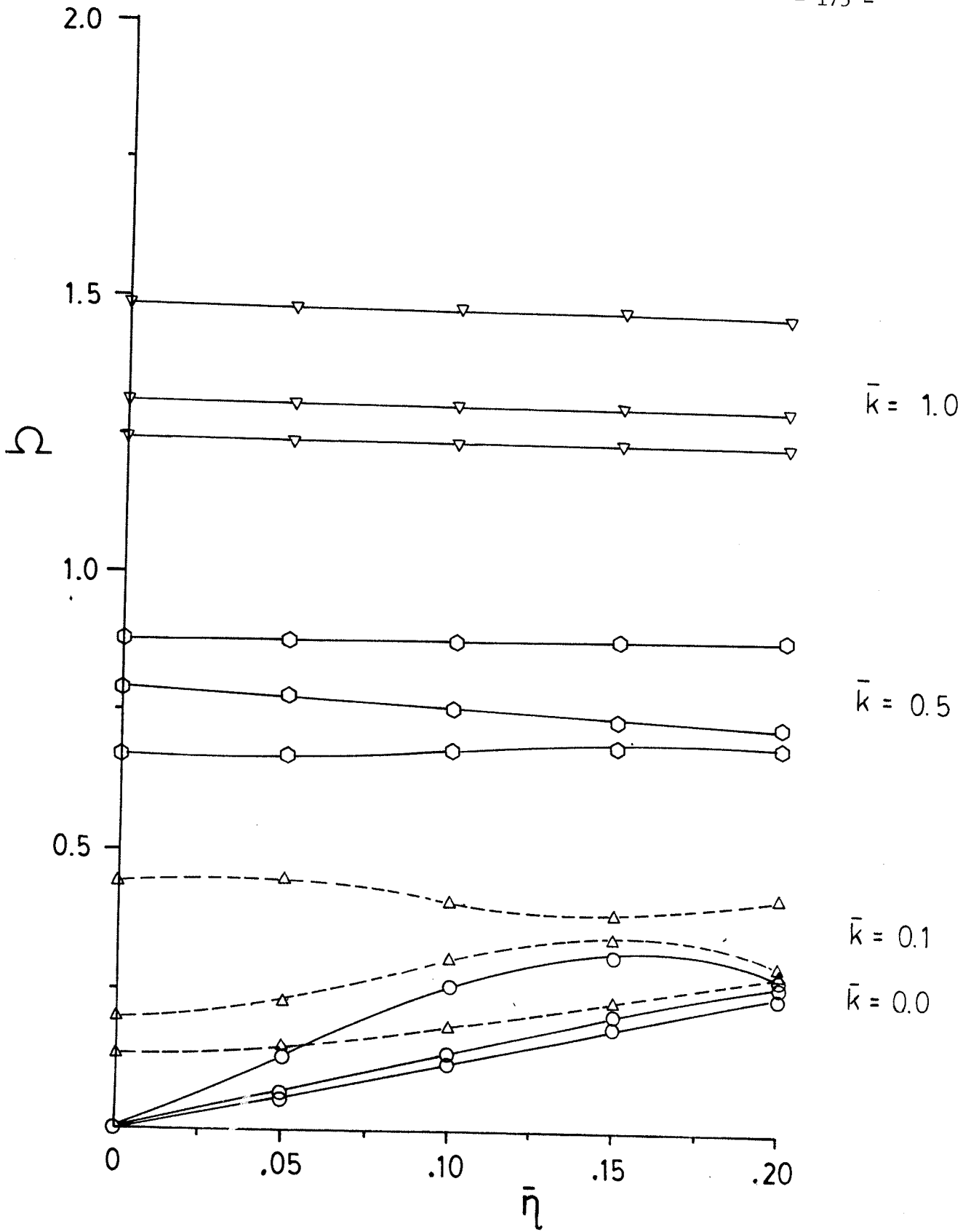


Fig. 4.44 Lowest 3 branches for curves of constant \bar{k} , $\alpha = 45^\circ$.

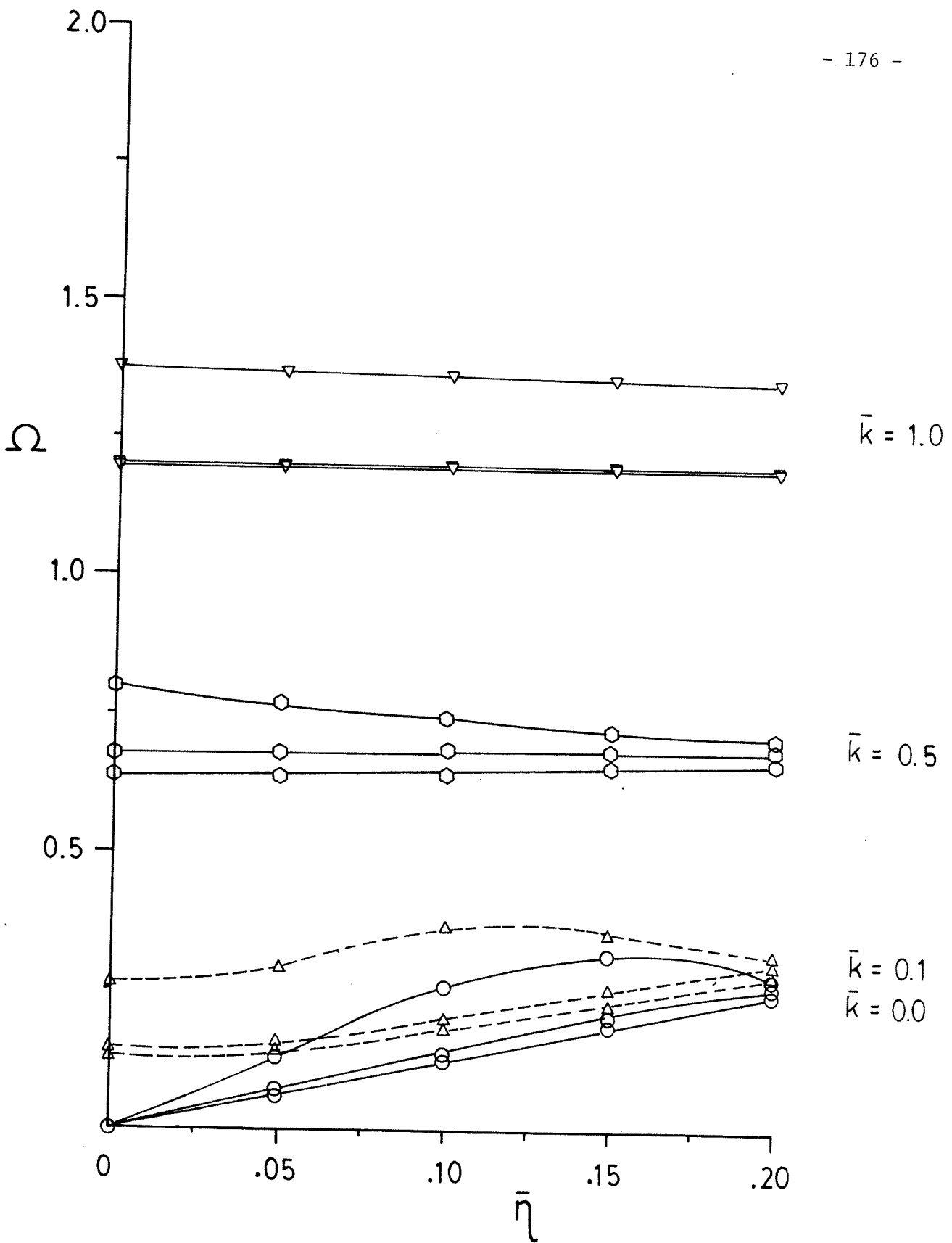


Fig. 4.45 Lowest 3 branches for curves of constant \bar{k} , $\alpha = 90^\circ$.

Fig. 4.46 Lowest branch for constant $\bar{\eta}$, $\alpha = 45^\circ$.

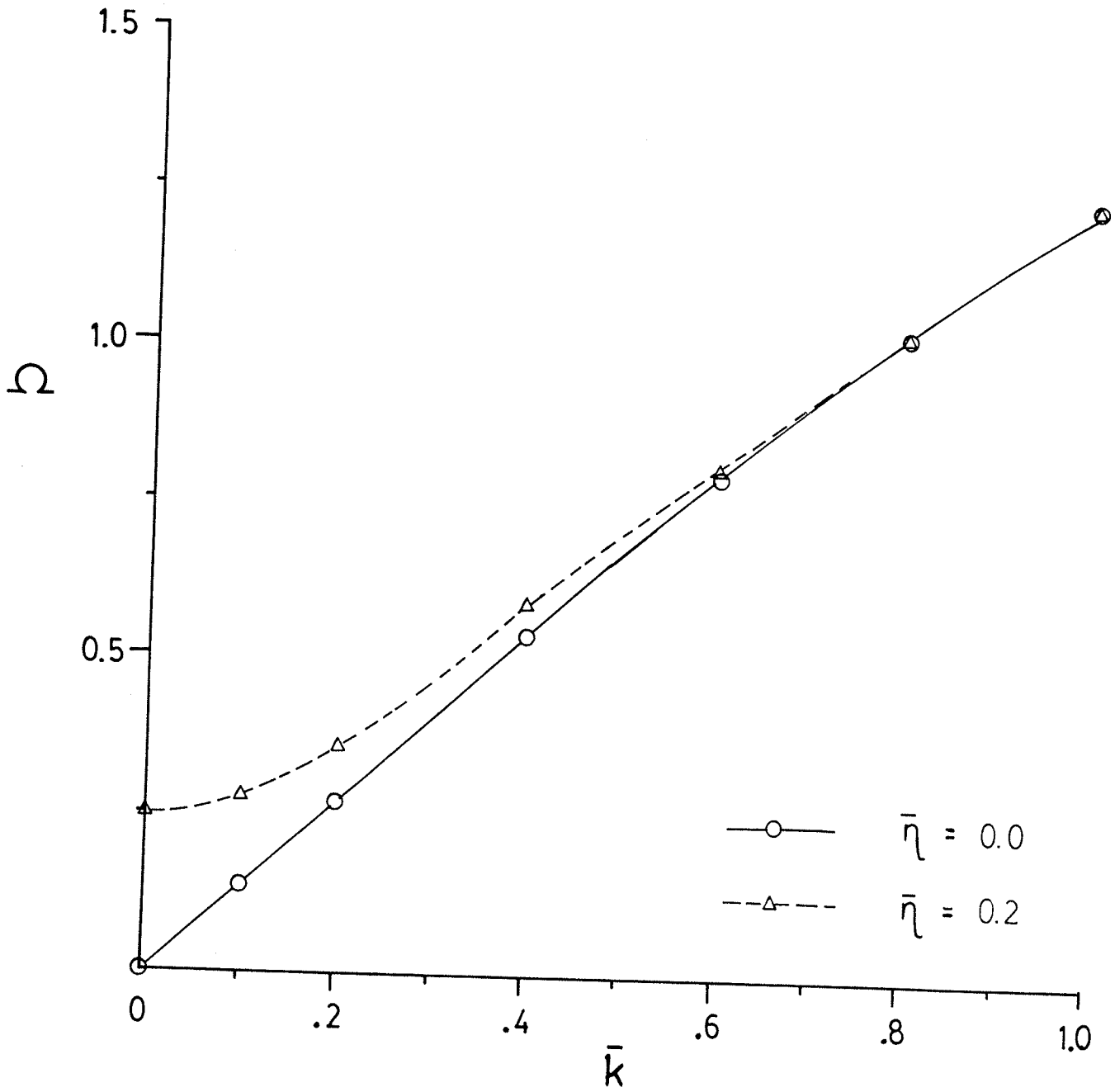


Fig. 4.47 Lowest 3 branches for wave propagating on x-y plane,
 $\alpha = 0^\circ$, $\phi = 45^\circ$; $\bar{d} = 9$.

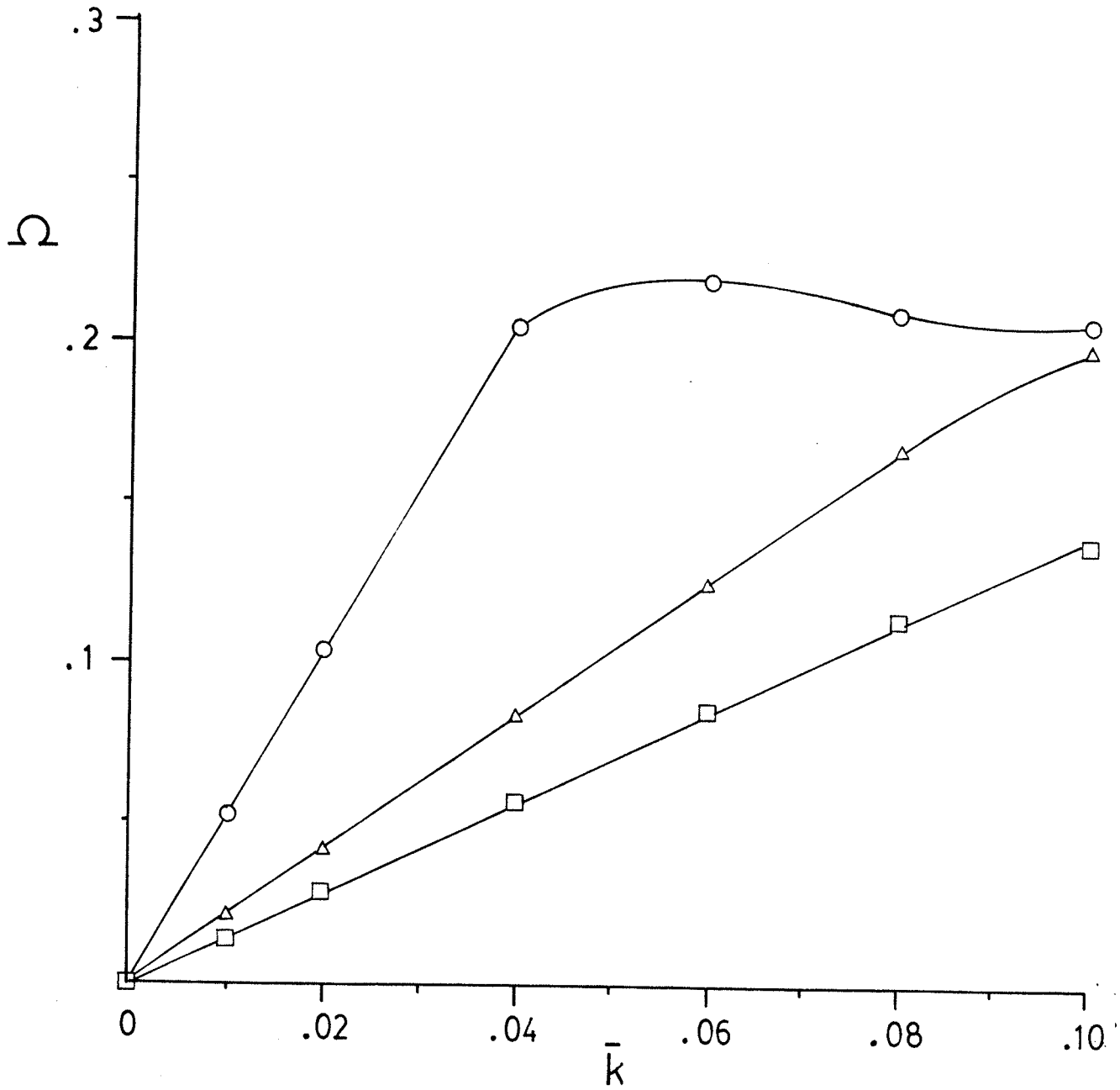
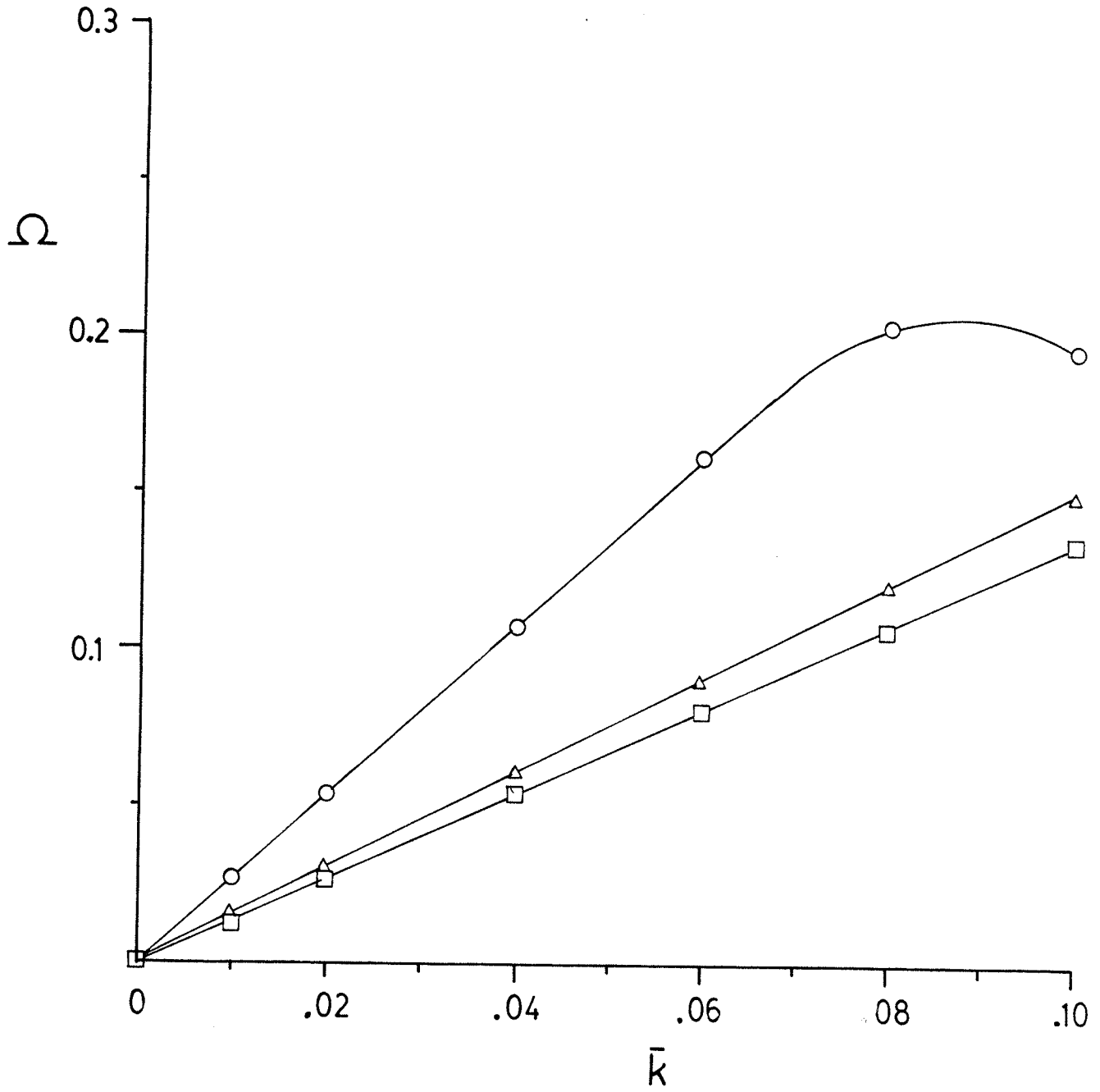


Fig. 4.48 Lowest 3 branches for wave propagating on y-z plane, $\alpha = 90^\circ$, $\phi = 45^\circ$; $\bar{d} = 9$.



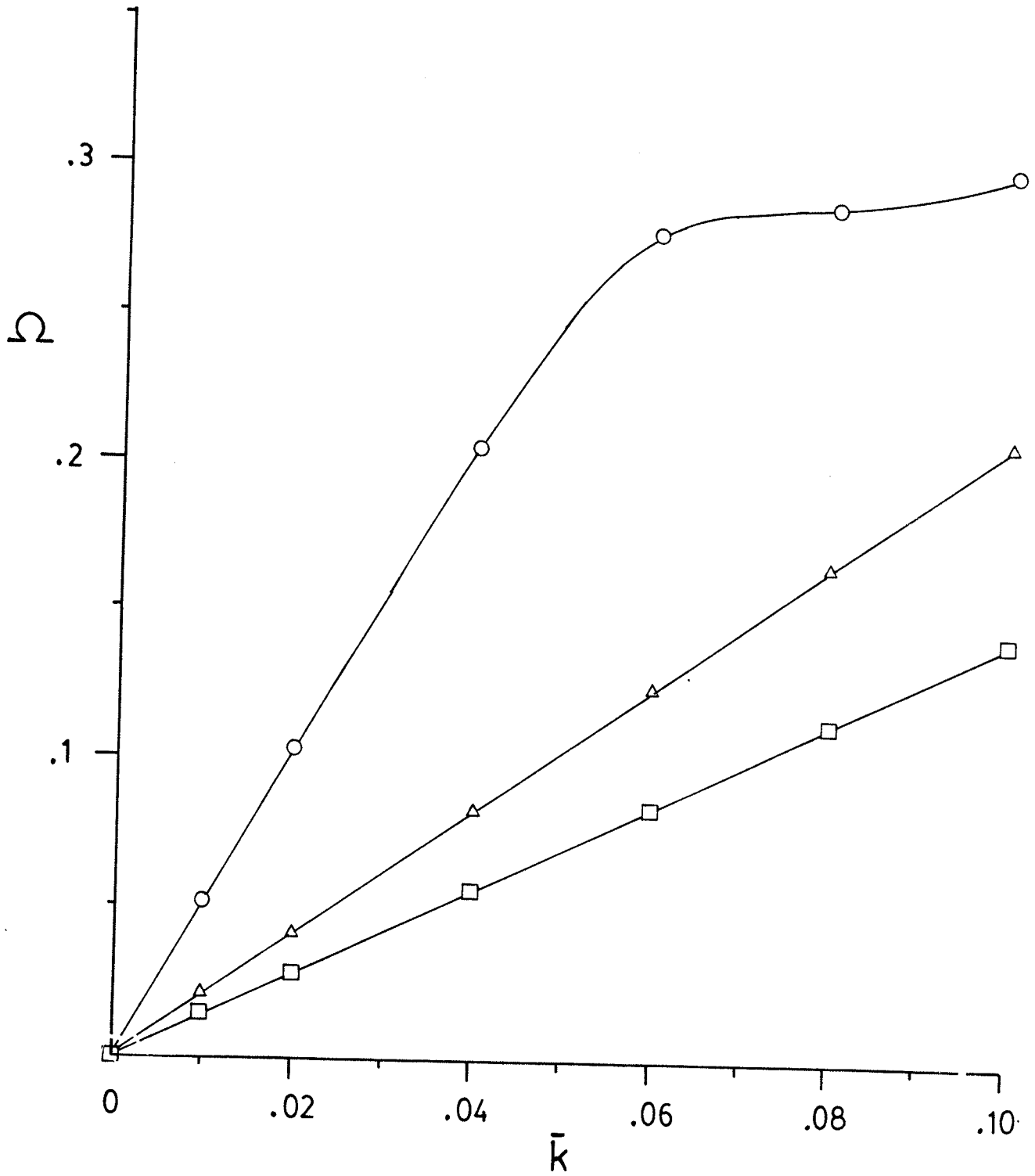
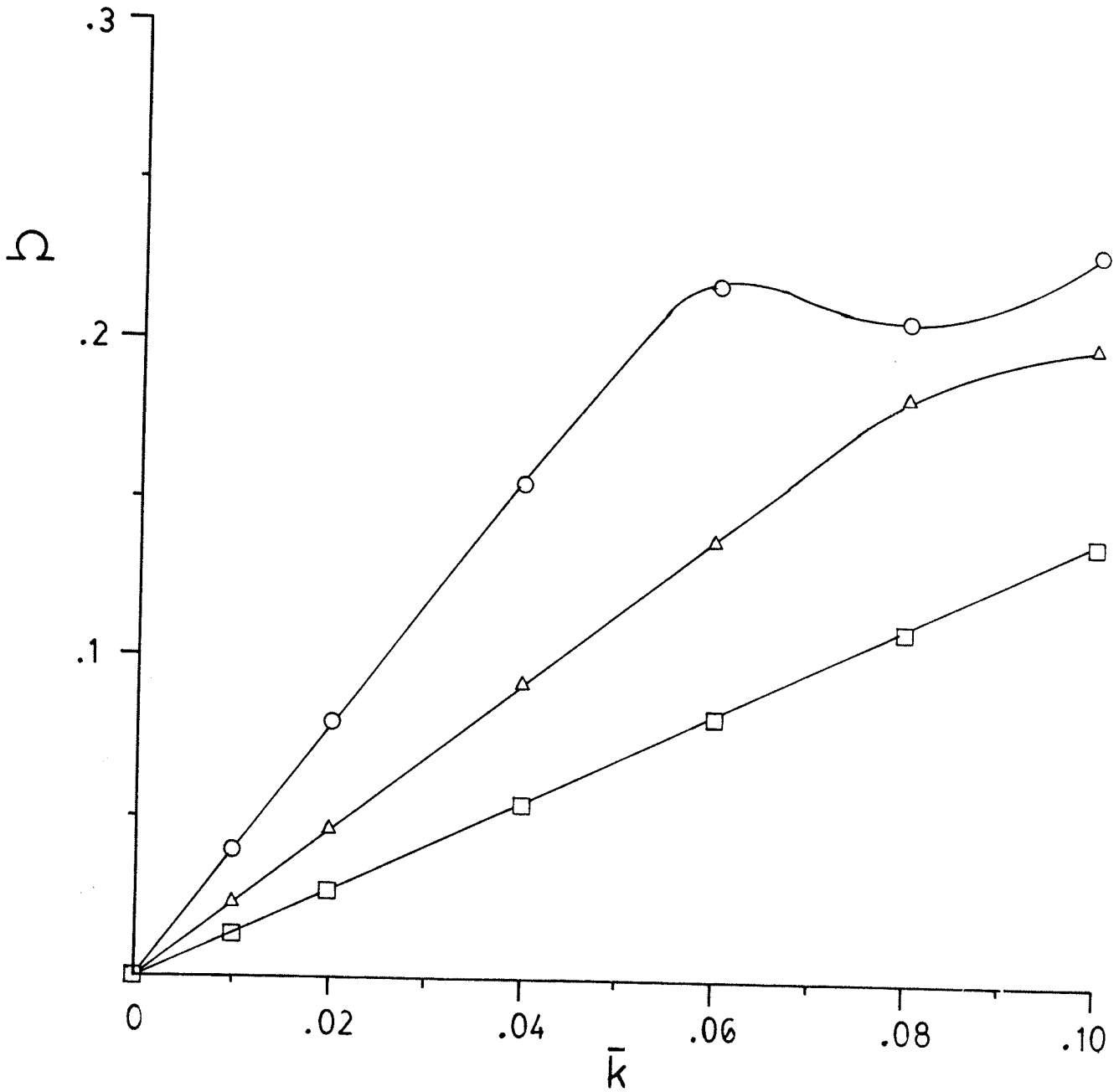


Fig. 4.49 Lowest 3 branches for wave propagating on x-z plane, $\alpha = 45^\circ$, $\phi = 0^\circ$; $\bar{d} = 9$.

Fig. 4.50 Lowest 3 branches for wave propagating at $\alpha = 45^\circ$, $\phi = 45^\circ$;
 $\bar{d} = 9$.



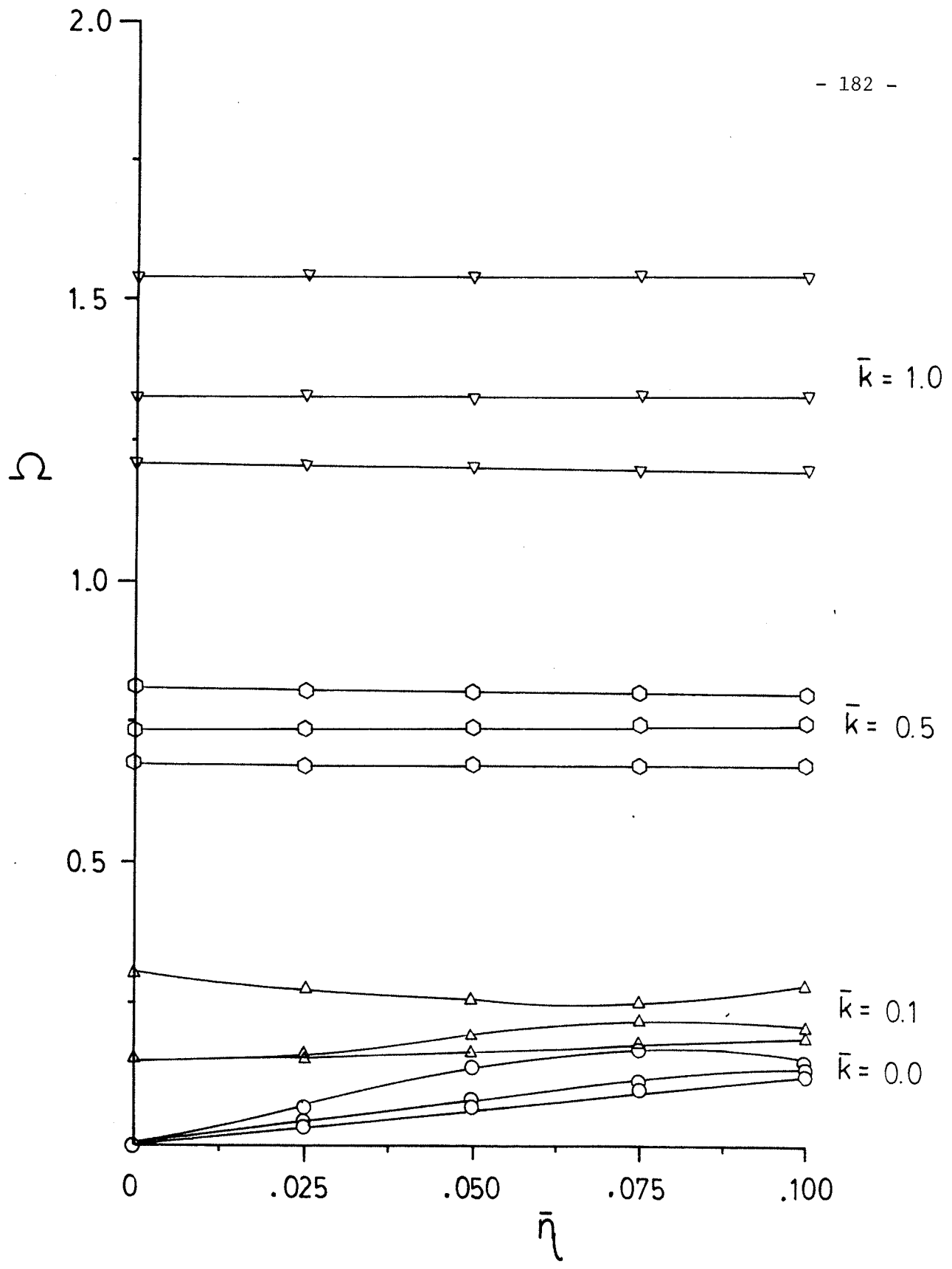


Fig. 4.51 Lowest 3 branches for curves of constant \bar{k} , $\alpha = 0.^\circ$; $\bar{d} = 9$.

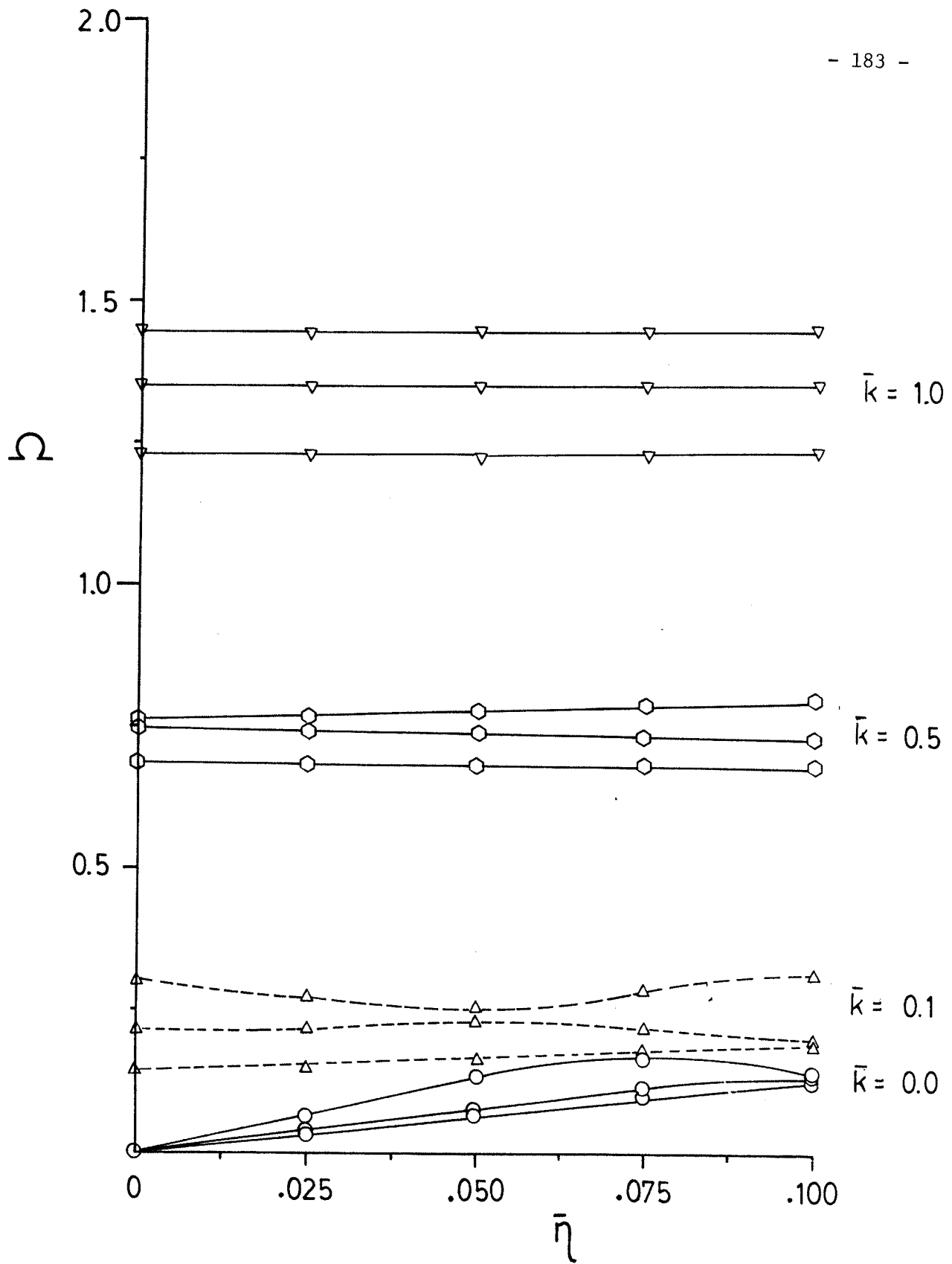


Fig. 4.52 Lowest 3 branches for curves of constant \bar{k} , $\alpha = 45^\circ$; $\bar{d} = 9$.

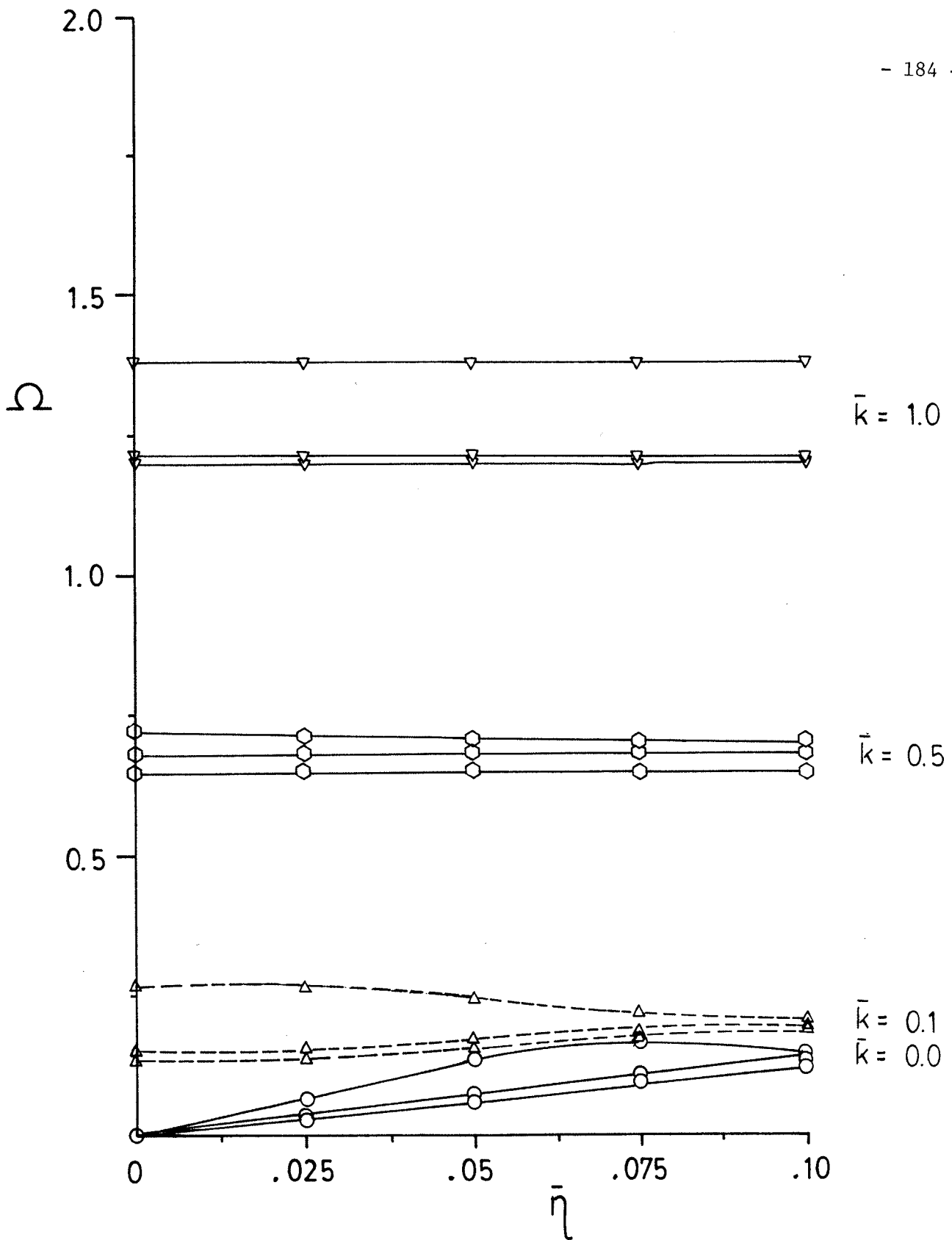


Fig. 4.53 Lowest 3 branches for curves of constant \bar{k} , $\alpha = 90^\circ$; $\bar{d} = 9$.

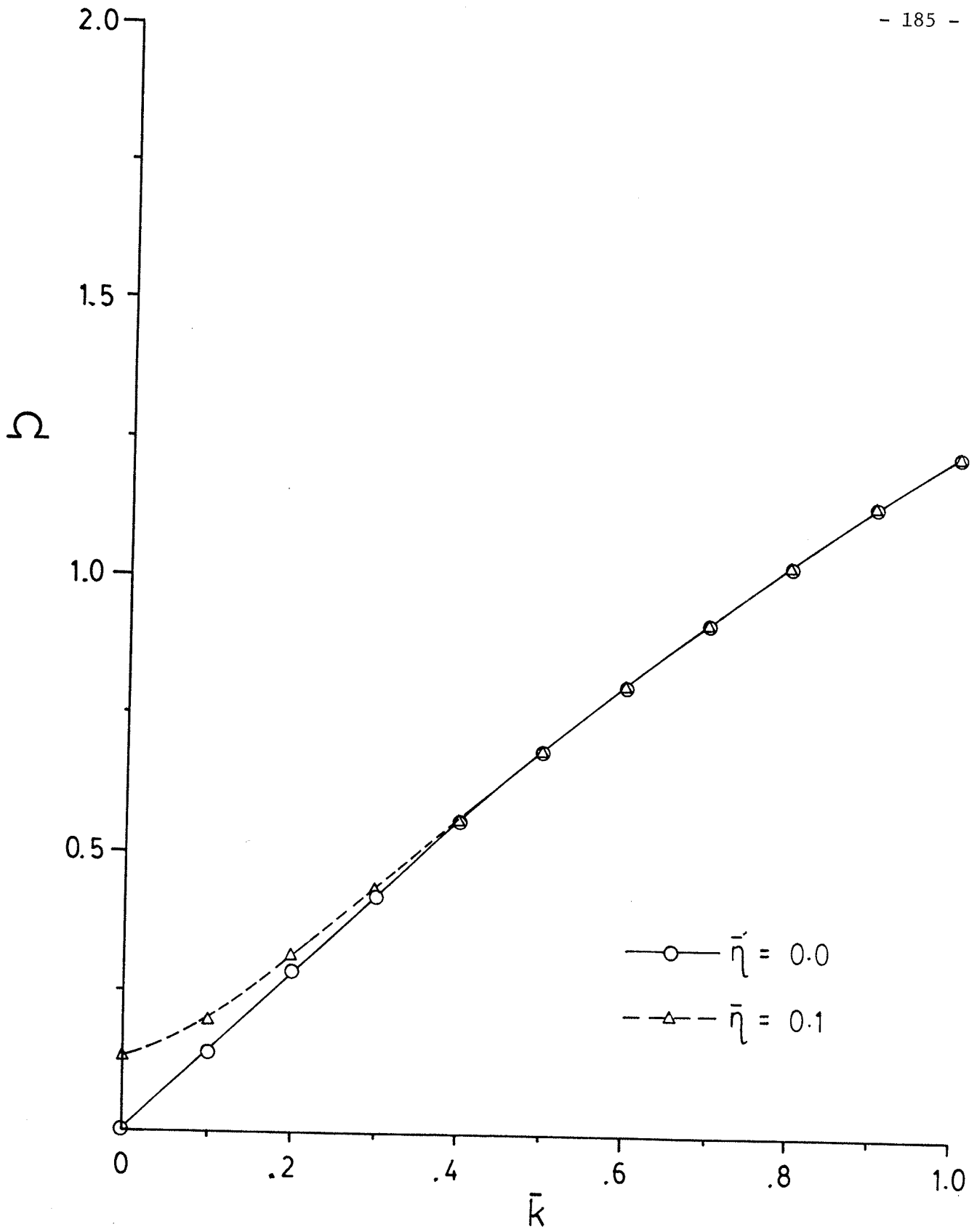


Fig. 4.54 Lowest branch for constant $\bar{\eta}$, $\alpha = 45^\circ$; $\bar{d} = 9$.

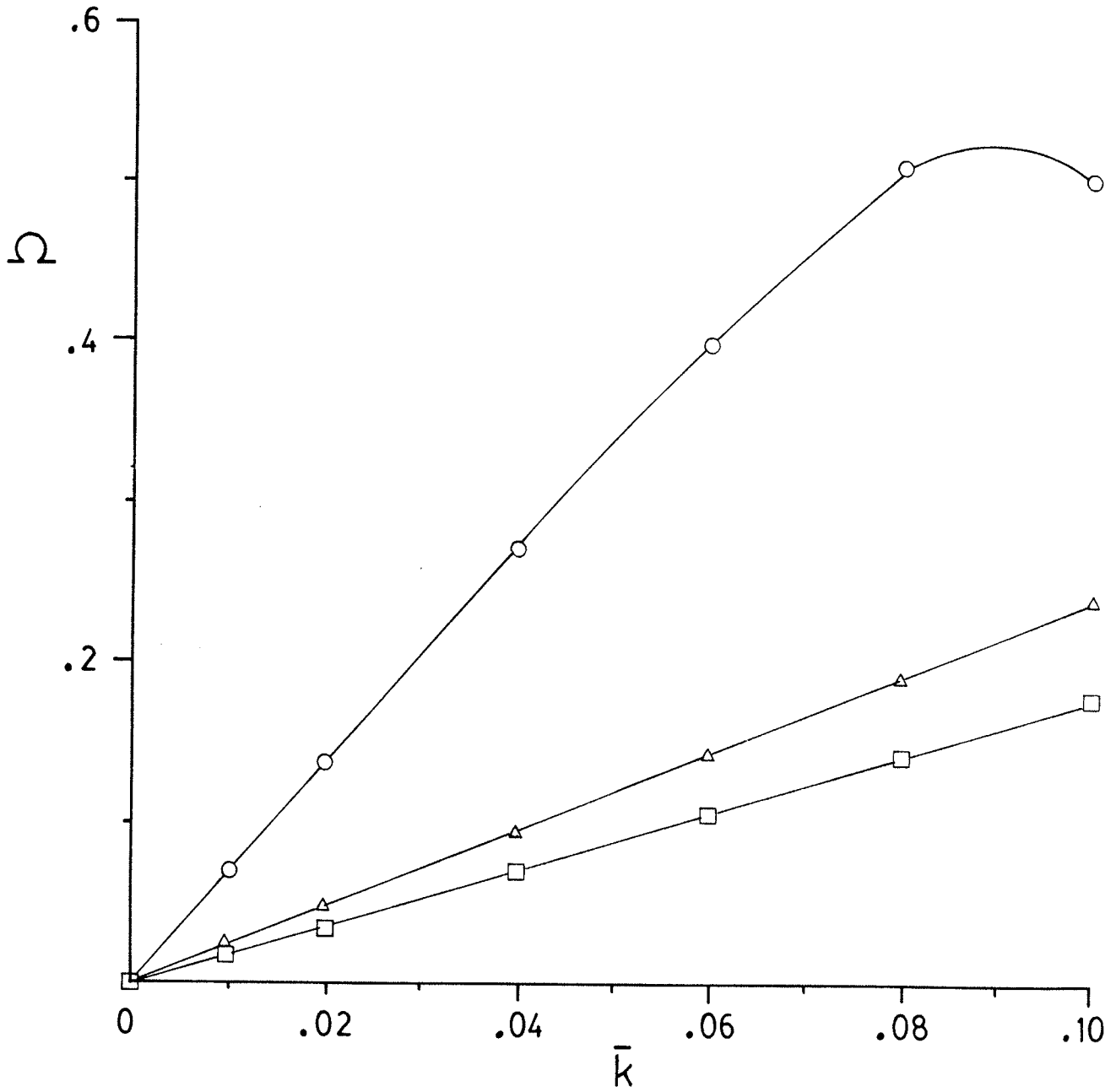


Fig. 4.55 Lowest 3 branches for wave propagating on x-y plane, $\alpha = 0^\circ$, $\phi = 45^\circ$.

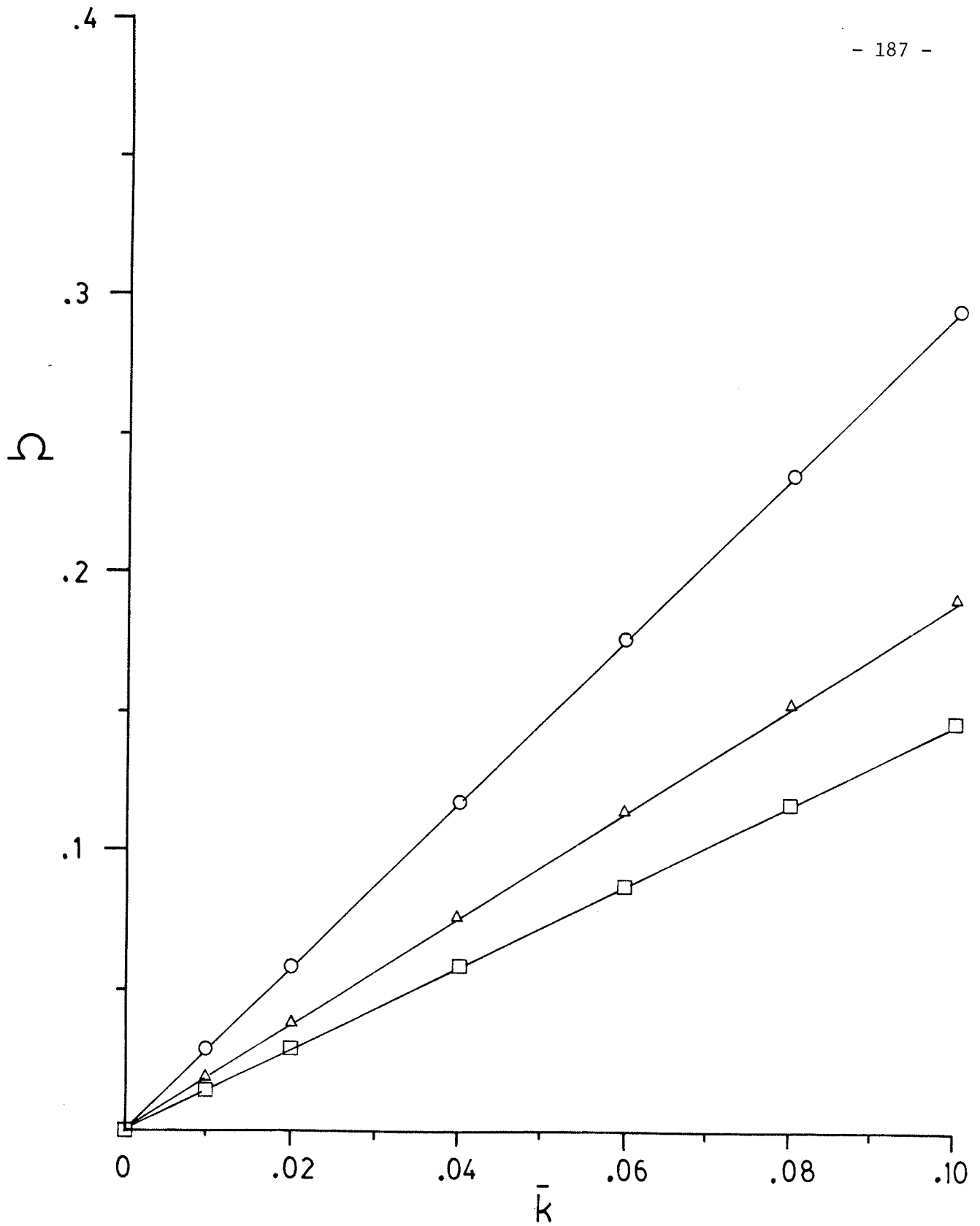


Fig. 4.56 Lowest 3 branches for wave propagating on y-z plane, $\alpha = 90^\circ, \phi = 0^\circ$.

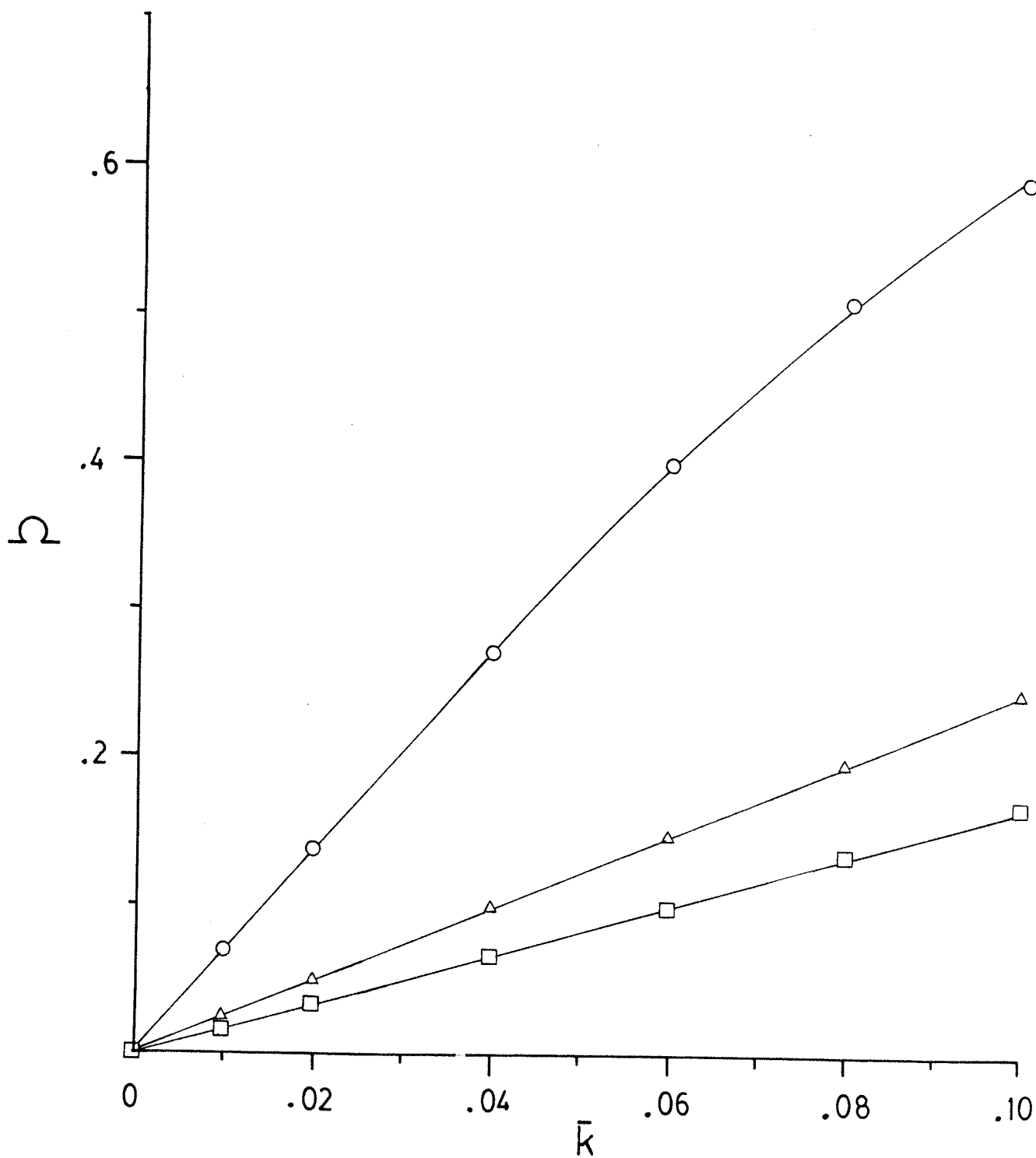


Fig. 4.57 Lowest 3 branches for wave propagating on x-z plane, $\alpha = 45^\circ$, $\phi = 0^\circ$.

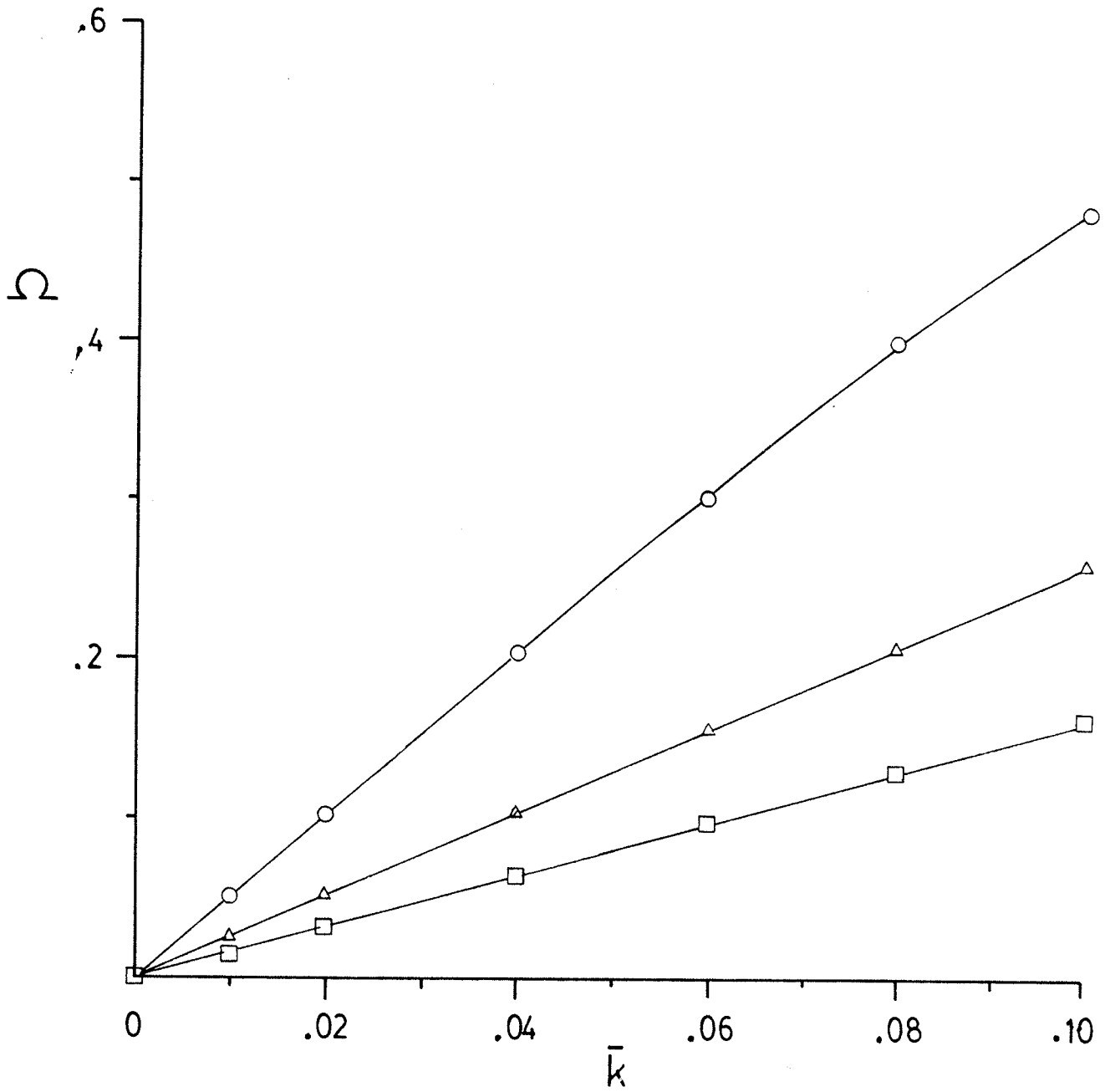


Fig. 4.58 Lowest 3 branches for wave propagating at $\alpha = 45^\circ$, $\phi = 45^\circ$.

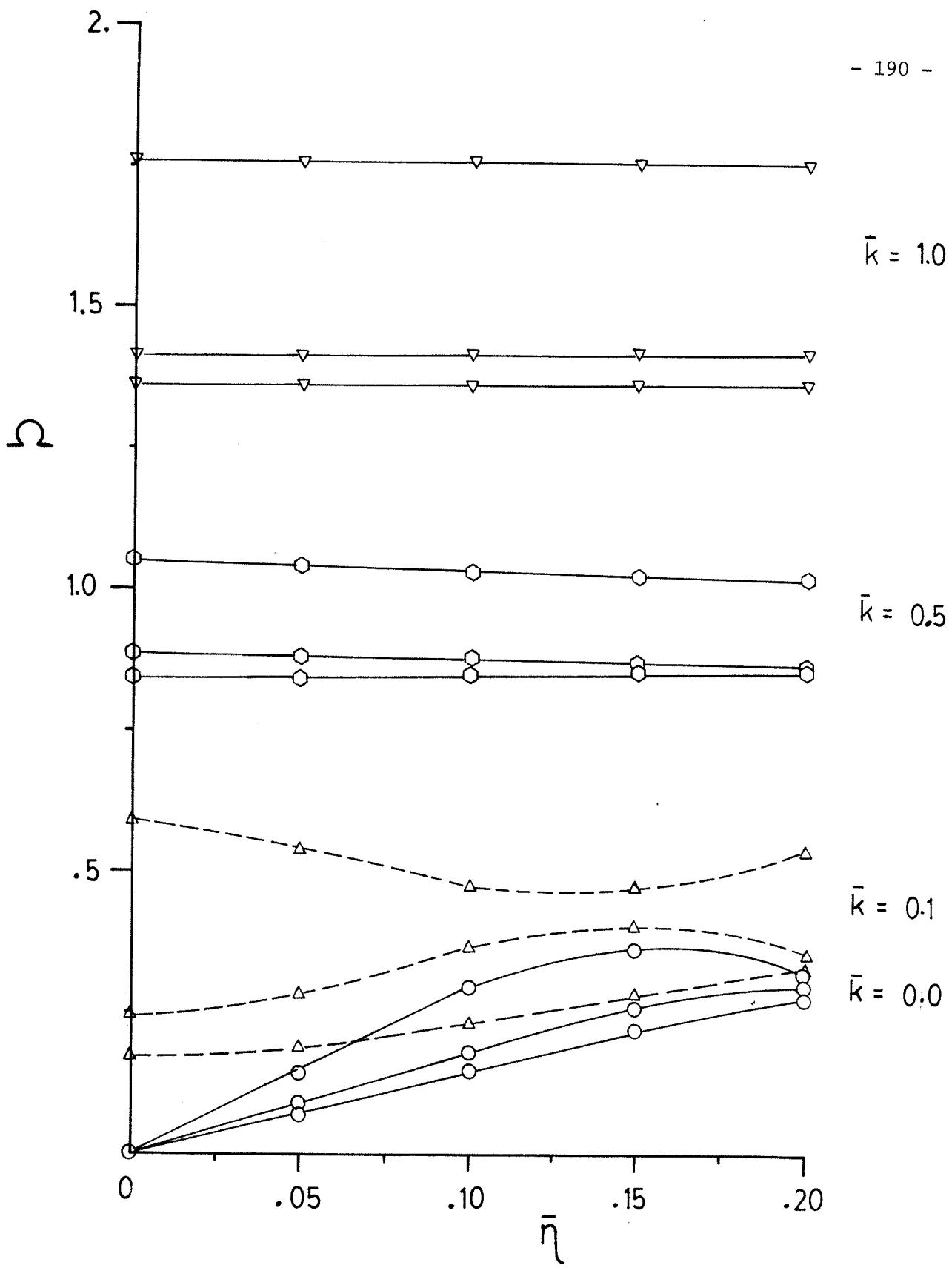


Fig. 4.59 Lowest 3 branches for curves of constant \bar{k} , $\alpha = 0^\circ$.

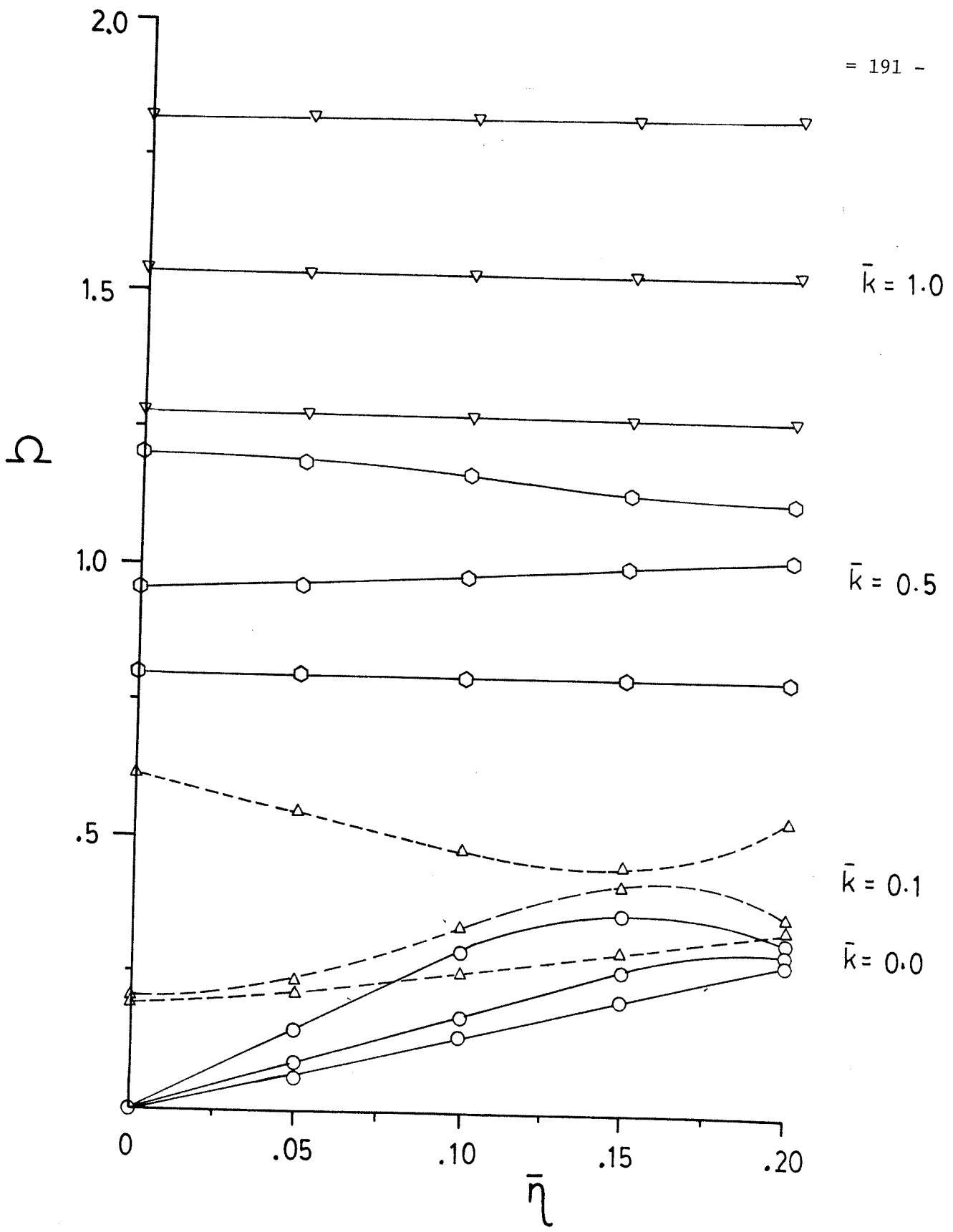


Fig. 4.60 Lowest 3 branches for curves of constant \bar{k} , $\alpha = 45^\circ$.

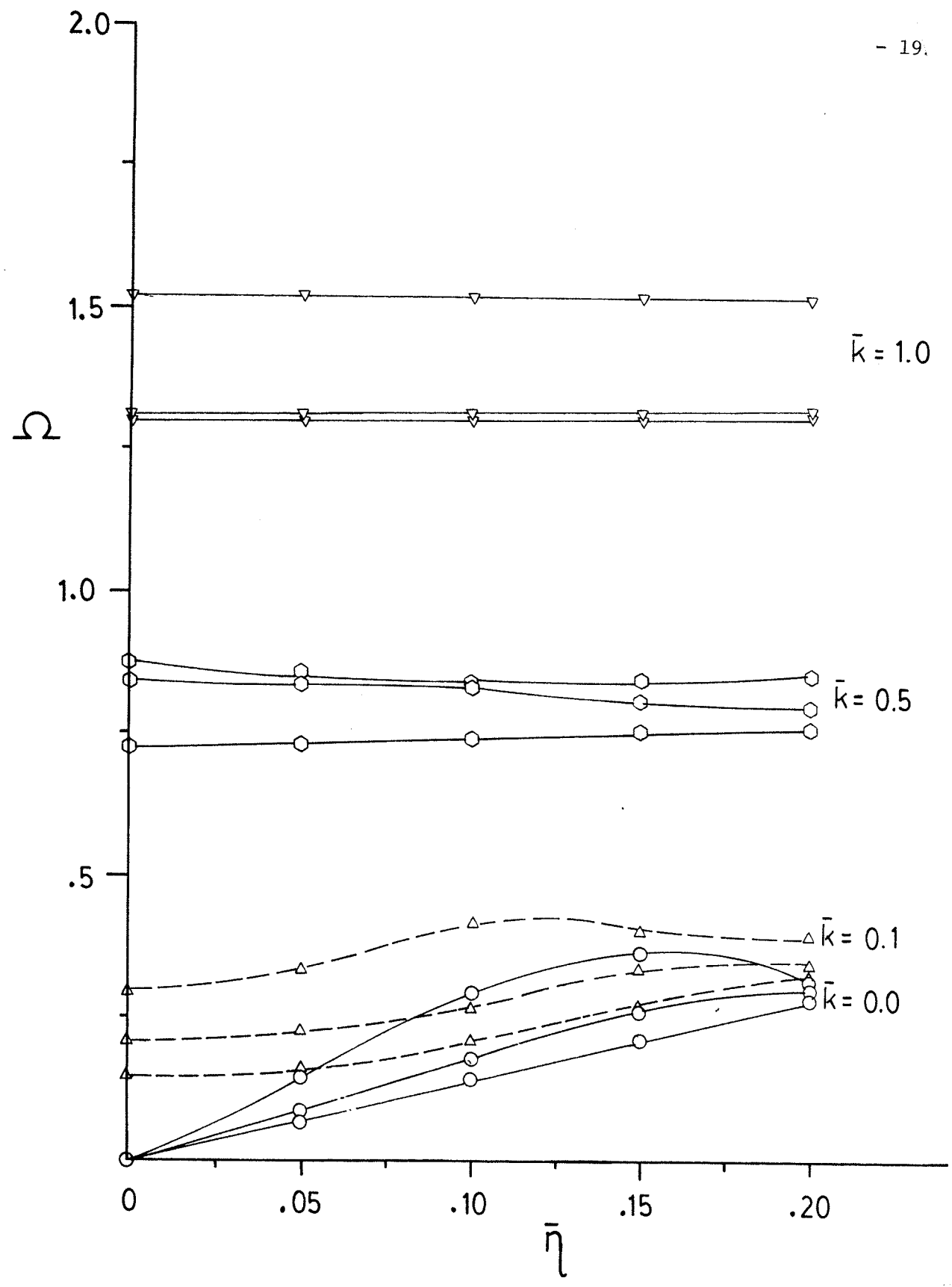


Fig. 4.61 Lowest 3 branches for curves of constant \bar{k} , $\alpha = 90^\circ$.

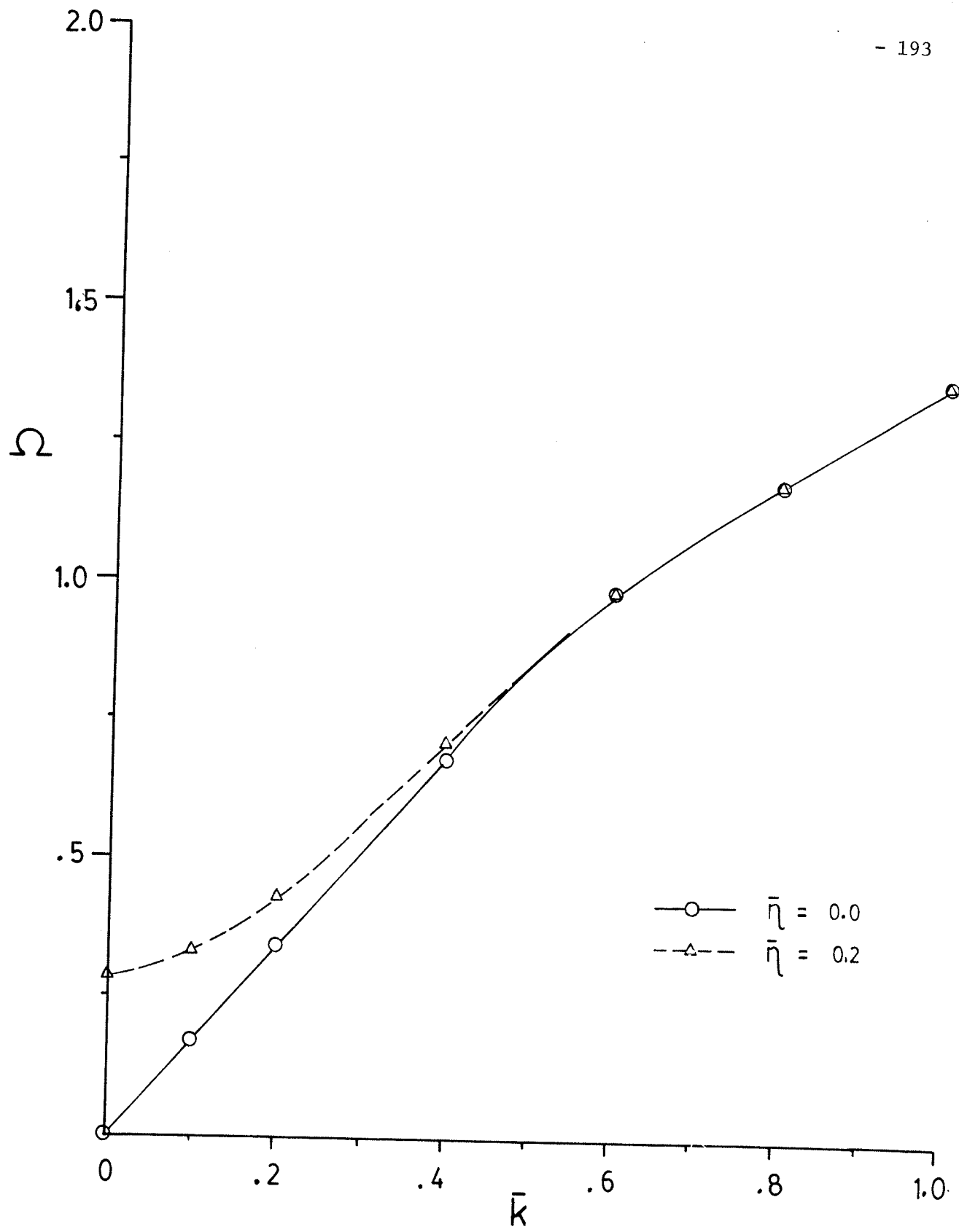


Fig. 4.62. Lowest branch for constant $\bar{\eta}$, $\alpha = 45^\circ$.

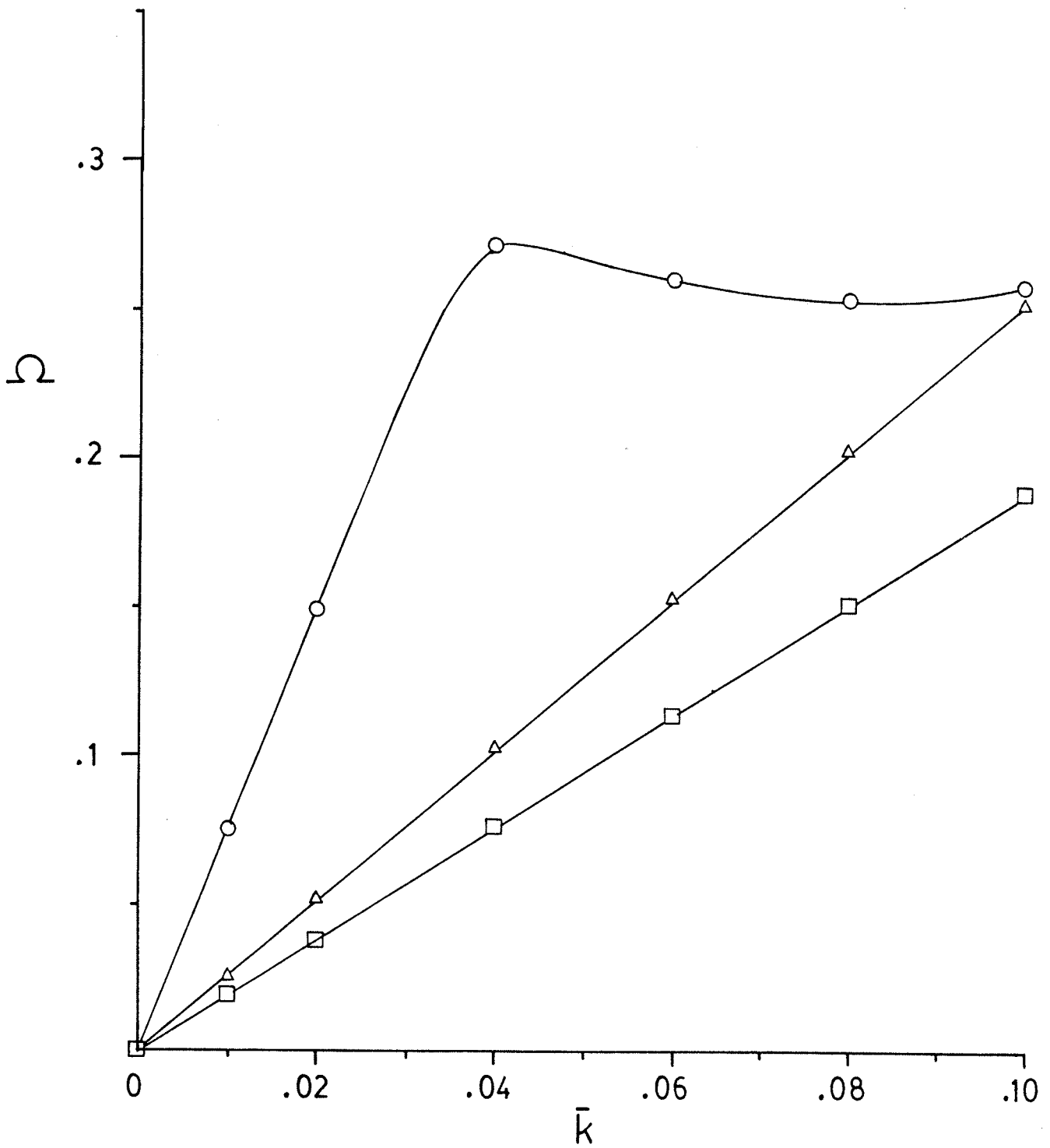
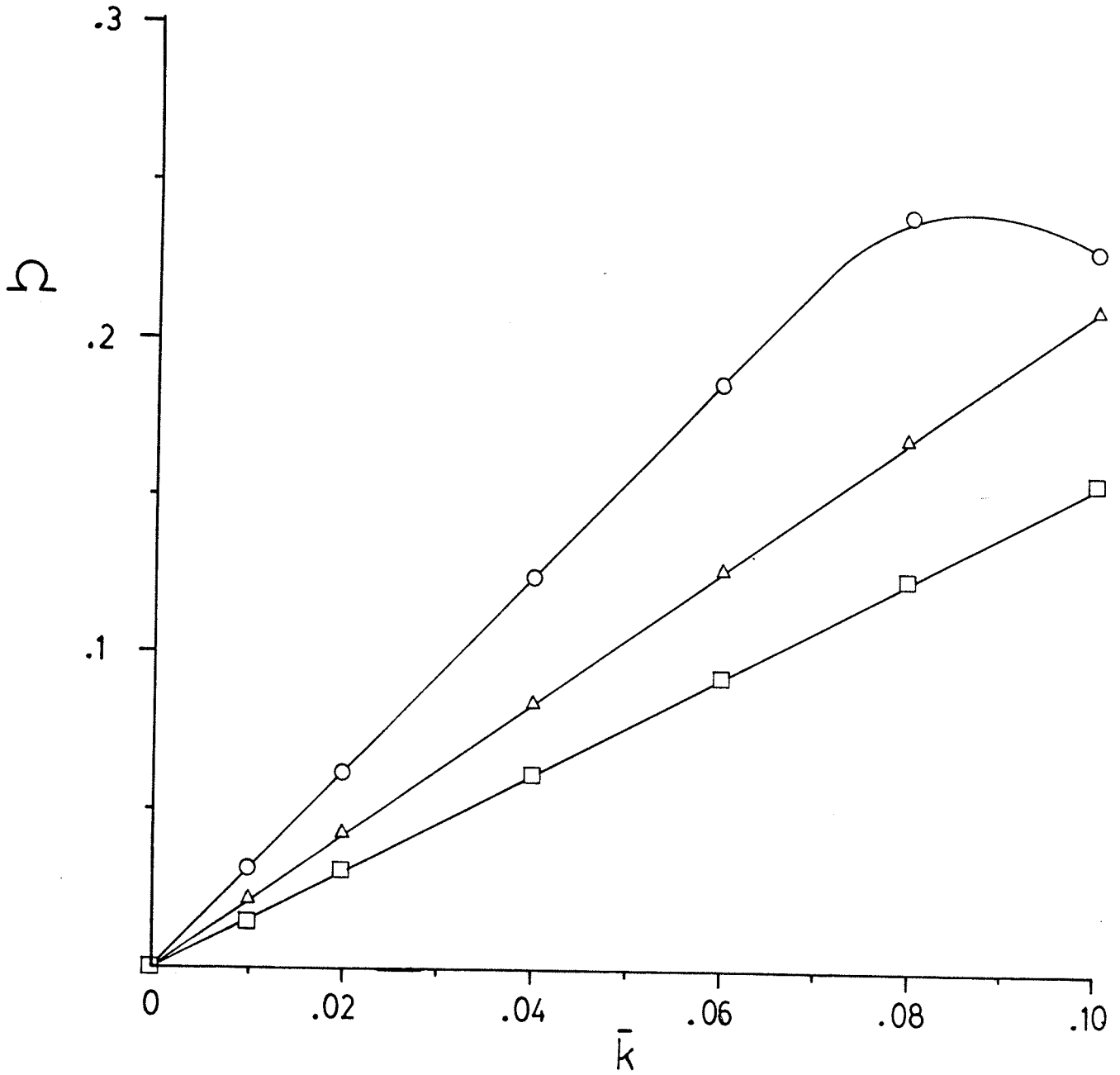


Fig. 4.63 Lowest 3 branches for wave propagating on x-y plane, $\alpha = 0^\circ$, $\phi = 42^\circ$; $\bar{d} = 9$.

Fig. 4.64 Lowest 3 branches for wave propagating at y-z plane,
 $\alpha = 90^\circ$, $\phi = 45^\circ$; $\bar{d} = 9$.



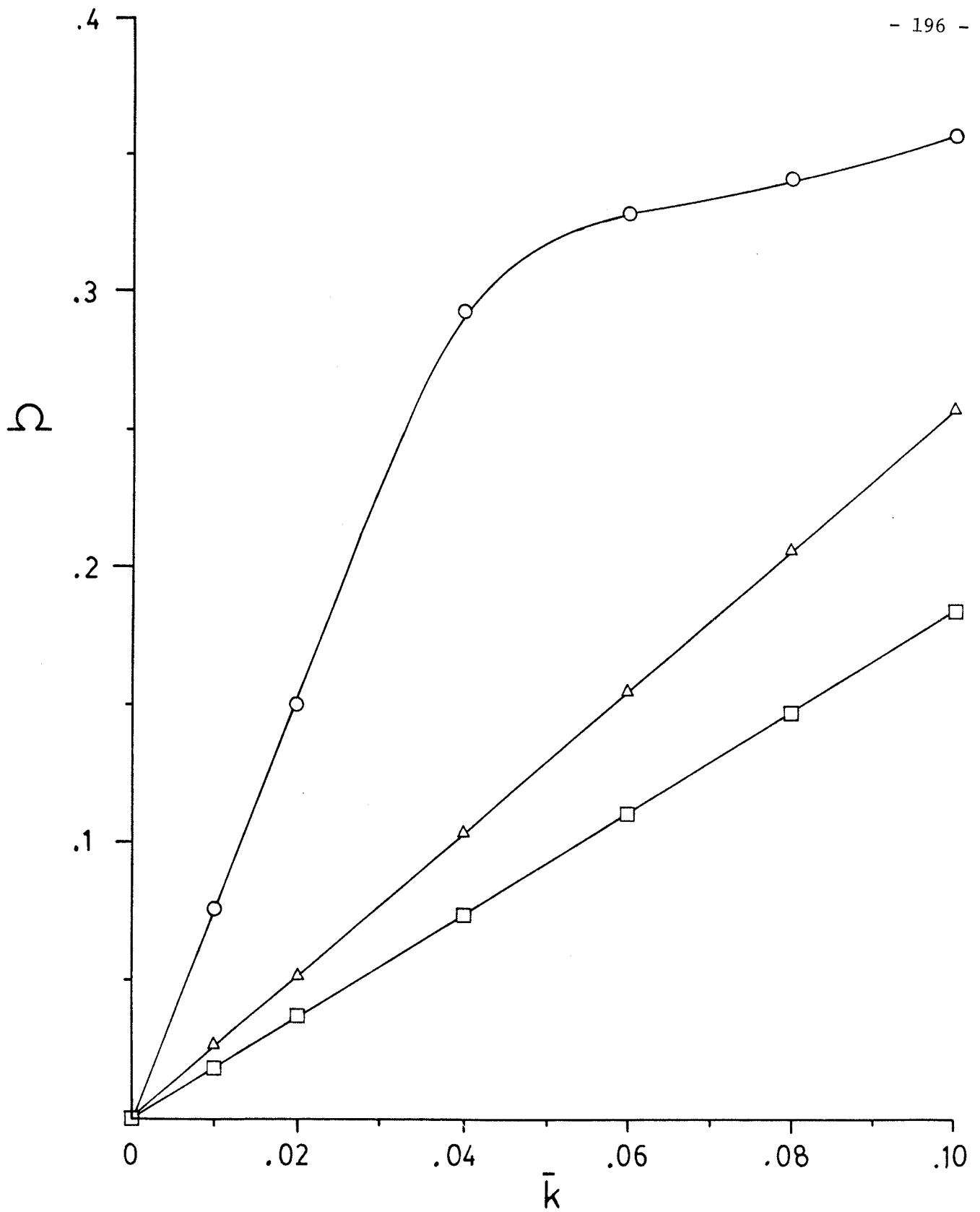


Fig. 4.65 Lowest 3 branches for wave propagating at x-z plane, $\alpha = 45^\circ$, $\phi = 0^\circ$; $\bar{d} = 9$.

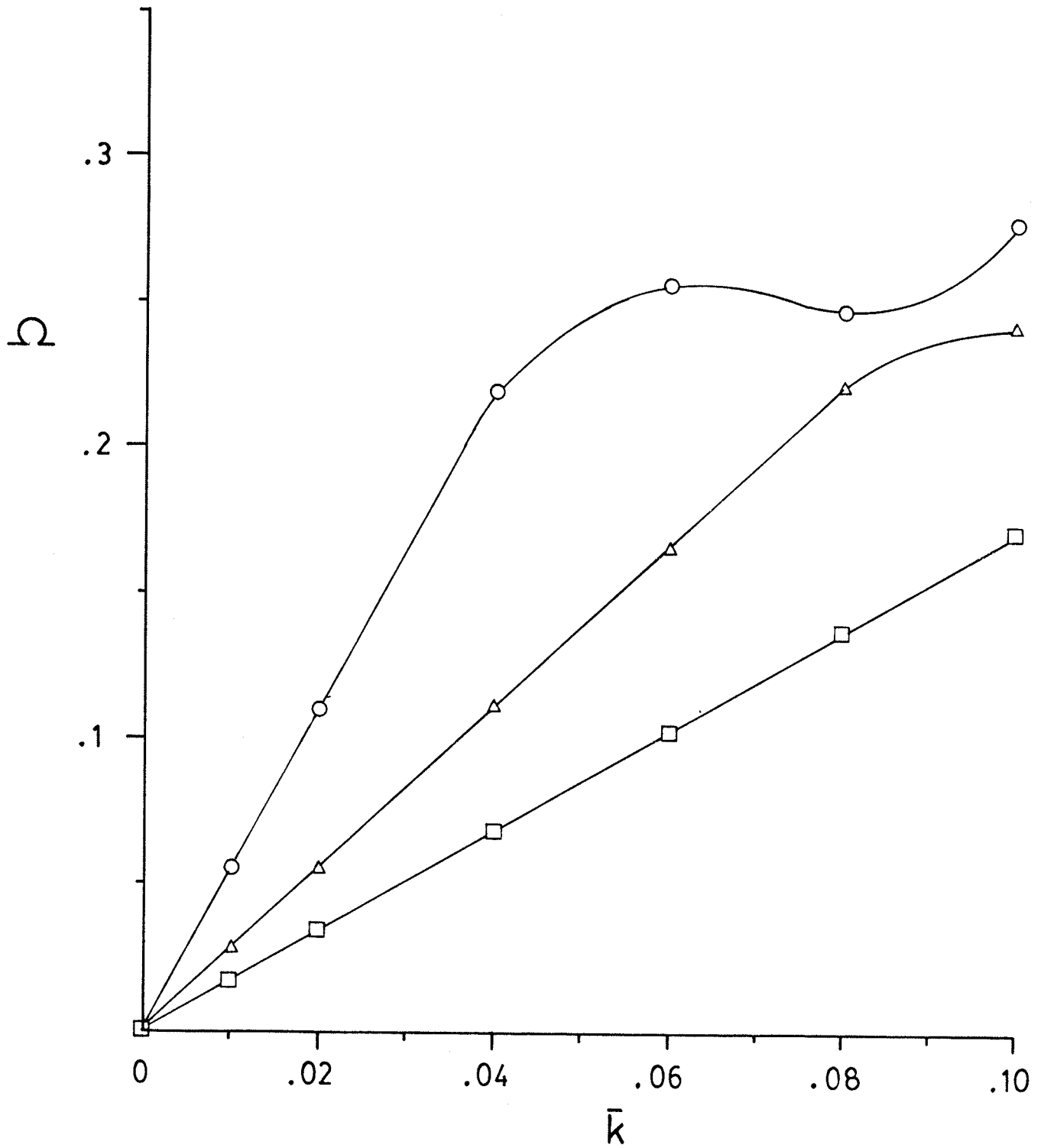


Fig. 4.66 Lowest 3 branches for wave propagating at $\alpha = 45^\circ$, $\phi = 45^\circ$; $\bar{d} = 9$.

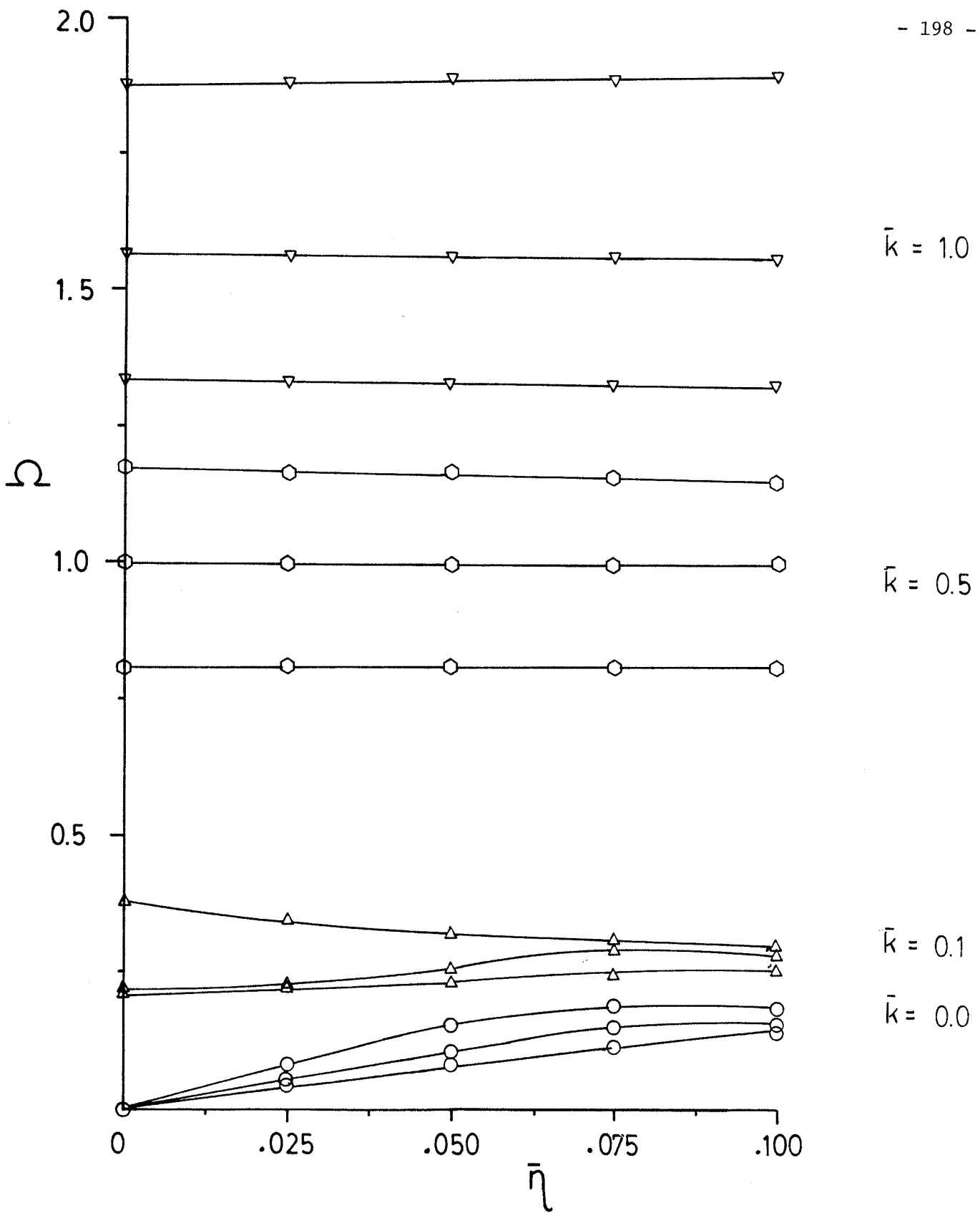


Fig. 4.67 Lowest 3 branches for curves of constant \bar{k} , $\alpha = 0^\circ$; $\bar{d} = 9$.

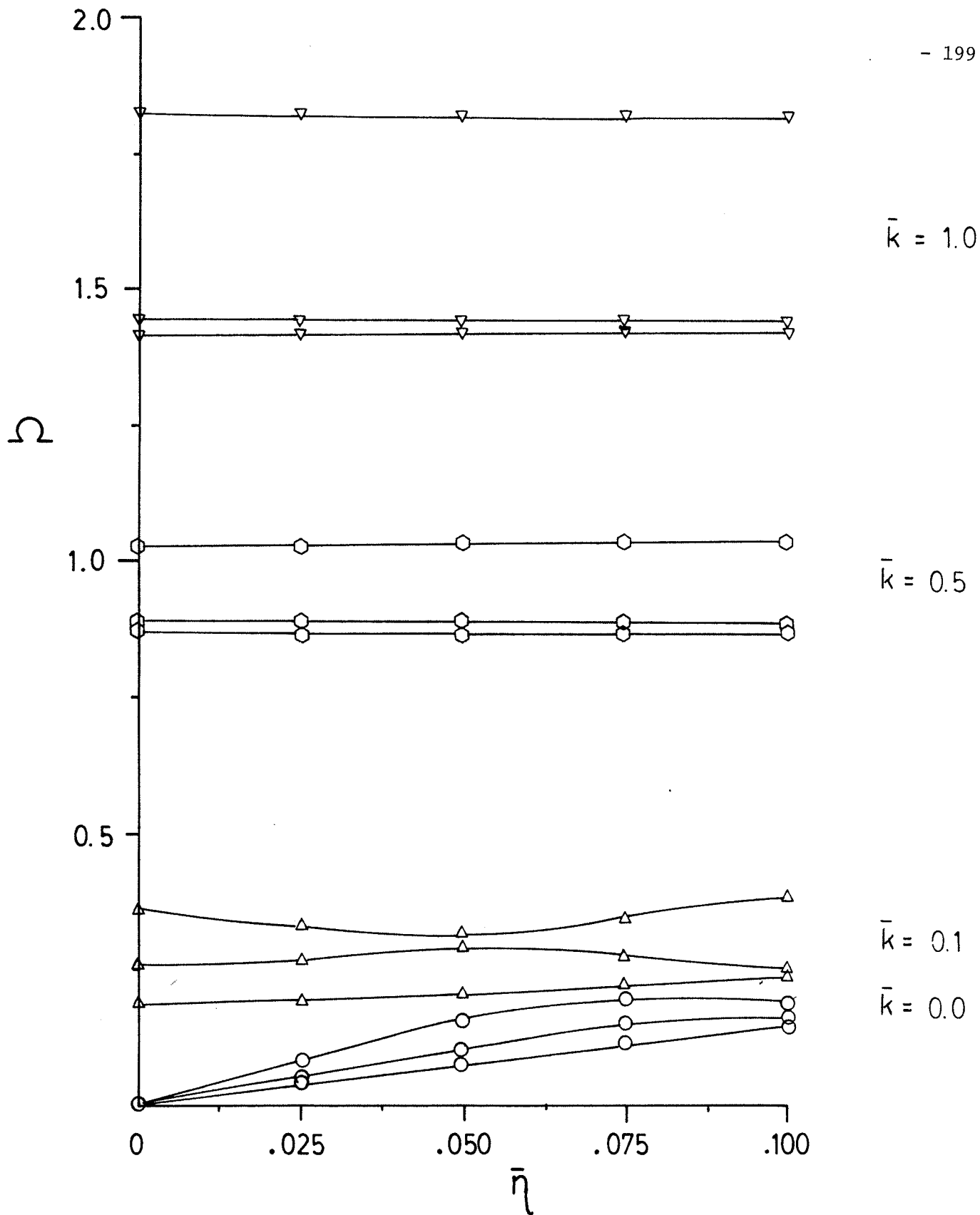


Fig. 4.68 Lowest 3 branches for curves of constant \bar{k} , $\alpha = 45^\circ$; $\bar{d} = 9$.

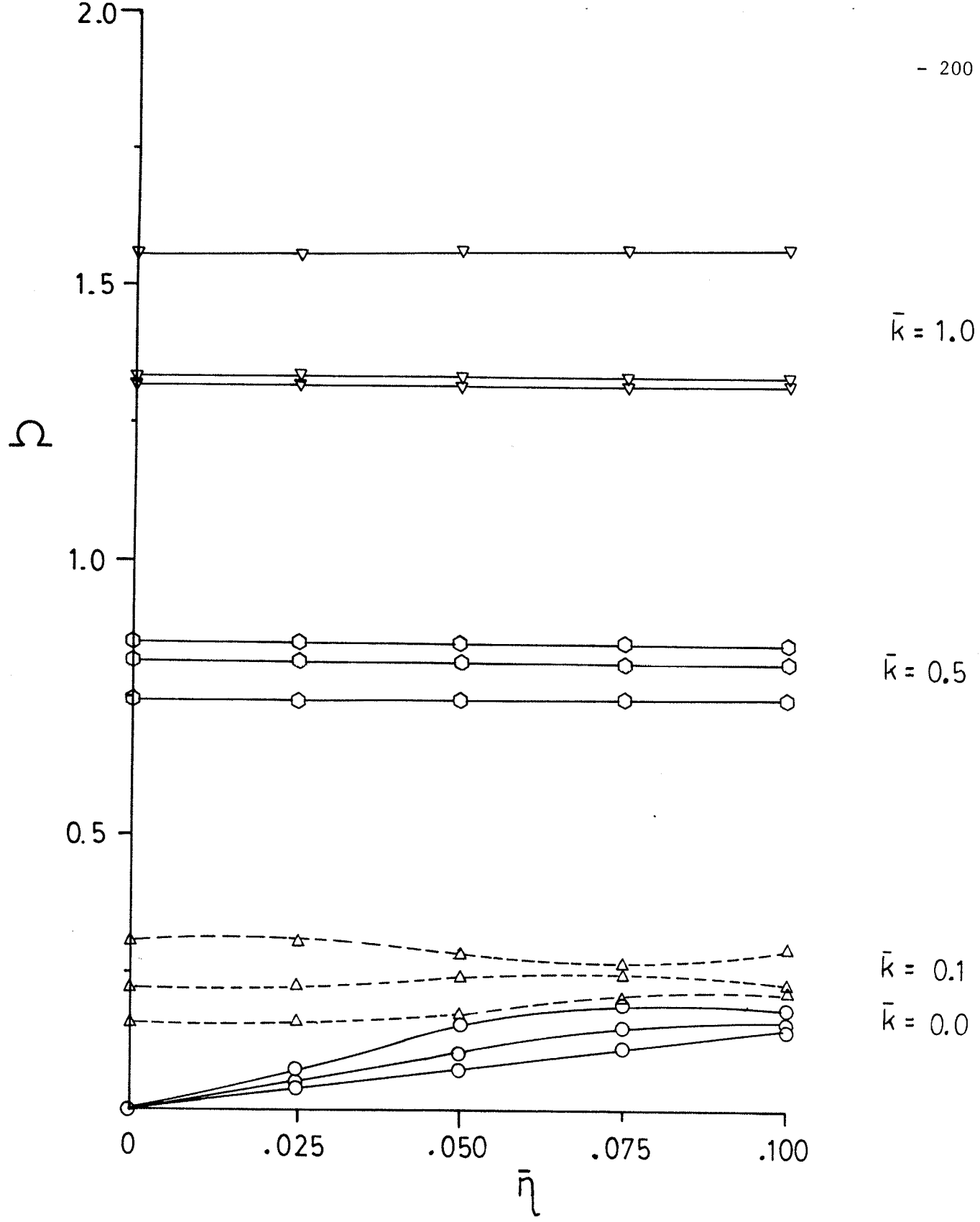


Fig. 4.69 Lowest 3 branches for curves of constant \bar{k} , $\alpha = 90^\circ$; $\bar{d} = 9$.

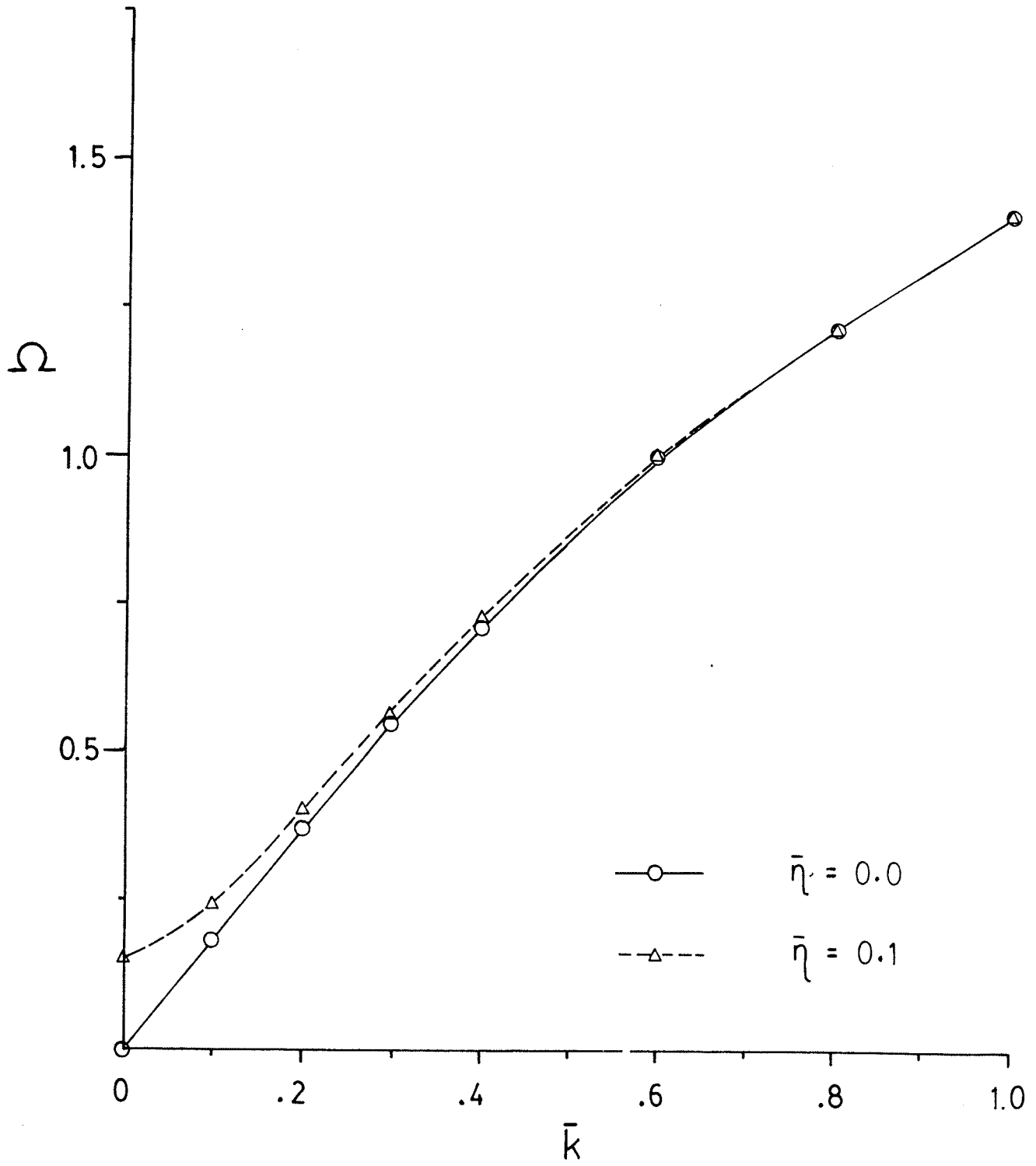


Fig. 4.70 Lowest branch for constant $\bar{\eta}$, $\alpha = 45^\circ$; $\bar{d} = 9$.

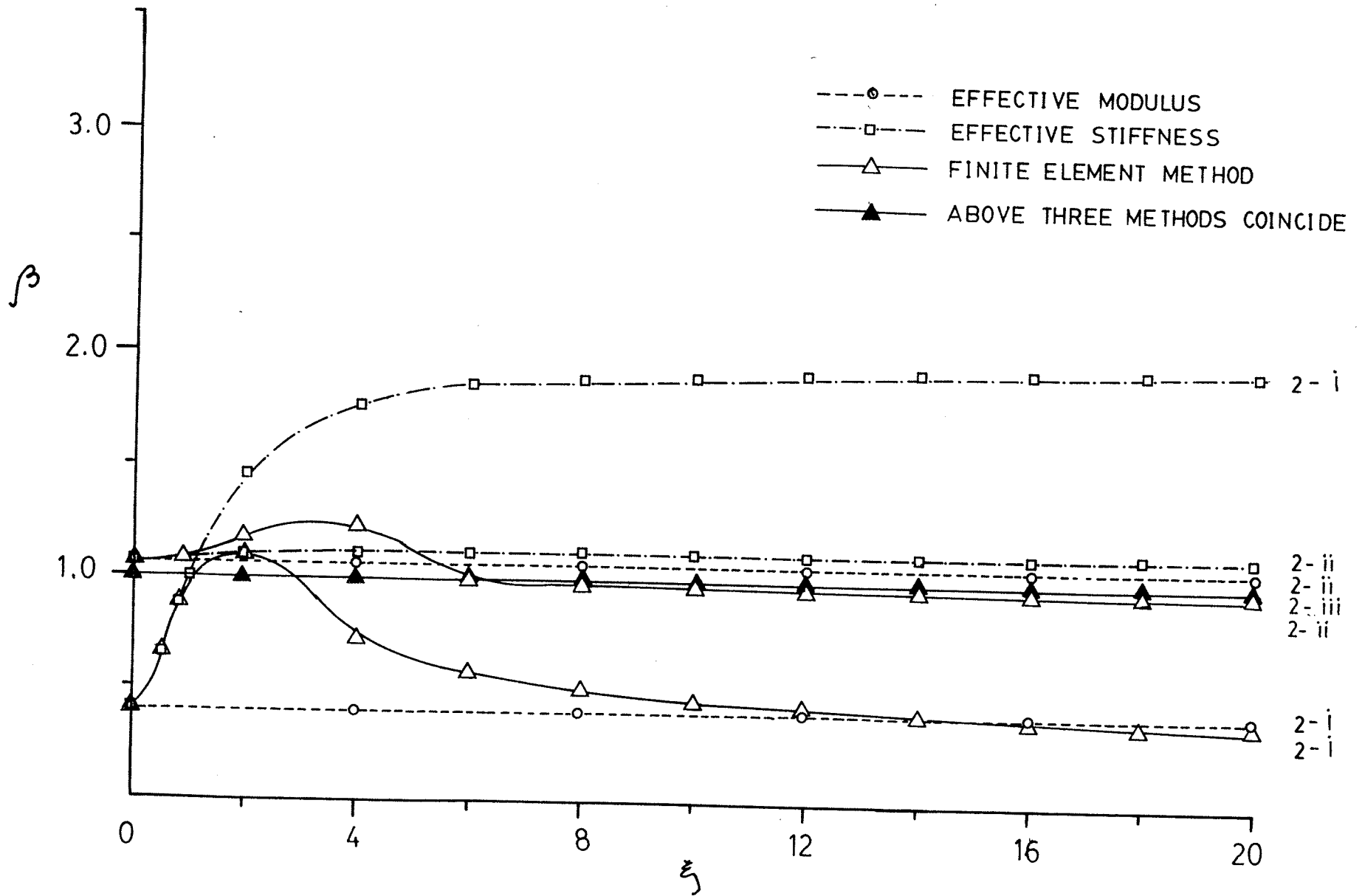


Fig. 4.71 Lowest SV mode for wave propagating through 3 isotropic media with different thicknesses.

Fig. 4.72 Lowest SH mode for wave propagating through 3 isotropic media with different thicknesses.

